INTERNATIONAL DOCTORAL
SCHOOL OF THE USC

Alberto
García Martín-Caro

PhD Thesis

Solitons and effective field theories in the Physics of strong interactions

Santiago de Compostela, 2023

Doctoral Programme in Nuclear and Particles Physics

Universidad de Santiago de Compostela

Escuela de doctorado internacional

Programa de doctorado en Física de Partículas y Nuclear

Solitons and effective field theories in the Physics of Strong Interactions

From low energy nuclear physics to Neutron Stars

por

Alberto García Martín-Caro

Bajo la supervisión de:

Christoph Adam
Ricardo A. Vázquez López

Instituto Galego de Física de Altas Enerxías

Santiago de Compostela, Julio de 2023

SUPERVISOR AUTHORISATION

Solitons and effective field theories in the physics of strong interactions

Mr Christoph Adam

STATES:

That this thesis corresponds to the work carried out by Mr Alberto García Martín-Caro, under my supervision, and hereby authorise its presentation, taking into account that it meets all the relevant requirements stated in the Doctoral Studies Regulations of the USC, and as its director it does not incur in the causes of abstention established in the 40/2015 Law.

In accordance with what is stated in the Regulations for Doctoral Studies, it is also declared that this doctoral thesis can be defended based on the modality of Monographic with reproduction of publications, in which the participation of the PhD student was decisive for its elaboration and the publications adjust to the Research Plan.

In Santiago de Compostela, 17 of June 2023

A mis padres,
a mi hermana
y a mi tio Charly

"It takes love over gold
And mind over matter
To do what you do that you must,

When the things that you hold
Can fall and be shattered
Or run through your fingers like dust"

– Dire Straits, *Love Over Gold*

Agradecimientos

"The person who finishes a Journey is rarely the same as the one who starts it"
– Long Road Home *(card flavor text)*

La tesis ha sido para mí una especie de viaje, en un sentido figurado pero también muy literal. Como en todos los viajes, ha habido momentos mejores y peores. Me gustaría agradecer aquí a todas las personas que han hecho de este un viaje memorable, y que me han ayudado de alguna u otra manera a poder llevarlo a su fin.

En primer lugar, debo agradecer a mis directores, Christoph y Ricardo, por haberme dado la oportunidad de empezar este trabajo sin apenas conocerme, y por dedicarme siempre el tiempo que fuese necesario para atender, y casi siempre resolver, las no pocas dudas que me han ido surgiendo estos años. Esta tesis también está dedicada a la memoria de Ricardo, que desgraciadamente no ha podido estar presente para leer el resultado final de un trabajo que comenzó en base a una de sus ideas. Su contagioso entusiasmo por la física ha sido y será una inspiración para mí.

A mis compañeros de celda, Mike y Jorge, que habéis sido mis hermanos en Santiago y en Cracovia, con quien he compartido discusiones sobre física, pero también muchas risas y anécdotas (y comilonas), os agradezco el haber hecho que mi paso por el IGFAE fuera infinitamente más ameno. Esta tesis es, literalmente, en parte también vuestra.

He tenido la suerte de encontrar en mis colaboradores Andrzej y Kasia dos grandes científicos y excelentes personas, y estoy muy agradecido por todo el tiempo que hemos compartido. Gracias también a Carlos Naya, por ejercer de mentor y guía turístico por Cracovia, y a Chris Halcrow, por estar siempre dispuesto a ayudar y a hablar sobre física.

I also would like to thank the people of the nuclear theory group at BNL for their hospitality during the months that I stayed there, especially Rob Pisarski and Joao, who made my life much easier and our physics discussions very enjoyable. Also to Yoshitaka Hatta, for his insightful ideas and a very fruitful collaboration.

Esta tesis no habría sido posible sin el apoyo de mi familia, especialmente de mis padres, y también de mi hermana y mi tio Charly, a quienes he sentido siempre a mi lado pese a la distancia que en ocasiones nos separaba.

A Manuela, que me animó desde el minuto uno a empezar este proyecto, le agradezco su amor incondicional y su paciencia durante toda esta etapa. Los cuatro años de esta tesis se han hecho cortos a tu lado. Te Kiero Mazo.

Gracias a la gente que conocí en Santiago y que me han acompañado estos cuatro años: Elena, Bala y la gente del CIQUS, y también a mis amigos de Alcorcón: David, Pablo, Arias, Edu, Guille, Fredy, Rober, Isma, Vito, Joseba, Yisus, Tito, Dani, Marcos, Lore, Karen, Albin, Sara, Gema y Ari, que me han recibido siempre con alegría cada vez que estaba de vuelta en El Barrio.

Gracias también a la gente que conocí durante la carrera y me han hecho un poco más feliz durante todo este recorrido. Especialmente, a los miembros del GdA (Grupete de Amiguetes), a Jose Canario (por sus buenas recomendaciones en cuanto a física, juegos y sitios para comer hamburguesas en Madrid), a Gerar y a Javi Olmedo, por escuchar mis desvaríos con paciencia, y a Merce y Luis, que fueron (y son) excelentes mentores.

Por último, me gustaría agradecer a todas las personas que me han apoyado desde que empecé a pensar en dedicarme a esto, a aquellas que están y que ya no están. Gracias de corazón.

Esta tesis ha sido financiada por el Ministerio de Ciencia, Innovación y Universidades y por el Fondo Social Europeo a través de la *Ayuda para contratos predoctorales para la formación de doctores* 2018, con referencia PRE2018-086479.

Abstract

The theory of Quantum Chromodynamics (QCD) elegantly describes the strong interaction, the origin of nuclear forces, in terms of quarks and gluon degrees of freedom as a (quantum) non-abelian gauge field theory. However, the emergence of complex phenomena (such as dynamical spontaneous symmetry breaking and color confinement) due to nonperturbative quantum effects at low energies makes it extremely challenging to explain the phenomenology of strongly-interacting matter at a quantitative level from the first principles of QCD in such regime. On the other hand, this low energy regime is precisely the most relevant to the understanding of nuclear physics, namely, the structure of atomic nuclei and their interactions, as well as the properties of cold, ultra-dense matter such as that expected to be found in the interior of Neutron Stars (NS). Indeed, being the final product of the gravitational collapse of massive stars, NS are the densest known compact objects in the Universe after black holes. As opposed to the physics of nuclei, which has been the subject of experiments in heavy-ion colliders and other research facilities, the matter at the cores of NS is not well understood at all despite the almost 50 years passed since they were first discovered, and even after a tremendous theoretical effort there are many aspects of the Equation of State of dense nuclear matter which remain speculative. It has been only recently that we have gained access to some of the properties of NS matter with the advent of Gravitational Wave (GW) astronomy. In 2014, the first observation of a GW from a NS binary merger was announced by the LIGO collaboration. It is expected that more of such events will be measured in the near future, hence the description of the nature and properties of dense nuclear matter is of extreme relevance in current theoretical physics.

In this thesis we aim to provide a unified framework to the study of both nuclear physics and dense nuclear matter phenomenology from the point of view of the Skyrme model approach. The principal feature of the Skyrme model, as oposed to other chiral EFTs, is that the concrete interaction terms in the phenomenological lagrangian are chosen to precisely allow for stable solitonic configurations (Skyrmions). These are then identified as baryons, such as protons and neutrons. The model also allows to obtain stable multi-skyrmion configurations, which can be identified with nucleon bound states, i.e. atomic nuclei. We review the computation of some well known properties of light nuclei (such as mass, charge radii and electromagnetic form factors) within a generalized Skyrme model, and compute other quantities such as the gravitational form factors, the mass and scalar radii, or beta-decay multipolar matrix elements, for the first time in a soliton approach.

Moreover, by imposing periodic boundary conditions on a finite box, one can obtain infinite crystalline solutions, called Skyrmion crystals, which we identify with symmetric, infinite nuclear matter at a finite density in order to find the equation of state for matter inside Neutron Stars as predicted by the Skyrme model. We also describe the effects of

quantum isospin as a function of density, which allows us to determine the behavior of the symmetry energy, and study the particle fractions in beta-equilibrated matter, including the possibility of kaon condensation in dense Skyrmion matter.

Finally, we obtain NS solutions using different Skyrme-based equations of state, and study their properties under rotation and tidal deformation, which in turn allow us to compute observable magnitudes that can be accesible with current GW observations.

Contents

Scope, structure and methodology

"Theory will only get you so far"

– E. Lawrence to J.R. Oppenheimer,
in *Oppenheimer*, by C. Nolan

The main body of this thesis is divided into two parts, each of them subdivided into two chapters. The common thread between them is the Skyrme model, a nonlinear (classical) field theory which presents topologically nontrivial solitons, also known as Skyrmions. The main motivation for this model comes from the necessity of finding a simple description of the low-energy phenomenology of strongly interacting matter, which is known to be described at high energies by perturbative QCD. Our major aim in this thesis is to investigate whether the Skyrme model, in spite of its simplicity, can be applied to describe strongly interacting matter in a wide range of energy and density scales, from the properties and interactions of free nucleons to the interior of neutron stars at several times the nuclear saturation density. Our approach focuses not only on a qualitative description, but on the quantitative level, trying to obtain valuable predictions that may be checked against either experimental observations at the laboratory or astrophysical observations from gravitational wave and multimessenger astrophysical signals. To reach this goal, there are three important tasks that we have addressed in the thesis:

1. *Computation of nuclear physics magnitudes:* Since the Skyrme model was first proposed, most global properties of nucleons and nuclei have been computed, such as classical binding energies, moments of inertia, mean radii and even form factors for the simplest cases. In the first part of this thesis we introduce a generalization of the Skyrme model that includes, apart from the terms originally introduced by Skyrme in its seminal work, a term that is sextic in derivatives (which may be thought of as coming from integrating out the ω meson, the lightest of vector mesons). Moreover, we review the process of obtaining classical Skyrmion solutions and the canonical quantization of their zero modes, neglecting the back-reaction on the classical solitonic configurations. This semi-classical approximation is called the *rigid rotor approximation*. This allows to obtain the quantum ground states of Skyrmions in order to identify them with nucleon and nuclei quantum states. We end the first chapter with a discussion of the instanton approximation of Skyrmions, and how the concept of constrained instantons may help in the search for a semi-analytical expression that approximates the Skyrmion solution.

   In the second chapter of the thesis, we show how to compute many different physical magnitudes associated to nucleons and nuclei within the Skyrme model approach. Some of these have already been computed several times in the literature (although maybe not in the generalised model), while others, like the multipole form factors

associated to beta decay, the charge densities, the gravitational form factors and the neutron skin radii, are new to our best knowledge. In order to compute all these quantities we just assume the rigid rotor approximation, and employ the numerical solutions obtained in the previous chapter.

On the other hand, before comparing to the experimental values, one needs to fit the free parameters appearing in the model to some values. There is not a general consensus on which physical quantity one should fit the parameters to, and the one that is most often used is, for historical reasons, the one proposed in [ANW83b], which fits the energies of the proton and the Delta baryon. The physical adequacy of such a fit has been put into doubt due to the ultra-relativistic character of the delta baryon, and also the general idea of fitting the classical energies (or semiclassical, if one includes corrections using a zero-mode quantization) can be argued against, since there may be significant contributions to the total energy, coming from the zero point energy of vibrational modes and other pionic quantum corrections that are assumed to cancel out when computing binding energies. Therefore, a natural question, that we address, is wether one can find a better set of magnitudes that one can fit the parameters to in order to make not only qualitative, but also quantitative predictions for medium and large nuclei. We also discuss on how the different physical magnitudes can be affected by the inclusion of the sextic term.

2. *Computation of the nuclear matter EOS in the high density regime:* After studying the properties of light nuclei, in the second part of this thesis we turn our focus to the classical Skyrmion crystal solutions (also including the sextic term) for different sizes of the unit cell (or equivalently, different densities). In practice, we employ the same numerical methods (gradient descent functional minimization), but slightly modified to account for the periodic boundary conditions. Furthermore, we have quantized these crystal solutions in order to include the effects of a finite isospin chemical potential, which becomes relevant for higher densities. Formally, the quantization of isospin degrees of freedom follows the same lines as for isolated skyrmions, but charge neutrality requires the introduction of a leptonic background that neutralizes the system (since the ground state of quantum skyrmion crystals is electrically charged, as we carefully show in chapter 3). The whole system can then be identified with $npe\mu$ matter at finite density. The Equation of State (EOS) is then computed by straightforward application of the thermodynamical definitions of energy and pressure densities. Finally, we extend our analysis to include the effects of strangeness (a quantum number related to the presence of a third type of quark, the strange quark) in order to study the possibility of kaon condensation at sufficiently high densities. It turns out that the Skyrme model predicts the condensation of kaons at a relatively small threshold density, well below the maximum densities that can be reached inside a neutron star.

3. *Extraction of signatures of the NS EOS from GW and astrophysical observations* In the last chapter of the thesis, we comment on the previous approaches of studying static Neutron Star (NS) solutions within the Skyrme model, in particular, the Bogomoln'y-Prasad-Sommerfeld (BPS) submodel, and review the theory of slowly rotating and tidally deformed neutron stars. The idea is to be able to obtain information not only from global observables such as the mass-radius curves, but other

interesting properties that can be extracted from gravitational wave observations, such as love numbers and quadrupolar moments. As it turns out, there is a set of universal relations that some of these properties should satisfy, the *I-Love-Q* relations, first proposed by Yagi and Yunes [YY13b] . We show that these relations are indeed satisfied for Skyrme based NSs, remarkably even in the case in which the stars are not described in terms of a barotropic equation of state.

We end this document with a summary of the principal results, a comment on the main conclusions obtained from them and an overview of possible further work directions in the last section.

Methodology

In general, there is not a standard, step-by-step way of proceeding in theoretical high energy physics. In the making of this thesis, we have mainly followed the Feynman-esque interpretation of the scientific method[1], as applied to theoretical physics. It starts by developing a theoretical model, either using an effective theory approach or a more phenomenological one (by directly "guessing" it, as Feynman would put it), from some basic principles such as symmetry, unitarity, etc. The model will, in general, include some free parameters such as coupling constants or mass/energy scales. To make contact with the real world phenomenomena, one must fit the free parameters of these theoretical models to a given set of observables. A good choice of relevant observables is important, as they must be available in terms of experimental data and/or empirical observations, but also one must be able to calculate them independently from the theoretical model. These calculations are usually quite involved technically, and sometimes require some kind of approximation that makes them more tractable. Thus, the number of free parameters defines the *predictive power* of a model, as once their values have been fitted to a set of observables, all other independent observables will be, in principle, determined, their values coming out as predictions. Of course, the number and accuracy of its predictions will ultimately determine the validity of such a model (and the approximations that have been taken) as a good description of the natural phenomena under consideration. We will devote this thesis to the computation of different observables as predicted by the Skyrme model, guided by the principles of Quantum Mechanics and General Relativity, and analyze the accuracy of the predicted values of such observables as compared to the corresponding empirical data.

The methods employed for analytical computations in this thesis come from standard nuclear, particle and high energy physics theoretical tools: basic notions of geometry and topology are necessary to work with the classical Skyrme model, plus the formalism of canonical quantization, as well as perturbation theory and representation theory techniques for the computation of nuclear form factors. However, as it is often the case in

[1] During one of his acclaimed lectures, Richard Feynman described the procedure of finding a new law in theoretical physics in three simple steps: "*First, we guess it. [...] Then we compute the consequences of the guess to see what it would imply, [...] and then we compare those computation results to nature.*", to which he added "*If it disagrees with experiment, it's wrong. And that simple statement is the key to science. It doesn't make a difference how beautiful your guess is. It doesn't make a difference how smart you are, who made the guess, or what his name is, if it disagrees with experiment, it's wrong. That's all there is to it.*" A video of this lecture is available in YouTube: Feynman on the Scientific Method.

modern theoretical physics, a satisfactory answer to the more relevant questions cannot be found with analytical methods alone, and numerical computations become essential. In our case, they are necessary for obtaining the classical Skyrmion solutions, which implies the minimization of a complicated energy functional. In order to solve this problem for different topological sectors, we developed a `C++` code based on a gradient-descent numerical method, described in appendix A. On the other hand, the last chapter of this thesis is more focused on the methods of General Relativity. In particular, the Einstein equations are solved (numerically) for static, spherically symmetric spacetimes, for which a simple `Python` script that integrates the corresponding system of ODEs is enough. Afterwards, we apply perturbation theory on top of such a background, which yields a slightly more complicated set of differential equations that can nevertheless be solved using a similar script. Details can be found in chapter 4 and appendix B.

In most cases, derivations of the main results are explicitly shown within the text, or, in the cases when they are not particularly illuminating, have been relegated to an appendix (with the exception of the first appendix, in which the numerical gradient flow algorithm is detailed). Some of the analytical computations have been hugely simplified by the use of symbolic computer algebra software such as *Sympy* [Meu+17], and MATHEMATICA® notebooks [Wol23]. Moreover, most figures in this thesis have been obtained using *Matplotlib* [Hun07] and the native MATHEMATICA® plotting packages. We have also made use of PGF/TikZ and the *TikZ-Feynman* LaTeXpackage [Ell17].

Notation and conventions

"Es mísero, sórdido, y aún diría tétrico,
someterlo todo al sistema métrico"

– Javier Krahe, *Un Burdo Rumor*

Units, metric and indices

Even though the results presented in this thesis are of theoretical nature, and have been obtained either with analytical or computational methods, in most cases we will ultimately be interested in the comparison between our results and the corresponding experimental data. It is also a common practice to choose a convenient system of units, to perform analytical calculations or computer simulations, in order to rewrite the relevant equations in terms of dimensionless constants. For instance, in the first part of this thesis, it will be useful to choose the following combinations of constants

$$E_s = \frac{3\pi^2 f_\pi}{e}, \quad x_s = \frac{\hbar c}{f_\pi e}, \tag{1}$$

as units of energy and length, respectively, where $f_\pi = 130\,\mathrm{MeV}$ is the pion decay constant, and e is a dimensionless parameter whose meaning will be clarified in chapter 1.

In order to simplify the analytic expressions, it will probe useful to choose units in which $\hbar = c = 1$, so that time and length will have the same dimensions, and so will mass and energy, with the latter being inverse of the former. However, when comparing the value of physical magnitudes obtained in a simulation with their corresponding experimentally measured values, dimensionless computational units must be brought to physical units. Depending on the particular problem at hand, we will either use GeV and MeV (for nuclear physics) or solar masses ($M_\odot = 1.9885 \times 10^{30}\,\mathrm{kg}$, for gravitational physics) as typical dimensions of energy. Similarly, for nuclear physics calculations we will mainly use the Fermi ($1\,\mathrm{fm} = 10^{-15}\mathrm{m}$) as unit of length, while the typical distance scales in neutron star physics are more easily measured in km.

This choice of units will affect the values of the different fundamental constants that will be relevant on each case, which must also be taken in the correct units. For example, we will use, for computing nuclear magnitudes in physical units, the value

$$\hbar c = 197.3269804\ \mathrm{MeV} \cdot \mathrm{fm},$$

while for computations involving the gravitational field, we will use the following value of Newton's constant:

$$G/c^4 = 1.48\,\frac{\mathrm{km}}{M_\odot}.$$

Unless otherwise specified, we will work in a 4 dimensional spacetime, with Lorentzian metric, for the most part of the thesis. The sign convention for the metric signature will, however, differ between the two different parts of this thesis. Indeed, in the first part, we will choose the mostly minus convention, $(+---)$, as it is common in particle physics. On the other hand, for the last chapter of the thesis we will change it and work with the mostly plus metric convention, $(-+++)$, because it is the standard choice in gravitational physics, and will be most convenient for comparing our results with the literature. Furthermore, as it is standard in high energy physics literature, we will denote spacetime indices with greek letters $(\alpha, \beta, \mu, \nu \cdots)$, which run from 0 to 3, and with latin indices $(i, j, k, l, \cdots)$ the components of the associated spatial three-vectors, and, most generally, the components of any three-vector defined in other spaces (such as the $\mathfrak{su}(2)$ Lie algebra). Occasionally, we will refer to vector quantities in higher-dimensional spaces with capital letter indices. For example, indices representing color degrees of freedom will be typically denoted by $(\mathrm{A}, \mathrm{B}, \cdots)$. Some tensorial quantities present both spacetime and flavor space index structures. In such cases, as a general rule of thumb we will prefer to use latin indices from the first letters of the alphabet $(a, b, c, \cdots)$ for denoting indices associated to flavor space, while the spatial indices will generally be denoted by latin letters from the middle part of the alphabet $(i, j, k, l, \cdots)$. Additionally, we will denote a three-vector, without any mention to a specific coordinate basis, by boldfaced letters, ($\mathbf{x}, \boldsymbol{\sigma}$, etc.). Further, we will make use of the square braket notation for a pair of antisymmetrized indices of any kind, so that

$$A_{[i}B_{j]} = \frac{1}{2}(A_iB_j - A_jB_i). \tag{2}$$

Spin and flavor

Throughout this thesis, the set of three 2×2 matrices denoted by σ^a represent the Pauli matrices,

$$\sigma^1 = \begin{pmatrix} 0 & 1 \\ -1 & 0 \end{pmatrix}, \quad \sigma^2 = \begin{pmatrix} 0 & -i \\ i & 0 \end{pmatrix}, \quad \sigma^3 = \begin{pmatrix} 1 & 0 \\ 0 & -1 \end{pmatrix}, \tag{3}$$

and we will denote the same numerical matrices also by the letter τ, depending on wether they act on spin or isospin spaces, respectively. Additionally, we define the Pauli spin three-vector $\boldsymbol{\sigma} = (\sigma^1, \sigma^2, \sigma^3)$, and $\boldsymbol{\tau}$ its analogue in isospin space.

The Pauli matrices represent a basis of generators of the $\mathfrak{su}(2)$ Lie algebra, so they are traceless and fulfill:

$$\sigma_a\sigma_b = i\epsilon_{abc}\sigma_c + \delta_{ab}\mathbf{1}, \tag{4}$$

where ϵ_{ijk} is the totally anti-symmetric Levi-Civita tensor, $\epsilon_{123} = +1$, and $\mathbf{1}$ is the 2×2 identity matrix.

When dealing with three quark flavors (or color degrees of freedom) we will also use

the standard Gell-Mann representation of the $\mathfrak{su}(3)$ generators,

$$\lambda_1 = \begin{pmatrix} 0 & 1 & 0 \\ 1 & 0 & 0 \\ 0 & 0 & 0 \end{pmatrix}, \quad \lambda_2 = \begin{pmatrix} 0 & -i & 0 \\ i & 0 & 0 \\ 0 & 0 & 0 \end{pmatrix}, \quad \lambda_3 = \begin{pmatrix} 1 & 0 & 0 \\ 0 & -1 & 0 \\ 0 & 0 & 0 \end{pmatrix},$$
$$\lambda_4 = \begin{pmatrix} 0 & 0 & 1 \\ 0 & 0 & 0 \\ 1 & 0 & 0 \end{pmatrix}, \quad \lambda_5 = \begin{pmatrix} 0 & 0 & -i \\ 0 & 0 & 0 \\ i & 0 & 0 \end{pmatrix}, \quad \lambda_6 = \begin{pmatrix} 0 & 0 & 0 \\ 0 & 0 & 1 \\ 0 & 1 & 0 \end{pmatrix}, \tag{5}$$
$$\lambda_7 = \begin{pmatrix} 0 & 0 & 0 \\ 0 & 0 & -i \\ 0 & i & 0 \end{pmatrix}, \quad \lambda_8 = \frac{1}{\sqrt{3}} \begin{pmatrix} 1 & 0 & 0 \\ 0 & 0 & 0 \\ 0 & 0 & -2 \end{pmatrix}.$$

We will also use the standard representation of the Dirac gamma matrices $\gamma^\mu = (\gamma^0, \boldsymbol{\gamma})$,

$$\gamma^0 = \begin{pmatrix} \mathbf{1} & 0 \\ 0 & -\mathbf{1} \end{pmatrix}, \qquad \gamma^i = \begin{pmatrix} 0 & \sigma^i \\ -\sigma^i & 0 \end{pmatrix}, \tag{6}$$

and the pseudoscalar Dirac matrix,

$$\gamma_5 = i\gamma^0\gamma^1\gamma^2\gamma^3 = \begin{pmatrix} 0 & \mathbf{1} \\ \mathbf{1} & 0 \end{pmatrix}. \tag{7}$$

List of Abbreviations

Throughout this thesis, we have made use of abbreviations in order to facilitate the reading of most technical parts to the expert reader, who will most probably be familiar with most of them. However, we acknowledge that an extensive use of abbreviations may be a source of confusion for a non-expert reader. Therefore, we present all of them, alphabetically, in the following list.

ADM Arnowitt-Desser-Misner

ADHM Atiyah-Drinfeld-Hitchin-Manin

BCC Body-Centered Cubic

BCPM Barcelona-Catania-Paris-Madrid

BNL Brookhaven National Laboratory

BPS Bogomoln'y-Prasad-Sommerfeld

BPST Belavin-Polyakov-Schwarz-Tyupkin

DEC Dominant Energy Condition

DU Direct Urca

DVCS Deeply Virtual Compton Scattering

EFT Effective Field Theory

EIC Electron Ion Collider

EMT Energy Momentum Tensor

EOS Equation of State

FCC Face Centered Cubic

FFs Form Factors

FR Finkelstein-Rubinstein

GFFs Gravitational Form Factors

GR General Relativity

GSM Generalized Skyrme Model

GW Gravitational Waves

ITO Irreducible Tensor Operator

LHC Large Hadron Collider

LIGO Laser Interferometer Gravitational-wave Observatory

NICER Neutron star Interior Composition ExploreR

NLSM Nonlinear Sigma Model

NS Neutron Star(s)

NST Neutron Skin Thickness

ODEs Ordinary Differential Equations

QCD Quantum Chromodynamics

QED Quantum Electrodynamics

QGP Quark Gluon Plasma

RHIC Relativistic Heavy Ion Collider

RME Reduced Matrix Element

TOV Tolman-Oppenheimer-Volkoff

SEC Strong Energy Condition

SM Standard Model

SSB Spontaneous Symmetry Breaking

vev vacuum expectation value

WZW Wess-Zumino-Witten

YMH Yang-Mills-Higgs

Introduction

"Es cosa averiguada [...] que no se sabe nada, y que todos son ignorantes, y aun esto no se sabe de cierto, que a saberse ya se supiera algo; sospéchase."
– Francisco de Quevedo, *El mundo por de dentro*

The modern understanding of fundamental interactions in physics is based on two great theoretical pillars, namely the theory of General Relativity (GR) and the Standard Model of particle physics. The former is a classical theory which describes the gravitational interactions in terms of the curvature of spacetime, based in the concept of invariance under general coordinate transformations. The latter, instead, consists on a complex quantum field theory that collects our current knowledge of the different pieces that conform the matter content of the universe, as well as their interactions through the strong, weak, electromagnetic and Higgs fields.

Within the Standard Model (SM), fundamental interactions are the result of invariance of the physical laws under local (gauge) symmetries. The complete gauge symmetry group of the Standard Model is $SU(3)_C \times SU(2)_W \times U(1)_W$, i.e. the product of that of Quantum Chromodynamics (QCD), corresponding to strong interactions, and the symmetry group of the Glashow-Weinberg-Salam model of electroweak interactions. Each of these gauge symmetries is associated with a set of bosonic, spin 1 fields that mediate them (one for each generator of the corresponding group). Therefore, the gauge fields that mediate the strong (color) interactions are 8 (gluons), whereas in the electroweak sector we have two electrically charged weak gauge bosons, $W^{\pm}_{\mu}$, one neutral weak boson Z^0_{μ} and the neutral photon γ. In the matter sector, the SM postulates the existence of six flavours of strongly-interacting, spin 1/2 fermions, the quarks. Additionally, there exists another six fermionic fields, called leptons, of which three (the electron, muon and τ) are electrically charged. Leptons do not interact with the color gauge field, but they still can interact with quarks via the electroweak gauge bosons.

As with the leptons, the quark flavors can be arranged into three pairs (generations) according to their masses. For example, while the masses of the first generation of quarks, u and d, are both smaller than 5 MeV, the next smallest massive quark, the strange quark, has a mass of ~ 95 MeV. Therefore, the particles of higher generations will be unstable, and tend to decay into their lower-generation analogues, in flavor-changing processes mediated by the weak bosons. This means that ordinary matter, including all the atoms that form all the different elements in the universe[2], is mainly made up of particles from

[2]A caveat about this statement concerns the possible existence of *Dark Matter*, a hypothetical kind

the first generation, i.e. u and d quarks, electrons and neutrinos.

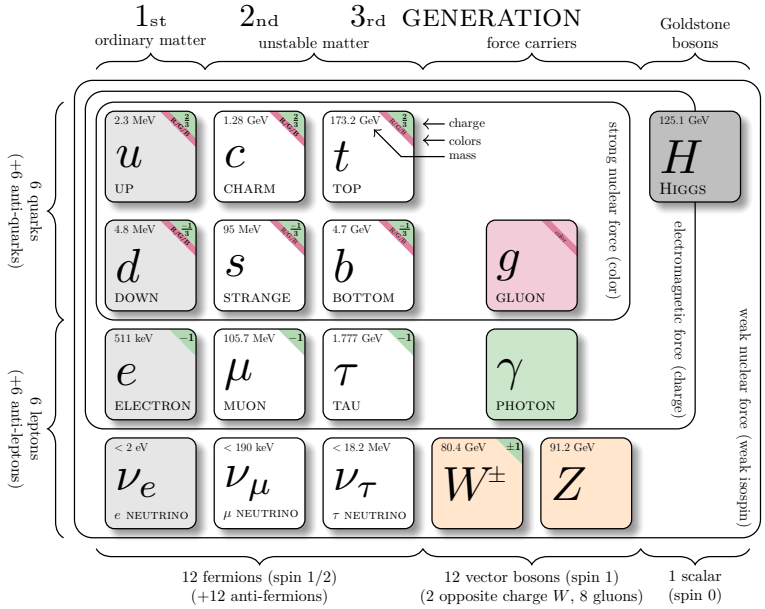

Figure 1: A diagram with the particle content currently included in the Standard Model. Modified from [Bur16].

Notwithstanding the great success of QCD in describing the strong interaction phenomenology at very high energies (such as those achieved at the Large Hadron Collider (LHC)), we are unable to achieve the same level of precision when trying to describe strong interactions in the low-energy regime, using the full machinery of perturbative quantum field theory. However, experimentally it is well known that in such regime, the fundamental fields of QCD become confined into colorless bound states, called HADRONS, such as the proton and the neutron. Despite being colorless, protons and neutrons (collectively known as NUCLEONS) and other hadrons can interact via the residual strong force between their color-charged constituents. In particular, due to such residual interaction, nucleons can bind together to form atomic nuclei.

Indeed, an outstanding problem in modern nuclear physics is to determine the properties of atomic nuclei as nucleon bound states from the fundamental theory of QCD, as well as their excitations and decay properties. This is an egregious task, since there are hundreds of experimentally observed NUCLIDES (bound states with a definite number of protons and neutrons), corresponding to the isotopes of the more than a hundred different elements known to date. Most of them are not stable, but radioactive, and decay either via nuclear fission or weak-mediated reactions (see fig. 2 for a chart of known nuclides and their measured half-life).

of matter whose presence in the universe can be inferred due to its gravitational effects at cosmological scales. The SM does not include such matter, as no direct detection of dark matter particles has been produced up to date, so one can safely ignore it for practical purposes when concerned with the physics of low energy particle interactions.

Therefore, a satisfactory description of nuclear phenomenology should be able to include also the processes due to the other forces in the Standard Model, i.e. nuclear transitions due to the electromagnetic and weak forces. The simplest example of the latter is the β decay of the neutron, mediated by the charged W^- boson.

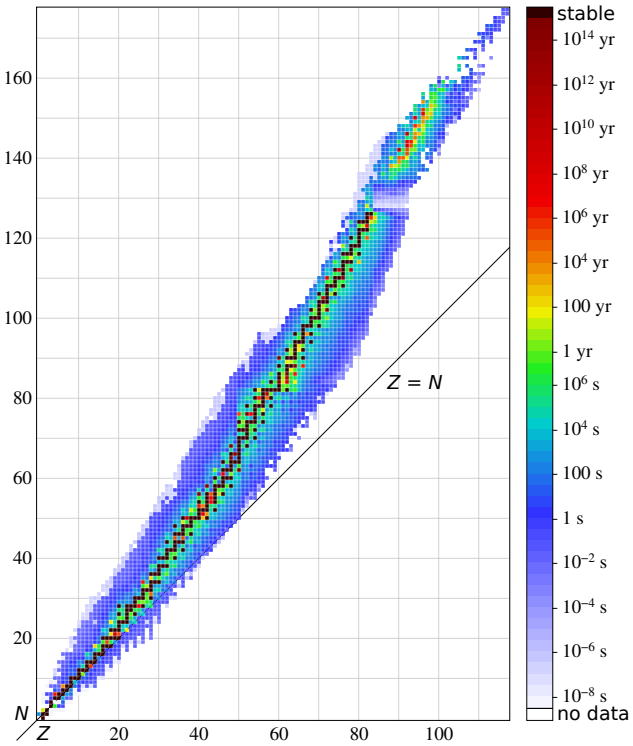

Figure 2: Chart of stability of known nuclides, being N the neutron number and Z the proton number, colored by half life. Taken from [Ben09].

Low energy QCD and chiral effective theories

Mathematically, QCD is a non-abelian gauge theory in which the most fundamental degrees of freedom are carried by the quark and gluon fields, and very compactly expressed in terms of the QCD Lagrangian

$$\mathscr{L}_{\text{QCD}} = \bar{\psi}(x)(i\gamma^\mu D_\mu - M)\psi(x) - \frac{1}{4}F^{\text{A}}_{\mu\nu}F^{\mu\nu}_{\text{A}}. \tag{8}$$

It describes a set of $N_f = 6$ quark flavors (*up, down, strange, charm, top*, and *bottom*) as massive, spin 1/2 fields that transform in the fundamental representation of the $SU(3)_C$ (color) gauge group. In other words, quarks carry color charge, that can be of three different types (with the corresponding anti-type). The color force is mediated by 8 gluon gauge fields (one for each generator of the gauge group), which, as opposed to the photon in the electromagnetic force, do carry color charge on their own. This means that gluons can interact between them, a characteristic trait of nonabelian gauge theories with profound implications in their particle spectrum. Indeed, the gluonic self-interaction implies that,

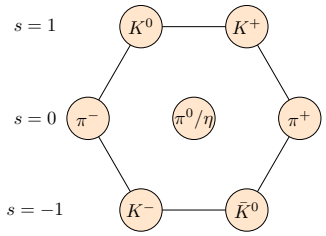

Figure 3: Meson octet of the approximate $SU(3)$ flavor symmetry.

as opposed to regular electromagnetism, the renormalized coupling constant of QCD decreases with the energy scale. This means that, while at large energies quarks and gluons barely interact with each other (a phenomenon usually referred to as asymptotic freedom), at energies lower than a certain energy scale $\Lambda_{QCD} \sim 200\,\text{MeV}$[3], the coupling constant grows arbitrarily, giving rise to what is known as COLOR CONFINEMENT. Due to such phenomenon, quarks are never observed outside the bound states they compose, the hadrons. Being colorless states, hadrons can only appear in the singlet representation of $SU(3)_C$, which may be achieved by combining a quark and an antiquark to form MESONS ($\mathbf{3} \otimes \bar{\mathbf{3}} = \mathbf{1} \oplus \mathbf{8}$), or three quarks to form BARYONS ($\mathbf{3} \otimes \mathbf{3} \otimes \mathbf{3} = \mathbf{1} \oplus \mathbf{8} \oplus \mathbf{8} \oplus \mathbf{10}$)[4]. Experimentally, both baryons and mesons are found to be arranged in "multiplets" of approximately the same masses, which points towards the existence of an underlying approximate symmetry of the QCD Lagrangian (see *eg* the pseudo-scalar meson octet in fig. 3). Historically, this idea lead Gell-Mann and Ne'eman to propose the *eightfold way* model, in which the basic unit is an eight-member multiplet (octet), with mesons and baryons belonging either to one octet or multiplets that could be made form them. Later, Gell-Mann and Zweig introduced the concepts of quarks and flavor, and derived the eightfold way model in terms of a simple $SU(3)$ symmetry between quarks flavors. Indeed, in the CHIRAL LIMIT $M \to 0$, the symmetry group of the QCD Lagrangian is given by [DGH23]:

$$\overbrace{\underbrace{SU(3)_C}_{\text{color}}}^{\text{gauge (local)}} \times \overbrace{\underbrace{SU(N_f)_L \times SU(N_f)_R}_{\text{chiral}} \times \underbrace{U(1)_V}_{\text{baryon}} \times \underbrace{U(1)_A}_{\text{axial}}}^{\text{flavor (global)}} \tag{9}$$

The vector symmetry $U(1)_V$ is an exact symmetry of the QCD Lagrangian, and thus it has an associated Noether charge, the baryon number B. Quarks (antiquarks) carry $B = \frac{1}{3}(-\frac{1}{3})$, so hadrons are split up into baryons ($B = 1$) and mesons ($B = 0$). Atomic nuclei are particles with $B > 1$, which are not seen as fundamental, but as bound states of individual baryons. On the other hand, while the axial $U(1)_A$ symmetry is exact in the classical theory, it is broken in the quantum theory due to the axial anomaly [DGH23].

Finally, even in the chiral limit, the chiral subgroup of the flavor symmetry group is spontaneously broken to its diagonal subgroup $SU(N_f)_{R+L}$ at low energies, and a quark condensate forms the physical vacuum of the flavor sector. By Goldstone's theorem, there

[3] The specific definition and its particular value depends on the renormalization scheme.

[4] Color singlets may also appear as combination of two or more gluon fields to form glueballs, or higher combinatons of quarks such as tetraquarks, pentaquarks, etc. These states are, however, barely relevant for the study of low energy nuclear physics processes due to their high masses.

must be N_f^2-1 massless, Nambu-Goldstone bosonic fields (one for each broken generator), formed by colorless, bound states of quarks. Such states are interpreted as oscillations around the quark condensate vacuum, and identified with the (pseudoscalar) mesons, as they are the lightest of hadrons, their small mass coming only from the fact that the chiral symmetry is explicitly broken by the quark mass term.

Therefore, the lightest degrees of freedom in the SM correspond to the only massless gauge boson, i.e. the photon, the (almost massless) pseudo-Nambu-Goldstone bosons associated to spontaneous chiral symmetry breaking, i.e. the mesons, and the leptons. Of these, the only non-fundamental particles are the mesons, and, as argued, trying to deduce their properties and interactions directly in terms of quark and gluon interactions is tremendously complicated. An alternative route to describe the dynamics of an underlying, (known or unknown) quantum field theory such as QCD in terms of the interactions between light degrees of freedom is presented by the Effective Field Theory (EFT) framework, in which only the knowledge of the relevant degrees of freedom (and the symmetries that their interactions should preserve) is needed to construct an effective Lagrangian, valid up to a certain energy scale.

Chiral effective theories

Adopting the EFT philosophy allows to impose strong constraints on the allowed interaction terms in any effective Lagrangian involving the lowest energy excitations of QCD, the pseudoscalar mesons, as the Goldstone bosons of the approximate chiral symmetry based on symmetry arguments alone. Such EFTs are usually called CHIRAL EFFECTIVE THEORIES, in which Goldstone bosons are parametrized via the so-called coset construction [Pic20]. Indeed, for a general spontaneous symmetry breaking of a global symmetry group G into the subgroup H, a number $N = \dim(G) - \dim(H)$ of Goldstone bosons will be generated, which we can collect into a scalar field of N components, $\boldsymbol{\phi} = (\phi^1(x), \cdots, \phi^N(x))$. The action of G over $\boldsymbol{\phi}$ will be given by some mapping

$$\begin{aligned} \mathbf{F}_g : G \times \mathbb{R}^N &\to \mathbb{R}^N \\ (g, \boldsymbol{\phi}) &\mapsto \boldsymbol{\phi}' = \mathbf{F}_g(\boldsymbol{\phi}) \end{aligned} \tag{10}$$

which satisfies the group composition law $\mathbf{F}'_g(\boldsymbol{\phi}') = \mathbf{F}'_g(\mathbf{F}_g(\boldsymbol{\phi})) = \mathbf{F}_{g'g}(\boldsymbol{\phi})$, and $\boldsymbol{\phi} = \mathbf{F}_e(\boldsymbol{\phi})$, with $e \in G$ the identity element. Then, after Spontaneous Symmetry Breaking (SSB), a choice of vacuum $\boldsymbol{\phi}_0$ is made. Since the vacuum manifold is invariant under the unbroken subgroup, we must have $\boldsymbol{\phi}_0 = \mathbf{F}_h(\boldsymbol{\phi}_0)$ for all $h \in H$, i.e.

$$\boldsymbol{\phi} = \mathbf{F}_g(\boldsymbol{\phi}_0) = \mathbf{F}_{gh}(\boldsymbol{\phi}_0), \tag{11}$$

so the Nambu Goldstone fields can be identified with the elements of the coset space G/H. If we now choose a group representative $\xi \in G$ for each (left) coset equivalence class gH (or equivalently, for each field configuration $\boldsymbol{\phi}$), the action of G over them is

$$\xi(\boldsymbol{\phi}) \to g\xi(\boldsymbol{\phi}) = \xi(\boldsymbol{\phi}')h(g, \boldsymbol{\phi}), \tag{12}$$

hence, in general, one needs a compensating transformation by $h^\dagger(g, \boldsymbol{\phi})$ to get back to the chosen coset representative after acting with any group element.

In the case of chiral symmetry of N_f flavors, the SSB pattern is

$$SU(N_f)_L \times SU(N_f)_R \longrightarrow SU(N_f)_{L+R} \tag{13}$$

so that under a gauge transformation by $g \equiv (g_L, g_R)$, each coset representative $(\xi_L(\boldsymbol{\phi}), \xi_R(\boldsymbol{\phi}))$ will transform as

$$(\xi_L, \xi_R) \mapsto (g_L \xi_L, g_R \xi_R) h^\dagger_{R+L}(g, \boldsymbol{\phi}). \tag{14}$$

One can take advantage of the fact that the compensating transformation is the same in both right and left coset representatives to define the following parametrization,

$$U[\boldsymbol{\phi}(x)] = \xi_R \xi_L^\dagger = \exp(i\phi^a(x) T^a) \tag{15}$$

where we have choosen the representative such that $\xi_R = \xi_L^\dagger = u = \exp(i\phi^a(x)T^a/2)$, and T_a represents the generators of the broken subgroup. With this parametrization, chiral symmetry transformations act linearly on the chiral field: $U \xrightarrow{G} g_R U g_L^\dagger$, but nonlinearly on the mesonic fields ϕ_a, $a = 1, \cdots N = N_f^2 - 1$.

Although the construction of an EFT for the mesonic fields as Goldstone bosons of chiral symmetry can be systematically addressed, the inclusion of higher energy states such as baryons is a more difficult task, as they are genuinely non-perturbative states. Indeed, in the chiral limit, one should naively expect that the absence of a mass scale in the Lagrangian implies that all states should be massless. However, the spontaneous chiral symmetry breaking generates a nonzero quark bilinear vacuum expectation value (vev), which in turn translates into a dynamically generated mass term for baryons of order $\sim$ 1 GeV. Hence, the spontaneous breaking of chiral symmetry, which is a purely dynamical effect induced by the (nonperturbative) strong gluonic interactions, is responsible for the principal mass generation mechanism of baryons. This is the main reason why the computation of baryon properties from the first principles of the full Standard Model is extremely difficult, and only have been possible for the lightest of them through powerful computational techniques such as LATTICE QCD, in which space-time is discretized into a lattice of points, and the equations of QCD are reformulated in terms of these lattice points [Rot12]. See Sec. 17 of [Wor+22] for a technical review, and Sec. 15 of the same reference for a state of the art review of hadron spectroscopy predictions from lattice QCD.

Due to the complicated nature of such calculations, usually phenomenological models are employed to describe baryons and nuclear interactions instead. In some of these models, nucleon fields are explicitly included in the effective lagrangian, describing their (residual) strong interactions with mesons as force carriers, whilst other models describe the baryons and nuclei as topological solitons, i.e. semi-classical, topologically nontrivial extended field configurations. This thesis will be mainly devoted to one of such models, namely, the Skyrme model [Sky61] in which baryons (and heavier nuclei) are understood as topological solitons of a nonlinear field theory of mesons, which corresponds to a chiral EFT for low-energy QCD in the large N_c (Number of colours) expansion [Wit83a]. Before introducing the model in chapter 1, let us briefly review the topological aspects of nonlinear field theories and how the concept of topological solitons emerges from them.

Non-linear field theory, topology and solitons

Consider a nonlinear scalar field theory, in which a scalar field $\boldsymbol{\phi}$ is defined on a $d+1$ dimensional spacetime $\mathcal{M}$ with topology $\mathbb{R} \times X$, X being a smooth Riemannian submanifold

equipped with a metric g, so that we can write the metric of $\mathcal{M}$ as

$$ds^2 = dt^2 - g_{ij}dx^i dx^j. \tag{16}$$

The field $\boldsymbol{\phi} = \boldsymbol{\phi}(t, \mathbf{x})$ takes values in a Riemannian target manifold Y, so that each field configuration can be seen as a map

$$\begin{array}{rcl} \boldsymbol{\phi} : \mathbb{R} \times X & \longrightarrow & Y \\ (t, \mathbf{x}) & \longmapsto & \boldsymbol{\phi}(t, \mathbf{x}), \end{array} \tag{17}$$

In general, one defines a local coordinate system such that $\boldsymbol{\phi}(t, \mathbf{x}) = (\phi_1(t, \mathbf{x}), \cdots, \phi_n(t, \mathbf{x}))$, with $n = \dim Y$. Many important kinds of nonlinear scalar field theories fall within the category of the so-called Nonlinear Sigma Model (NLSM), which is described by an action functional of the form:

$$S[\boldsymbol{\phi}] = \frac{1}{2} \int_{\mathcal{M}} h_{ab}(\boldsymbol{\phi}) \partial_\mu \phi^a(x) \partial^\mu \boldsymbol{\phi}^b(x) \; d^{d+1}x, \tag{18}$$

where h_{ab} is the Riemannian metric of Y, whose components are in general nontrivial functions of the fields and encode the (generically non-polynomial) interactions of these. It transforms as a symmetric 2-tensor on Y, such that the action is invariant under arbitrary reparametrizations $\boldsymbol{\phi} \mapsto \boldsymbol{\phi}'(\boldsymbol{\phi})$ of the fields. Further symmetry properties of the NLSM are related to the isometries of the target manifold Y and hence depend on the specific model. If the target manifold Y turns to be a simple submanifold of a higher dimensonal Euclidean space, the corresponding nonlinear theory can be written as a linear field theory in which the fields are subject to a nonlinear constraint [MS04].

The concept of homotopy

Topology is the branch of mathematics that focuses on identifying which of the properties of spaces are invariant under any continuous transformation, or homeomorphism. Loosely speaking, a manifold is said to be topologically non-trivial when any of such properties is not equivalent to that of the trivial (flat) space of the same dimension. As for a given nonlinear field theory, whether or not the target manifold Y is topologically non-trivial will have direct consequences in the phenomenology and spectrum of allowed states, both in its classical and quantum versions. Indeed, at any given instant of time t_0, the field configuration can be seen as a map

$$\boldsymbol{\phi}(t_0, \mathbf{x}) \equiv \boldsymbol{\phi}_{t_0} : X \longrightarrow Y, \tag{19}$$

and, if $\boldsymbol{\phi}$ is continuous in both space and time, there will be a continuous deformation between the field configuration at t_0 and at any other instant in time, given by the corresponding Hamiltonian evolution. We say that two maps $\boldsymbol{\phi}_{t_0}$ and $\boldsymbol{\phi}_t$ related by a continuous transformation (homotopy) are homotopic, and define the HOMOTOPY CLASS of a map $\boldsymbol{\phi}_t$ as the class of equivalence defined by all mappings that are homotopic to it.

The homotopy class of $\boldsymbol{\phi}_{t_0}$ (as a map between the manifolds X and Y) will be, by definition, unchanged in time. Thus, in general, we may see $\boldsymbol{\phi}_{t_0}$ as an element of the space of continuous maps $\mathrm{Maps}(X \to Y)$, which is generally disconnected, each connected component corresponding to a different homotopy class of maps. In particular, any property that

does not depend on the specific map $\boldsymbol{\phi}_{t_0}$ but only on its homotopy class will be conserved in time. This kind of conserved magnitudes are called TOPOLOGICAL INVARIANTS.

The number of homotopy classes of maps between two manifolds X and Y depends on the topology of the specific manifolds. In the case in which the base manifold is the $n-$dimensional sphere, the number of homotopy classes of mappings from S^n to Y is given by the $n-$th HOMOTOPY GROUP of Y, denoted by $\pi_n(Y)$.

Topological degree

In general, different solitonic configurations corresponding to different topological sectors (i.e. homotopy equivalence classes) will be characterized by the associated topological invariants. In particular, for any two compact, oriented manifolds X, Y of the same dimension, $\dim Y = \dim X = d$, the TOPOLOGICAL DEGREE (or Brouwer degree) of a differentiable map $\Psi : X \mapsto Y$ is defined as

$$\deg \Psi = \frac{1}{\mathrm{Vol}(Y)} \int_X \Psi^*(\Omega) \in \mathbb{N}, \tag{20}$$

where Ω is a volume form on Y, i.e.

$$\int_Y \Omega = \mathrm{Vol}(Y), \tag{21}$$

and its pullback to X by Ψ, $\Psi^*(\Omega)$, defines a volume form on X.

In terms of local coordinates, if $\Omega = \omega(y^\alpha) dy^1 \wedge \cdots \wedge dy^d$ and

$$\begin{array}{rccc} \Psi : & X & \longrightarrow & Y \\ & x^\mu & \longmapsto & \psi^\alpha(x^\mu), \end{array} \tag{22}$$

then

$$\begin{aligned} \Psi^*(\Omega) =& \omega(\psi^\alpha(x)) \frac{\partial \psi^1}{\partial x^{\mu_1}} dx^{\mu_1} \wedge \cdots \wedge \frac{\partial \psi^d}{\partial x^{\mu_d}} dx^{\mu_d} = \omega(\psi^\alpha(x)) \det \frac{\partial \psi^\alpha}{\partial x^\mu} dx^1 \wedge \cdots \wedge dx^d) = \\ =& \omega(\psi^\alpha(x)) \mathcal{J}_\Psi(x) dx^1 \wedge \cdots \wedge dx^d, \end{aligned} \tag{23}$$

where $\mathcal{J}_\Psi(x)$ is the Jacobian of Ψ at x.

The topological degree defined as (20) is independent of the choice of Ω, integer-valued ($\deg \Psi \in \mathbb{Z}$) and invariant under homotopy transformations. This means that its value is the same for any other map $\tilde{\Psi} \in \mathrm{Maps}_{[\Psi]}(X \to Y)$, i.e. in the same homotopy class as Ψ. The independence on the choice of volume form can be seen by taking a different volume form $\tilde{\Omega}$ on Y, with the same normalization as Ω. Since both Ω and Ω are closed $d-$ forms, they may differ only by an exact $d-$form Δ, i.e. $\Omega = \tilde{\Omega} + \Delta$. Therefore, $\Psi^*(\Omega) = \Psi^*(\tilde{\Omega}) + \Psi^*(\Delta)$, but $\Psi^*(\Delta)$ is an exact $d-$form on X, which integrates to zero.

Also, the homotopy invariant property of the topological degree comes from the fact that is an integer, thus it can not change under continuous deformations of Ψ. One can see that $\deg \Psi \in \mathbb{Z}$ by proving the following result:

$$\deg \Psi = \sum_{i=1}^{n} \mathrm{sgn}\left[\mathcal{J}_\Psi(x^{(i)})\right], \tag{24}$$

where $x^{(i)} \in X$ are the pre-images of an arbitrary point of the target manifold $y_0 \in Y$ under Ψ, i.e. $\Psi(x^{(i)}) = y_0$, $i = 1, \cdots, n$. Note that $\deg \Psi$ does not depend on the choice of y_0. To prove this, take a normalized volume form Ω and let us deform it into one concentrated in a small neighborhood of $y_0 \in Y$ (but still normalized), i.e. $\Omega \to \tilde{\Omega} \simeq \delta^{(d)}(y - y_0) dy^1 \wedge \cdots \wedge dy^d$. Therefore, from the properties of the $d-$dimensional delta function:

$$\begin{aligned} \deg \Psi = \int \Psi^*(\tilde{\Omega}) = \int \sum_{i=1}^{n} \frac{\delta^{(d)}(x - x^{(i)})}{|\mathcal{J}_\Psi(x^{(i)})|} \mathcal{J}_\Psi(x^{(i)}) dx^1 \wedge \cdots \wedge dx^d = \\ = \sum_{i=1}^{n} \operatorname{sgn}\left[\mathcal{J}_\Psi(x^{(i)})\right] \int \delta^{(d)}(x - x^{(i)}) dx^1 \wedge \cdots \wedge dx^d = \sum_{i=1}^{n} \operatorname{sgn}\left[\mathcal{J}_\Psi(x^{(i)})\right]. \end{aligned} \tag{25}$$

The topological degree is therefore an integer that represents the number of times the target manifold Y "wraps" around the base manifold X under the mapping of ψ.

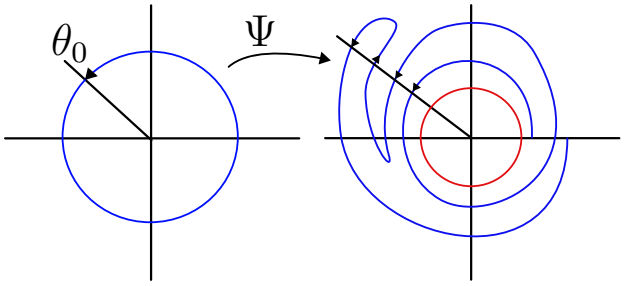

Figure 4: Example of topological degree for a map Ψ between 1-dimensional manifolds (1-spheres), also known as winding number, since it counts the number of times the first circle "winds" into the second due to Ψ.

Topological Solitons

In a nonlinear field theory, a minimal energy configuration (classically stable configuration) in which the energy density is smooth and localized (or concentrated) at some finite region of space is called a SOLITON. These stable field configurations are called TOPOLOGICAL SOLITONS if their stability can be understood by topological arguments (for example, they represent field configurations which are homotopically inequivalent to the vacuum). The existence of different homotopy classes (i.e. a nontrivial homotopy group of the target manifold) is the basis for the stability of topological solitons.

In order to find topological soliton solutions for a given field theory, it is important to investigate whether that particular theory presents the required topological structure. Indeed, let us consider a scalar field theory defined in flat space, namely, $X = \mathbb{R}^d$, with no further boundary conditions imposed. If the theory is linear, any field configuration $\boldsymbol{\phi}(x)$ can be deformed by the homotopy $(1 - \tau)\boldsymbol{\phi}$, with $\tau \in [0, 1]$, so that every configuration is homotopic to the trivial one, $\boldsymbol{\phi} = 0$. Hence, linear fields with no constraints are topologically trivial in flat space. For nonlinear fields, field configurations are mappings from $\mathbb{R}^d$ to Y, and, since $\mathbb{R}^d$ is contractible to a point, the only topological invariant is the component of Y where the field takes its value, i.e. the field configurations are clasified by $\pi_0(Y)$, namely, the connected components of Y.

Hence, it turns out that classical field theories in flat space require both some form of nonlinear interaction and some nontrivial boundary conditions for the field configurations in order to present topological solitons. Note that, while these properties are required, they do not imply at all the existence of (stable) topological solitons in a given theory.

Let us now focus on field configurations with localized, finite energy density, i.e. configurations whose energy density decays rapidly as $|x| \to \infty$. This requirement is equivalent to imposing some boundary conditions on the field configurations, which affect their topological classification. Indeed, consider a multiplet of n scalar fields $\boldsymbol{\phi} = (\phi^1, \cdots, \phi^n)$. For time independent configurations, the total energy will be given by the static energy functional:

$$E[\boldsymbol{\phi}] = \frac{1}{2}\int \left[h_{ab}(\boldsymbol{\phi})\partial_i\phi^a(x)\partial^i\phi^b(x) + V(\boldsymbol{\phi}, \partial_i\boldsymbol{\phi})\right] d^dx \equiv \int \varepsilon(\boldsymbol{\phi})\ d^dx. \tag{26}$$

Assuming that this energy takes its minimum value on a submanifold $V \subset Y$ (the vacuum manifold of the theory), any configuration $\boldsymbol{\phi}_0$ with localized energy density must take values on V at spatial infinity. Also, we assume that $\boldsymbol{\phi}_0$ has FINITE ENERGY, so the field must tend to a constant value $y_0 \in V$ at infinity, independent of direction (to avoid divergent gradient energy).[5] This boundary condition is equivalent to a topological compactification $\mathbb{R}^d \to S^d_\infty$, where $S^d_\infty = \mathbb{R}^d \cup \{\infty\}$ is homeomorphic to the d dimensional sphere. Therefore, these field configurations define maps:

$$\boldsymbol{\phi} : S^d \longrightarrow Y. \tag{27}$$

Thus, the topological character of the configuration $\boldsymbol{\phi}(x)$ is determined by the homotopy class of the map $\boldsymbol{\phi}$, which is an element of the (d)-th homotopy group of the target manifold, $\pi_d(Y)$ [MS04]. Any soliton configuration will be characterized by the topological degree of the corresponding mapping $\boldsymbol{\phi}$. As it is a topological invariant, the topological degree can be associated to a conserved charge of the soliton.

In a chiral effective theory, in which mesons are parametrized as coordinates in the chiral coset space, finite energy solitons in $3+1$ dimensions are allowed, since the third homotopy group of such space is nontrivial:

$$\pi_3\left(\frac{SU(N_f)_L \times SU(N_f)_R}{SU(N_f)_{\text{diag}}}\right) = \pi_3(SU(2)) = \mathbb{Z}. \tag{28}$$

Solitons in these type of theories are usually called SKYRMIONS, after Tony R. Skyrme, who proposed them for the first time as models for baryons even before QCD was developed [Sky61]. Hence, the associated topological charge of a Skyrmion is identified with the baryon number. We will postpone the discussion of the model originally developed by Skyrme, as well as the properties of its solitonic solutions (Skyrmions) to the first section of chapter 1.

In modern theoretical physics, solitonic solutions can be found in a very wide range of different models and theories. The topologically nontrivial, particle-like solutions first discussed by Skyrme aroused general interest on the study of solitonic solutions in other nonlinear models, and in the mid seventies many different solutions were found. 't Hooft

[5] Note that this is not necessary the case in 1+1 dimensional theories, since the spatial infinity consists of two disconnected points

[t H74] and Polyakov [Pol74] discussed magnetic monopoles, Nielsen and Olesen found string-like solutions [NO73], and Zeldovich et al. [ZKO74] studied domain walls.

Even though they are best understood as extended solutions of a classical field theory, after the discovery of INSTANTONS by Polyakov, Belavin et al. [Bel+75] and their implications [t H76] it became clear that extended classical solutions are also important to compute processes in quantum field theory. This idea triggered a very fruitful relation between topology and physics, which led to many important developments in the next decades, such as the discovery of index theorems (and the subsequent geometrical understanding of quantum anomalies [AG85]), or the invention of topological quantum field theory [Wit88].

Subsequently, many researchers found applications of topological solitons in other areas of physics. In the context of cosmology, the possibility of formation of different TOPOLOGICAL DEFECTS such as cosmic strings, monopoles or domain walls after a symmetry-breaking phase transition from theories of grand unification in the early universe was proposed by Kibble [Kib76]. The formation of such defects was found to yield specific imprints in the cosmic microwave background radiation during subsequent years. Although most of these models were eventually ruled out by observations in favor of inflationary models as candidates to explain the formation of structures in the universe, others, such as cosmic strings are still interesting [JBR23]. Moreover, a cosmological network of cosmic strings sources a background of Gravitational Waves (GW) in a very wide range of frequencies, which could be observed in the near future with Earth and space-based gravitational wave interferometers [BOS18; Auc+23].

On the other hand, topological solitons are ubiquitous in condensed matter physics. Some examples are vortices in superconductors [Abr57], two-dimensional skyrmion-like defects [Müh+09] and domain walls in magnetic materials [Hub75], and ferroelectrics [TCA01; Nah+15]. Indeed, topology plays an essential role in current condensed matter research, with the study of TOPOLOGICALLY ORDERED states [Wen90], characterized by the existence of topologically-protected, gapless surface states, and their classification in terms of the symmetries of the associated Hamiltonian [Chi+16]. Examples of such states are the fractional quantum Hall states [Wen93] and other strongly correlated quantum liquid states, as well as topological insulators or superconductors [Sch+08].

Nuclear matter and Neutron stars

The phases of QCD matter

The terms QCD matter or strong-interaction matter are used to broadly refer to matter governed by QCD in its various forms. In spite of the apparent simplicity of the QCD Lagrangian (8), the theory of strong interactions presents a very rich phase structure at finite temperatures and densities, with a plethora of phase transitions often characterized by the breaking (or restoration) of some symmetry.

Due to quark confinement, at low energies strongly interacting matter appears only in the form of colorless states, i.e. hadrons and their bound states, the nucleons and nuclei. However, the asympotic freedom of QCD allows for a different phase of matter, with quasi-free quarks and gluons, at sufficiently high energies (or, equivalently, temperatures). This new phase of strongly interacting matter is called the Quark Gluon Plasma (QGP)

[Shu09], and can be experimentally probed in heavy ion collision experiments, produced in research facilities such as LHC at CERN, and the Relativistic Heavy Ion Collider (RHIC) at Brookhaven National Laboratory (BNL) [Gyu04; KMR17]. These experiments allowed to create and study the properties of QGP, which can be described as a nearly perfect fluid made of quarks and gluons that, however, remains strongly coupled. These experiments are able to generate conditions as they are expected to have been present in our universe microseconds after the Big Bang, hence are relevant to cosmology. A profound study of this phase of QCD matter is, however, very complicated in this kind of experiments, since the QGP that is formed during the collission of heavy ions is far from equilibrium, and only survives for a very short time. Therefore, much of our present-day knowledge about hot QCD matter at vanishing baryon chemical potential is obtained from lattice QCD studies. The transition from the hadronic (confined) phase to the QGP is called the DECONFINEMENT transition, which is actually believed to be a crossover between the two phases at a temperature at which the mean scale of momentum transfer is of order of the characteristic QCD scale $\Lambda_{QCD} \sim 200\,\mathrm{MeV}$, i.e. $T \sim 10^{12}\,\mathrm{K}$. When strong-interaction matter becomes deconfined, quark and gluons are not bounded to form colorless states anymore, and the chiral condensate "melts", resulting in the restoration of the spontaneously-broken chiral symmetry, which is often called CHIRAL TRANSITION.

On the other hand, it is expected that deconfinement (and chiral symmetry restoration) could also happen for much smaller temperatures, but sufficiently high densities. Indeed, at asymptotically large densities, the strong interaction becomes sufficiently weak due to asymptotic freedom, and one can study QCD at finite density perturbatively. In this case, calculations have shown that the ground state of quarks at sufficiently small temperature presents a *Cooper pair instability*, i.e. a condensate of quark pairs will become the ground state. Since a pair of quarks cannot form a color singlet, the condensation of quark pairs spontaneously breaks the local $SU(3)_C$ color gauge invariance, in the same fashion as how the gauge symmetry associated to electromagnetism is broken in standard superconductivity, producing a sort of "Meissner effect" for gluons. Such a new phase of QCD matter is called COLOR-SUPERCONDUCTING PHASE [Alf+08]. Moreover, the quarks forming a Cooper pair condensate in a color-superconducting phase, as opposed to electrons, possess color, flavor and spin degrees of freedom. As a consequence, there will be various configurations in which two qarks can pair, resulting into different color-superconducting phases, associated to the different color/flavor/spin index structure of the corresponding Cooper pairs [RW00].

At lower baryon densities, up to approximately twice the NUCLEAR SATURATION (baryon number) density $n_0 \approx 0.16\,\mathrm{fm}^{-3}$ (or equivalently the saturation mass density $\rho_0 \approx 2.7 \times 10^{14}\mathrm{g/cm}^3$), strong-interaction matter in the hadronic phase can be very successfully described by perturbative methods in the framework of chiral effective field theory. Beyond these baryon densities, however, the exploration of the QCD phase diagram becomes very challenging and our knowledge about this region is rather especulative. The main reason is that current collider experiments cannot probe such high densities, and lattice simulations become limited by the so-called *sign problem* [Goy+17]. In lattice QCD simulations, Monte Carlo methods are typically used to sample the space of possible configurations of the system. The sign problem arises when simulating systems at finite density, where the partition function of the system becomes complex due to the presence of a non-zero chemical potential. This leads to an oscillatory sign in the in-

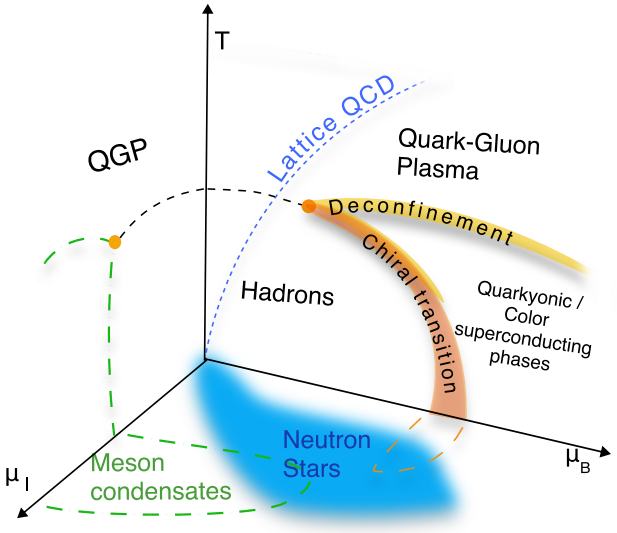

Figure 5: Schematic nuclear matter phase diagram

tegrand, making the Monte Carlo sampling difficult. This problem makes it extremely challenging or even impossible to obtain accurate results from lattice QCD simulations at sufficiently high densities, and we must resort to other theoretical approaches, the most common ones being those based either on perturbative methods for chiral effective field theories [DHW21], relativistic mean field theories (such as quantum hadro-dynamics [SW97]), many-body quantum montecarlo simulations [Car+15; Tew+16], or holographic methods [Jär22; Hoy+16].

The discussion above suggests that there are two fundamental parameters which describe the phase diagram of pure QCD matter at equilibrium: the temperature T and the baryon number density n_B (or, equivalently, the associated chemical potential μ_B). However, this is not the full picture, since a realistic description of matter should include the rest of interactions in the SM, ie. the electroweak sector. Therefore, realistic nuclear matter at equilibium is not only in thermodynamical, but also in chemical (electroweak) equilibrium. Hence, it is the equilibrium under weak processes (such as β decay or electron capture) which precisely dictates the amount of particles of each nature at each point in the $T - \mu_B$ plane. As these processes do not preserve flavor quantum numbers, the QCD phase diagram should be extended by including each of the different chemical potentials associated to each quark flavor. In practice, it is enough to consider the ISOSPIN CHEMICAL POTENTIAL, μ_I, which is related to the difference in number densities between protons and neutrons (or, more generally, u and d quarks). Thus, a complete phase diagram of nuclear matter at equilibrium sould be thought of as a two-dimensional surface embedded into a three-dimensional space labelled by T, μ_B and μ_I[6]. A sketch based on our current knowledge of such space is presented in fig. 5. In the region in which the isospin chemical potential dominates over the other two parameters, additional, exotic phases of matter have been proposed in which electrically charged mesons may conden-

[6]We leave out other parameters that are also relevant to the physics of neutron stars, such as the external magnetic field. QCD matter in the presence of a magnetic field does also present interesting phenomenology, such as the chiral soliton lattice [SS08].

sate in a spontaneous symmetry breaking scenario [KT01; Man19], in order to relieve the neutron degeneracy pressure. While the study of QCD matter at extreme temperatures is crucial to understand the conditions of matter in the early universe, matter at ultra-high densities (of up to several times that of nuclei) only occurs in the cores of extremely compact stars, the NEUTRON STARS.

Neutron stars

The concept of a Neutron Star (NS) i.e. a stellar object made only by ultra-degenerate neutrons, was proposed by Baade and Zwicky shortly after the neutron was discovered by Chadwick. (Although L. D. Landau proposed the idea of a stellar object with nuclear density even before the neutron was discovered). However, they remained as a theoretical object for almost 30 years, until Hewish, Bell et al. [Hew+68] first identified a NS as a radio PULSAR (pulsating star) in 1967. Since then, around two thousand other neutron stars have been identified, either isolated or in a binary system, the latter usually in the form of an *x-ray pulsar*. The estimated total number of neutron stars in our galaxy is of the order of 10^8 [RDH21].

NS are the final product of the gravitational collapse of progenitor stars with masses $8 \lesssim M/M_\odot \lesssim 12$. Lighter stars result in the formation of *white dwarfs*, while with increasing mass the formation of black holes becomes increasingly likely. Neutron stars are the remnants of core-collapse SUPERNOVA (type II) explosions: At the end of a massive star's life, the "nuclear fuel" is used up until it cannot sustain the gravitational pressure anymore, leading to a gravitational collapse of the core, which generates an outward travelling shock wave [Bet90]. This supernova explosion expels the outer layers into space and leaves behind a proto-neutron star. The proto-neutron star is initially hot with temperatures up to 10 MeV, and radii of more than 20 km. Within the first seconds of its generation, the star cools down by neutrino emission , and electron-capture processes (inverse beta decay) due to the high degeneracy of electrons lower the proton-neutron ratio [Pon+99]. During this process, the star shrinks to its final size, until beta equilibrium is reached. After a timescale of 100 s, the neutron star is cooled to temperatures much smaller than the associated Fermi temperature of the degenerate matter it contains, so temperature effects are not relevant for the description of neutron stars.

As the core of the star collapses, its rotation rate increases due to conservation of angular momentum. Therefore, newly formed NS can reach extreme spinning rates, and rotate at up to several hundred times per second. Some neutron stars emit beams of electromagnetic radiation that make them detectable as pulsars. Their magnetic fields are between 10^8 and 10^{15} times stronger than Earth's magnetic field [PMG09].

Apart from their extreme magnetic fields and rotation frequencies, NS are the densest objects in our universe, surpassed only by black holes. The typical radii of such objects are in the range $10 - 14$ km, while the typical masses are of the order of our Suns mass, i.e., $M \sim 1.4 M_\odot$. This can give an idea of the mean density of these stars, which can reach more than five times that of nuclear saturation. A NS is bound by gravitation, while the neutron degeneracy pressure as well as repulsive forces from nuclear interactions, i.e., strong interactions, stabilize the star and prevent it from contracting further. The requirement of local charge neutrality and β-decay equilibrium implies that the star is composed of mostly neutron-rich nuclear matter with only a small fraction of protons and electrons, i.e. matter inside a NS presents a high isospin asymmetry.

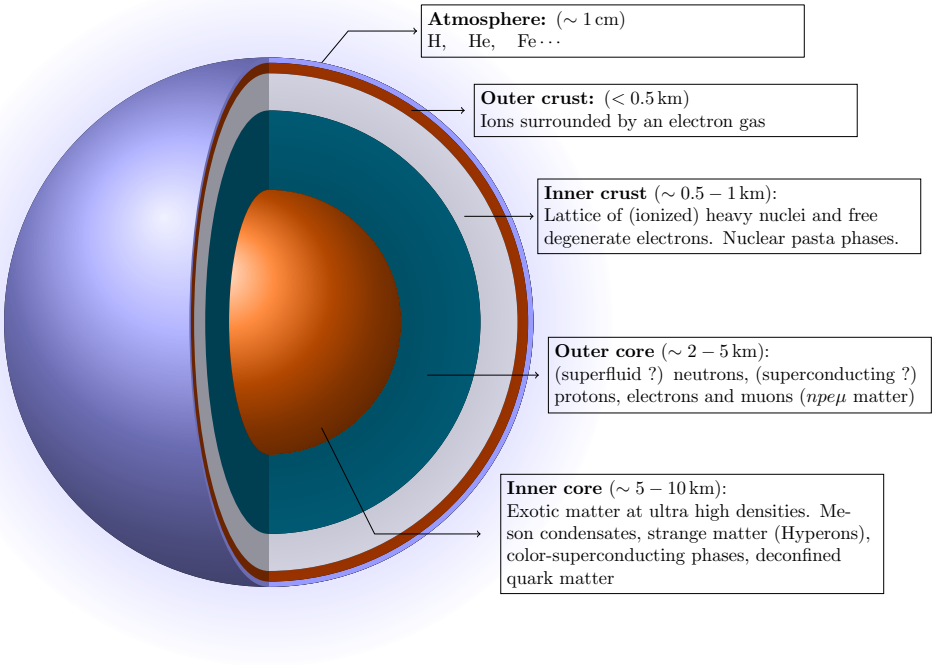

Figure 6: The general structure of a Neutron Star

Therefore, the relevant region of the QCD phase diagram for NS is precisely that of (almost) zero T, but high μ_B and μ_I (see fig. 5), what makes these objects one of our most valuable sources of information for determining nuclear properties in this region.

The internal structure of the NS can be described in terms of layers. The outermost layer consists of nuclei forming a lattice, thus giving rise to a solid crust with a thickness of 0.5 km [CH08]. The nuclei are surrounded by a degenerate electron gas and become increasingly more neutron-rich deeper into the crust because of the increasing density. A liquid of free neutrons starts to form in the inner part of the crust. Eventually, the lattice composed of nuclei vanishes and the nuclei disintegrate into homogeneous neutron-rich matter, marking the beginning of the outer core consisting of superfluid neutrons and of a small fraction of superconducting protons. The central densities in the inner region of the core are conjectured to be from several up to ten times the nuclear saturation density. Such high densities might give rise to strong-interaction matter in various forms, and novel phases of dense baryonic matter are expected to occur in the inner core of NS, containing additional particle species such as Δ isobar resonances [Gle85; DLP14; Dra+14; Cai+15; LSW18], hyperons [Gle85], or pion or kaon condensates [HSS75; CNS77; KN88; GS99; PBG00]. However, as argued, the precise phase structure of cold, strongly interacting matter at both finite baryon and isospin chemical potential is still very speculative, and there have been theoretical proposals of even more exotic scenarios, where a transition to deconfined, color superconducting quark matter takes place inside the core [HPS93; BL99; Ann+20], or a new state of matter in which both hadronic and quark degrees of freedom coexist, the so-called quarkionic matter [MP07; MR19]. Studies of the dynamical features of compact stars, such as the occurrence of phase transitions during mergers or the cooling rate of proto-neutron stars may produce complementary data, as they may

strongly depend on the specific microscopic degrees of freedom as well as on the EOS.

Therefore, one of the principal challenges of current astrophysical research is to obtain information about the EOS of ultra-dense matter from neutron star observations. In particular, apart from their masses and radii, other interesting observable properties of NS are their quadrupole moments, spin angular velocity (angular momentum), and deformability against tidal forces—which is encoded in the so-called Love numbers [Hin08; PPL10]. All these properties can be constrained by their imprints into the waveform of a gravitational wave signal emitted by an inspiraling binary neutron star system. Indeed, binary NS systems are one of the most promising sources of GW within the detection range for already-operating second generation observatories, such as Advanced LIGO [Aas+15], Advanced VIRGO [HH18; Abb+18], or KAGRA [Aku+19], and future third generation ones such as the Einstein Telescope [Mag+20], the Cosmic Explorer [Rei+19] or LISA [Ama+17]. The observation of GW emitted during the coalescence of the stars in such systems—especially in the last part of the merging, in which the stars are subject to large tidal deformations due to the extremely strong gravitational fields involved—will shed light onto the Equation of State EOS of matter at very high densities, well beyond the nuclear saturation point. A particularly interesting property of compact stars is the apparently universal relation between the moment of inertia, the Love numbers and the quadrupole moment (I-Love-Q relations) of such stars. These I-Love-Q relations, firstly proposed by K. Yagi and N. Yunes in [YY13b], when applied to NS, allow to break the degeneracy between the quadrupole moment and the NS spins in the gravitational waveforms of inspiraling NS binaries. Therefore, a much more precise determination of the (dimensionless) averaged spin can be reached in such measurements [YY13a].

Part I

The Physics of Light Nuclei

CHAPTER 1

Light nuclei as topological solitons

Articles partially reproduced in this chapter: [GHH23; Gar22]. See *permissions*.

> *"It seems this whole subject is a monument of austere beauty... covered with minus signs, like bird droppings"*
>
> – John Baez, *on Classical Mechanics*

1.1 The Skyrme model and its generalizations

The Skyrme model [Sky61] is a phenomenological, effective-field-theoretic model of interacting Goldstone bosons originally proposed to describe strongly interacting matter in a low energy regime. In this model, the fundamental degrees of freedom are a set of four scalar fields subject to a constraint, which are more conveniently parametrized in terms of an $SU(2)$-valued field. The resulting three degrees of freedom can be identified with the pions in a nonlinearly-realized chiral effective theory, much like other EFT-based approaches to low-energy QCD, such as chiral perturbation theory. Moreover, baryons, nucleons and nuclei, whose existence can not be inferred from QCD directly by perturbative methods, naturally appear within the Skyrme model as (topological) solitonic configurations of the underlying bosonic degrees of freedom, and whose existence is allowed by the topological properties of the $SU(2)$ group manifold, as explained in the introduction.

Although it was first proposed by Tony H. Skyrme in the sixties, it did not cause much interest, as other alternative explanations for the structure of baryons in terms of constituent particles (quarks) were also developed at the same time, which in turn led to the establishment of the current fundamental theory of strong interactions, QCD. However, twenty years later, it was shown by E. Witten that Skyrmions could be interpreted as a description of baryons in the large N_c limit of QCD. Such observation triggered a period of extraordinarily high activity during the next couple of decades, in which many properties of nucleons [ANW83b] and nuclei [BC86; WSH86; Bat+09; LM14; HKM17; NS18a; BH18] were reproduced using this model, tipically within a 30% accuracy. Furthermore, different generalizations of the original model proposed by Skyrme have been also proposed, in order to reduce the typically quite large binding energies of Skyrmions, which translates into unphysically large binding energies of atomic nuclei. The first addition was the pion mass term, which explicitly breaks chiral symmetry to its diagonal subgroup. Further generalizations include the addition of new, physically motivated terms, e.g., the so-called sextic term [Jac+85; ASW10a], generalized potentials [GHS15; Gud16] or new degrees of freedom, e.g., vector mesons [NS18a; Mei+86; MZ86; Mar91; ASW10a; Sut10]

In the last years, there has been significant progress in the application of the Skyrme model to the description of atomic nuclei. The first source of this development is the use of the vibrational quantization. Here the Hilbert state is built not only on the zero modes, as in the standard rigid rotor quantization [ANW83a], but also the lightest massive deformations are take into account. This approach elevated the Skyrme model to a quantitative tool for the understanding of excitation bands of light nuclei [Bat+09; LM14; HKM17; Man22]. In addition, it has very recently been shown how the spin-orbit interaction leading to a phenomenologically consistent nucleon-nucleon force emerges in the Skyrme model [HH20]. These results have contributed to establish the Skyrme model approach as a well-motivated proposal for the description of nuclear matter.

The Generalized Skyrme Model (GSM) that we will consider is given by the following Lagrangian density,

$$\begin{aligned} \mathscr{L}_{\mathrm{SK}} = \quad \mathscr{L}_2 + \mathscr{L}_4 + \mathscr{L}_6 + \mathscr{L}_0 = \\ = -\frac{f_\pi^2}{16}\,\mathrm{Tr}\{L_\mu L^\mu\} + \frac{1}{32e^2}\,\mathrm{Tr}\{[L_\mu, L_\nu]^2\} - \lambda^2\pi^4 B_\mu B^\mu + \frac{m_\pi^2 f_\pi^2}{8}\,\mathrm{Tr}\{U - \mathbf{1}\}, \end{aligned} \tag{1.1}$$

where $U \in SU(2)$ contains the fundamental mesonic degrees of freedom, parametrized as the coordinates of the $SU(2)$ group element

$$U = \sigma\mathbf{1} + i\pi_a\tau_a \equiv i\phi^\alpha\bar{\tau}_\alpha, \quad \phi^\alpha = (\sigma, \boldsymbol{\pi}), \quad \bar{\tau}_\alpha = (-i\mathbf{1}, \boldsymbol{\tau}), \tag{1.2}$$

with τ^a $(a = 1, 2, 3)$ being the Pauli matrices. $L_\mu = U^\dagger\partial_\mu U$ are the components of the associated left-invariant Maurer-Cartan form, $\mathbf{1}$ is the 2×2 identity matrix, and B^μ is the topological current,

$$B^\mu = \frac{\epsilon^{\mu\nu\rho\sigma}}{24\pi^2}\,\mathrm{Tr}\{L_\nu L_\rho L_\sigma\}. \tag{1.3}$$

Note that $B^0 d^3x$ is a three-form proportional to the pull-back (under the map (1.2)) of the volume form on the target space S^3, i.e.

$$B^0 d^3x = \frac{1}{2\pi^2} U^*(d\Omega_3), \tag{1.4}$$

so that, by the definition of the topological degree of a map [MS04], the integral

$$B = \int B^0 d^3x = \frac{1}{24\pi^2}\int \varepsilon^{ijk}\,\mathrm{Tr}\{L_i L_l L_k\} d^3x. \tag{1.5}$$

will be integer-valued. The Skyrme model thus presents topological solitons (Skyrmions), whose topological charge (1.5) is identified with the baryon number.

Although only the first two terms (namely, the quadratic and quartic terms in L_μ) in (1.1) were originally considered by Skyrme [Sky61], the other two terms have been subsequently included in order to achieve a better agreement with nuclear phenomenology. Indeed, the potential term explicitly breaks chiral symmetry and provides a mass term for the pions. On the other hand, the sextic term in L_μ, first proposed in [Jac+85] (see also [AN84]), can be seen as an effective point-like interaction that describes the repulsive exchange of omega vector mesons, which becomes relevant at sufficiently high densities. Such a term has recently proven to be crucial for an accurate description of the high density equation of state of neutron stars, allowing to reach sufficiently high maximum masses and sound velocities above the conformal limit [Ada+20; Ada+23].

Obtaining classical Skyrmions

As occurs with most nonlinear field theories in three dimensions, analytical expressions for the topologically nontrivial solutions to the equations of motion of the Skyrme model have not been found, and even for the simplest case one needs to resort to numerical methods. In this thesis, we will be interested in obtaining static solutions of the Skyrme field, and for numerical purposes we adopt the usual Skyrme units of energy and length,

$$E_s = \frac{3\pi^2 f_\pi}{e}, \quad x_s = \frac{1}{f_\pi e}, \tag{1.6}$$

unless otherwise specified. The static energy functional in these units becomes

$$\begin{aligned} 24\pi^2 E &= \int d^3x \left[-\frac{1}{2}\,\mathrm{Tr}\left\{L_i^2\right\} - \frac{1}{4}\,\mathrm{Tr}\left\{[L_i, L_j]^2\right\} + 8\lambda^2\pi^4 f_\pi^2 e^4 (B^0)^2 + \left(\frac{m_\pi}{f_\pi e}\right)^2 \mathrm{Tr}\{\mathbf{1} - U\}\right] \\ &= \int d^3x \left[(\partial_i\phi_\alpha)^2 + (\partial_i\phi_\alpha\partial_j\phi_\beta - \partial_i\phi_\beta\partial_j\phi_\alpha)^2 + c_6\left(\epsilon_{\alpha\beta\gamma\delta}\phi_\alpha\partial_1\phi_\beta\partial_2\phi_\gamma\partial_3\phi_\delta\right)^2 + c_0(1-\sigma)\right], \end{aligned} \tag{1.7}$$

where $\epsilon_{\alpha\beta\gamma\delta}$ is the totally antisymmetric Levi-Civita tensor with $\epsilon_{0123} = 1$ and we have defined $c_6 = 2\lambda^2 f_\pi^2 e^4$ and $c_0 = 2m_\pi^2/(f_\pi e)^2$.

Thus, (static) classical solutions minimize the functional (1.7), subject to the vacuum boundary conditions. To compute such solutions numerically, one starts with an *ansatz* for the fields that belongs to the same homotopy class of the wanted solution, and then applies a gradient-descent-based algorithm (see appendix A), which smoothly transforms the ansatz into the true solution. It is well known that the field configuration space of the Skyrme model presents local minima and becomes very complicated in the large baryon charge sectors, so the choice of a good initial ansatz is crucial in order to achieve the convergence to the wanted, global minimum on each topological sector. As usual, symmetry arguments can be a good guiding principle to find acceptable ansatze at a given topological sector.

The full symmetry group of the massless Skyrme Lagrangian is given by the direct product of the Poincaré and chiral groups. However, we are interested in solutions that minimize the energy functional (measured on a given reference frame). The internal symmetry group of such functional is the same as the Lagrangian, but the Poincaré symmetry is broken to the Euclidean subgroup corresponding to spatial rotations and translations, $E_3 = SO(3) \times \mathbb{R}^3$. Thus, the symmetry group of the energy functional is

$$\widetilde{G} = E_3 \times SU(2)_L \times SU(2)_R \simeq E_3 \times SO(4)_{chiral}. \tag{1.8}$$

The action of an element of such group on the Skyrme field is given by

$$U(\mathbf{x}) \to g_L U(R_S \cdot \mathbf{x} + \mathbf{a}) g_R^\dagger \tag{1.9}$$

where $\mathbf{a} \in \mathbb{R}^3$, $R_S \in SO(3)$ represents the spatial rotations and $g_{L/R} \in SU(2)_{L/R}$ are the left and right-handed chiral transformations, respectively.

Moreover, the presence of nontrivial boundary conditions imposed on the relevant field configurations may further reduce their symmetry. Indeed, in the case of finite energy

field configurations a boundary condition of the form $U(\mathbf{x}) \xrightarrow{|\mathbf{x}|\to\infty} \mathbf{1}$ must be imposed (i.e. the Skyrme field must decay to its vacuum value far from the center of the soliton). Such boundary condition not only allows us to classify the field configurations into different topological sectors labeled by their homotopy class within the third homotopy group of the target space $\pi_3(SU(2)) = \mathbb{Z}$, but also reduces the symmetry of such configurations since the vacuum is only preserved under the subgroup $G = E_3 \times \mathrm{diag}[\mathrm{SU(2)_L} \times \mathrm{SU(2)_R}] \simeq \mathrm{E_3} \times \mathrm{SU(2)_I}$, i.e. transformations of the form (1.9) with $g_L = g_R = g \in SU(2)_I$. The remaining internal symmetry group is called the ISOSPIN GROUP, since it corresponds to the isospin degrees of freedom when the solitons (Skyrmions) are identified with baryons and nucleons of low-energy QCD and nuclear physics.

A further reduction of the symmetry group G may occur on individual configurations minimizing the energy functional for each topological sector. For instance, the $B = 1$ Skyrmion does present the full group G as a symmetry of its energy density isosurfaces, whereas the spatial rotations are broken to $O(2) = SO(2) \times \mathbb{Z}_2$ for the $B = 2$ Skyrmion, which presents a toroidal shape. As B increases, the symmetry of the configurations minimizing the static energy becomes more complicated, and for $B \geq 3$ it is given by a point group, the $B = 3$ Skyrmion presenting tetrahedral symmetry, the $B = 4$ cubic symmetry and so on.

It is clear then that a good initial ansatz will present the same point symmetry than the true solution. By examining the symmetries of low baryon charge Skyrmions, and their symmilarity to monopole solutions, Houghton, Manton and Sutcliffe proposed the RATIONAL MAP approximation, [HMS98], in which the angular profile of a $B = N$ Skyrmion configuration is described in terms of a map between 2-spheres,

$$R(z) = \frac{p(z)}{q(z)}, \tag{1.10}$$

with z the coordinate of the Riemann sphere, and $p(z), q(z)$ two polynomials, at least one of them of degree N (the other can be of lower degree). A given rational map of degree N defines then a Skyrmion field of the same degree via

$$U(\mathbf{x}) \equiv U(r, z) = \exp[if(r)\mathbf{n}(R(z)) \cdot \boldsymbol{\tau}], \tag{1.11}$$

where

$$\mathbf{n}(R(z)) = \frac{1}{1 + |R|^2}(2\,\mathrm{Re}(R), 2\,\mathrm{Im}(R), 1 - |R|^2) \tag{1.12}$$

is the unit vector obtained via the stereographic projection of the image of the Riemann sphere under the rational map R, and $f(r)$ is just a radial profile that can be obtained by minimizing the corresponding one-dimensional problem.

The rational map idea makes it easier to construct a numerical ansatz in a given topological sector and with a given point symmetry. In our computations, we construct a numerical ansatz based on the rational maps proposed in [MMW07] for each topological sector up to $B = 8$, and allow this initial configuration to relax to the true minimizer via the accelerated gradient descent algorithm described in appendix A. We remark that this is an increasingly difficult task for values of the topological charge $B \gtrsim 8$, not only due to the increase of the solution's mean radius, which requires a numerical simulation on a lattice with an increasing number of points, but also because of the flatness of the field

configuration landscape, which in general presents multiple local minima with very similar energies but different symmetries and shapes, as recently shown by Gudnason and Halcrow [GH22]. This fact points towards the failure of the rigid quantization approximation—in which quantum effects do not modify the classical shape of the Skyrmions—for higher baryon charges in general. We have, nevertheless, constructed also solutions with large baryon charge and cubic symmetry, namely, the $B = 32 = 4 \times 2^3$ and $B = 108 = 4 \times 3^3$ Skyrmions, which are expected to not be affected by spin nor isospin quantum effects in their ground state, and are considered to be the minimum energy configurations due to their high degree of symmetry. These solutions are illustrated in fig. 1.1a ($1 \leq B \leq 8$) and fig. 1.1 ($B = 32, 108$) where energy density iso-surfaces are plotted. For $B = 8$, we consider two energy-degenerate solutions[2] with different symmetries.

1.2 Skyrmion quantization and light nuclei spectra

Nucleons and nuclei are described within the Skyrme model as classical solitonic configurations through the identification of the Skyrmion topological charge and the baryon number of nuclear states. However, other quantum numbers such as the spin and isospin of quantum nuclear states are not described at the classical level. Hence, a quantization of the Skyrmion field is needed in order to take into account the relevant quantum numbers. This is done in the semi-classical approach by promoting the zero modes of the soliton to dynamical degrees of freedom.

To do so, we introduce the rotational and iso-rotational degrees of freedom through a pair of time-dependent $SU(2)$ transformations of the classical (static) solitonic solution, representing the iso-rotation and the spatial rotation zero modes, respectively, as well as a time dependent vector $\mathbf{X}(t)$ representing the translational zero modes (1.9):

$$U(t, \boldsymbol{x}) = A(t)U_0(R_B(t)(\boldsymbol{x} - \boldsymbol{X}(t)))A^\dagger(t), \tag{1.13}$$

where $R_B^{ij} = \frac{1}{2}\operatorname{Tr}\{\tau^i B \tau^j B^\dagger\} \in SO(3)$ is the corresponding rotation matrix in space. $A(t), B(t) \in SU(2)$ and $\boldsymbol{X}(t)$ together form the COLLECTIVE COORDINATES of the soliton.[3] The semi-classical quantization of the Skyrmion then consists of substituting (1.13) into the Skyrme Lagrangian (1.1), which yields the Lagrangian of an effective dynamical system in terms of the collective coordinates $\{A(t), B(t), \boldsymbol{X}(t)\}$, and quantizing such a system via standard canonical methods. Performing this substitution yields

$$L_{\text{col}} = \int d^3x \mathcal{L}_{\text{SK}} = -\mathcal{M} + \frac{1}{2}\mathcal{M}\dot{X}_i\dot{X}_i + \frac{1}{2}a_i U_{ij} a_j - a_i W_{ij} b_j + \frac{1}{2}b_i V_{ij} b_j, \tag{1.14}$$

where

$$a_j = -i \operatorname{Tr} \tau_j A^{-1}\dot{A}, \quad b_j = i \operatorname{Tr} \tau_j \dot{B} B^{-1},$$

[2] The difference in energies of both solutions is less than 1%. The precise number (and even its sign) will depend on the parameter values.

[3] For spherically symmetric solutions, rotation in coordinate space can be undone by that in isospin space, and one can devise a simpler quantization procedure without introducing the matrix $B(t)$ [ANW83b]. The present treatment is more general and can be used also for non-spherical solutions that we shall be mainly interested in.

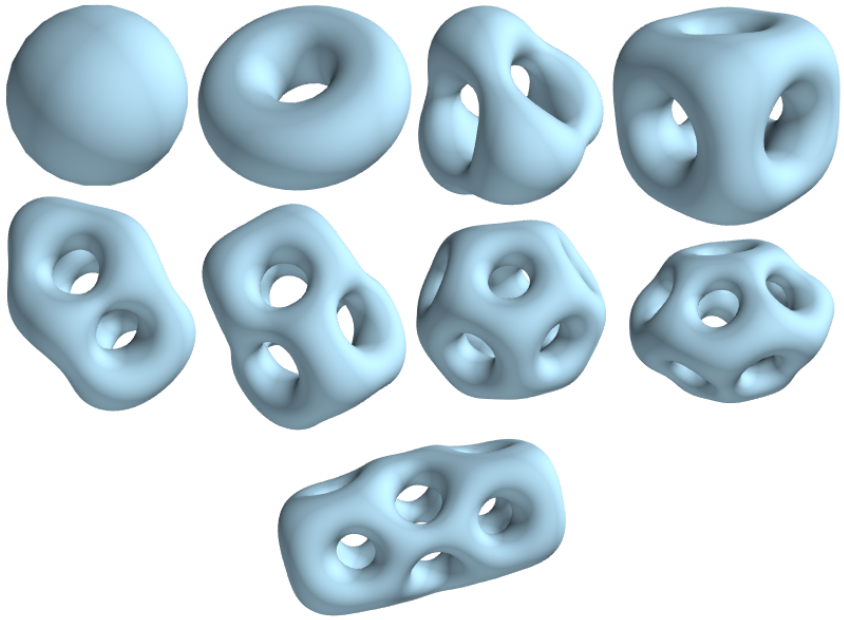

(a) Skyrmions with baryon number from 1 to 8, including the two energy-degenerate solutions with different symmetries, 8*a* (second row) and 8*b* (third row).

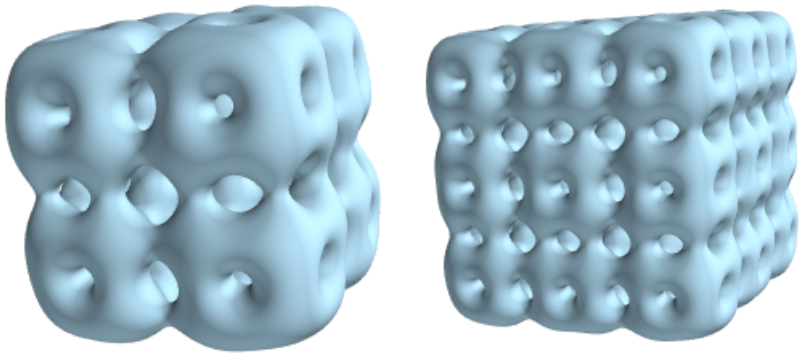

(b) The $B = 32$ and $B = 108$ Skyrmions. They present a manifest cubic symmetry, as they can be thought of being composed of individual $B = 4$ "bricks".

Figure 1.1: Energy density iso-surfaces of the classical Skyrmion configurations used in this chapter. The surfaces are not to scale, as the relative size grows with the total baryon charge.

are the angular velocities in isospace and physical space, respectively. We have also introduced the corresponding inertia tensors

$$U_{ij} = \frac{1}{24\pi^2}\int d^3x\Big[-\mathrm{Tr}\big\{T_i^- T_j^-\big\} - \mathrm{Tr}\big\{\big[T_i^-, L_k\big]\,\big[T_j^-, L_k\big]\big\} + \\ + \frac{c_6}{16}\,\mathrm{Tr}\big\{T_i^-[L_a, L_b]\big\}\,\mathrm{Tr}\big\{T_j^-[L_a, L_b]\big\}\Big], \tag{1.15}$$

$$V_{ij} = \frac{1}{24\pi^2}\int d^3x\,\epsilon_{ilm}\epsilon_{jnp}x_l x_n\Big[-\mathrm{Tr}\{L_p L_m\} - \mathrm{Tr}\{[L_p, L_k]\,[L_m, L_k]\} + \\ + \frac{c_6}{16}\,\mathrm{Tr}\{L_p[L_a, L_b]\}\,\mathrm{Tr}\{L_m[L_a, L_b]\}\Big], \tag{1.16}$$

$$W_{ij} = \frac{1}{24\pi^2}\int d^3x\,\epsilon_{jlm}x_l\Big[\mathrm{Tr}\big\{T_i^- L_m\big\} + \mathrm{Tr}\big\{\big[T_i^-, L_k\big]\,[L_m, L_k]\big\} - \\ - \frac{c_6}{16}\,\mathrm{Tr}\big\{T_i^-[L_a, L_b]\big\}\,\mathrm{Tr}\big\{L_m[L_a, L_b]\big\}\Big], \tag{1.17}$$

given in terms of the $\mathfrak{su}(2)$-valued currents

$$L_k = U_0^\dagger \partial_k U_0 = iL_{k,a}\tau^a, \qquad \text{with} \quad L_{k,a} = 2\partial_k\phi^{[0}\phi^{a]} + \epsilon_{abc}\phi^b\partial_k\phi^c \tag{1.18}$$

$$T_i^\pm = \frac{i}{2}U_0^\dagger\,[\tau_i, U_0]_\pm \equiv iT_{k,a}^\pm\tau^a, \qquad \text{with} \begin{cases} T_{k,a}^+ = \phi^0\phi^0\delta_{ka} + \phi_k\phi_a + \epsilon_{kla}\phi^0\phi^l \\ T_{k,a}^- = \phi^b\phi^b\delta_{ka} - \phi_k\phi_a + \epsilon_{kla}\phi^0\phi^l \end{cases} \tag{1.19}$$

For notational simplicity, here and below we do not distinguish upper (x^i, τ^a) from lower (x_i, τ_a) indices for three-dimensional vectors and tensors when we deal with purely three-dimensional expressions.

Once we have the Lagrangian (1.14) (and thus the corresponding Hamiltonian), we may perform the quantization of the system by finding an irreducible representation of the algebra of observables associated to the quantum degrees of freedom defined on the Hilbert space of states, $\mathcal{H}$. We start by noting that the term quadratic in the time derivatives of the translational coordinates X_i in (1.14) is the standard kinetic term of a non-relativistic free particle. The associated observables will be the translational coordinates X_i and momenta $P_i = \mathcal{M}\dot{X}_i$, and the corresponding quantum operators satisfy the standard canonical commutation relations,

$$[\hat{X}_i, \hat{P}_i] = i\delta_{ij}. \tag{1.20}$$

Hence, the corresponding states associated to the translational zero modes will be those of a quantum, non-relativistic free particle. Let $\mathcal{H}_{\text{f.p.}}$ be the Hilbert space of such states. A complete basis for $\mathcal{H}_{\text{f.p.}}$ is given by the set of momentum eigenstates, $|\boldsymbol{p}\rangle$.

On the other hand, a transformation of the form (1.13) with $\boldsymbol{X} = 0$ corresponds to an element $g = (A, B) \in SU(2) \times SU(2) \equiv G$ of the most general symmetry group of the Skyrme Lagrangian. Therefore, the quantum mechanical spin and isospin states of a Skyrmion belong to the Hilbert space $\mathcal{H}_G = L^2(G, \mu)$ of square integrable functions on G [4] with the inner product

$$\langle\psi, \phi\rangle = \int_G d\mu(g)\psi^*(g)\phi(g), \tag{1.21}$$

[4] Actually, on some cover of G [Kru03].

where $d\mu(g)$ is the Haar measure on G. The observables associated to these states correspond to the rotational and iso-rotational collective coordinates A, B and their canonically conjugate momenta, the body-fixed isospin and spin angular momentum operators K_j and L_j, obtained in terms of the angular velocities a_j and b_j via the relations,

$$\begin{aligned} K_i &= U_{ij}a_j - W_{ij}b_j, \\ L_i &= -W_{ij}^T a_j + V_{ij}b_j, \end{aligned} \tag{1.22}$$

where T denotes transpose. These operators are related to the usual space- fixed isospin and spin angular momentum operators I_j and J_j via

$$I_i = -R_{ij}(A)K_j, \quad J_i = -R_{ij}\left(B\right)^T L_j, \tag{1.23}$$

implying $\boldsymbol{I}^2 = \mathbf{K}^2$ and $\boldsymbol{J}^2 = \mathbf{L}^2$. The set of operators, $\boldsymbol{I}, \boldsymbol{J}, \boldsymbol{K}$ and $\boldsymbol{L}$, form an irreducible representation of the Lie algebra of $\mathcal{O}_{I,K} \otimes \mathcal{O}_{L_n J}$, the symmetry group of two rigid rotators, and obey the commutation relations

$$[I_i, I_j] = i\epsilon_{ijk}I_k, \quad [K_i, K_j] = i\epsilon_{ijk}K_k, \quad [J_i, J_j] = i\epsilon_{ijk}J_{k1}, \quad [L_i, L_j] = i\epsilon_{i,jk}L_k. \tag{1.24}$$

From these, we may produce a complete set of commuting observables to define an eigenstate basis of $\mathcal{H}_G$. We construct such a basis with states of the form

$$|G\rangle = |i, i_3, k_3\rangle \otimes |j, j_3, l_3\rangle \equiv |i, i_3, k_3; j, j_3, l_3\rangle\,, \tag{1.25}$$

where j and j_3 correspond to the eigenvalues of the corresponding total angular momentum and the third component of angular momentum operators. Thus the total Hilbert space $\mathcal{H} = \mathcal{H}_{\text{f.p.}} \otimes \mathcal{H}_G$ is spanned by the states $|i, i_3, k_3; j, j_3, l_3; \boldsymbol{p}\rangle$, where $-i \leq i_3, k_3 \leq i$ and $-j \leq j_3, l_3 \leq j$. In particular, the subspace of fixed i, i_3, j, j_3 and momentum $\boldsymbol{p}$, labelled by the states $|k_3, l_3\rangle$, is $(2i+1)(2j+1)-$dimensional.

Spin and statistics of Skyrmions

Up to now, we have not taken into account the baryon quantum number in the quantization of a Skyrmion. Indeed, if we are to identify the quantum skyrmion states to physical nucleons and nuclear states, we need to be able to account for the fermionic character of the nucleons and some nuclei. This character is in principle not imposed by the symmetries nor the classical solutions of the Skyrme Lagrangian in the $SU(2)$ case[5], but for the topological properties of the configuration space.

A rigorous way to do this starts by noticing that the configuration space of the classical solutions of the model is not connected, and divided into connected components Q_B labeled by the topological charge. For the vacuum boundary condition at spatial infinity, Q_B is topologically equivalent to $\text{Maps}_{\text{B}}(\text{S}^3 \to \text{S}^3)$, and it is easy to see also that all Q_B are homeomorphic to the others, and, in particular, to $Q_0 \equiv Q$. However, it turns out that Q_B (for any B) is not simply connected. Indeed, it can be shown [Giu93] that it has a nontrivial fundamental homotopy group

$$\pi_1(Q_B) = \pi_4(S^3) = \mathbb{Z}_2, \tag{1.26}$$

[5] in the three flavor case, the Wess-Zumino-Witten term forces the spin-statistics theorem, and the fermionic character of a given Skyrmion is related to the baryon charge and the number of colors of the underlying UV-theory.

so that functions f on Q_B are not single-valued in general. It was noted by Finkelstein and Rubinstein that if the configuration space is not simply connected, then the wave functions have to be defined not on configuration space, but on some covering of the configuration space. In the case of Skyrmions, the corresponding Hilbert space $\mathcal{H}$ will correspond to normalized, square integrable functions on the universal double cover of Q_B, CQ_B. An element $[q] \in CQ_B$ is defined as a path starting in $q_0 \in Q_B$ and ending in $p \in Q_B$ up to homotopy. Indeed, $[q] \neq [q \cdot a]$, where $[a]$ corresponds to the loop generating the fundamental group of Q_B, although both project to the same point p in Q_B. Also, from eq. (1.26) it is clear that $[p \cdot a \cdot a] = [p]$. Now let $\psi([p]) \in \mathcal{H}$, and let $[r] \in CQ_B$ be the loop in configuration space corresponding to a spatial rotation of 2π of the Skyrmion solution $U_0 \in Q_B$ around any axis. We say that the Skyrmion admits a *fermionic quantization* if $[r]$ generates the fundamental group of Q_B, i.e. if $[q \cdot r] \neq [q]$ ($[r]$ is a non-contractible loop). Then, we may impose

$$\psi([q \cdot r]) = -\psi([q]), \tag{1.27}$$

and thus the Skyrmion aqcuires a non-trivial phase under a 2π rotation. This in fact implies, for any axis $\mathbf{n}$,

$$e^{i2\pi \mathbf{n}\cdot\mathbf{L}}\psi = -\psi \implies l \text{ is half integer.} \tag{1.28}$$

Although imposing this condition is a matter of choice (at least, in the $SU(2)$ case), the spin-statistics theorem follows from such condition. Indeed, one can show:

- In general, if B is odd, then rotation by 2π is a non-contractible loop, while if B is even, then it is contractible. Thus, spin is half-integer if B is odd, and integer if B is even [Giu93].

- The loop induced by the permutation of two $B = 2n + 1$ Skyrmions is non-contractible [FR68]. This result links spin with statistics.

Also, the fermionic quantization of Skyrmions allows for the rigurous treatment of the Finkelstein-Rubinstein (FR) constraints. Indeed, let H be the (possibly discrete) subgroup of G describing the symmetry of the classical Skyrmion configuration, and let

$$H_k = \{h_k, h_k'\} = \left\{ e^{-\frac{i\theta}{2}\hat{\mathbf{n}}\cdot\tau}, e^{-\frac{i\theta'}{2}\hat{\mathbf{n}}'\cdot\tau} \right\} \tag{1.29}$$

belong to the generating set of H. Then, the physical states $|\Psi\rangle$ must satisfy

$$e^{i\theta\hat{\mathbf{n}}\cdot\mathbf{L}} e^{i\theta'\hat{\mathbf{n}}'\cdot\mathbf{K}} |\Psi\rangle = \chi_{\mathrm{FR}} |\Psi\rangle , \tag{1.30}$$

where $\chi_{\mathrm{FR}} = +$ or $-$ depending on whether the loop in the cover space CQ_B associated to the symmetry generated by H_k is contractible or not. Eq. (1.30) represents the Finkelstein-Rubinstein constraint associated with the symmetry generated by H_k [Irw00; Giu93].

$B = 1$ Skyrmion. Nucleon states.

Let us now focus in the quantization of spin and isospin of the $B = 1$ Skyrmions. As argued, in this case the symmetry of the classical solution implies that total spin and isospin quantum numbers are linked, and hence the quantization procedure simplifies. The physical Hilbert space is spanned by the basis $|X\rangle = |ii_3j_3\rangle$ of states with fixed total spin (and isospin) and third components of spin and isospin.

We may parametrize the isospin collective coordinates as an element $A \in SU(2)$ by $A = a_0 + ia_k\tau_k$, where $a = (a_0, \mathbf{a})$ is subject to the constraint $a_0^2 + a_k a_k = 1$. Thus, the coordinate vector a can be thought of parametrizing a four-dimensional sphere, and hence, in the $|A\rangle$ representation, the wave function of each of the basis states corresponds to the (hyper-)spherical harmonics on S^3:

$$\psi(A) = \langle A|ii_3j_3\rangle = Y^{2i}_{i_3,j_3}(a), \tag{1.31}$$

with

$$Y^{2j}_{m,m'}(A) = [(2j+1)/2\pi^2]^{1/2}\mathscr{D}^j_{m,m'}(A), \tag{1.32}$$

where $\mathscr{D}^j_{m,m'}(A)$ are the Wigner's D-functions, associated to an irreducible, spin-j representation of the $SU(2)$ group. Let us write its explicit expression in terms of the matrix elements of an arbitrary 2×2 matrix B [BI66]:

$$B = \begin{pmatrix} a & b \\ c & d \end{pmatrix} \implies \mathscr{D}^j_{m,m'}(B) = [(j+m)!(j-m)!(j+m')!(j-m)!]^{1/2} \sum_{n_i>0} \frac{a^{n_1}b^{n_2}c^{n_3}d^{n_4}}{n_1!n_2!n_3!n_4!}, \tag{1.33}$$

with $n_1 + n_2 = j - m$, $n_3 + n_4 = j + m$, $n_1 + n_3 = j + m'$, $n_2 + n_4 = j - m'$. Indeed, the wavefunctions (1.32) are correctly normalized under the corresponding inner produt (1.21),

$$\int_{SU(2)} (Y^{2j}_{i_3,j_3}(A))^* Y^{2j'}_{i'_3,j'_3}(A) d\mu(A) = \delta_{jj'}\delta_{i_3i'_3}\delta_{j_3j'_3}, \tag{1.34}$$

where the Haar measure $\mu(A)$ can be written in this case as a volume element in terms of three angular variables parametrizing the three-sphere S^3.

In particular, for describing nucleon states we are interested in the lowest, half-integer spin and isospin states, i.e. the spin-1/2 representation of $SU(2)$. There are four of such states, [ANW83b] which are shown in table 1.1 together with their corresponding wavefunction in the $|A\rangle$ representation.

	$\lvert i_3, j_3\rangle$	$\psi(A)$
$\lvert p\uparrow\rangle$	$\left\lvert \frac{1}{2}\frac{1}{2}\right\rangle$	$\frac{1}{\pi}(a_1 + ia_2)$
$\lvert p\downarrow\rangle$	$\left\lvert \frac{1}{2}\frac{-1}{2}\right\rangle$	$-\frac{i}{\pi}(a_0 - ia_3)$
$\lvert n\uparrow\rangle$	$\left\lvert \frac{-1}{2}\frac{1}{2}\right\rangle$	$\frac{i}{\pi}(a_0 + ia_3)$
$\lvert n\downarrow\rangle$	$\left\lvert \frac{-1}{2}\frac{-1}{2}\right\rangle$	$-\frac{1}{\pi}(a_1 - ia_2)$

Table 1.1: Nucleon spin and isospin quantum states for the lowest energy nucleons.

Once we have characterized all the basis states, we are ready to calculate the matrix elements of any observable that can be expressed as an operator $\hat{F}(A)$ over the Hilbert

space $\mathcal{H}$. Indeed, for any pair of basis sates $|ii_3j_3\rangle, |i'i'_3j'_3\rangle$, we may write the matrix element as an integral over $SU(2)$:

$$\langle ii_3j_3|\,\hat{F}(A)\,|i'i'_3j'_3\rangle = \int_{SU(2)} (Y^{2i}_{i_3,j_3}(A))^* F(A) Y^{2i'}_{i'_3,j'_3}(A) d\mu(A). \tag{1.35}$$

Quantization of multiskyrmions ($B > 1$).

In general, the classical field configuration of a $B > 1$ Skyrmion presents a non-trivial symmetry characterized by a finite point group H. Hence, the corresponding allowed quantum states of spin and isospin will correspond to different linear combinations of the basis vectors (1.25). To find these combinations explicitly, the group H has to be known in terms of a set of generators, $\{H_k\}$ that can be written as a product of a rotation $\mathcal{R}_k$ and an isorotation $\mathcal{R}'_k$. Then, the FR constraints may be written as in eq. (1.30). To consistently do this, as explained above, it is important to know as well whether each of the symmetries H_k corresponds to a contractible or a non-contractible loop in configuration space. Once all the generators H_k have been parametrized in terms of products of rotations and isorotations, one needs to find a solution of the Finkelstein-Rubinstein system of constraints on each subspace of fixed i, j. Solving the system of FR constraints is equivalent to finding a set of common eigenvectors in this subspace of a particular set of matrices.

Indeed, according to the general transformation law of angular momentum states under a rotation $\mathcal{R}(\alpha, \beta, \gamma)$ parametrized in terms of the Euler angles α, β, γ (in the $Z - Y - Z$ convention):

$$\mathcal{R}(\alpha, \beta, \gamma)\,|j, m\rangle = \sum_{m'} D^j_{mm'}(\alpha, \beta, \gamma)\,|jm'\rangle\,, \tag{1.36}$$

where $D^j_{mm'}(\alpha, \beta, \gamma)$ is the Wigner D-matrix, correponding to the irreducible, spin-j representation of the rotation group.

Hence, for each H_k, a solution of the corresponding FR constraint is given by a state $|\Psi\rangle$ which is both an eigenstate of $\mathcal{R}_k(\alpha, \beta, \gamma)$ with eigenvalue λ_k and of $\mathcal{R}'_k(\alpha', \beta', \gamma')$ with eigenvalue λ'_k, and such that $\lambda_k \times \lambda'_k = \chi_{\rm FR}$. On each subspace given by a fixed value of total spin and isospin, this is equivalent to finding a common eigenvector of the correponding Wigner D-matrices. The allowed (physical) states will be those which satisfy all the FR constraints.

To conclude this section, we review the application of the above formalism to obtain the ground states and lowest energy excitations of some simple nuclei such as the deuteron, the tritium or the $B = 6$ nuclides.

Let us start by the $B = 2$ case. Following [MMW07], the FR constraints associated to the continuous axial symmetry and the discrete $\mathbb{Z}_2$ symmetry are, respectively

$$(L_3 + 2K_3)\,|\psi\rangle = 0, \qquad e^{i\pi L_1} e^{i\pi K_1}\,|\psi\rangle = -\,|\psi\rangle\,. \tag{1.37}$$

The minimum energy state that also solves the above constraints is the spin-1, isospin singlet, which can be identified with the deuteron state with polarization λ:

$$\left|{}^2\mathrm{H}, \lambda\right\rangle = |1, \lambda, 0\rangle \otimes |0, 0, 0\rangle\,, \qquad (\lambda = 0, \pm 1). \tag{1.38}$$

Another example that will be interesting for us in the following chapter is the spin $\frac{1}{2}$, (^{3}H,^{3} He) isospin doublet:

$$\left|{}^3\mathrm{H}/{}^3\mathrm{He}, s\right\rangle = \left|\tfrac{1}{2}, s, \tfrac{1}{2}\right\rangle \left|\tfrac{1}{2}, {}^{+}\!/_{-}\tfrac{1}{2}, \tfrac{-1}{2}\right\rangle - \left|\tfrac{1}{2}, s, \tfrac{-1}{2}\right\rangle \left|\tfrac{1}{2}, {}^{+}\!/_{-}\tfrac{1}{2}, \tfrac{1}{2}\right\rangle, \tag{1.39}$$

that arises as the ground state of the physical Hilbert space in the $B = 3$ topological sector [MMW07; Car91a].

Finally, we will be also interested in the low energy states of the $B = 6$ sector. The lower energy states that solve the corresponding FR constraints are the spin-1, isospin 0 state $|1, j_3, 0\rangle\,|0, 0, 0\rangle$ corresponding to the ground state of the lithium-6 nucleus ^{6}Li, and the isospin triplet $|0, 0, 0\rangle\,|1, i_3, 0\rangle$ formed by the helium-6 and beryllium-6 ground states plus the spin-0 excited state of ^{6}Li.

1.3 Skyrmions from instantons

In a seminal paper [AM89], M. Atiyah and N. Manton proposed that a (static) Skyrme field configuration $U(\mathbf{x})$ with baryon number k may be obtained as the holonomy of an SU(2) Yang-Mills k-instanton configuration along the Euclidean time direction, formally

$$U(\mathbf{x}) = \mathcal{P}\exp\left(-\int_{-\infty}^{\infty} A_4(\mathbf{x}, x_4)dx_4\right), \tag{1.40}$$

with $\mathcal{P}$ denoting path ordering of the exponential. Such a construction is almost gauge invariant, since the effect of a gauge transformation of A_μ by $g(x)$ is just a conjugation of U by the asymptotic values $g(\pm\infty)$. This can be understood as an isospin rotation of the corresponding Skyrme field.

In order to better understand the statement above, let us quickly review the concept of instantons of a Yang-Mills theory, for example, in the case of $SU(2)$ gauge group in four dimensions.

The vacuum structure of an SU(2) Yang-Mills theory in $3+1$ dimensions is nontrivial, in the sense that it presents a discrete set of degenerate classical minima. These minima are associated to static (in the temporal gauge), pure gauge configurations of the form $A_\mu = \Omega^{-1}(\mathbf{x})\partial_\mu\Omega(\mathbf{x})$, with $\mathrm{SU}(2) \ni \Omega(\mathbf{x}) \to 1$ as $|\mathbf{x}| \to \infty$. Mathematically, these configurations can be seen as continuous mappings $\mathbb{R}^3 \cup \{\infty\} \sim S^3 \to \mathrm{SU}(2) \sim S^3$, which are classified by their third homotopy group, $\pi_3(S^3) = \mathbb{Z}$. In other words, vacuum gauge field configurations are separated in different homotopy classes, labeled by an integer $n[\Omega]$, which can be obtained as an integral

$$n[\Omega] = -\frac{1}{24\pi^2}\int_{S^3} d^3x\epsilon^{ijk}\,\mathrm{Tr}\left(\Omega^{-1}\partial_i\Omega\Omega^{-1}\partial_j\Omega\Omega^{-1}\partial_k\Omega\right). \tag{1.41}$$

Vacuum configurations with different topological degree cannot be continuously deformed into each other without generating non-vacuum gauge fields, so these vacua are separated by a potential barrier in the quantum theory. The tunneling transition between classically degenerate vacua of a quantum theory is generally described by INSTANTONS, which are solutions of the Euclidean field equations, i.e absolute minimizers of the Euclidean action

$$S_\mathrm{E} = \frac{1}{4g^2}\int \mathrm{Tr}(F_{\mu\nu}F_{\mu\nu})d^4x, \tag{1.42}$$

with $F^a_{\mu\nu} = \partial_\mu A^a_\nu - \partial_\nu A^a_\mu + \epsilon^{abc} A^b_\mu A^c_\nu$ is the gauge field strength tensor, and $A_\mu = -ig\frac{\tau^a}{2}A^a_\mu$ is the Lie algebra-valued Yang-Mills field.

Instanton solutions are localised in spacetime, and can also be classified by their homotopy class when seen as mappings on $\mathbb{R}^4$ that asymptote to pure gauge configurations on its boundary, S^3_∞ (so that their action remains finite). Therefore, we can also think of Yang-Mills instantons as topological solitons in the Euclidean version of the theory, with topological charge (instanton number) given by

$$n = -\frac{1}{16\pi^2}\int d^4x \,\mathrm{Tr}\,({}^\star F^{\mu\nu} F_{\mu\nu}), \tag{1.43}$$

where $\star$ denotes the Hodge dual of the field strength tensor: ${}^\star F_{\mu\nu} = \frac{1}{2}\epsilon_{\mu\nu\rho\sigma}F^{\rho\sigma}$.

These tunnelling solutions are usually necessary in order to understand various non-perturbative processes in the Standard Model and other (super)Yang-Mills theories. In particular, they play an important role in QCD, where they have been used to solve the axial U(1) problem [t H86] or to explain chiral symmetry breaking [Dia96].

A priori, Yang-Mills instantons in a $SU(2)$ gauge theory and solitons in the Skyrme model are completely different objects: the former are vector(gauge) fields in an (Euclidean) 4-dimensional spacetime which take values in the $\mathfrak{su}(2)$ Lie algebra, while the latter are scalar fields in three spatial dimensions, taking values in the $SU(2)$ group manifold. Additionally, the two types of solitons minimize very different energy functionals: the Skyrme energy and the Euclidean Yang-Mills action, respectively. Nevertheless both of these solitons are equivalent in terms of topology, as they are described by the same homotopy group. Atiyah and Manton were the first to realize this, and found a topological charge-preserving mapping between them, given by (1.40)

Moreover, the moduli space of SU(2) instanton configurations of charge k, including the choice of gauge at infinity, is a connected manifold of dimension $8k$ [AHS77; JR77]. Hence, the set of Skyrme fields with $B = k$ obtained via the Atiyah-Manton construction (1.40) will be an $8k-1$ dimensional manifold, as a global time translation of the instanton leaves the Skyrme field unchanged. This manifold is sometimes called the *moduli space of $B = k$ instanton-generated Skyrmions*, since even though the Skyrme fields so-constructed are not exact solutions to the Skyrme field equations, some are good approximations to minimal energy Skyrmions and other field configurations describing their low energy dynamics in that topological sector. The Atiyah-Manton approximation was further developed in [LM94; HOA91; Sut94], and it was also extended in order to include instantons at finite temperature, [Cor18; CH22] and skyrmions from gravitational instantons [Dun13]. Its application to describe low energy interactions between nuclei was studied shortly after it was first proposed [AM93; HOA91], and has been put forward recently in [HW21; HH22].

The useful idea that Skyrmions can be seen as instantons in a higher dimensional space has been thoroughly studied in the holographic context. In Sutcliffe [Sut10], it is explicitly shown that the Skyrme model appears, together with a Kaluza-Klein tower of vector mesons, after a dimensional reduction of a $4+1$ dimensional Yang-Mills theory. This phenomenon is also realized in several holographic QCD models. In particular, the Sakai-Sugimoto model, a holographic dual of QCD with N_f massless quarks proposed in [SS05a]. The low energy effective action of such a model consists of a five-dimensional Yang-Mills and Chern-Simons theory on a curved background. In this model, the massless

pion and an infinite tower of massive (axial-)vector mesons are interpreted as Kaluza-Klein states associated with the holographic direction, and baryons are identified as D4-branes wrapped on a non-trivial four-cycle in the D4 background. Such a D4-brane is realized as an instanton configuration in the worldvolume gauge theory. Also, the pion effective action obtained from the Kaluza-Klein reduction of the $4+1d$ Yang-Mills theory is precisely that of the Skyrme model, in which baryons appear as solitons. It can be shown that the baryon number of a Skyrmion, i.e the winding number carried by the pion field, is equivalent to the instanton number in the Yang-Mills theory. In this way, the Sakai-Sugimoto model presents two dual descriptions of baryons, as wrapped D-branes (instantons) and as Skyrmions in the Kaluza-Klein-reduced theory.

Apart from QCD-like theories, instanton-mediated processes are also important in more complicated gauge theories presenting the Higgs mechanism, such as the electroweak sector of the Standard Model, where they are associated to the violation of baryon number [Esp90]. Such transitions become relevant only at very high energies and have been proposed as a plausible source of baryon number violation leading to baryogenesis in the early universe [RS96]. However, the Higgs mechanism poses a slight complication concerning instantons in these gauge theories. Indeed, there are no solutions to the Euclidean field equations, i.e. no exact minima of the Euclidean action in sectors with nonzero topological degree. The reason, as we will discuss below, is that the action for instanton-like configurations, with a nontrivial Higgs field, depends on the instanton size and decreases as it tends to zero. To evaluate the functional integral in that case one introduces a constraint that fixes the size of the configuration [t H76], then minimizes the action under this constraint and finally integrates over all possible values of the instanton size. The constrained solutions that one uses to calculate instantonic contribution to the path integral in the Higgs phase are called CONSTRAINED INSTANTONS.

Constrained instantons in Yang-Mills-Higgs theories

We now consider an SU(2) Yang-Mills-Higgs (YMH) theory on four dimensional Euclidean space $\mathbb{R}^4$, given by the Lagrangian

$$\mathscr{L} = \frac{1}{g^2}\left\{\frac{1}{4}F^a_{\mu\nu}F^a_{\mu\nu} + \kappa\left[(D_\mu\phi)^\dagger D_\mu\phi + \frac{1}{4}(\phi^\dagger\phi - \mu^2)\right]\right\}, \tag{1.44}$$

where $D_\mu = \partial_\mu - i\frac{\tau^a}{2}A^a_\mu \equiv \partial_\mu + A_\mu$ is the associated covariant derivative, ϕ an SU(2) Higgs doublet g and κ the gauge and Higgs couplings, respectively. Finally, μ^2 is the vacuum expectation value of the Higgs field in the spontaneously broken phase, in which the gauge field acquires a mass $m = \sqrt{\frac{\kappa\mu^2}{2}}$ due to the Higgs mechanism.

For $\mu = 0$, the (Euclidean, $4d$) YMH field equations present instanton solutions which are the same as in the pure Yang-Mills case, with $\phi = 0$. In the 't Hooft gauge [t H76], these solutions read

$$A_\mu(x) = \frac{1}{2}\sigma_{\mu\nu}\partial_\nu \log\alpha(x), \tag{1.45}$$

with α a solution of the Laplace equation in $\mathbb{R}^4$, $\partial^2\alpha = 0$, and $\sigma_{\mu\nu}$ the $\mathfrak{so}(4)$ Lie algebra

generators, defined as [6]

$$\sigma_{\mu\nu} = \frac{1}{4i}(\sigma_\mu \sigma_\nu^\dagger - \sigma_\mu^\dagger \sigma_\nu), \qquad \text{with} \quad \sigma_\mu = (\boldsymbol{\tau}, i\mathbf{1}_2). \tag{1.46}$$

In particular, the $k = 1$-instanton is given by

$$\alpha(x) = 1 + \frac{\lambda^2}{|x - X|^2} = 1 + t, \quad t \doteq \frac{\lambda^2}{|x - X|^2}, \tag{1.47}$$

with $\lambda \in \mathbb{R}$, $X \in \mathbb{R}^4$ the MODULI parameters determining the size and position of the instanton in Euclidean space, respectively, which are associated with ZERO MODES of the soliton [Sut94].

On the other hand, for $\mu \neq 0$, the nontrivial vacuum expectation value of the Higgs field breaks conformal symmetry, and there cannot exist an exact instanton solution of the coupled field equations. This can be easily seen by applying Derrick's scaling argument [Aff81]. Indeed, rescaling any instanton field configuration with $\phi \neq 0$ as

$$A_\mu(x) \to a A_\mu(ax), \quad \phi(x) \to \phi(ax), \tag{1.48}$$

the action becomes ($y = ax$):

$$S = \int d^4y \frac{1}{g^2}\left\{\frac{1}{4}F^a_{\mu\nu}(y)F^a_{\mu\nu}(y) + \frac{\kappa}{a^2}\left[(D_\mu\phi(y))^\dagger D_\mu\phi(y) + \frac{1}{4a^2}(\phi^\dagger\phi - \mu^2)\right]\right\}, \tag{1.49}$$

and since all terms in the integrand are positive, the action can always be made smaller by taking the limit $a \to \infty$. Since the expression for $aA_\mu(ax)$ is exactly equal to $A_\mu(x)$ with λ replaced by λ/a, we get that the action-minimizing instanton has zero size. However, the nontrivial topology of the space of field configurations is not affected by the Higgs mechanism, so that instanton-like field configurations with nonzero topological degree still exist as approximate solutions of the field equations. These are the so-called constrained instantons, and have been used to approximately calculate nonperturbative contributions to the path integral in the standard model and (super) Yang-Mills theories at the Higgs phase [t H76; Nie05; RS96].

The constrained instanton idea is based on the existence of a finite number of destabilizing directions in the gauge field space, along which the action always decreases, so that one introduces constraints that prevent deformations in these directions. Then, one just minimizes the action for fields subject to such constraints. For the spontaneously broken phase of SU(2) YMH theory, the destabilizing direction is that parametrized by the rescaling parameter a (note that this would correspond to a zero mode in the pure Yang-Mills phase), so one needs to impose a constraint that fixes the instanton size λ at some value.[7] The contribution to the path integral coming from these configurations is then obtained by integration over all (fixed) values of λ. Remarkably, the Higgs mechanism resolves the infrared divergence problem due to large instantons dominating the path integral measure on an otherwise scale-symmetric field theory such as pure Yang-Mills, since these become suppressed on the Higgs phase [t H76; Esp90; Shi22].

[6] we are using the conventions in [Esp90]

[7] Also, the constraint must allow finiteness of the action, which is a nontrivial demand for choosing a valid constraint, see [NN00].

The YMH equations coming from the Lagrangian (1.44) are

$$D_\mu F^a_{\mu\nu} + \frac{\kappa}{2}\left(-i\phi^\dagger \tau^a \overleftrightarrow{\partial}_\mu \phi - A^a_\mu \phi^\dagger \phi\right) = 0, \tag{1.50}$$

$$D^2\phi - \phi(\phi^\dagger\phi - \mu^2) = 0. \tag{1.51}$$

One could naively try to find instantonic solutions to the YMH equations. The finite action condition in the broken phase implies that gauge fields must become pure gauge configurations asymptotically, and the Higgs field must tend to a point in the corresponding vacuum manifold,

$$A_\mu(x) \to \Omega\partial_\mu\Omega^{-1}, \quad \phi(x) \to \Omega\phi_{\text{vac}}, \quad x \to \infty, \quad \Omega(x) \in \text{SU}(2) \tag{1.52}$$

with ϕ_{vac} a general base point of the Higgs potential vacuum manifold. Without loss of generality, we may choose $\phi_{\text{vac}} = (0, \mu)^\intercal$. Therefore, a general ansatz for the (spherically symmetric) $k = 1$ instanton would be of the form

$$A_\mu = \tilde{\xi}(x)\Omega\partial_\mu\Omega^{-1}, \qquad \phi(x) = (1 - \chi(x))\Omega\phi_{\text{vac}}, \tag{1.53}$$

where $\Omega = i\frac{\sigma_\mu x^\mu}{\sqrt{x_\mu x_\mu}}$ is an element of the first nontrivial homotopy class in $\pi_3(\text{SU}(2))$, and $\tilde{\xi}, \chi$ are functions of the radial Euclidean coordinate $r = |x|$ which satisfy the conditions $\tilde{\xi}, \chi \to 1, 0$ as $r \to \infty$. This ansatz corresponds to the generalization of the Belavin-Polyakov-Schwarz-Tyupkin (BPST) instanton solution [Bel+75] in the regular gauge to the Higgs phase, and was used in [Kli93] to find a constrained instanton solution using a specific constraint. In particular, for $\mu = 0$, i.e. the pure Yang-Mills case, the instanton solution is given in this gauge by $\tilde{\xi} = r^2/(r^2 + \lambda^2)$.

However, we will find it useful to gauge-transform (1.53) into a new form, in which $\phi \to \phi_{\text{vac}}$. This can be achieved with a gauge transformation by Ω^{-1}, which brings the ansatz into the so-called singular gauge:

$$A_\mu(x) = \frac{x^\nu \sigma_{\mu\nu}}{x^2}\xi(r) = -\sigma_{\mu\nu}\partial_\nu a(r), \quad \phi(x) = (1 - \chi(x))\phi_{\text{vac}}, \tag{1.54}$$

where ξ is a function related to the original $\tilde{\xi}$, and $\xi = a'/r$. With this gauge choice, the boundary conditions $A_\mu(x) \xrightarrow{x\to\infty} 0$, $\phi(x) \xrightarrow{x\to\infty} (0, \mu)^\intercal$, are satisfied, and eqs. (1.50) and (1.51) linearize for $A_\mu(x)$ and $\chi(x)$ in the $x \to \infty$ limit,

$$\left[-\delta_{\mu\nu}\partial^2 + \partial_\mu\partial_\nu + m^2\right]A_\mu = 0, \qquad m = \sqrt{\frac{\kappa\mu^2}{2}} \tag{1.55}$$

$$(-\partial^2 + \mu^2)\chi = 0. \tag{1.56}$$

Any solution of the linearized equations that satisfies the correct boundary conditions is given by

$$\chi \propto G(x; \mu), \qquad A_\mu \propto \sigma_{\mu\nu}\partial_\nu G(x; m), \tag{1.57}$$

with

$$G(x; \alpha) = \frac{\alpha}{r}K_1(\alpha r) \tag{1.58}$$

the Green function associated to the four dimensional, Euclidean Klein-Gordon operator, $-\partial^2 + \alpha^2$, and $K_n(z)$ is the modified Bessel function of degree n.

Unfortunately, as previously shown using Derrick's argument, the boundary conditions we have imposed are not compatible with a regular solution of the full system of YMH equations. Nonetheless, it was argued in [Aff81] that a perturbative solution can be constructed if we add extra terms to the right-hand sides of such equations, with coefficients that can be adjusted order by order in perturbation theory to obtain the desired boundary conditions. The presence of these extra terms is equivalent to adding a constraint at the level of the action, so the obtained solutions are constrained instantons. This procedure was further extended in [NN00] with the additional requirement that the perturbative solution yields a finite value for the action functional, and a constrained instanton solution in the Higgs phase of SU(2) YMH theory was calculated perturbatively in the parameter μ up to $\mathcal{O}(\mu^4)$. The solution looks like the standard self-dual instanton near its core, but decays exponentially (instead of polynomially) as $\exp(-\mu r)$ far from the center.

The perturbative method starts with the singular gauge ansatz (1.54), defining two real functions $\alpha = \exp(a)$ and $f = \mu(1-\chi)$ which depend on x in terms of the parameter $t = \frac{\lambda^2}{r^2}$. Then, these functions are expanded as

$$\alpha = \sum_{n=0}^{\infty} \alpha_{2n}, \qquad f = \sum_{n=0}^{\infty} f_{2n+1}, \tag{1.59}$$

where the subscript on each function indicates the lowest power of μ appearing on it. Introducing this ansatz into the YMH Lagrangian, the equations of motion for α and f are ($' = d/dt$) [NN00]:

$$(\alpha^{-3}t^3\alpha'')' = \frac{\kappa\lambda^2}{8} f^2\alpha^{-3}\alpha', \quad \alpha^2 f'' - \frac{3}{4}(\alpha')^2 f = \frac{\alpha^2\lambda^2 f}{8t^3}(f^2-\mu^2), \tag{1.60}$$

which can be solved by quadrature at each order. The required boundary conditions plus finiteness of the action impose that these equations are modified order by order by adding certain terms at the right hand side. These terms (and the corresponding constraint) must then be computed at each order in μ, and are unique up to $\mathcal{O}(\mu^4)$ [NN00]. This can be done iteratively, starting with the zeroth-order instanton solution, $\alpha_0(t) = 1+t$, and substituting in the equation for f, which yields $f_1 = \mu/\sqrt{1+t}$. This solution already satisfies the boundary condition for ϕ, so no modification of the equation for f is needed at this order. In fact, the equation for f does not need to be modified at any order [NN00]. On the other hand, at second order, the modification of the equation for α turns out to be unique, (i.e. the corresponding constraint is unique up to $\mathcal{O}(\mu^4)$), and therefore, one can solve for α_2 unambiguously. Further details on the perturbative construction can be found in [NN00], in which a recurrence relation for obtaining the leading term on each higher order component α_{2n} was found. Moreover, it was also shown that the leading order terms in the series of $\alpha(t)$ presents a convergence towards $G(x,m)$ at large distances (which was expected from the asymptotic linearized equations).

However, for our purposes, the perturbative solution is unsatisfactory, because it will always diverge for some value of r at any given truncation order [Gar22]. After computing the corresponding holonomy, this translates into a Skyrme field that does not satisfy the correct boundary conditions at infinity. A simple way around this problem is just to consider the asymptotic solution, namely

$$\alpha(x) = 1 + \frac{\lambda^2 m}{r} K_1(mr), \tag{1.61}$$

which does of course yield well-behaved Skyrmions at infinity, as we show in the next section.

Apart from the perturbative method, an alternative approach for constructing constrained instanton configurations in YMH theory was used in [Wan94], in which instead of fixing the constraint and trying to solve the equation for the corresponding constrained instanton, the reverse method is followed. One chooses a particular functional form for the constrained instanton, and the corresponding constraint may be systematically calculated afterwards due to the freedom in choosing the constraint in the first place. The only requirement in choosing the constrained instanton shape a priori is that it satisfies some constraint-independent boundary conditions at the origin and far from its center. Indeed, if one considers again the BPST-like ansatz, the (dimensionless) functions ξ, χ can depend on $r = |x|$ only through two dimensionless combinations, λ/r and mr. We may expand these functions both for small ($r \ll \lambda$) and large ($r \gg m^{-1}$) distances in terms of these two combinations, as [Esp90; Wan94]:

$$\begin{aligned}\xi(r) &= \xi_0(\tfrac{\lambda}{r}) + (mr)^2\xi_1(\tfrac{\lambda}{r}) + \cdots = \\ &= (\tfrac{\lambda}{r})^2\xi^0(mr) + (\tfrac{\lambda}{r})^4\xi^1(mr) + \cdots,\end{aligned} \tag{1.62}$$

$$\begin{aligned}\chi(r) &= \chi_0(\tfrac{\lambda}{r}) + (mr)^2\ln(mr)\chi_1(\tfrac{\lambda}{r}) + \cdots = \\ &= (\tfrac{\lambda}{r})^2\chi^0(mr) + (\tfrac{\lambda}{r})^4\chi^1(mr) + \cdots .\end{aligned} \tag{1.63}$$

Thus for recovering the pure Yang-Mills solution in the $m \to 0$ limit we require

$$\xi_0(\tfrac{\lambda}{r}) = \frac{2\lambda^2}{r^2+\lambda^2}, \qquad \chi_0(\tfrac{\lambda}{r}) = 1 - \sqrt{\frac{r^2}{r^2+\lambda^2}}, \tag{1.64}$$

where χ_0 above corresponds to the scalar field profile in the instanton background without backreaction [t H76].

On the other hand, the linearized equations at large distances impose

$$\xi^0(mr) = m^2r^2K_2(mr), \qquad \chi^0(mr) = \tfrac{1}{2}mrK_1(mr). \tag{1.65}$$

A pair of functions proposed by Wang in [Wan94] satisfying eqs. (1.62) to (1.65) are

$$\xi(r) = \frac{\lambda^2m^2K_2\left(mr\right)}{[1+\lambda^2m^2K_2(mr)/2]}, \quad \chi(r) = \left[1 - \left(\frac{r^2}{r^2+\lambda^2mrK_1\left(mr\right)}\right)^{\frac{1}{2}}\right]. \tag{1.66}$$

Obviously, the expressions in eq. (1.66) are associated with a particular constraint at the level of the action, which could be calculated, at least formally. Of course, they are not unique, and a different pair of functions satisfying the correct boundary conditions could have been chosen.

1.3.1 The constrained instanton approximation for the Skyrmion

Let us now explicitly apply the Atiyah-Manton construction to the simplest case, the $B = 1$ Skyrmion. Indeed, the $B = 1$ Skyrmion solution is well known, and can be written using the so-called HEDGEHOG ANSATZ:

$$U(\mathbf{x}) = e^{if(\rho)\mathbf{n}^a\sigma_a}, \qquad \text{where} \qquad \rho = |\mathbf{x}|, \quad \mathbf{n} = \frac{\mathbf{x}}{\rho}, \tag{1.67}$$

and $f(\rho)$ is the radial profile of the Skyrmion, which, for the $B = 1$ case, must satisfy $f(0) = \pi$ and $f(\infty) = 0$. Introducing the hedgehog ansatz into the static energy functional (1.7) (with $\lambda = 0$ for simplicity), one obtains

$$E = 4\pi \int \left(\rho^2 f'^2 + 2\left(f'^2 + 1\right) \sin^2 f + \frac{\sin^4 f}{\rho^2} + 2m^2\rho^2(1 - \cos f) \right) d\rho, \tag{1.68}$$

where we have renamed the constant $c_0 = 2m^2$ for convenience.

Hence the problem of minimizing the energy functional reduces to a one dimensional problem, whose solution can be obtained by solving a second order differential equation for f. These 1-instantons generate, after calculating the corresponding holonomy as in (1.40), a seven-dimensional manifold of B = 1 Skyrme hedgehogs, the coordinates being the position, orientation and scale size, and whose radial profile is given by

$$f(\rho) = \pi \left[1 - \left(1 + \frac{\lambda^2}{\rho^2} \right)^{-1/2} \right]. \tag{1.69}$$

Although instantons are scale invariant, the energy of the associated Skyrmion configurations depends on the particular value of the (in principle, arbitrary) parameter λ. Therefore, its value must be fixed so that the energy of the resulting Skyrme field is minimized, which reduces the moduli space by one dimension. It turns out that, for the massless case, the value of this scale is $\lambda^2 = 2.11$, with an energy of $E^{\text{inst}}_{m=0} = 1.243 \times 12\pi^2$, which is only 1% above that of the true Skyrmion solution.

Despite its success in describing the moduli space of massless pion Skyrmions, the instanton approximation does not work in the massive pion case. This can be understood by noting that the asymptotic decay of the instanton generated profile function is $f \sim \lambda^2/(2\rho^2)$, which has the correct form for massless pions, but decays too slowly for the massive pion case, ultimately generating configurations with infinite energy. Thus this form of the instanton holonomy method is not applicable to massive pions.

However, as we have seen in the previous section, we are still able to find instanton-like configurations in YMH theory that preserve their topological properties and nevertheless present an exponential radial decay due to the Higgs mechanism. Hence, constrained instantons are natural candidates for generating exponentially decaying Skyrme hedgehogs via the Atiyah-Manton construction. Indeed, from the ansatz in the previous section we get

$$A_4(\mathbf{x}, x_4) = -in^a\tau_a \left(\rho \frac{\lambda^2}{(x_4^2 + \rho^2)^2} \frac{\alpha'}{\alpha} \right), \tag{1.70}$$

with $\alpha(t)$ given by (1.61). The profile function generated by the constrained instanton approximation can therefore be written

$$f(\rho) = \int_{-\infty}^{\infty} \frac{\rho\lambda^2}{(x_4^2 + \rho^2)^2} \frac{\alpha'(t)}{\alpha(t)} dx_4. \tag{1.71}$$

On the other hand, if we choose to use the nonperturbative configuration generated by the functions (1.66) for constructing the constrained instanton, the profile function of the corresponding Skyrmion can be directly obtained as

$$f(\rho) = \int_{-\infty}^{\infty} \frac{\rho\lambda^2 m^2 K_2(m\sqrt{x_4^2 + \rho^2})}{2(x_4^2 + \rho^2)[1 + \lambda^2 m^2 K_2(m\sqrt{x_4^2 + \rho^2})/2]} dx_4. \tag{1.72}$$

As pointed out in [Esp90], the Lagrangian eq. (1.44) is invariant under independent global rotations of A_μ and ϕ, even after substituting the ansatz (1.54). Thus, in the constrained instanton the gauge and Higgs field orientations are not correlated. Furthermore, the Higgs field orientation is completely fixed once we choose a specific point in the vacuum manifold, ϕ as the vacuum state in the spontaneously broken phase. On the other hand, the orientation of A_μ remains a symmetry of the YMH action and therefore has to be treated as a collective coordinate along with the position of the constrained instanton. Of course, these collective coordinates will be inherited by the Skyrmion field configurations generated by constrained instanton configurations, so that the structure of the instanton-generated Skyrmion moduli space is preserved even after the addition of the Higgs field.

Obviously, the constrained instanton solution has lost its scale invariance due to a finite Higgs vev, so the scale parameter λ does not represent a zero mode anymore, but a quasi-zero mode, since it parametrizes a family of local minima of the action when the constraint is imposed. Therefore, we still have the freedom of choosing the value that better fits the true Skyrmion energy. Also, even for a given, specific constraint, its value will not be unique, but will depend on the value of the other free parameter, namely, the gauge field mass m, which coincides with the (dimensionless) pion mass parameter of the Skyrme field. Therefore, there's a one parameter family of Skyrmion solutions, each with different values of m, and the best value of λ for each one can be understood as a function $\lambda(m)$.

At the end of the day, constrained instantons also generate a seven dimensional Skyrmion moduli space, as fixing the Higgs vev at infinity does not break translation invariance, nor global gauge symmetry of the gauge field solution.

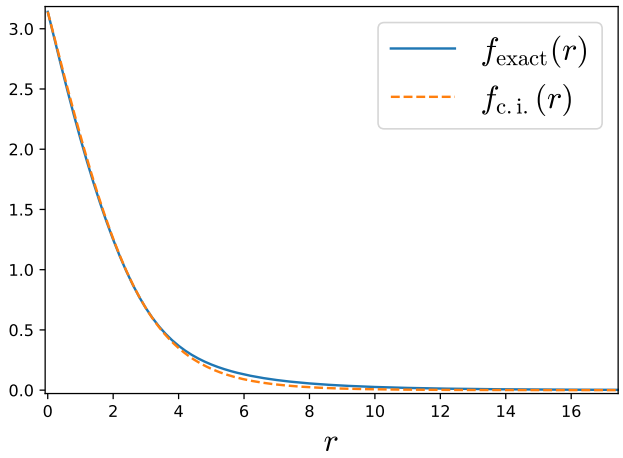

Figure 1.2: Solution of the Skyrme field profile for $m = 0.5$, and its corresponding best approximation using a constrained instanton

As we can see from fig. 1.2, the similarity between the true solution in the massive pion case and the constrained instanton approximation is astounding, and even better than the regular instanton approximation in the massless case. Indeed, the difference in energies between both cases is smaller than 1%, for instance, $E_{m=0.5} = 1.433 \times 12\pi^2$ and $E^{\text{c.inst}}_{m=0.5} = 1.438 \times 12\pi^2$. In this case, we have $\lambda^2(m = 0.5) = 1.47$. In table 1.2 we show the energies for each case in units of 12π.

m	0	0.5	3
E_{real}	1.232	1.433	2.170
$E_{\text{inst}}^{\text{pert}}$	1.243	1.438	2.250
$E_{\text{inst}}^{\text{n.pert}}$	1.243	1.435	2.224

Table 1.2: Energies of $B = 1$ hedgehog obtained by numerically solving the Skyrme field equations (E_{real}) and by the constrained instanton approximation, both using the perturbative configuration ($E_{\text{inst}}^{\text{pert}}$) and Wang's proposal ($E_{\text{inst}}^{\text{n.pert}}$).

Now an interesting question is whether we can say anything about higher baryon number skyrmions. In the pure Yang-Mills case, the self duality of instantons allows for the construction of the most general k instanton configuration via the powerful method of Atiyah-Drinfeld-Hitchin-Manin (ADHM) local data [Ati+78]. In [CH22], this method was used to describe multi-Skyrmion moduli spaces in terms of the ADHM data of the corresponding instanton approximation.

In our case, however, self duality is broken, and the problem of finding expressions for $k > 1$ constrained instantons, considerably harder. We could try to construct a k constrained instanton as a superposition of k individual 1-instantons, with arbitrary widths and positions, using a generalization of the 't Hooft ansatz to our case, i.e. taking

$$\alpha(x) = 1 + \sum_{i=1}^{k} \frac{\lambda_i^2 m}{|x - X_i|} K_1(m|x - X_i|), \tag{1.73}$$

where λ_i, X_i correspond to the sizes and Euclidean positions of each constrained instanton. Unfortunately, this ansatz does not reproduce the full picture, as it does not allow for different orientations of the individual instantons. A modification of the 't Hooft ansatz that includes the relative orientation between instantons and does not modify the topological degree was proposed in [Par+02]. It's based on the introduction of $3k$ additional parameters, namely, the Euler angles of a $SU(2)$ rotation matrix R_n. Then, the fourth component of the gauge field is given by

$$A_4(\mathbf{x}, x_4) = -i\frac{1}{\alpha} \sum_{i=1}^{k} R_i \tau_a \partial_a \left[\frac{\lambda_i^2 m}{|x - X_i|} K_1(m|x - X_i|) \right] R_i^\dagger, \tag{1.74}$$

which yields the correct number of collective coordinates on each topological sector. To what extent the gauge field configuration given in eq. (1.74) does actually reproduce the moduli space of multi-Skyrmions in the massive pion case after calculating its holonomy along x_4 is out of the scope of this paper. Nevertheless, it is an interesting calculation that may allow us to study the effect of a nonzero pion mass in the Skyrmion-Skyrmion interactions. Such configuration, in the $k \to \infty$ limit could be used as well to approximate the (half-)Skyrmion crystals, since it is the constrained-instanton version of that proposed in [Par+02]. Indeed, a nonzero pion mass provides a natural cutoff for the individual instantons, which decay exponentially, and the holonomy can be calculated directly without needing to impose an artificial cutoff on instanton tails.

1.4 Final remarks

In this first chapter, we have reviewed the basic procedure to obtain nuclear states as quantized Skyrmions from a (generalized) Skyrme model. It starts by computing the corresponding energy minimizing-configuration at each topological sector, which required of numerical methods. Then, the canonical quantization method is applied to zero-mode degrees of freedom (given by rotations in space, or spin, rotations in flavor space (isospin) and translations in three dimensional space) of each solution, which yields a well-defined Hilbert space for semi-classical, nonrelativistic nuclear states. As we will show in the next chapter, some of these states will be relevant for the computation of diverse nuclear properties that involve the matrix elements of nuclear currents.

We remark that the above procedure of soliton quantization is of very general nature, and does not depend on the specific model that one is considering. Indeed, the link between spin and statistics of quantized solitons is well established also outside of the Skyrme model. For example, the same topological principle applied in lower dimensional examples gives place to particle-like solitons with fractional spin and exotic statistics [WZ83].

Finally, after explaining the Atiyah-Manton construction of approximate Skyrmions from the holonomy of Yang-Mills instantons, we have presented a slight improvement on the instanton approximation of the $B = 1$ skyrmion with nonzero pion mass. It is given by a (relatively) simple analytic expression based on the concept of constrained instantons. Obviously, having a short, semi-analytical approximation to the $k = 1$ Skyrmion with massive pions can also be useful to study some dynamical aspects of the model without the need to rely in numerical methods to solve the corresponding Euler Lagrange equation. We would like to remark that a different method of generating Skyrmions with massive pions via computing the holonomy of instantons along circles in $\mathbb{R}^4$ was proposed in [AS05]. The field configurations obtained this way correspond to Skyrmions with massless pions in hyperbolic space, which are shown to be a good approximation to Skyrmions in flat space with a nonzero pion mass, when the curvature parameter is related to the pion mass in a certain way. This idea results also in a very good approximation to the real solutions, but a drawback of this method is that the moduli space structure is not preserved, since the position of the skyrmion is related to a fixed point in the base manifold and it is not a free parameter (as there is not translation symmetry in hyperbolic space). However, the instanton approximation is most useful for studying low energy dynamical processes involving two or more Skyrmions, since it allows to (approximately) describe the corresponding moduli space. In principle, the extension of our approach to describe a multi-skyrmion moduli space is possible, although not straightforward. A first step would be to find constrained multi-instanton solutions, and study the corresponding moduli space.

CHAPTER 2

The inner structure of light nuclei

Articles partially reproduced in this chapter: [GHH23]. See *permissions*.

"The Weak or the Strong,
Who got it goin' on?"

– Biggie Smalls, *Dead Wrong*

2.1 Introduction

Due to the color confinement phenomenon, it is difficult to probe the dynamics of quarks and gluons directly in experiments. Instead, we can learn about their dynamics by scattering leptons off hadrons, or by scattering hadrons on other hadrons, which in turn reveals information on how hadrons interact with the force carrying particles in the standard model, i.e. the gauge vector bosons (photons, W and Z bosons) and also with mesons (e.g. pions), which mediate the (residual) strong force between hadrons. Some of the relevant processes involving the nucleon are shown in fig. 2.1, for example, the electron scattering (which probes the electromagnetic interaction), the neutrino scattering (much weaker, mediated by a neutral current), the β decay which produces an $(e, \bar{\nu}_e)$ pair and is mediated by a charged weak boson, or the nucleon-nucleon interaction via a pion exchange.

The study of such processes reveals information of the internal structure of nucleons and nuclei, encoded into the so called FORM FACTORS: scalar, Lorentz-invariant quantities that determine the strength of a given interaction channel as a function of the momentum transfer.

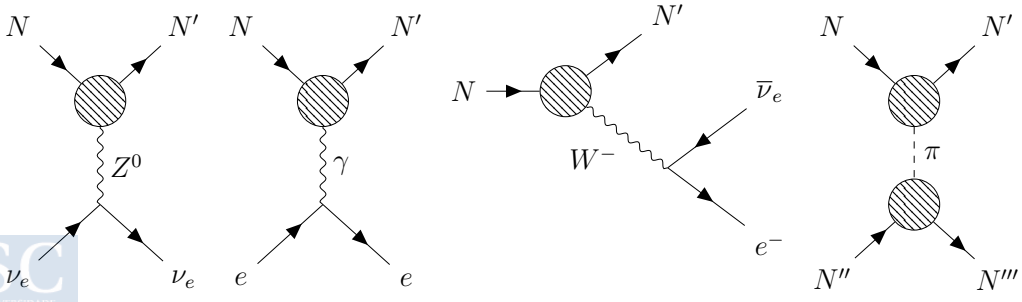

Figure 2.1: Feynman diagrams of nuclear scattering processes at tree level.

Despite this variety of processes, their corresponding scattering amplitudes all share a very simple structure at tree level, in terms of two fermionic (each either hadronic or leptonic) currents and a propagator. For instance, for a massive vector boson exchange interaction, the corresponding matrix element will be

$$\mathcal{M} = \langle l'(p_1')|\, J_l^\mu\, |l(p_1)\rangle \, \frac{i}{q^2 - M_V^2}(-\eta_{\mu\nu} + q_\mu q_\nu / M_V^2)\, \langle N'(p_2')|\, J_h^\mu\, |N(p_2)\rangle\,, \tag{2.1}$$

where quantities of the form

$$\langle \lambda'(p')|\, J_{a\cdots}^{\mu\cdots}\, |\lambda(p)\rangle \tag{2.2}$$

denote CURRENT MATRIX ELEMENTS, i.e. the interaction vertex between the one-particle states λ and λ', with respective momenta p and p'. These currents are operators which can, in general, present any Lorentz index structure (they can be either scalar, pseudoscalar, vector, axial-vector or even tensors), and also additional index structures representing, for example, flavor degrees of freedom. Since leptons are fundamental particles, their currents can be easily deduced via the Feynman rules from the SM Lagrangian. For example, the electron-photon vertex is given by the Feynman rules of Quantum Electrodynamics (QED) [DGH23]:

$$\langle e(p')|\, J_{l,\mathrm{em}}^\mu\, |e(p)\rangle = -ie\bar{u}_e(p')\gamma^\mu u_e(p), \tag{2.3}$$

with γ^μ the gamma matrices, u_e is a Dirac spinor representing the electron state, and e is its charge. On the other hand, the equivalent current for the nucleon-photon vertex can not be read straightforwardly from the Lagrangian, due to their composite nature. Instead, one can define an effective vertex Γ^μ such that

$$\langle N'(p')|\, J_{h,\mathrm{em}}^\mu\, |N(p)\rangle = -ie\bar{u}_{N'}(p')\Gamma^\mu(p', p)u_N(p). \tag{2.4}$$

This effective vertex (denoted by a "blob" in the second diagram of fig. 2.1) is not known a priori, but its tensorial structure can be determined by imposing the symmetries it should satisfy. Indeed, in the electromagnetic case, Γ^μ should transform like a vector. Also, it can only depend on the four vectors p, p' and γ^μ, as well as on scalar functions of the MOMENTUM TRANSFER $t^2 = -q^2$, to preserve Lorentz invariance. Thus, in general, we will have

$$\Gamma^\mu = \gamma^\mu A + q^\mu B + k^\mu C, \tag{2.5}$$

with $q = p' - p$, $k = p' + p$ and A, B, C are arbitrary scalar functions of t^2. Current conservation implies the Ward identity $q_\mu \Gamma^\mu = 0$, which further imposes $C = 0$ [2]. Then, Gordon's identity

$$\bar{v}\,(p')\,\gamma^\mu v(p) = \bar{v}\,(p')\left[\frac{k^\mu}{2m} + \frac{i\sigma^{\mu\nu}q_\nu}{2m}\right] v(p) \tag{2.6}$$

allows us to write the general expression for the (spin $\frac{1}{2}$) nucleon electromagnetic current matrix element as

$$\langle N(p')|\, J_{h,\mathrm{em}}^\mu\, |N(p)\rangle = \bar{u}_N(p')\left[\gamma^\mu F_1(t) + \frac{i\sigma^{\mu\nu}q_\mu}{2M_N}F_2(t)\right]u_N(p), \tag{2.7}$$

[2] While $q_\mu k^\mu$ vanishes identically, the γ^μ term only vanishes on-shell.

where $2\sigma^{\mu\nu} = i[\gamma^\mu, \gamma^\nu]$, M_N is the nucleon mass and $F_{1,2}$ are the so-called Pauli and Dirac form factors.

An analogue reasoning could be done for the charged weak currents, which can be readily obtained from the SM coupling between weak isospin lepton doublets $\psi_l = (u_l, u_{\nu_l})$ to the charged weak bosons [GM09],

$$\mathcal{L}_{\mathrm{J}} = \frac{g}{\sqrt{2}}\left(W^+_\mu l^\mu_- + W^-_\mu l^\mu_+\right) \longrightarrow l^\mu_\pm = \langle l(p')|\, J^\mu_{l,\pm}\, |l(p)\rangle = \bar{\psi}_l \gamma^\mu (1-\gamma^5)\tau_\mp \psi_l, \tag{2.8}$$

where $\tau_\pm = (\tau_1 \pm i\tau_2)/2$, and $\gamma_5 = i\gamma^0\gamma^1\gamma^2\gamma^3$. Particularized to the electron and neutrino fields, the weak leptonic current reads $l^\mu = \bar{u}_\nu \gamma^\mu (1-\gamma_5) u_e$. We observe that the weak charged currents are composed of both vector ($v^\mu_i = \bar{\psi}_l \gamma^\mu \frac{1}{2}\tau_i \psi_l$) and axial-vector ($a^\mu_i = \bar{\psi}_l \gamma^\mu \gamma_5 \frac{1}{2}\tau_i \psi_l$) fermion bilinears. Hence, the associated hadronic currents will also be composed of a vector and an axial-vector part, each with different form factors. For instance, the nucleon's axial current will also be characterized by two form factors (assuming isospin symmetry):

$$\langle N'(p')|\, A^\mu_i\, |N(p)\rangle = \bar{u}_{N'}(p')\frac{\tau_i}{2}\left[\gamma^\mu G_A(t) + \frac{iq_\mu}{2M_N} G_P(t)\right]\gamma_5 u_N(p), \tag{2.9}$$

where $G_A(t)$ and $G_P(t)$ are the axial and the induced pseudoscalar form factors, respectively.

The Breit frame. Form factor phenomenology

In general, a free Dirac spinor can be decomposed into two two-component Pauli spinors,

$$u_N = \sqrt{E_{\mathbf{p}} + M_N}\begin{pmatrix}\phi_N & \xi_N\end{pmatrix}, \quad \text{with} \quad \xi_N = \frac{\boldsymbol{\sigma}\cdot\mathbf{p}}{E_{\mathbf{p}} + M_N}\phi_N, \quad \text{and} \quad E^2 = M_N^2 + \mathbf{p}^2. \tag{2.10}$$

Such a decomposition breaks Lorentz invariace, i.e. it is frame dependent. We may thus choose a particularly useful reference frame, the so-called Breit frame, in which the initial and final momenta of the nucleus are equal in magnitude and with opposite sign: $\mathbf{p}_i = -\mathbf{p}_f = \mathbf{q}/2$. The vector $\mathbf{q}$ is therefore the momentum transferred to/by the lepton pair after the interaction, and there is no energy transfer, $q^\mu = p^\mu_f - p^\mu_i = (0, \mathbf{q})$

In the Breit frame, the following relations hold :

$$\bar{u}_N(-\mathbf{p})u_N(\mathbf{p}) = 2E, \quad \bar{u}_N(-\mathbf{p})\gamma_5 u_N(\mathbf{p}) = \phi^\dagger_N \boldsymbol{\sigma}\cdot\mathbf{q}\phi_N, \tag{2.11}$$

$$\bar{u}_N(-\mathbf{p})\gamma^0 u_N(\mathbf{p}) = 2M, \quad \bar{u}_N(-\mathbf{p})\gamma^i u_N(\mathbf{p}) = i\epsilon^{ijk} q^k \phi^\dagger_N \sigma^j \phi_N, \tag{2.12}$$

$$\bar{u}_N(-\mathbf{p})\gamma^0\gamma_5 u_N(\mathbf{p}) = 0, \quad \bar{u}_N(-\mathbf{p})\gamma^i\gamma_5 u_N(\mathbf{p}) = \phi^\dagger_N(2E\sigma^i_T + 2M\sigma^i_L)\phi_N, \tag{2.13}$$

where we have defined

$$\sigma^i_T = \sigma^i - q^i\frac{\mathbf{q}\cdot\boldsymbol{\sigma}}{|\mathbf{q}|^2}, \qquad \sigma^i_L = q^i\frac{\mathbf{q}\cdot\boldsymbol{\sigma}}{|\mathbf{q}|^2}. \tag{2.14}$$

Then, we may write the electromagnetic and axial current off-forward nucleon matrix

elements in the Breit frame as

$$\langle N(p')|\, J^0_{h,\mathrm{em}}\, |N(p)\rangle = e2M_N G_E(t)\phi^\dagger_N\phi_N, \tag{2.15}$$

$$\langle N(p')|\, J^i_{h,\mathrm{em}}\, |N(p)\rangle = ieG_M(t)\epsilon^{ijk}q^k\phi^\dagger_N\sigma^j\phi_N, \tag{2.16}$$

$$\langle N'(p')|\, A^0_a\, |N(p)\rangle = 0, \tag{2.17}$$

$$\langle N'(p')|\, A^i_a\, |N(p)\rangle = \phi^\dagger_{N'}\frac{\tau_a}{2}\left[2EG_A(t)\sigma^i_T + 2M\left(G_A(t)+\frac{t}{2M}G_P(t)\right)\sigma^i_L\right]\phi_N, \tag{2.18}$$

where

$$G_E(t) = F_1(t) + \frac{t}{4M^2}F_2(t), \qquad G_M(t) = F_1(t) + F_2(t) \tag{2.19}$$

are the electric and magnetic (Sachs) form factors [Sac62]. The values of these Form Factors (FFs) at zero momentum transfer are fixed by gauge and Lorentz symmetry to the electric charges and magnetic moments of the corresponding nucleon

$$G^p_E(0) = 1, \qquad G^p_M(0) = \mu_p, \tag{2.20}$$

$$G^n_E(0) = 0, \qquad G^p_M(0) = \mu_n, \tag{2.21}$$

with $\mu_p = 2.79$ and $\mu_n = -1.91$ in units of the nuclear magneton ($\mu = \frac{e\hbar}{2m_p}$).

Electromagnetic form factors of nucleons and nuclei have been measured over the last decades to an impressive level of precision in nuclear scattering experiments such as those at JLab [Pun+15; Cam+14; Arr+23]. The same form factors have been obtained for nucleons and small nuclei using the formalism of chiral perturbation theory [Pia+13] and functional methods [Eic+16].

On the other hand, the computation of the electromagnetic FFs of the nucleon in the Skyrme model was first carried out by Braaten et al. [BTW86]. The same computations for other chiral-soliton models have been carried out several times in the literature, including vector meson contributions as well as in the three-flavour case (see [Wei08] for a pedagogical review). Nevertheless, not much has been done concerning the electromagnetic FFs of light nuclei in the Skyrme model (or any similar solitonic approach to nuclei). Indeed, subsequent papers by Braaten and Carson [BC89] and Carson [Car91b] worked out the formalism to compute FFs of the non spherically-symmetric $B = 2$ (Deuteron) and $B = 3$ (Tritium-Helium) ground states. Almost two decades later, Manton and Wood [MW08] and later Karliner et al. [KKM16] computed the form factors of zero isospin nuclei (in the $B = 4N$) sector. However, a systematic analysis of these FFs still remains to be done for multi-Skyrmions.

Here, we will not be interested in repeating these analyses, but we will adapt some of these methods to the computation of other form factors that, to our knowledge, have not been studied within the Skyrme model, namely, the weak decay multipolar form factors and the gravitational form factors.

2.2 Electroweak form factors of Skyrmions

As reviewed in section 1.2, quantized Skyrmions can be interpreted as models for light nuclei. An important question is then how well does the Skyrme model predict not only

the quantum states and energies of light nuclei, but all other properties concerning their structure and interactions. In particular, information about the inner structure of hadrons can be obtained from the study of form factors

2.2.1 Hadronic currents

In order to compute form factors from the Skyrme model, we first need to identify in the chiral theory the hadronic current operators that couple to electromagnetic and charged weak bosons. Let us consider for instance the electromagnetic current of the first two quark flavors from the interaction terms of the SM:

$$j^{\mu}_{\mathrm{em};q} = \bar{\psi}_f Q_f \gamma^{\mu} \psi_f = \bar{\psi}_f (\tfrac{1}{2}\sigma_3 + \tfrac{1}{6}\mathbf{1})\gamma^{\mu}\psi_f = v^{\mu}_3 + \frac{1}{2} v^{\mu}_0. \tag{2.22}$$

In other words, the photon couples to hadrons via the third isospin vector current and the baryon current, so that the associated charges satisfy the Gell-Mann-Nishijima relation:

$$Q = \frac{1}{2}B + T_3. \tag{2.23}$$

The baryon number current has been already defined in eq. (1.3). On the other hand, an explicit expression for (the classical version of) the vector and axial-vector currents can be obtained from Noether's theorem, given that the infinitesimal version of vector and axial vector tranformations yield

$$U \to U' = U + \epsilon^k \delta U^{\mathrm{v(a)}}_k, \qquad \delta U^{\mathrm{v(a)}}_k = \frac{i}{2}[\tau^k, U]_{-(+)}, \tag{2.24}$$

and from the definition of the corresponding Noether current,

$$I^{\mu}_k = -\frac{1}{24\pi^2}\Big[\mathrm{Tr}\big\{L^{\mu} T^{-}_k\big\} + \mathrm{Tr}\big\{\big[L_{\nu}, L^{\mu}\big]\big[L^{\nu}, T^{-}_k\big]\big\}\Big], \tag{2.25}$$

$$A^{\mu}_k = -\frac{1}{24\pi^2}\Big[\mathrm{Tr}\big\{L^{\mu} T^{+}_k\big\} + \mathrm{Tr}\big\{\big[L_{\nu}, L^{\mu}\big]\big[L^{\nu}, T^{+}_k\big]\big\}\Big]. \tag{2.26}$$

where $T^{\pm}_k$ are the $\mathfrak{su}(2)$ currents defined in eq. (1.19).

These currents depend non-trivially on the Skyrme field $U(x)$. As we are interested in the emission of a gauge boson from a nucleus, we first need to find the correct classical solution within the desired baryon charge sector. Even when the classical Skyrmion configuration is found, the task is not finished yet, since there is no distinction between protons and neutrons in the Skyrme model at the classical level. The current that couples to the weak bosons can be understood as describing a classical source for the charged bosons, but it does not correspond to quantum current operator appearing in the Hamiltonian. To be able to describe such a transition, one must introduce the quantum spin and isospin degrees of freedom. This is usually done within the semi-classical approach to the quantization of Skyrmions. Basically, we introduce time-dependent collective coordinates for the zero modes associated to isospin rotations ($A \in SU(2)_I$), spatial rotations ($B \in SU(2)_S$) and translations ($\mathbf{X} \in \mathbb{R}^3$) as explained in section 1.2 .

We are now interested in writing the corresponding quantum operator associated to the isoscalar, vector and axial-vector Noether currents, eqs. (1.3), (2.25) and (2.26). To

simplify the calculations, let us split the hadronic currents into their timelike and spacelike components: $I^a_\mu = (I^a_0, \mathbf{I}^a)$, $A^a_\mu = (A^a_0, \mathbf{A}^a)$. The associated quantum operators may be obtained by substituting the Skyrme field with collective coordinates (1.13) into the classical expressions. Following the notation in [Car91b], we have:

$$\hat{I}^a_0 = -R^{ab}(A)[u_{bk}(\mathbf{x}')a^k - w_{bk}(\mathbf{x}')b^k], \tag{2.27}$$

$$\hat{I}^a_i = R^{ab}(A)R^T_{ij}(B)I^b_j(\mathbf{x}'), \tag{2.28}$$

$$\hat{A}^a_0 = -R^{ab}(A)[\tilde{u}_{bk}(\mathbf{x}')a^k - \tilde{w}_{bk}(\mathbf{x}')b^k], \tag{2.29}$$

$$\hat{A}^a_i = R^{ab}(A)R^T_{ij}(B)A^b_j(\mathbf{x}'). \tag{2.30}$$

where $\mathbf{x}' = R(B)(\mathbf{x} - \mathbf{X})$, and we have used $A^\dagger \tau^a A = R_{ab}(A)\tau^b$, with $R_{ab}(A) = \frac{1}{2}\operatorname{Tr}\{\tau^a A^\dagger \tau^b A\}$ the $SO(3)$ rotation matrix representing the $SU(2)$ element A.

Although their classical expressions are written in a covariant form, the canonical quantization procedure implies the choice of a reference frame, so quantized Skyrmions are nonrelativistic objects in nature. It is therefore natural to choose the Breit frame when computing the form factors. Let us first consider the matrix element of the current operators between two spatial momentum eigenstates. For an arbitrary hadronic operator, its partial matrix element with respect to momenta in the Breit frame can be written

$$\langle -\mathbf{q}/2|\, F[R(B)(\mathbf{x} - \mathbf{X})]\, |\mathbf{q}/2\rangle = e^{i\mathbf{q}\cdot\mathbf{x}} \int d^3x' \exp\{-i\mathbf{q}\cdot R(B)^T\mathbf{x}'\}F(\mathbf{x}'). \tag{2.31}$$

The exponential inside the integral in the rhs of eq. (2.31) can be expanded in partial waves:

$$\exp\{-i\mathbf{q}\cdot R(B)^T\mathbf{x}'\} = 4\pi \sum_{l=0}^{\infty}(-i)^l j_l(qr) \sum_{m=-l}^{l} Y_{lm}(\hat{\mathbf{q}})Y^*_{lm}(R(B)^T\hat{\mathbf{x}}'), \tag{2.32}$$

being $j_l(x)$ the spherical Bessel functions, and $Y_{lm}(\hat{\mathbf{x}})$ the spherical harmonics.

Thus, when computing matrix elements with respect to the other part of the quantum states (namely, the spin and isospin part), one can just truncate the above expression and compute only the matrix elements of the terms that will be relevant to the process at hand. For illustrative purposes, let us first quickly review the computation of the electromagnetic form factors in the simplest case, the nucleons.

Example: Nucleon form factors

In the $B = 1$ sector, the classical configuration that minimizes the energy can be written in the hedgehogh form (1.67), in terms of a scalar function $f(r)$ (with $r = |\mathbf{x}|$). Further, as argued in chapter 1, the FR constraints associated to its spherical symmetry reduce the allowed states to those with equal total spin and isospin, hence only one of such transformations is really independent. The above arguments allow to write the hadronic

currents for the $B = 1$ sector as

$$\hat{I}_0^a(0) = -\left(\mathbf{X}^2\delta_{ij} - X^iX^j\right)\frac{h(\mathbf{X}^2)}{3u}[K^i, R^{aj}(A)]_+ + \mathcal{O}\big(P^i\big), \tag{2.33}$$

$$\hat{I}_i^a(0) = -\epsilon^{ijk}X^j h(\mathbf{X}^2)R^{ak}(A), \tag{2.34}$$

$$\hat{B}_0(0) = b(\mathbf{X}^2), \tag{2.35}$$

$$\hat{B}_i(0) = \frac{b(\mathbf{X}^2)}{u}\epsilon^{ijk}X^jK^k + \mathcal{O}\big(P^i\big), \tag{2.36}$$

where $h(x)$ and $b(x)$ are two scalar functions given by (in Skyrme units) [BTW86]:

$$h(r) = \frac{1}{12\pi^2}\left[\frac{\sin^2 f}{r^2} + 4\frac{\sin^2 f}{r^2}\left(\left(\frac{\mathrm{d}f}{\mathrm{d}r}\right)^2 + \frac{\sin^2 f}{r^2}\right)\right], \tag{2.37}$$

$$b(r) = -\frac{\sin^2 f}{2\pi^2 r^2}\frac{\mathrm{d}f}{\mathrm{d}r}, \tag{2.38}$$

u is the spin moment of inertia, $|\mathbf{q}| \equiv q$ and we have ommited the part of the operators that's linear in the center of mass momentum $\mathbf{P}$, whose contribution will vanish in the Breit frame. Indeed, for instance the nucleon matrix elements of the isospin charge in the Breit frame are

$$\begin{aligned}
&\langle -\mathbf{q}/2, i_3', k_3'|\, \hat{I}_0^a\, |\mathbf{q}/2, i_3, k_3\rangle = \\
&= -\langle \mathbf{q}/2|\, (\mathbf{X}^2\delta_{ij} - X^iX^j)\frac{h(\mathbf{X}^2)}{3u}\, |\mathbf{q}/2\rangle \left\langle \tfrac{1}{2}, i_3', k_3'\right|\, [K^i, R^{aj}(A)]_+ \left|\tfrac{1}{2}, i_3, k_3\right\rangle \\
&= \frac{1}{3u}\int h(r)r^2 j_0(qr)d^3x\, \langle i_3'|\, \tau_3\, |i_3\rangle\, \delta_{k_3',k_3},
\end{aligned} \tag{2.39}$$

and the rest of the current matrix elements can also be readily computed:

$$\langle -\mathbf{q}/2, i_3', k_3'|\, \hat{I}_i^a\, |\mathbf{q}/2, i_3, k_3\rangle = -i\frac{2}{3}i_3\epsilon^{ijk}q^j\int r\frac{j_1(qr)}{q}h(r)d^3x\, \langle k_3|\, \sigma_k\, |k_3\rangle\,, \tag{2.40}$$

$$\langle -\mathbf{q}/2, i_3', k_3'|\, \hat{B}_0\, |\mathbf{q}/2, i_3, k_3\rangle = \int b(r)j_0(qr)d^3x\delta_{i_3',i_3}\delta_{k_3',k_3}, \tag{2.41}$$

$$\langle -\mathbf{q}/2, i_3', k_3'|\, \hat{B}_i\, |\mathbf{q}/2, i_3, k_3\rangle = -i\frac{1}{2u}\epsilon^{ijk}q^j\int r\frac{j_1(qr)}{q}b(r)d^3x\, \langle k_3|\, \sigma_k\, |k_3\rangle\,. \tag{2.42}$$

In the above calculations, we have made use of the following useful identities [BTW86]:

$$\langle -\mathbf{q}/2|\, f\left(\mathbf{X}^2\right)\, |\mathbf{q}/2\rangle = \int d^3x j_0(qr)f\left(r\right), \tag{2.43}$$

$$\langle -\mathbf{q}/2|\, f\left(\mathbf{X}^2\right)X^j\, |\mathbf{q}/2\rangle = -\frac{i}{q}q^j\int d^3x j_1(qr)rf\left(r\right), \tag{2.44}$$

$$\langle -\mathbf{q}/2|\, f\left(\mathbf{X}^2\right)\left(X^iX^j - \tfrac{1}{3}\mathbf{X}^2\delta^{ij}\right)\, |\mathbf{q}/2\rangle = -\left(q^iq^j - \tfrac{1}{3}q^2\delta^{ij}\right)\int d^3x\frac{j_2(qr)}{q^2}r^2f(r). \tag{2.45}$$

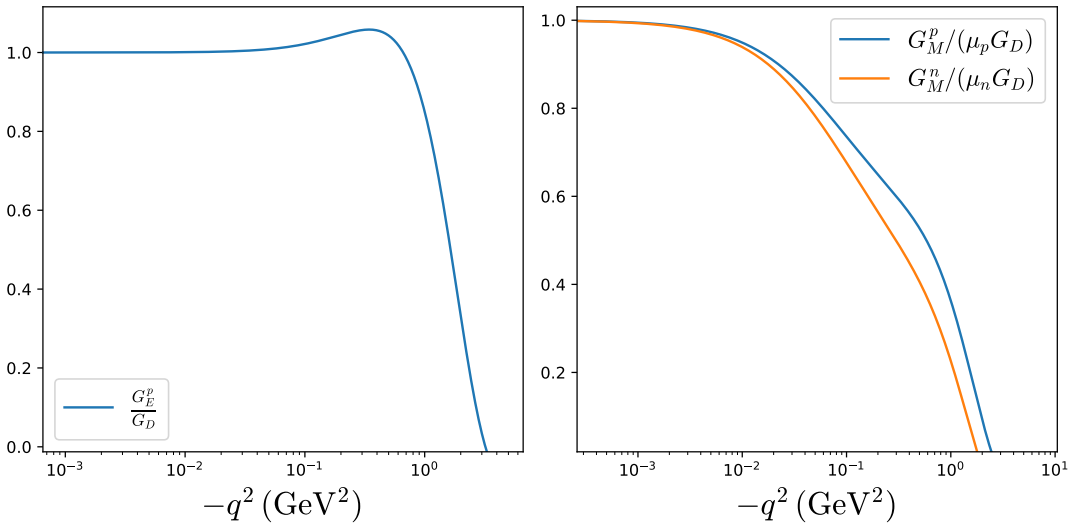

Figure 2.2: Electric (left) and magnetic (right) Sachs form factors of the nucleons, normalized to the dipole parametrization.

as well as the isospin matrix element:

$$\langle -\mathbf{q}/2, i_3', k_3'|\, \tfrac{1}{2}[K^i, R^{aj}]_+ \,|\mathbf{q}/2, i_3, k_3\rangle = -\frac{1}{6}\delta^{ij}\,\langle i_3'|\,\tau^a\,|i_3\rangle\,\langle k_3'|k_3\rangle\,. \tag{2.46}$$

We can now identify the Sachs form factors of the nucleons by noting that the electromagnetic current can be written $J^\mu_{\text{em}} = \frac{1}{2}B^\mu + I_3^\mu$:

$$G_E(i_3, q) = \int \left[b(r) + \frac{2}{3}i_3\frac{h(r)}{u}\right] j_0(qr)d^3x, \tag{2.47}$$

$$G_M(i_3, q) = M_N \int \left[\frac{b(r)}{2u} + \frac{2}{3}i_3 h(r)\right]\frac{j_1(qr)}{q} r d^3x. \tag{2.48}$$

Experimentally, it turns out that these form factors can be well approximated, for momentum transfers of order $-q^2 \lesssim 10\,\mathrm{GeV}$, by the following dipole parametrization, [Pun+15]

$$G_D(t) = (1 + t/M_D^2)^{-2}, \qquad M_D \approx 0.84\,\mathrm{GeV}\,. \tag{2.49}$$

We show in fig. 2.2 our results for the electromagnetic FFs of the nucleons in the Skyrme model with the Adkins-Nappi-Witten choice of parameter values, (see table 2.1) that fit the masses of the proton and the Δ resonance [ANW83a]. Unless otherwise stated, we shall make use of this choice of parameter values for the rest of this chapter.

label	f_π	e	λ^2	m_π
value	133.71	4.628	0	138

Table 2.1: Parameter values that fit to the proton and Δ masses.

2.2.2 Application to nuclear beta decay

For larger baryon number (hence larger total spin/isospin states) the decomposition of the hadron currents in terms of form factors becomes more involved. In general, one is interested in extracting from the hadronic current, the relevant multipolar operators that participate in a particular electromagnetic or weak interaction process. Let us now focus on a particularly interesting application, the determination of the matrix elements of operators involved in the β-decay process of nuclei. Let us first consider the case of the nucleon β decay, in which a neutron becomes a proton after the emission of an electron-antineutrino pair. This process is mediated by a charged weak boson (see the third diagram in fig. 2.1). As we are interested in energy scales way lower than the weak boson masses, the weak boson can be integrated out from the lagrangian to obtain an effective four fermion interaction term,

$$\mathscr{L}_{\text{int}} = \frac{G}{\sqrt{2}}\left[J_\mu^+ l_-^\mu + \text{h.c.}\right], \tag{2.50}$$

where $G = g^2/(4\sqrt{2}M_W^2)$ is the effective coupling constant, g is the weak gauge field coupling, M_W is the W boson mass, and l_μ^a and J_μ^a correspond to the leptonic and hadronic currents, respectively.

The corresponding matrix element will thus have the form

$$\mathcal{M} = -\frac{G}{\sqrt{2}}\int d^3x e^{-i\mathbf{q}\cdot\mathbf{x}} \left\langle N'(p')\right| l^\mu J_\mu \left|N(p)\right\rangle . \tag{2.51}$$

The hadronic current matrix element for a nucleon is usually written in its non relativistic form in terms of the nucleon fields and two experimentally determined coupling constants, namely, the vector and axial-vector couplings, which describe the Fermi and Gamow-Teller transitions, respectively. Indeed, consider the simplest case of the neutron decay. Then, the effective hadronic current can be written

$$J^{+\mu} = \bar{u}_p(x)\gamma^\mu(C_V + C_A\gamma_5)u_n(x). \tag{2.52}$$

As we saw, a Dirac spinor can be decomposed into two two-component bispinors, $u^T = (\phi, \xi)$ (2.10). In the non-relativistic limit, the components of the bispinor ϕ are much larger than those of ξ, and the latter can be neglected. Then:

$$\left\{\bar{u}_p\gamma^0 u_n, \bar{u}_p\gamma^i u_n\right\} \to \left\{\phi_p^\dagger\phi_n, 0\right\}, \qquad \text{Fermi transition} \tag{2.53}$$

$$\left\{\bar{u}_p\gamma^0\gamma_5 u_n, \bar{u}_p\gamma^i\gamma_5 u_n\right\} \to \left\{0, \phi_p^\dagger\sigma^i\phi_n\right\}, \qquad \text{Gamow-Teller transition} \tag{2.54}$$

We see that the vector part of the hadron current only contributes to the temporal component, and yields the Fermi-like matrix elements. On the other hand, the only contribution to the spatial components of the current comes from the axial part, and yields the Gamow-Teller matrix elements.

Also, we can easily write the generalization of the above matrix elements to the case of a nuclear transition from the initial state $|i\rangle$ to the final state $|f\rangle$ as

$$\text{Fermi: } \left\langle f\right|\hat{T}_+\left|i\right\rangle , \quad \text{Gamow-Teller: } \left\langle f\right|\boldsymbol{\sigma}\hat{T}_+\left|i\right\rangle , \tag{2.55}$$

where T_+ is the isospin-raising operator, and $\boldsymbol{\sigma}$ is the vector of Pauli matrices. Therefore, assuming the nonrelativistic approximation and a negligible momentum transfer to the nucleus, the transition matrix element takes the form:

$$S_{if} \sim \frac{G}{\sqrt{2}} 2\pi\delta(E_e + E_\nu - \Delta E_{fi}) \times \Big[C_V \langle f| \hat{T}_+ |i\rangle j_l^0(0) + C_A \langle f| \sigma_i \hat{T}_+ |i\rangle j_l^i(0) \Big]. \quad (2.56)$$

The matrix element (2.56) describes the so called *allowed β decays*, in which leptons are produced with zero spatial angular momentum. *Forbidden transitions* can be described but the full spatial and momentum dependence of the transition operator must be taken into account as well.

In general, the problem of calculating the β decay of an arbitrary unstable nucleus is reduced in the first approximation to the calculation of the Fermi and Gamow-Teller matrix elements for allowed decays. However, due to the non-perturbative nature of low-energy QCD, calculating these matrix elements from first principles becomes impossible, and one needs to develop a model for the nucleus that can be used to calculate the nuclear wavefunctions. In the following, we will derive the form of these matrix elements from the Skyrme model.

2.2.3 Calculating relevant matrix elements

Now the first issue we need to address is to identify the hadronic current entering the effective Fermi interaction term (2.50) within the Skyrme model. A natural course of action would be to construct a current that presents the same tensorial structure as that for elemental particles, which is given by the standard model Feynman rules. Indeed, for fundamental leptons and quarks, the weak charged currents present both a vector and an axial-vector parts, in the combination $v_\mu - a_\mu$. Further, the isospin index structure is determined by the fact that the current must connect the two states of an isospin doublet, hence it must be proportional to $\tau_\pm$ (see eq. (2.8)). We thus conclude that the hadronic charged weak current that enters the Fermi contact interaction term must be of the form

$$J^\mu_{V-A} = I^\mu_+ - A^\mu_+. \quad (2.57)$$

This is consistent with the so-called Conserved Vector Current hypothesis, which states that the isovector components of the electromagnetic and weak currents are only different components of the same, conserved isospin vector current, I^μ_a.

We also remark that the same result could be obtained by promoting the (global) $SU(2)\times U(1)$ chiral symmetry to a local one, and introducing an external gauge field that represents the electroweak gauge bosons. The interaction between the Skyrme field and the charged weak fields can thus be introduced through the following covariant derivative [SS05b; KCP05]:

$$\partial_\mu U \to D_\mu U + iUW_\mu, \qquad W_\mu = -\frac{g}{\sqrt{2}}(W^+_\mu \tau_+ + W^-_\mu \tau_-) \equiv W^a_\mu \tau_a, \quad a = \{+,-\} \quad (2.58)$$

which must substitute the partial derivatives in the Skyrme action. Then, the corresponding current operator can be computed as the functional derivative of the effective action with respect to the external current, $j^\mu_a = \delta S/\delta W^\mu_a$. This is a well-known "trick" to compute hadronic currents in chiral effective theories, see e.g. [Pic95].

Once the hadronic weak current operator has been identified, the next step is to compute its matrix elements connecting different nuclear momentum, spin and isospin eigenstates. In the first approximation, we can truncate the expansion of eq. (2.32) at the zero-th term, which is equivalent to the zero momentum transfer approximation in the Breit frame. As we have commented above, this is sufficient to describe ALLOWED β decays. Moreover, we can in principle calculate also matrix elements corresponding to FORBIDDEN decays, which are however less likely to occur and thus have much longer half-lives. The degree to which a transition is forbidden depends on how far we must take the partial wave expansion to find a nonzero matrix element. The first term beyond the zero term opens the $J = 1$ channel, and yields first-forbidden decays, the next gives second-forbidden, etc [KHS88].

After the partial matrix elements of the relevant operators with respect to momentum eigenstates are computed (which is trivial in the Breit frame for the zero-momentum transfer approximation), it remains to compute the matrix elements between spin and isospin states of the initial and final nuclear wavefunctions. This task cannot be fulfilled in general, and we need specific examples in order to make explicit calculations.

Gamow-Teller matrix element for neutron and tritium decay

In general, the spin and isospin part of the nuclear wavefunction in the Skyrme model is constrained by the symmetries of the classical configuration. A review of the quantization procedure of a classical multi-Skyrmion configuration, and some examples of the quantum states associated to the lowest topological sectors ($B = 1 - 8$) can be found in [MMW07], or chapter 1.

The simplest cases of β decay whose matrix elements we can try to calculate are those for the neutron ($B = 1$) and tritium ($B = 3$). The total spin and isospin quantum numbers of the initial and final wavefunctions are the same in both cases,

$$i = j = k = l = \frac{1}{2}, \tag{2.59}$$

i.e. the neutron and proton form an isospin doublet, as the wavefunctions for ^{3}He and ^{3}H. We are interested in calculating the matrix element between such states of the (spatial part of the) axial current part of the Weak decay current, since it yields the Gamow-Teller matrix element in the forward limit, as argued above.

Spherical symmetry (in the $B = 1$ case) and tetrahedral symmetry (in the $B = 3$ case) makes the classical current $A_i^a(\mathbf{x})$ proportional to the identity, so that

$$\langle -\mathbf{q}/2|\, \hat{A}_i^a \,|\mathbf{q}/2\rangle = \int R^{ab}(A) R_{ij}^T(B) A_j^b(\mathbf{x}) d^3x = R^{ab}(A) R_{ib}^T(B)\alpha, \quad \int A_j^b(\mathbf{x}) d^3x = \alpha \delta_j^b. \tag{2.60}$$

We can label states within the fixed total spin and isospin subspace by their third components of spin and isospin. The matrix element of (2.60) between states with arbitrary i_3, j_3 within the multiplet are given by [Car91b]

$$\langle i_3', j_3'|\, R_{ab}(A) R_{bi}(B) \,|i_3, j_3\rangle = -\frac{1}{3}(\tau_a)_{i_3' i_3}(\sigma_i)_{j_3' j_3}, \tag{2.61}$$

and therefore

$$\langle i_3', j_3', -\mathbf{q}/2|\, \hat{A}_i^a \,|i_3, j_3, \mathbf{q}/2\rangle = -\frac{2}{3}(\tau_a/2)_{i_3' i_3}(\sigma_i)_{j_3' j_3}\alpha. \tag{2.62}$$

Remembering that the axial part of the weak hadronic current actually involves the combination $A_i^+ = A_i^1 + iA_i^2$, we have

$$\langle i_3', j_3', -\mathbf{q}/2|\, \hat{A}_i^+ \,|i_3, j_3, \mathbf{q}/2\rangle = -\frac{2}{3}\alpha \,\langle f|\, \hat{T^+}\sigma_i \,|i\rangle\,, \tag{2.63}$$

where $\hat{T^+} = \frac{1}{2}(\tau_1 + i\tau_2)$ is the isospin raising operator. Comparing with eq. (2.56), we may identify $C_A = -\frac{2}{3}\alpha$. This result was first obtained in [Car91b] for the tritium decay. The axial coupling he obtained is roughly half of the experimental value, although it may be improved with the sextic term and a different calibration of the parameters.

Computation of general multipolar matrix elements

We are ultimately interested in the computation of the hadronic current matrix elements that are relevant for the β-decay process of an arbitrary nucleus, i.e.

$$^A_Z X \to {}^A_{Z+1}X' + e + \bar{\nu}, \tag{2.64}$$

without assuming the zero momentum transfer limit. The most general expression for the matrix element (2.51) in the Skyrme model is

$$\begin{aligned}
\mathcal{M} =& -\frac{G}{\sqrt{2}}\int d^3x e^{-i\mathbf{k}\cdot\mathbf{x}} \left\langle i_3 + \tfrac{1}{2}, J_f, M_f, -\mathbf{q}/2\right| l_\mu \hat{J}^\mu_{V-A}(\mathbf{x}) \left|i_3, J_i, M_i, \mathbf{q}/2\right\rangle = \\
=& -\frac{G}{\sqrt{2}}\int d^3x e^{i(\mathbf{q}-\mathbf{k})\cdot\mathbf{x}} \langle f| \int d^3x' e^{-i\mathbf{q}\cdot R(B)^T\mathbf{x}'} l_\mu J^\mu_{V-A}(\mathbf{x}') \,|i\rangle = \\
=& -\frac{G}{\sqrt{2}}\delta(\mathbf{q}-\mathbf{k}) \langle f| \int d^3x e^{-i\mathbf{k}\cdot\mathbf{x}} [l_0 J^0_{V-A}(R(B)\cdot\mathbf{x}) - l^i R^T_{ij}(B) J^i_{V-A}(R(B)\cdot\mathbf{x})] \,|i\rangle\,,
\end{aligned} \tag{2.65}$$

where we have defined the initial and final eigenstates

$$|i/f\rangle = \left|{}^A Z/{}^A(Z+1), J_{i/f}, M_{i/f}\right\rangle, \tag{2.66}$$

and we have relabelled the third component of isospin by the proton number of the nucleus. We now proceed to rewrite the exponential in a suitable multipolar expansion. Following [Wal04], we decompose the spatial part of the leptonic current in a spherical vector basis, $\boldsymbol{l} = \hat{\mathbf{e}}_0^\dagger l_3 + \sum_{\lambda=\pm1} \hat{\mathbf{e}}_\lambda^\dagger l_\lambda$, where we define the following orthonormal unit vectors:

$$\hat{\mathbf{e}}_0 = \frac{\mathbf{k}}{k}, \qquad \hat{\mathbf{e}}_{\pm1} \equiv \mp\frac{1}{\sqrt{2}}(\hat{\mathbf{e}}_{\mathbf{k}_1} \pm i\hat{\mathbf{e}}_{\mathbf{k}_2}), \tag{2.67}$$

being $\hat{\mathbf{e}}_{\mathbf{k}_1}$ two arbitrary, unitary vectors that are orthogonal between them and with $\hat{\mathbf{e}}_0$. Taking into account the following identities ($k = |\mathbf{k}|$):

$$\begin{aligned}
\hat{\mathbf{e}}^\dagger_{\mathbf{k}\lambda} e^{-i\mathbf{k}\cdot\mathbf{x}} = -\sum_{J\geq1}^{\infty} \sqrt{2\pi(2J+1)}(-i)^J \Big\{ &\lambda j_J(kx)\boldsymbol{\mathcal{Y}}^{-\lambda}_{JJ}(\hat{\mathbf{x}}) + \\
&+ \frac{1}{k}\nabla\times\left[j_J(kx)\boldsymbol{\mathcal{Y}}^{-\lambda}_{JJ}(\hat{\mathbf{x}})\right]\Big\}\Big|_{\lambda=\pm1},
\end{aligned} \tag{2.68}$$

$$\hat{\mathbf{e}}^\dagger_{\mathbf{k}0} e^{-i\mathbf{k}\cdot\mathbf{x}} = \frac{i}{k}\sum_{J\geq0}^{\infty} \sqrt{4\pi(2J+1)}(-i)^J \nabla\left[j_J(kx)Y_{J0}(\hat{\mathbf{x}})\right], \tag{2.69}$$

in terms of the spherical Bessel functions $j_J(x)$, the spherical harmonics Y_{JM}, and *vector spherical harmonics* $\boldsymbol{\mathcal{Y}}^{\lambda}_{JJ}$, defined as [Wal04]:

$$\boldsymbol{\mathcal{Y}}^{M}_{LJ}(\hat{\mathbf{x}}) = \sum_{M',\lambda'} \langle L1M'\lambda'|JM\rangle\, Y_{LM'}\hat{\mathbf{e}}_{\mathbf{k}\lambda'}, \tag{2.70}$$

one can show that the matrix element can be rewritten as

$$\begin{aligned}\mathcal{M} = -\frac{G_F}{\sqrt{2}}\langle f|\Bigg\{ &-\sum_{J\geqslant 1}\sqrt{2\pi(2J+1)}(-i)^J \sum_{\lambda=\pm 1} l_\lambda\left[\lambda\mathcal{M}_{J-\lambda}(k) + \mathcal{E}_{J-\lambda}(k)\right] \\ &+\sum_{J\geqslant 0}\sqrt{4\pi(2J+1)}(-i)^J\left(l_3\mathcal{L}_{J0}(k) - l_0\mathcal{C}_{J0}(k)\right)\Bigg\}|i\rangle,\end{aligned} \tag{2.71}$$

in terms of four different types of multipole Irreducible Tensor Operator (ITO) [Wal04; Kin+23]

$$\mathcal{C}_{JM}(k) = \int d^3x j_J(kr) Y_{JM}\left(\hat{\mathbf{x}}\right) J^0_{V-A}(R(B)\cdot\mathbf{x}), \tag{2.72}$$

$$\mathcal{L}_{JM}(k) = \frac{i}{k}\int d^3x \nabla\left[j_J(kr) Y_{JM}\left(\hat{\mathbf{x}}\right)\right]\cdot R^T(B)\cdot \boldsymbol{J}_{V-A}(R(B)\cdot\mathbf{x}), \tag{2.73}$$

$$\mathcal{E}_{JM}(k) = \int d^3x \nabla\times\left[j_J(kr)\boldsymbol{\mathcal{Y}}^M_{JJ}\left(\hat{\mathbf{x}}\right)\right]\cdot R^T(B)\cdot \boldsymbol{J}_{V-A}(R(B)\cdot\mathbf{x}), \tag{2.74}$$

$$\mathcal{M}_{JM}(k) = \frac{i}{k}\int d^3x \left[j_J(kr)\boldsymbol{\mathcal{Y}}^M_{JJ}\left(\hat{\mathbf{x}}\right)\right]\cdot R^T(B)\cdot \boldsymbol{J}_{V-A}(R(B)\cdot\mathbf{x}). \tag{2.75}$$

Therefore, the amplitude of any process of the form (2.64) will depend on the relevant matrix elements of the above multipole operators. Furthermore, since these are irreducible tensor operators, the matrix elements of a generic multipole $\mathcal{T}_{JM}$ between initial and final nuclear states can be written in terms of the Reduced Matrix Element (RME) $\langle J_f||\mathcal{T}_J||J_i\rangle$ by virtue of the Wigner-Eckart theorem:

$$\langle J_f M_f|\,\mathcal{T}_{JM}\,|J_i M_i\rangle = \frac{\langle J_i J M_i M|J_f M_f\rangle}{\sqrt{2J_i+1}}\langle J_f||\mathcal{T}_J||J_i\rangle. \tag{2.76}$$

Example: Multipole operators of ^{6}He beta decay

Once we have shown that the weak Hamiltonian can be expanded in an infinite sum of multipole operators with definite total angular momentum J and parity, let us now focus on a particular example: the pure Gamow-Teller transition ^{6}He$(0+) \to {}^6$Li$(1+)$, which only receives contributions from operators with $J = 1$ between the initial state $|{}^6\text{He}, 00\rangle$ and the final state $|{}^6\text{Li}, 10\rangle$. This transition has been measured with extraordinary accuracy [Cir+19], and the prediction of the contribution from each of the relevant multipolar terms has became a benchmark for many different theoretical approaches [Kin+23; VBG09]

The simplest of these operators is $C_1(k) \equiv \langle 1||\mathcal{C}_1(k)||0\rangle$, which can be computed using the Wigner-Eckart theorem (2.76),

$$C_1(k) = \frac{\langle 1,0|\,\mathcal{C}_{10}(k)\,|0,0\rangle}{\langle 0100|10\rangle} = \langle 1,0|\,\mathcal{C}_{10}(k)\,|0,0\rangle\,. \tag{2.77}$$

We will now go through the step by step computation of such matrix element to demonstrate the power of this formalism in the Skyrme model. We start by extracting the explicit dependence of the multipole operator $\mathcal{C}_{JM}(k)$ on the zero mode collective coordinate operators. We first note that the dependence on the spin rotation matrix can be factorized from (2.72) by changing the integration variable, to get

$$\mathcal{C}_{JM}(k) \equiv \sum_{M'} \mathscr{D}^1_{MM'}(B^\dagger) \int d^3x j_J(kx) Y_{JM'}(\hat{\mathbf{x}})\, J^0_{V-A}(\mathbf{x}), \tag{2.78}$$

where we have taken into account that the spherical harmonics of degree l transform in the $(2l+1)$dimensional IRREDUCIBLE REPRESENTATION (irrep) of the rotation group. We remark that this transformation property is in fact a characteristic shared by all four operators in eqs. (2.72) to (2.75), due to their ITO nature. On the other hand, the weak hadronic current operator can be written in terms of the vector and axial-vector isospin currents as

$$\begin{aligned}
\hat{J}^0_{V-A}(\mathbf{x}) &= \hat{I}^0_+(\mathbf{x}) - \hat{A}^0_+(\mathbf{x}) = \\
&= e^c_{\lambda=+1} \frac{1}{2} \left[\frac{(u_{ab} - \tilde{u}_{ab})(\mathbf{x})}{u} [R_{ca}(A), K^b]_+ + \frac{(w_{ab} - \tilde{w}_{ab})(\mathbf{x})}{v} [R_{ca}(A), L^b]_+ \right] \\
&\approx - \sum_{\lambda'=0,\pm1} \frac{1}{2} [\mathscr{D}^1_{1\lambda'}(A), K^b]_+ e^a_{\lambda'} \left[\frac{(u_{ab} - \tilde{u}_{ab})(\mathbf{x})}{u} \right] = \\
&= - \sum_{\lambda',\sigma=0,\pm1} \frac{1}{2} [\mathscr{D}^1_{1\lambda'}(A), K^\sigma]_+ e^a_{\lambda'} \left[\frac{(u_{ab} - \tilde{u}_{ab})(\mathbf{x})}{u} \right] e^{\dagger b}_\sigma,
\end{aligned} \tag{2.79}$$

In the second step we have made use of the fact that for the $B = 6$ Skyrmion, the sphericity condition (2.133) is very well satisfied, and we have also made the approximations

$$w \ll u, \qquad \frac{(w - \tilde{w})_{ab}}{v} \ll \frac{(u - \tilde{u})_{ab}}{u} \tag{2.80}$$

which are also very good for the case at hand(indeed, the neglected terms amount up to a few percent of the leading terms).

Combining eqs. (2.78) and (2.79), we have

$$\begin{aligned}
\mathcal{C}_{JM}(k) &= \sum_{M',\lambda',\sigma=0,\pm1} \mathscr{D}^1_{MM'}(B^\dagger) \frac{1}{2} [\mathscr{D}^1_{1\lambda'}(A), K^\sigma]_+ \int d^3x j_J(kx) Y_{JM'}(\hat{\mathbf{x}})\, e^a_{\lambda'} \left[\frac{(\tilde{u}_{ab} - u_{ab})(\mathbf{x})}{u} \right] e^{\dagger b}_\sigma \\
&\equiv \mathscr{D}^1_{MM'}(B^\dagger) \frac{1}{2} [\mathscr{D}^1_{1\lambda'}(A), K^\sigma]_+ \Gamma^{\lambda'\sigma}_{JM'}(k).
\end{aligned} \tag{2.81}$$

In the last step of (2.81), we have ommited the summation symbol and adopted Einstein's summation convention also for repeated spherical indices (M', λ'). This factorized expression allows us to compute the matrix element between the desired nuclear states, which, using the notation of eq. (1.25), are given by

$$\left|{}^6\mathrm{He}; 0, 0\right\rangle = |1, -1, 0; 0, 0, 0\rangle\,, \qquad \left|{}^6\mathrm{Li}; 1, 0\right\rangle = |0, 0, 0; 1, 0, 0\rangle\,. \tag{2.82}$$

Hence we have

$$\begin{aligned}
&\left\langle {}^6\mathrm{Li}; 1, 0\right| \mathcal{C}_{10}(k) \left|{}^6\mathrm{He}; 0, 0\right\rangle = \\
&= \langle 1,0,0|\, \mathscr{D}^1_{0M'}(B^\dagger)\, |0,0,0\rangle \, \langle 0,0,0|\, \frac{1}{2}[\mathscr{D}^1_{1\lambda'}(A), K^\sigma]_+ \, |1,-1,0\rangle \, \Gamma^{\lambda'\sigma}_{1M'}(k) = \\
&= \frac{1}{2} \langle 1,0,0|\, \mathscr{D}^1_{0M'}(B^\dagger)\, |0,0,0\rangle \Big[- \langle 0,0,0|\, \mathscr{D}^1_{1\lambda'}(A)\, |1,-1,1\rangle \, \Gamma^{\lambda' 1}_{1M'}(k) + \\
&\qquad + \langle 0,0,0|\, \mathscr{D}^1_{1\lambda'}(A)\, |1,-1,-1\rangle \, \Gamma^{\lambda' -1}_{1M'}(k) \Big], \qquad (2.83)
\end{aligned}$$

where we have used the following relation between the angular momentum operators in the spherical basis and the ladder operators:

$$\begin{aligned}
K^{\sigma=-1} &= \frac{1}{\sqrt{2}} \left(K^x - iK^y\right) = \frac{K_-}{\sqrt{2}}, \\
K^{\sigma=0} &= K^z, \\
K^{\sigma=1} &= -\frac{1}{\sqrt{2}} \left(K^x + iK^y\right) = -\frac{K_+}{\sqrt{2}}. \qquad (2.84)
\end{aligned}$$

The matrix element of a Wigner D-function between angular momentum eigenstates can be straightforwardly calculated in terms of Clebsch-Gordan coefficients. We define the coefficients

$$\begin{aligned}
\chi^{(j_1,m_1,m_1')}_{(j_3,m_3,m_3')}(j_2, m_2, m_2') &= \langle j_1, m_1, m_1'|\, \mathscr{D}^{j_2}_{m_2 m_2'}(A)\, |j_3, m_3, m_3'\rangle = \\
&= \frac{\sqrt{(2j_1+1)(2j_3+1)}}{2\pi^2} \int d\mu(A) \mathscr{D}^{j_1 *}_{m_1 m_1'}(A) \mathscr{D}^{j_2}_{m_2 m_2'}(A) \mathscr{D}^{j_3}_{m_3 m_3'}(A) = \\
&= \sqrt{\frac{2j_3+1}{2j_1+1}} \, \langle j_2 j_3 m_2 m_3 | j_1 m_1 \rangle \, \langle j_2 j_3 m_2' m_3' | j_1 m_1' \rangle \,, \qquad (2.85)
\end{aligned}$$

where we have used the property $\mathscr{D}^{j*}_{mm'}(A) = \mathscr{D}^{j}_{m'm}(A^\dagger)$ and the $SU(2)$ integration formula [BC89]:

$$\int d\mu(B) \mathscr{D}^i(B)_{m_1 m_1'} \mathscr{D}^j(B)_{m_2 m_2'} \mathscr{D}^k\left(B^\dagger\right)_{m_3' m_3} = \frac{2\pi^2}{2k+1} \, \langle ij m_1 m_2 | k m_3 \rangle \, \langle ij m_1' m_2' | k m_3' \rangle \,. \qquad (2.86)$$

Note that the integral above does not depend on the $SU(2)$ elements, and neither do the coefficients defined in (2.85). We thus arrive to our final result:

$$\begin{aligned}
C_1(k) &= \left\langle {}^6\mathrm{Li}; 1, 0\right| \mathcal{C}_{10}(k) \left|{}^6\mathrm{He}; 0, 0\right\rangle = \\
&= \frac{1}{2} \sum_{M', \lambda' = -1}^{1} \chi^{(1,0,0)}_{(0,0,0)}(1,0,M') \Big[\chi^{(0,0,0)}_{(1,-1,-1)}(1,1,\lambda') \Gamma^{\lambda' -1}_{1M'}(k) - \chi^{(0,0,0)}_{(1,-1,1)}(1,1,\lambda') \Gamma^{\lambda' 1}_{1M'}(k) \Big] = \\
&= \frac{1}{6}(-\Gamma^{-1,1}_{1,0}(k) + \Gamma^{1,-1}_{1,0}(k)) = \frac{1}{3} \Gamma^{ab}_{1,0}(k) e_1^{[a} e_{-1}^{b]} = i \frac{1}{3} \Gamma^{[xy]}_{1,0}(k) = \\
&= \frac{i}{4\sqrt{3\pi}} \int j_1(kr) \frac{z}{r} \frac{(\tilde{u}_{xy} - u_{xy})(\mathbf{x}) - (\tilde{u}_{yx} - u_{yx})(\mathbf{x})}{u} d^3x \qquad (2.87)
\end{aligned}$$

If we take into account that, for the decay we are considering, the momentum transfer is of order $q/m_\pi \lesssim 0.03$, the spherical Bessel functions can be approximated by

$$j_j(x) \sim \frac{x^l}{(2l+1)!!} \tag{2.88}$$

and thus, at the first nontrivial order in the momentum transfer expansion [Kin+23] we find:

$$C_1(k) \sim -\frac{i}{3}\frac{k}{m_\pi}C_1^{(1)} + \mathcal{O}\big(k^2/m_\pi^2\big), \qquad C_1^{(1)} = \frac{m_\pi}{2\sqrt{3\pi}}\int z\frac{(\tilde{u}_{[xy]} - u_{[xy]})(\mathbf{x})}{u}d^3x \tag{2.89}$$

numerically, we obtain $C_1^{(1)} \sim 10^{-4}$, i.e. this multipole contribution is very supressed in the beta decay of ^{6}He.

Indeed, the multipole operators that will be most relevant will be those that are of order $\mathcal{O}(k^0)$ in the momentum transfer, which will in general yield the leading contribution to Fermi and Gamow-Teller allowed transitions. Let us consider for example the leading Gamow-Teller multipole, $\mathcal{L}_{10}$. In the low momentum transfer approximation,

$$\nabla\left[j_1(kx)Y_{1M}\left(\hat{\mathbf{x}}\right)\right] = \frac{k}{3}\Big(Y_{1M}\left(\hat{\mathbf{x}}\right)\frac{\mathbf{x}}{r} + r\nabla Y_{lm}(\hat{\mathbf{x}})\Big) + \mathcal{O}(kr). \tag{2.90}$$

Also, as in the previous case, a change of variables in (2.73) allows us to write

$$\mathcal{L}_{10}(0) \sim i\sum_{M'}\mathscr{D}^1_{0M'}(B^\dagger)\int d^3x\frac{1}{3}\Big(Y_{1M'}(\hat{\mathbf{x}})\frac{\mathbf{x}}{r} + r\nabla Y_{1M'}(\hat{\mathbf{x}})\Big)\mathbf{J}_{V-A}(\mathbf{x}), \tag{2.91}$$

and we have

$$\begin{aligned} L_1(0) &= \left\langle {}^6\mathrm{Li};1,0\right|\mathcal{L}_{10}(0)\left|{}^6\mathrm{He};0,0\right\rangle = \\ &= \frac{i}{3}\sum_{M',\lambda'=-1}^{1}\chi^{(1,0,0)}_{(0,0,0)}(1,0,M')\chi^{(0,0,0)}_{(1,-1,0)}(1,1,\lambda')\int\Big(Y_{1M'}\frac{\mathbf{x}}{r} + r\nabla Y_{1M'}\Big)(I^i_{\lambda'} - A^i_{\lambda'})d^3x = \\ &= -i\frac{1}{9}\sqrt{\frac{3}{4\pi}}\int[I^3_3(\mathbf{x}) - A^3_3(\mathbf{x})]d^3x = \frac{-i}{3}L_1^{(0)}, \end{aligned} \tag{2.92}$$

from which an effective value for the axial coupling constant can be extracted [Kin+23]. Numerically, we obtain $L_1^{(0)} \sim 0.19$, which is a 20% of its measured value, too small even for the Skyrme model standards.

2.3 Gravitational form factors

The Gravitational Form Factors (GFFs) of a nucleon describe the scattering of a graviton with a nucleon, or, equivalently, the response of a nucleon to the passing of a (quantized) gravitational wave. Obviously, a direct measurement of such quantity is not available, as this would require a controlled experimental setup to scatter a nucleon from isolated gravitons. However, indirect ways to measure these form factors in lepton-nucleon scattering experiments have been proposed, such as in the Deeply Virtual Compton Scattering (DVCS) process, in which a high-energy electron is scattered off a nucleon by

exchanging a virtual photon. Then, a highly energetic real photon is emitted from one of the quarks inside the nucleon, which carries information on the quark's transverse position and longitudinal momentum. This can be seen as an effective, two-photon interaction with the nucleus, which can thus probe spin-2 correlation functions such as those appearing in the GFFs.

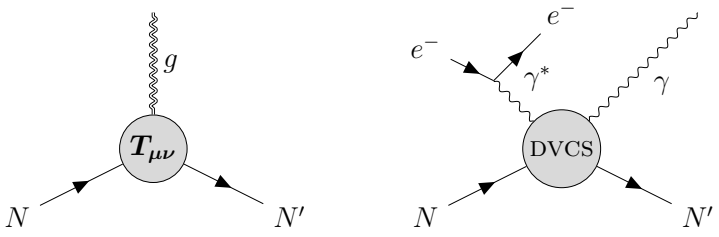

Figure 2.3: Hypothetical graviton emission process from a nucleon (left) and Deeply Virtual Compton Scattering (right)

The GFFs are form factors associated with the QCD Energy Momentum Tensor (EMT) $T_{\mu\nu}$ [KO62; Pag66]. Much like the electromagnetic form factors, they contain a wealth of information about the structure of the nucleons, or more generally hadrons and nuclei. However, unlike the latter which have enjoyed more than 70 years of continual theoretical and experimental efforts, it was not until recently that GFFs started to attract community-wide attention [PS18]. A major catalyst is the Electron Ion Collider (EIC) project [Abd+22] poised to uncover the mass and spin structure of the nucleons and nuclei. Since the EMT encodes mechanical properties such as mass, angular momentum, internal forces and their distribution, the study of GFFs is perfectly aligned with the core missions of the EIC. In a sense, the GFFs are more 'quintessentially QCD' than the electromagnetic form factors, since they can be defined without reference to QED.

Indeed, the off-forward nucleon matrix element of the QCD EMT can be parameterized as

$$\langle p'|T_{\mu\nu}|p\rangle = \bar{u}(p')\Big[\gamma_{(\mu}P_{\nu)}A(t) + \frac{iP_{(\mu}\sigma_{\nu)\rho}q^{\rho}}{2M_N}B(t) + \frac{q_\mu q_\nu - \eta_{\mu\nu}q^2}{4M_N}D(t)\Big]u(p), \tag{2.93}$$

where $P_\mu = (p_\mu + p'_\mu)/2$ and $q = p' - p$ is the momentum transfer with $t = q^2$. $A_{(\mu}B_{\nu)} = \frac{A_\mu B_\nu + A_\nu B_\mu}{2}$ denotes symmetrization. $u(p)$ is the nucleon spinor normalized as $\bar{u}(p)u(p) = 2M_N$ with M_N being the mass of the nucleon. The same formula applies to all the spin-1/2 nuclei with trivial changes. The gravitational form factors A, B, D are scalar, renormalization-group invariant functions of t. In the zero momentum transfer limit, i.e. $t = 0$, the values of $A(t = 0)$ and $B(t = 0)$ are constrained to 1 and 0 due to momentum and angular momentum conservation, respectively. However, the so-called D-term $D = D(t = 0)$ is not constrained by any symmetry, and this is our main object of interest, as it is related to the 'pressure' distribution inside hadrons and nuclei [PS18]. Its value at vanishing momentum transfer $D(t = 0)$, often referred to as the *D-term*, is a fundamental constant similar to the magnetic moment. While the value is presently unknown, even for the nucleons, in principle the form factor $D(t)$ can be experimentally accessed in DVCS [AT07] and near-threshold quarkonium photo- and electro-production in electron-nucleon scattering [HY18; BH20; HS21; GJL21; MZ22]. The same methods could be used to measure the $D(t)$ of light nuclei at the EIC.

The application of the Skyrme model to GFFs has been so far limited to the $B = 1$ sector (nucleons and their excited states) [Ceb+07; PPS16; KS21] which is relatively tractable due to the spherical symmetry of the classical solution. In fact, all the known Skyrmion solutions with $B > 1$ are not spherically symmetric. Yet, each solution possesses a (discrete) symmetry group, and techniques from group theory can greatly facilitate the extraction of form factors as we have illustrated in the previous sections in the context of the electromagnetic and weak form factors. In this section, we shall adapt this method to the computation of GFFs.

It should be mentioned that the form factor $D(t)$ for nuclei has been calculated in other models [Pol03; LT05; GS06] and its dependence on the atomic number has been studied. We shall compare our result with these previous calculations at the end of the next sextion.

The EMT of the model can be obtained via the Hilbert prescription, i.e. minimally coupling the scalar chiral field to a nontrivial background metric $g_{\mu\nu}$, and vary the action with respect to this metric. For our sign convention this can be written:

$$T^{\mu\nu} = -\frac{2}{\sqrt{-g}}\frac{\delta S}{\delta g_{\mu\nu}} = -\frac{2}{\sqrt{-g}}\frac{\partial(\mathscr{L}\sqrt{-g})}{\partial g_{\mu\nu}}. \tag{2.94}$$

The minimal coupling to a gravitational field is a trivial task for all terms in the GSM lagrangian but the sextic. Indeed, the sextic term contribution to the action in a gravitational field is

$$S = -\int d^4x\sqrt{-g}\lambda^2\pi^4 g_{\mu\nu}\frac{B^\mu B^\nu}{-g}. \tag{2.95}$$

Note that the definition of B^μ involves a Levi-Civita tensor, hence it transforms as a tensor density of rank one and each must include a factor of $|g|^{-\frac{1}{2}}$ [Ada+15c]. Then, we have

$$-\frac{2}{\sqrt{-g}}\frac{\delta(\mathscr{L}\sqrt{-g})}{\delta g_{\mu\nu}} = \lambda^2\pi^4\frac{2}{\sqrt{-g}}\left[\frac{B^\mu B^\nu}{\sqrt{-g}} + g_{\alpha\beta}B^\alpha B^\beta\frac{\delta|g|^{-\frac{1}{2}}}{\delta g_{\mu\nu}}\right] = 2\lambda^2\pi^4\left[\frac{B^\mu B^\nu}{|g|} - \frac{g^{\mu\nu}}{2|g|}g_{\alpha\beta}B^\alpha B^\beta\right], \tag{2.96}$$

and T^{00} has overall positive sign. To compute T_{00} with the Hilbert prescription one should also take into account that $B_\mu = g_{\mu\nu}B^\nu$.

Therefore, the full Skyrme EMT for our sign convention is given by

$$\begin{aligned} T_{\mu\nu} =& \frac{1}{2}\operatorname{Tr}\{-2L_\mu L_\nu + \eta_{\mu\nu}L_\rho L^\rho\} - \frac{1}{4}\operatorname{Tr}\big\{-4[L_\mu, L_\rho][L_\nu, L^\rho] + \eta_{\mu\nu}[L_\rho, L_\sigma]^2\big\} \\ &+ 8\pi^4 c_6 B_\mu B_\nu - 4\pi^4 c_6 B_\rho B^\rho\eta_{\mu\nu} + c_0(1-\sigma)\eta_{\mu\nu}. \end{aligned} \tag{2.97}$$

We shall be mainly interested in the $\mu\nu = i, j$ (spatial) components. The relevant traces we need to compute are:

$$\operatorname{Tr}\{-L_iL_j\} = \operatorname{Tr}\big\{\partial_iU^\dagger\partial_jU\big\} = 2\partial_i\phi^\alpha\partial_j\phi^\alpha, \tag{2.98}$$

$$\begin{aligned} \operatorname{Tr}\{L_iL_jL_kL_l\} &= \operatorname{Tr}\big\{\partial_iU^\dagger\partial_jU\partial_kU^\dagger\partial_lU\big\} = \\ &= 2\partial_i\phi^\alpha\partial_j\phi^\beta\partial_k\phi^\gamma\partial_l\phi^\delta(2\delta_{\alpha\beta}\delta_{\gamma\delta} + \delta_{\alpha\gamma}\delta_{\beta\delta} - \delta_{\alpha\delta}\delta_{\beta\gamma} - \epsilon_{\alpha\beta\gamma\delta}) \end{aligned} \tag{2.99}$$

and contractions of these. We have used the properties of the τ_α (see e.g. appendix D in [Esp90]).

2.3.1 The D term

In this section, we outline our strategy to compute the $D(t)$ form factor for the $B = 1$ (nucleons), $B = 2$ (deuteron) and $B = 3$ (helium-3 and triton) solutions. These three examples are representative of different situations one encounters in the computations of $D(t)$ in the Skyrme model. Despite the differences, however, under certain assumptions we shall arrive at the same formula in all cases. This motivates us to extrapolate our discussion to solutions with arbitrary values of B. The actual computation of the form factor is carried out in the next section.

$B = 1$: the nucleons

The $D(t)$ form factor can be isolated by working in the Breit frame ($\boldsymbol{p}' = -\boldsymbol{p} = \boldsymbol{q}/2$, $t = -\boldsymbol{q}^2$) and taking the spatial $i, j = 1, 2, 3$ components:

$$\langle p'|T_{ij}|p\rangle = 2P^0 \frac{D(t)}{4M_N}(q_i q_j - \boldsymbol{q}^2\delta_{ij}) \approx \frac{D(t)}{2}(q_i q_j - \boldsymbol{q}^2\delta_{ij}), \tag{2.100}$$

where we used the nonrelativistic approximation in the last expression. Classically, in the Skyrme model, $D(t)$ can be obtained by simply Fourier-transforming the classical EMT T^{cl}_{ij} (2.97). For spherically symmetric configurations such as the $B = 1$ solution, the EMT can be written in terms of the 'shear' and 'pressure' distributions

$$T^{cl}_{ij}(\mathbf{x}) = \left(\frac{x_i x_j}{x^2} - \frac{1}{3}\delta_{ij}\right)s(x) + p(x)\delta_{ij}. \tag{2.101}$$

(Below we shall write $|\mathbf{x}| = x$ and $|\boldsymbol{q}| = q$ for simplicity.) It then follows that

$$D(t) \;=\; -6M_N \int d^3x \left(x^i x^j - \frac{1}{3}\delta^{ij}x^2\right)\frac{j_2(qx)}{(qx)^2}T^{cl}_{ij}(\mathbf{x}). \tag{2.102}$$

In particular,

$$\begin{aligned} D(t=0) \;&=\; -\frac{2M_N}{5}\int d^3x \left(x_i x_j - \frac{1}{3}x^2\delta_{ij}\right)T^{cl}_{ij}(\mathbf{x}) \\ &=\; -\frac{4M_N}{15}\int d^3x\, x^2 s(x). \end{aligned} \tag{2.103}$$

We see that the D-term is related to the distribution of shear forces inside the nucleon, parametrized in the spherically symmetric case by the function $s(x)$. It is interesting to note that in the so-called BPS Skyrme model, a solution that saturates the Bogomolny bound exists [ASW10b]. For this particular solution, the EMT is that of a perfect fluid [Ada+15a], that is, the shear force vanishes. Therefore, the D-term is exactly zero in this limit. From physical point of view, the passing of a gravitational wave causes a volume preserving deformation of the nucleon, which is precisely a symmetry in the BPS model [ASW10b]. Therefore, in this limit, nucleons are transparent to gravitons.

Returning to general situations with $s(x) \neq 0$, we now consider the effect of quantization (1.13) and write the matrix element between momentum eigenstates as

$$\langle \boldsymbol{q}/2|T_{ij}[U(R(B)(\mathbf{x}-\mathbf{X}))]|-\boldsymbol{q}/2\rangle = e^{-i\boldsymbol{q}\cdot\mathbf{x}}R^T_{ia}(B)R^T_{jb}(B)\int d^3x' \exp\{i\boldsymbol{q}\cdot R^T(B)\mathbf{x}'\}T_{ab}(\mathbf{x}'), \tag{2.104}$$

where

$$T_{ab}(\mathbf{x}) = T^{cl}_{ab}[U_0(\mathbf{x})] + \mathcal{O}\big(I^2, J^2\big). \tag{2.105}$$

Both R^T and T_{ab} in (2.104) are operators which act on spin and isospin eigenstates (1.25). In general, the calculation of their matrix elements is a complicated task. However, since our main objective is to evaluate the $D(t)$-form factor for a wide variety of nuclei with different spin/isospin quantum numbers rather than focusing on a particular nucleus, we neglect the $\mathcal{O}(I^2, J^2)$ terms in (2.104). This may be partially justified by the large-N_c approximation.

Even after this approximation, (2.104) still contains the spatial rotation matrix R^T which acts on external spin states. To deal with it, we expand the exponential on the right hand side in partial waves $l = 0, 1, 2, \cdots$

$$\begin{aligned}\exp\big\{i\boldsymbol{q}\cdot R^T(B)\mathbf{x}\big\} \;=\; & j_0(qx) + iq_c R^T_{ck}(B)x_k\frac{3j_1(qx)}{qx} \\ & -\frac{1}{2}\left(q_cq_d - \frac{1}{3}\delta_{cd}q^2\right)R^T_{ck}(B)R^T_{dl}(B)\left(x_kx_l - \frac{1}{3}\delta_{kl}x^2\right)\frac{15j_2(qx)}{(qx)^2} + \cdots .\end{aligned} \tag{2.106}$$

In order to extract the $D(t)$-form factor, it suffices to focus on the $l = 2$ tensor term and read off the coefficient of q_iq_j. One then needs to evaluate the integral

$$T_{abkl} = \int d^3\mathbf{x}\left(x_kx_l - \frac{1}{3}\delta_{kl}x^2\right)\frac{15j_2(qx)}{(qx)^2}T^{cl}_{ab}(\mathbf{x}). \tag{2.107}$$

For a spherically symmetric solution, the tensorial structure is completely fixed by symmetry

$$T_{abkl} = \frac{1}{10}\left(\delta_{ak}\delta_{bl} + \delta_{il}\delta_{jk} - \frac{2}{3}\delta_{ij}\delta_{kl}\right)T_{cdcd}. \tag{2.108}$$

Note that the trace part $T^{cl}_{ab} \sim \delta_{ab}$ does not contribute to the integral (2.107). Substituting (2.108) into (2.104), we see that the R^T matrices disappear due to the orthogonality relation $RR^T = 1$ and we recover the formula (2.102).

One might wonder that, since we have neglected the $\mathcal{O}(J^2, I^2)$ terms in (2.105), what the effects of quantization are in the present calculation. The point is that if the classical solution is not spherically symmetric, the tensor T_{abkl} does not have the canonical form (2.108) in general. The introduction of the R-matrix then becomes crucial to restore the symmetry. We shall see examples of this below.

$B = 2$: the deuteron

We now turn to the $B = 2$ sector, the 'deuteron', with spin $J = 1$. For spin-1 nuclei, there are in general six independent gravitational form factors [Hol06] related to the fact that the nuclear wavefunction is not spherically symmetric. In particular, it is well-known that the deuteron wavefunction has quadrupole deformation. In terms of the EMT matrix element, this is most clearly shown by the following multipole expansion in the Breit frame in the nonrelativistic limit [PS19]

$$\begin{aligned}\langle p'\sigma'|T_{ij}|p\sigma\rangle =& \frac{1}{2}(q_iq_j - \delta_{ij}q^2)\mathcal{D}_1(t)\epsilon^*_{\sigma'}\cdot\epsilon_\sigma + \big(q_jq_kQ_{ik} + q_iq_kQ_{jk} - q^2Q_{ij} - \delta_{ij}q_kq_lQ_{kl}\big)_{\sigma'\sigma}\mathcal{D}_2(t) \\ & + \frac{1}{2M_D^2}(q_iq_j - \delta_{ij}q^2)q_kq_lQ_{kl,\sigma'\sigma}\mathcal{D}_3(t) + \cdots\end{aligned} \tag{2.109}$$

where M_D is the deuteron mass. ϵ_σ are the polarization vectors of the deuteron with spin $\sigma = \pm 1, 0$ measured along the x^3-direction (not helicity). $Q_{ij,\sigma'\sigma} \equiv \langle \sigma' | \hat{Q}_{ij} | \sigma \rangle$ is the matrix element of the quadrupole operator

$$\hat{Q}_{ij} = \frac{1}{2}\left(J_i J_j + J_j J_i - \frac{4}{3}\delta_{ij} \right), \tag{2.110}$$

where J_i is the spin-1 operator with matrix elements $\langle \sigma' | J_i | \sigma \rangle = -i\epsilon_{ijk}\epsilon^*_{\sigma' j}\epsilon_{\sigma k}$. While the quadrupole part is of interest in its own right (see recent extractions for the ρ-meson [FC19; PHS22]), we will only focus on the monopole part $\mathcal{D}_1$. The Q-dependent terms can be eliminated by averaging over the three spin states thanks to the identity

$$\sum_{\sigma}^{\pm,0} Q_{ij,\sigma\sigma} = 0. \tag{2.111}$$

Restricting ourselves to this simpler situation, we write

$$\frac{1}{3}\sum_{\sigma} \langle p'\sigma | T_{ij} | p\sigma \rangle = \frac{1}{2}(q_i q_j - \delta_{ij} q^2) D(t), \tag{2.112}$$

where we renamed $D(t) = \mathcal{D}_1(t)$ to emphasize the correspondence with (2.100).

Turning now to the Skyrme model, we recall that the classical $B = 2$ solution has toroidal symmetry [BC88] and is mainly characterized by a c-number quadrupole tensor Q_{ij} [PS19]

$$\begin{aligned} T^{cl}_{ij} \approx Y_2^{ij} s(x) + p(x)\delta_{ij} \quad &+ \quad 2s'(x)\left(Q_{ik}Y_2^{kj} + Q_{jk}Y_2^{ki} - \delta_{ij}Q_{ab}Y_2^{ab} \right) + p'(x)Q_{ij} \\ &- \frac{1}{M_D^2} Q^{kl}\partial_k\partial_l \left(p''(x)\delta^{ij} + s''(x)Y_2^{ij} \right), \end{aligned} \tag{2.113}$$

where we abbreviated $Y_2^{ij} = \frac{x_i x_j}{x^2} - \frac{\delta_{ij}}{3}$. In principle, Q_{ij} can be numerically extracted from a given Skyrmion configuration. But in parallel with the spin-averaging procedure above, we eliminate it by forming the moment (2.102) and using the integrals

$$\begin{aligned} &\int d^2\Omega Y_2^{ij} = 0, \qquad \int d^2\Omega Y_2^{ij}\left(Q_{ik}Y_2^{kj} + Q_{jk}Y_2^{ki} - \delta_{ij}Q_{ab}Y_2^{ab} \right) = 0, \\ &Q^{kl}\int d^2\Omega Y_2^{ij}\partial_k\partial_l \left(s''(x)Y_2^{ij} \right) = 0, \end{aligned} \tag{2.114}$$

where we used the traceless property $Q_{ii} = 0$. We thus see that the $D(t)$ form factor as defined in (2.112) can be calculated via the same formula (2.102) with the trivial replacement $M_N \to M_D$ even if the classical solution is not spherical.

$B = 3$ and beyond

Next we turn to the $B = 3$ sector relevant to the helium-3 nucleus (^{3}He) and the triton (^{3}H). Since they have spin 1/2, GFFs are parameterized by the same formula (2.93) as in the nucleon case. However, in the Skyrme model, the $B = 3$ classical solutions are not spherically symmetric, but rather has the shape of a tetrahedron [Car91a]. It is then

not obvious how one can recover the same set of form factors in the present semiclassical approach.

In order to answer this question, we need some elements of group theory. The tetrahedral group T_d [Tin64] consists of 24 discrete transformations such as a 120º rotation around one of the four vertices of a tetrahedron. It turns out that this symmetry imposes strong constraints on various moments of classical configurations [Car91b]. For example, consider the following integral

$$A_{ab} = \int d^3x T^{cl}_{ab}(\mathbf{x}) j_0(qx), \tag{2.115}$$

which appears in the $l = 0$ partial wave in (2.107). Let g be an element of the tetrahedral group. Changing variables as $\boldsymbol{x} \to g\boldsymbol{x}$, we find

$$A_{ab} = g^T_{ai} g^T_{bj} \int d^3x' T'^{cl}_{ij}(\mathbf{x}') j_0(qx') = g^T_{ai} g^T_{bj} A_{ij}, \tag{2.116}$$

where we used $T'^{cl}_{ij} = T^{cl}_{ij}$ due to symmetry. This means that $A_{ab} \propto \delta_{ab}$. Mathematically, the integral transforms as the singlet (A_1) representation contained in the product of two vector representations (T_1) of the tetrahedral group

$$T_1 \times T_1 = A_1 + E + T_1 + T_2, \tag{2.117}$$

along with the two-dimensional (E) and axial vector (T_2) representations [Tin64].

Consider, then, the transformation properties of the tensor T_{abkl} defined in (2.107) under the tetrahedral group. Since the trace part of the EMT T^{cl}_{ab} does not play a role, T_{abkl} can be viewed as the product of two symmetric and traceless tensors formed by T_1 vectors

$$(T_1 \times T_1) \times (T_1 \times T_1), \tag{2.118}$$

where $(T_1 \times T_1) = E + T_1$ denotes the traceless part. We are interested in the components that transform as the irreducible, singlet representation A_1. There are two such structures[3] which can be rearranged in the form [Car91b]

$$T_{abkl} = \frac{1}{10}\left(\delta_{ak}\delta_{bl} + \delta_{al}\delta_{bk} - \frac{2}{3}\delta_{ab}\delta_{kl}\right) T_{cdcd} + C_{abkl}. \tag{2.119}$$

The first structure is the same as before (2.108). The second tensor C is symmetric and traceless in any pair of indices (a, b, k, l) (see [Car91b] for the details). Plugging (2.119) into (2.104), we obtain

$$\begin{aligned} \langle \boldsymbol{q}/2 |\, T_{ij}(-R\boldsymbol{X}) \,| -\boldsymbol{q}/2 \rangle|_{l=2} \;=\; & -\left(q_i q_j - \frac{\delta_{ij}}{3} q^2\right) \frac{T_{cdcd}}{10} = \\ & -\frac{1}{2}\left(q_c q_d - \frac{1}{3}\delta_{cd} q^2\right) R^T_{ia}(B) R^T_{jb}(B) R^T_{ck}(B) R^T_{dl}(B) C_{ab,kl}. \end{aligned} \tag{2.120}$$

The operator in the second term is totally symmetric and traceless in the four indices i, j, c, d. It is thus a spin-4 operator whose matrix element between spin-1/2 states vanishes. The first term then leads to the same formula (2.102) for the D-form factor. We

[3] One coming from $E \times E = A_1 + A_2 + E$, the other from $T_1 \times T_1 = A_1 + E + T_1 + T_2$. The cross term $E \times T_1 = T_1 + T_2$ does not contribute to the trivial representation.

now appreciate the effect of the rotation matrix R in the present calculation. Had we neglected R's, namely, $R^T_{ia} \to \delta_{ia}$ etc. in (2.120), the second term would have contributed extra terms quadratic in q_i, in contradiction with the unique tensor structure (2.100) for a spin-1/2 nucleus. By introducing R's, we have minimally included quantum effects in order to restore the original spherical symmetry of the problem.

The above argument can be broadly generalized. Each Skyrmion solution possesses a symmetry group [BH18]. For $B \geq 3$, the group consists of discrete symmetry transformations and this puts strong constraints on the possible tensor structures of the integral (2.107). For example, the $B = 4$ solution (the helium-4 nucleus, or the 'alpha' particle) has cubic symmetry [BTC90]. The associated octahedral group O_h has irreducible representations which correspond to those of the tetrahedral group $A_1 \to A_{1g}$, $T_1 \to T_{1u}$, etc. We can then immediately conclude that the D-form factor is again given by (2.102).[4] A similar argument can be repeated for larger-B solutions. (Spin-averaging is understood for spin ≥ 1 nuclei.) We thus use (2.102) as a working definition for all nuclei in the Skyrme model.

2.3.2 Angular momentum form factor $J(t)$

Our approach can be straightforwardly generalized to the other GFFs. As an example, let us consider the angular momentum form factor

$$J(t) = \frac{1}{2}(A(t) + B(t)) \tag{2.122}$$

for spin-1/2 nuclei, where $A(t), B(t)$ are defined in (2.93). Physically, $J(t)$ represents the form factor associated with the total angular momentum of the system. The forward value $J(0) = 1/2$ is constrained by angular momentum conservation. In the Skyrme model, $J(t)$ has been computed for the $B = 1$ solutions [Ceb+07; KS21]. Here, for the first time, we compute it for the $B = 3$ (helium-3, triton) solution.

In the Breit frame, the J-form factor appears in the following components of the EMT matrix element: (2.93)

$$\frac{\langle p', s' | \, T_{00}(0) \, | p, s \rangle}{2P^0} = M \left[A(t) - \frac{t}{4M^2} \left[A(t) - 2J(t) + D(t) \right] \right] \delta_{ss'}, \tag{2.123}$$

$$\frac{\langle p', s' | \, T_{0i}(0) \, | p, s \rangle}{2P^0} = -J(t) \, i\epsilon_{ijk} \frac{\tau^j_{s's}}{2} q^k. \tag{2.124}$$

Note that the mixed (timelike-spacelike) components vanish in the classical limit which corresponds to a static configuration. Once the quantization of the Skyrmion is taken into account, we find a nonzero, operator-valued result

$$T_{0i} = I_{ij} a^j - J_{ij} b^j, \tag{2.125}$$

[4] For a spinless nucleus such as the helium-4, there are only two GFFs which we parameterize as

$$\langle p' | T_{\mu\nu} | p \rangle = 2A(t) P_\mu P_\nu + \frac{D(t)}{2} (q_\mu q_\nu - \eta_{\mu\nu} q^2). \tag{2.121}$$

where

$$I_{ij} = -\frac{1}{24\pi^2}[\mathrm{Tr}\{L_i T_j\} + \mathrm{Tr}\{[L_k, L_i]\,[L_k, T_j]\}], \tag{2.126}$$

$$J_{ij} = \frac{1}{24\pi^2}\epsilon_{jkl}x^k[\mathrm{Tr}\{L_i L_l\} + \mathrm{Tr}\{[L_a, L_i]\,[L_a, L_l]\}]. \tag{2.127}$$

Both of the above tensor densities transform as the product of a vector and an axial vector, i.e., they belong to the $T_2 \times T_1$ representation which does not contain an irreducible trivial component A_1. Therefore, their contribution must vanish at first order ($l = 0$) in the partial wave expansion (2.107). At the next order $l = 1$, we find

$$\begin{aligned}\langle \boldsymbol{q}/2|T_{0i}(-R\mathbf{x})|-\boldsymbol{q}/2\rangle|_{l=1} &= R^T_{ij}(B)\int d^3x \exp\{i\boldsymbol{q}\cdot R^T(B)\mathbf{x}\}T_{0j}(\mathbf{x}) \\ &= iR^T_{ij}(B)R^T_{kl}(B)q^k\int d^3x \frac{3j_1(qx)}{qx}[I_{jm}a^m - J_{jm}b^m]x^l. \end{aligned}\tag{2.128}$$

Defining the currents

$$I_{ijk}(q) = \int d^3x \frac{3j_1(qx)}{qx}I_{ij}x^k, \qquad J_{ijk}(q) = \int d^3x \frac{3j_1(qx)}{qx}J_{ij}x^k, \tag{2.129}$$

we can identify their irreducible component that transforms as $A_1 \in T_2 \times T_1 \times T_1$, which is totally antisymmetric in the three indices [Car91b]:

$$I_{ijk} = \epsilon_{ijk}\mathcal{I}(q), \qquad J_{ijk} = \epsilon_{ijk}\mathcal{J}(q), \tag{2.130}$$

where

$$\mathcal{I}(q) = \frac{1}{3!}\epsilon^{abc}I_{abc}(q), \qquad \mathcal{J}(q) = \frac{1}{3!}\epsilon^{abc}J_{abc}(q). \tag{2.131}$$

Substituting (2.130) into (2.128), we get

$$\begin{aligned}\langle \boldsymbol{q}/2|T_{0i}(-R\boldsymbol{X})|-\boldsymbol{q}/2\rangle &= iR^T_{ij}(B)R^T_{kl}(B)q^k\epsilon_{jml}[\mathcal{I}(q)a^m - \mathcal{J}(q)b^m] \\ &= i\epsilon_{ijk}q^k R^T_{jm}(B)[\mathcal{I}(q)a^m - \mathcal{J}(q)b^m]. \end{aligned}\tag{2.132}$$

At this point, we need to invert the relations in (1.22) between the spin and isospin velocities in terms of the associated angular momentum operators. This is a complicated task in general, but for the specific $B = 3$ solution at hand, the tensors defined in eqs. (1.15) to (1.17) are proportional to the identity, i.e.,

$$U_{ij} = u\delta_{ij}, \quad V_{ij} = v\delta_{ij}, \quad W_{ij} = w\delta_{ij}. \tag{2.133}$$

In that case, we have [Car91b]:

$$a^m = \frac{vK^m + wL^m}{uv - w^2}, \qquad b^m = \frac{wK^m + uL^m}{uv - w^2}, \tag{2.134}$$

and we may write

$$\begin{aligned}&R^T_{lm}(B)[\mathcal{I}(q)a^m - \mathcal{J}(q)b^m] = \\ &= \frac{1}{uv - w^2}\{[\mathcal{I}(q)(w - v) + \mathcal{J}(q)(w - u)]R^T_{lm}(B)L^m + [v\mathcal{I}(q) - w\mathcal{J}(q)]R_{lm}(B)M^m\},\end{aligned}\tag{2.135}$$

where we have defined the operator $\boldsymbol{M} = \boldsymbol{K} + \boldsymbol{L}$. Also, taking into account (1.23) and the fact that the $B = 3$ ground states are $\boldsymbol{M} = 0$ singlets [Car91a], we find our final result

$$J(t) = \frac{\mathcal{I}(q)(w - v) + \mathcal{J}(q)(w - u)}{uv - w^2}. \tag{2.136}$$

Comparing the definitions in eqs. (2.126), (2.127) and (2.131) with eqs. (1.16) and (1.17), we get the following relations

$$\lim_{q\to 0} \mathcal{I}(q) = -\frac{1}{6} W_{ii} = -\frac{1}{2} w, \quad \lim_{q\to 0} \mathcal{J}(q) = -\frac{1}{6} V_{ii} = -\frac{1}{2} v, \tag{2.137}$$

and thus $J(t = 0) = \frac{1}{2}$ as required by Lorentz invariance.

2.4 Numerical results

In order to compute the gravitational form factors of light nuclei, we start by generating the static energy-minimizing classical field configuration corresponding to each of the topological sectors.

After obtaining the classical solutions, we used the formula (2.102) (with M_N replaced by the respective nuclear masses) to compute the D-form factor for the first eight topological sectors, for which the ground state is well known, as well as for the $B = 32$ and $B = 108$ cubic Skyrmions. The results for the first three Skyrmions are shown in fig. 2.4. We have used the same values for the parameters in the Lagrangian as in [Ceb+07]. Thus the $B = 1$ result is in agreement with [Ceb+07], while the $B = 2, 3$ results are new. In the same plot, we also show the results obtained with a second set of parameters which includes a nonzero value of the sextic coupling constant $\lambda^2 = 3\,\mathrm{MeV\,fm}^3$. This choice is motivated by some previous studies on the symmetry energy of infinite nuclear matter within the same model [Ada+22b], as well as the EOS of neutron stars [Ada+23]. Finding classical solutions with nonzero λ via gradient-descent based algorithms becomes numerically more challenging for arbitrarily large values of this parameter. With our choice of $\lambda^2 = 3\,\mathrm{MeV\,fm}^3$, we have been able to obtain trustable solutions only up to $B = 32$. We find that the main effect of the sextic interaction is to increase the magnitude (in absolute value) of the D-term $D(0)$. This can be traced back to the fact that the sextic term represents a repulsive interaction, which makes the size of the soliton to grow to pick up more contributions from the large-radius region in the integral (2.102). However, apparently it contradicts with the recent observation [Fuj+22] in the Sakai-Sugimoto model [SS05a] that the repulsive interaction due to the omega meson exchange decreases the magnitude of the D-term. Unlike in [Fuj+22], in the present model the omega meson is treated as a static field represented by the sextic coupling [Jac+85], and induces only a diagonal term $T_{ij} \propto c_6 \delta_{ij}$ in the EMT (2.97) which does not directly contribute to the D-form factor. Thus the value of the D-term seems to be rather sensitive to different (static or dynamical) treatments for the omega meson field. This point deserves further study.

The results for the $B > 3$ solutions with $\lambda = 0$ are plotted in fig. 2.5 and fig. 2.6. All the curves start with a negative value, with their absolute value increasing with B, and cross zero at least once for some value of $|t|$. The number of nodes increases with B, and they appear earlier for higher values of B. The oscillation is caused by the spherical Bessel

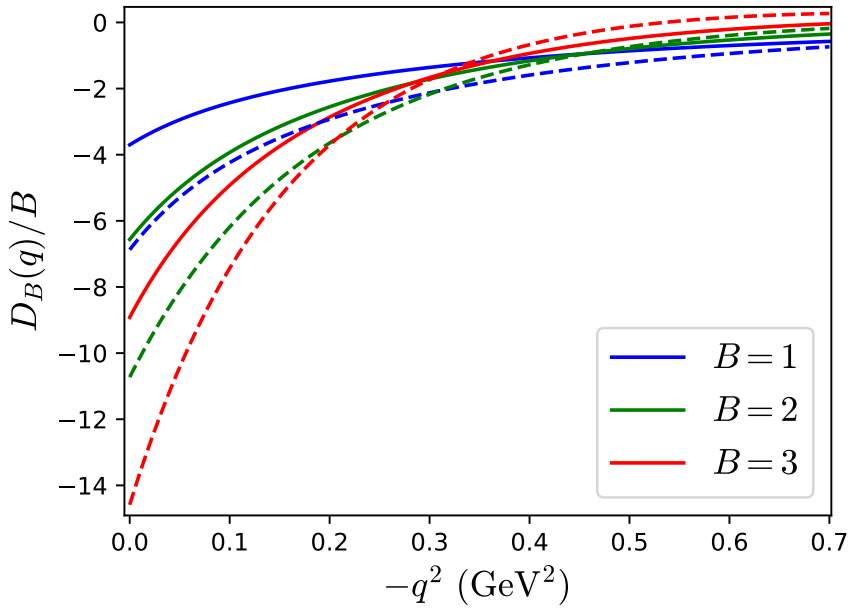

Figure 2.4: The D gravitational form factor of the Skyrmions with $B = 1, 2, 3$, normalized by B, for $\lambda = 0$ (solid) and $\lambda^2 = 3$ MeV fm^3 (dashed).

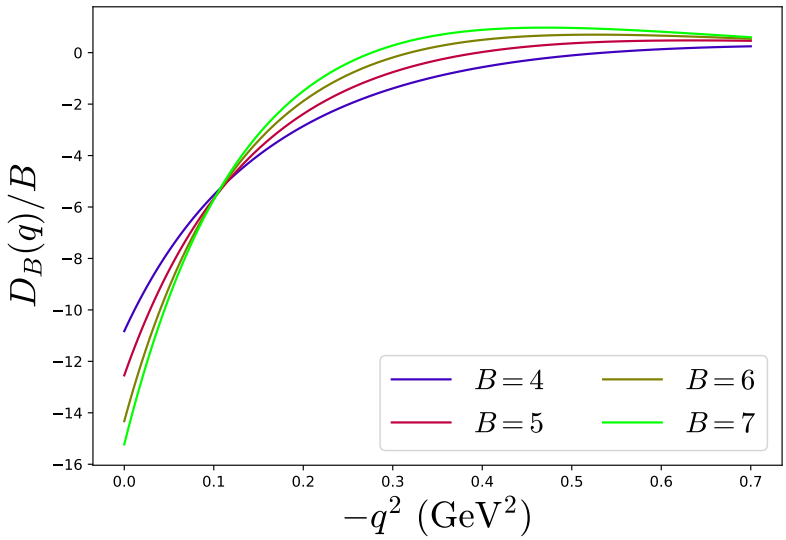

Figure 2.5: The D gravitational form factor of the Skyrmions with $B = 4, 5, 6$ and 7, normalized by B, for the $\lambda = 0$ case.

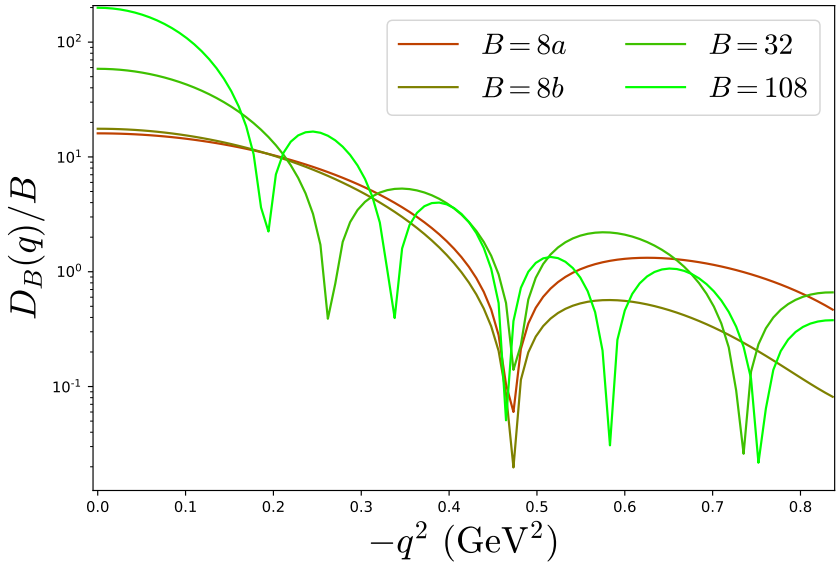

Figure 2.6: The D gravitational form factor (absolute value, not normalized by B) of the Skyrmions with $B = 8, 32, 108$, also for $\lambda = 0$. Cusps mean that the form factor flips signs and oscillates around zero.

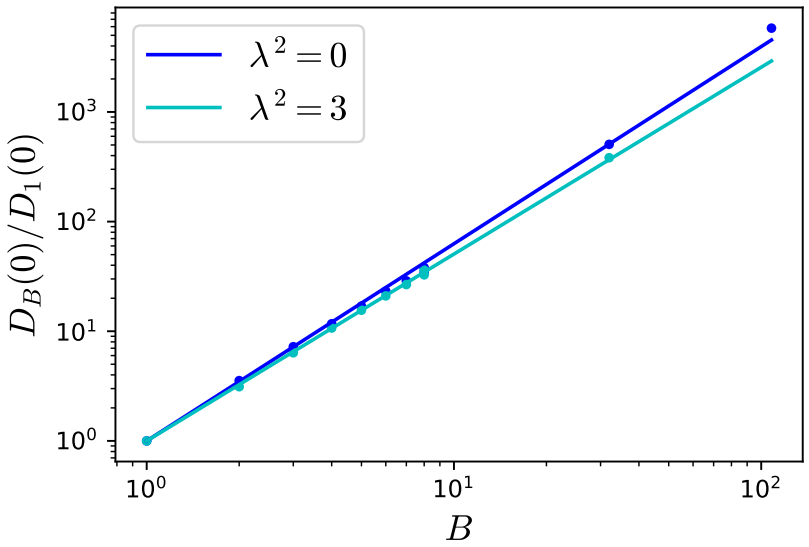

Figure 2.7: Dependence of the D term on the baryon charge B for Skyrmions with $B \leq 8$, $B = 32$ and $B = 108$. The cases $\lambda^2 = 0$ (dark blue) and $\lambda^2 = 3$ MeV fm^3 (light blue) are shown.

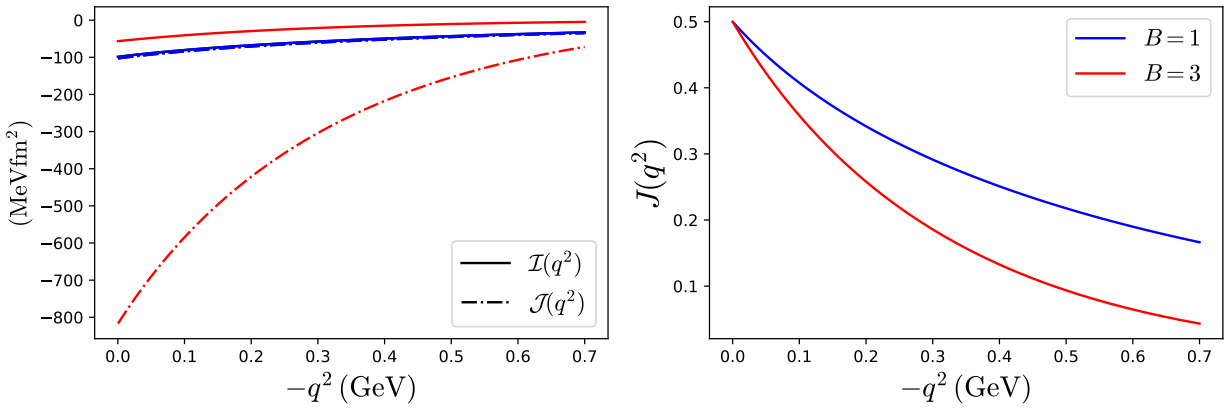

Figure 2.8: Left: Values of the functions $\mathcal{I}(q)$ and $\mathcal{J}(q)$ for the $B = 1$ and $B = 3$ cases. Right: The gravitational form factor $J(q^2)$ for the same nuclei.

function j_2 in (2.102) convoluted with the increasingly flatter density profile of larger-B solutions.

The particular values of the $D_B(0)$ for each topological sector will depend strongly on the specific values of the parameters of the model. However, their scaling with the topological charge, or atomic number, of the nuclei is a genuine prediction of the Skyrme model. , and will only depend on the different terms included in the Lagrangian. We have found that the B-dependence is very well fitted by a simple power-law $D_B(0) \propto B^\beta$, or equivalently,

$$\beta \equiv \frac{\log \frac{D_B(0)}{D_1(0)}}{\log B}, \tag{2.138}$$

is a constant as demonstrated in fig. 2.7. The value of β is found to be $\beta \approx 1.8$ for $\lambda^2 = 0$ and $\beta \approx 1.7$ for $\lambda^2 = 3\,\text{MeV}\,\text{fm}^3$. In comparison, we note that the liquid drop model of nuclei predicts $\beta = 7/3$ [Pol03] which is consistent with the result in the Walecka model $\beta \approx 2.26$ [GS06]. On the other hand, a microscopic approach using the nonrelativisitic nuclear spectral function predicts $\beta = 1$ [LT05].

Finally, in fig. 2.8 we show the results for the angular momentum form factor $J(q^2)$ together with the isospin $\mathcal{I}$ and rotation $\mathcal{J}$ currents defined in (2.130) for the $B = 1, 3$ solutions. For $B = 1$, $\mathcal{I}$ and $\mathcal{J}$ are equal due to the symmetry of the hedgehog configuration. The total J-form factor agrees with [Ceb+07]. For $B = 3$, we see that the angular momentum distribution is more localized at small momentum transfer, or at larger radius in position space.

2.5 Other probes of the nuclear structure

2.5.1 Charge density of nuclei

As argued in the previous section, electromagnetic FFs describe how the nucleon target reacts in an elastic scattering with a leptonic probe, and contain therefore information about the internal distribution of charge and magnetization. Since they were first measured, it has been customary to interpret FFs as Fourier transforms of charge and magnetization

spatial distributions. However, relativistic wave functions are frame dependent, hence such an interpretation is often restricted to the Breit frame [Sac62] (in the nonrelativistic case). Recently, the generalization of this interpretation to an arbitrary, relativistic reference frame was proposed in [Lor20] by introducing an appropriate kinematic factor in the Fourier integral,

$$\rho_c(r) = \int \frac{d^3\mathbf{q}}{(2\pi)^3} e^{-i\mathbf{q}\cdot\mathbf{r}} \frac{\langle p', \lambda \,|J^0_{em}(0)|\, p, \lambda\rangle_B}{2P^0_B} = \int \frac{d^3\mathbf{q}}{(2\pi)^3} e^{-i\mathbf{q}\cdot\mathbf{r}} \frac{G_E\left(-\mathbf{q}^2\right)}{\sqrt{1+\mathbf{q}^2/\left(4M^2\right)}} \tag{2.139}$$

which also resolves the apparent contradiction between the same magnitude obtained in the Breit and infinite momentum frames [Mil07].

Although, the issue of wether it makes sense to define a localized charge density for quantum objects such as nucleons has recentily been subject to some debate [Jaf21], this ambiguity was recently resolved in [Epe+22], where a redefinition of the charge density in terms of a new integral involving the electric form factor is shown to not depend on the particular wavefunction, as long as one can assume its spherical symmetry, i.e. in the rest frame of the system.

Furthermore, an accurate description of the charge densities of nucleons, and especially of the proton, has become one of the principal goals of theoretical nuclear physicists, as it is not only essential to the knowledge of strong forces in the non-perturbative regime but also to the understanding of other precission observables in quantum electrodynamics [GV22].

The electric charge density of Skyrmions

In the Skyrme approach, nucleons are semi-classical objects: one starts with a classical, localized soliton solution (the Skyrmion), and first quantize the zero-modes to find a quantum state. This is the so-called RIGID ROTOR QUANTIZATION. Further corrections to the wave function are expected to arise from vibrational modes, as well as from loop corrections from the meson fields. However, a natural starting point to compute local densities associated to any magnitude for Skyrmion solutions is to employ the rigid rotor approximation. Then, the task becomes fairly straightforward once the classical solutions are computed numerically, as it can be done directly without taking any intermediate steps involving the associated form factors. Indeed, the Gell-Mann-Nishijima formula tells us how to obtain the charge density of a Skyrmion field configuration,

$$Z = \frac{1}{2}B + I_3 \quad \longrightarrow \quad \rho = \frac{1}{2}B^0 + \left\langle I^0_3 \right\rangle, \tag{2.140}$$

where I^0_3 is the time-like component of the third isospin Noether current, and the brackets represent the expectation value on the quantum state of the Skyrmion. An explicit expression for (the classical version of) this current can be obtained from Noether's theorem, given that an infinitesimal isospin transformation

$$U \to U' = U + \epsilon^k \delta U_k, \qquad \delta U_k = \frac{i}{2}[\tau^k, U], \tag{2.141}$$

generates the Noether current (2.25). In particular, we have already written up the isospin charge current in eq. (2.27).

The quantum version of I_3^0 can be obtained by substituting the classical variable a_i with the corresponding quantum operators and Weyl ordering the products of two or more non-commuting operators. In the case of the angular velocity, we will use the quantum (body-fixed) angular momentum operators i.e. we need to invert (1.22). If we assume that the moment of inertia tensors satisfy the sphericity condition (2.133), the expectation value of I_3^0 in the isospin state $|\psi\rangle$ is given by

$$\begin{aligned}\left\langle I_3^0\right\rangle &= -\frac{1}{(uv-w^2)}\left\langle\psi\right|\left[R_{3a}u_{ab}(vK^b+wL^b)-R_{3a}w_{ab}(wK^b+uL^b)\right]_{\text{Weyl}}\left|\psi\right\rangle = \\ &= -\frac{1}{2}\left\langle\psi\right|\left[\frac{(u-v)u_{ab}+(u-w)w_{ab}}{(uv-w^2)}[R_{3a}K_b]_+ + \frac{wu_{ab}+uw_{ab}}{(uv-w^2)}[R_{3a},M_b]_+\right]\left|\psi\right\rangle\end{aligned} \tag{2.142}$$

where we have used the relation between the body-fixed and space-fixed angular momenta (1.23), and defined the grand spin operator $M_i = K_i + L_i$. Therefore, one just needs to compute the matrix elements

$$\mathcal{M}_{ab}(\psi) = \frac{1}{2}\left\langle\psi\right|\left[R_{3a},K_b\right]_+\left|\psi\right\rangle, \qquad \tilde{\mathcal{M}}_{ab}(\psi) = \frac{1}{2}\left\langle\psi\right|\left[R_{3a},M_b\right]_+\left|\psi\right\rangle \tag{2.143}$$

in order to obtain the charge density of the skyrmion in any given quantum state $|\psi\rangle$.

In the case of nucleons, spherical symmetry implies $u = v = w$ in eq. (2.142), so this expression is undefined. To get rid of the apparent divergence can rewrite the denominator as

$$\lim_{v,w\to u} uv - w^2 = (u+u)(u-u) \tag{2.144}$$

and the term $(u-u)$ cancels with the same term in the denominator, once take into account the fact that nucleons are grand spin singlets, i.e. satisfy $\mathbf{L}\left|\psi\right\rangle = -\mathbf{K}\left|\psi\right\rangle$. Therefore, we have, for nucleon states $|\psi\rangle = \left|\frac{1}{2},i_3,j_3\right\rangle$ [BTW86]:

$$\langle\psi|I_3^0|\psi\rangle = -\frac{u_{ij}}{2u}\left\langle\tfrac{1}{2},i_3,j_3\right|\left[R_{3j}K_i\right]_+\left|\tfrac{1}{2},i_3,j_3\right\rangle = -\frac{u_{ij}}{6u}\delta^{ij}\left\langle i_3|\tau^3|i_3\right\rangle\left\langle j_3|j_3\right\rangle \tag{2.145}$$

and thus the charge density of quantized $B = 1$ Skyrmions in the ground state is given by

$$\rho(\mathbf{x};i_3) = \frac{1}{2}B^0(r) - i_3\frac{\delta^{ij}u_{ij}(r)}{3u} \tag{2.146}$$

which, of course, presents spherical symmetry.

In fig. 2.9 we plot the radial profile of the charge densities for protons and neutrons as predicted by the Skyrme model. The dotted line data has been obtained from [Epe+22].

Indeed, this can be generalized to higher baryon charges. Another simple example is the $B = 3$ ground state $|\psi\rangle$ (1.39), which corresponds to the $({}^3H,{}^3He)$ isospin doublet. We start by noting that it is a grand spin singlet, so $\tilde{M}_{ij}$ will vanish, and we have

$$\left\langle\psi\right| I_3^0(\mathbf{x})\left|\psi\right\rangle = -\mathcal{M}_{ab}(\psi)\frac{(u-v)u_{ab}(\mathbf{x})+(u-w)w_{ab}(\mathbf{x})}{(uv-w^2)}, \tag{2.147}$$

$$\rho(\mathbf{x},\psi) = \frac{1}{2}B_0(\mathbf{x}) + \left\langle\psi\right| I_3^0(\mathbf{x})\left|\psi\right\rangle = \frac{1}{2}B_0(\mathbf{x}) - i_3\delta_{ab}\frac{(u-v)u_{ab}(\mathbf{x})+(u-w)w_{ab}(\mathbf{x})}{3(uv-w^2)}. \tag{2.148}$$

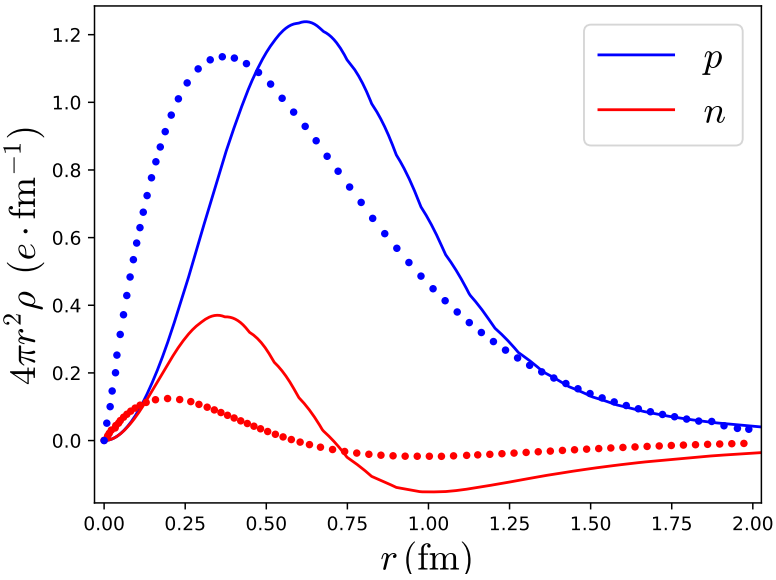

Figure 2.9: Radial profile of the electric charge density of nucleons

The charge densities of ^{3}H and ^{3}He ground states in the Skyrme model are not spherically symmetric, but preserve the symmetry of the classical solution (as required by the FR constraints). We plot a two-dimensional projection of these densities in fig. 2.10.

(a) ^{3}H (b) ^{3}He

Figure 2.10: Charge densities of helium and tritium ground states (in units of e)

Electromagnetic charge densities are a valuable source of information about the internal structure of nuclei and the strong force. Indeed, the distribution of charges inside a nucleus can reveal information about the isospin-asymmetric nuclear forces. In turn, we will see in subsequent sections how these are crucial to the understanding of matter inside compact stars.

2.5.2 Neutron skin thickness of Skyrmions

In standard nuclear physics, the Neutron Skin Thickness (NST) ΔR_{np} of a nucleus is defined as the difference between the mean square radius of neutrons and that of protons, i.e.

$$\Delta R_{np}({}^{B}X) = R_n - R_p, \qquad R_n = \sqrt{\frac{\int \rho_n r^2 d^3x}{B-Z}}, \quad R_p = \sqrt{\frac{\int \rho_p r^2 d^3x}{Z}}. \tag{2.149}$$

In the Skyrme model, nuclei are not described in terms of bound states of neutrons and protons, but, as shown in the last section, one can still compute an associated charge density to each quantum state. This can be identified with an effective "proton density". Furthermore, the neutron density will be given by

$$\rho_n = B_0 - \rho_p = \frac{1}{2}B_0 - \left\langle I_3^0 \right\rangle \tag{2.150}$$

so we can, in principle, compute the NST of a given nucleus once we know its associated quantum state in the Skyrme model.

For example, consider the $B = 3$ ground state $|\psi\rangle$ (1.39), which corresponds to the $({}^3H, {}^3He)$ isospin doublet. We start by noting that it is a grand spin singlet, so $\tilde{M}_{ij}$ will vanish, and we have

$$\begin{aligned} R_p^2(\psi) &= \frac{1}{Z}\int \left[\frac{1}{2}B_0 r^2 + \left\langle I_3^0 \right\rangle r^2\right] d^3x = \\ &= \frac{1}{Z}\left[\frac{1}{2}\int B_0 r^2 d^3x - \frac{M_{ij}(\psi)}{(uv-w^2)}\left[(v-w)u_{ij}^{(2)} + (u-w)w_{ij}^{(2)}\right]\right], \end{aligned} \tag{2.151}$$

where we have defined

$$u_{ij}^{(2)} \doteq \int u_{ij}(x) r^2 d^3x, \qquad w_{ij}^{(2)} \doteq \int w_{ij}(x) r^2 d^3x. \tag{2.152}$$

Further, by the tetrahedral symmetry of the $B = 3$:

$$u_{ij}^{(2)} = u^{(2)}\delta_{ij}, \qquad w_{ij}^{(2)} = w^{(2)}\delta_{ij} \tag{2.153}$$

so that

$$R_p^2(\psi) = \frac{1}{Z}\left[\frac{1}{2}B^{(2)} + \frac{(v-w)u^{(2)} + (u-w)w^{(2)}}{(uv-w^2)} i_3\right], \tag{2.154}$$

where we have defined $B^{(2)} = B r_{rms}^2$, r_{rms}^2 being the root mean square matter radius, and used that $M_{ii} = \langle\psi| R_{3i}K_i |\psi\rangle = -\langle\psi| I_3 |\psi\rangle = -i_3$.

Equivalently,

$$R_n^2(\psi) = \frac{1}{3-Z}\left[\frac{1}{2}B^{(2)} - \frac{(v-w)u^{(2)} + (u-w)w^{(2)}}{(uv-w^2)} i_3\right]. \tag{2.155}$$

Hence, we have

$$R_p({}^3He) = \sqrt{\frac{1}{4}\left[B^{(2)} + \frac{(v-w)u^{(2)} + (u-w)w^{(2)}}{(uv-w^2)}\right]} = R_n({}^3H), \tag{2.156}$$

$$R_n({}^3He) = \sqrt{\frac{1}{2}\left[B^{(2)} - \frac{(v-w)u^{(2)} + (u-w)w^{(2)}}{(uv-w^2)}\right]} = R_p({}^3H). \tag{2.157}$$

For our choice of parameters $f_\pi = 131.3\,\text{MeV}$, $e = 4.628$ and the physical value of the pion mass, we get

$$\Delta R_{np}(^3H) \approx 0.6\,\text{fm} = -R_{np}(^3He). \tag{2.158}$$

The measured charge radii of ^{3}He and ^{3}H are $1.959 \pm 0.03\,\text{fm}$ and $1.755 \pm 0.086\,\text{fm}$, respectively [Sic01]. Their difference measures the NST, $\Delta R_{pn}(^3\text{H})\big|_{\text{exp}} \approx 0.2\text{fm}$. For our choice of values of parameters, the predicted difference in charge radii of the ^{3}H $-^3$ He isodoublet comes out almost three times bigger than the experimentally measured value.

Now we turn to the question of whether we can compute the NST for larger nuclei, without the need to deal with the specific details of their quantization. From numerical simulations of a large set of solutions up to $B = 16$ [BH18], we see that the spherical symmetry approximation eq. (2.133) is very well satisfied (up to approximately a 7%), and also $w \ll u, v$, so we may neglect its value. Taking these approximations, eqs. (2.154) and (2.155) become

$$R_p^2(B, i_3) = \frac{1}{B + 2i_3}\left[B^{(2)} + 2\frac{u^{(2)}}{u}i_3\right] = \frac{1}{1-\delta}\left[r_{rms}^2 - \frac{u^{(2)}}{u}\delta\right], \tag{2.159}$$

$$R_n^2(B, i_3) = \frac{1}{B - 2i_3}\left[B^{(2)} - 2\frac{u^{(2)}}{u}i_3\right] = \frac{1}{1+\delta}\left[r_{rms}^2 + \frac{u^{(2)}}{u}\delta\right], \tag{2.160}$$

where

$$\delta = -\frac{2i_3}{B} = \frac{N-Z}{B} \tag{2.161}$$

is the ISOSPIN ASYMMETRY, with N and Z the corresponding numbers of neutrons and protons in the nucleus. Given eqs. (2.159) and (2.160), we can get a rough estimate for the NST of *any* nucleus from the Skyrme model, just by computing the corresponding classical solution.

To understand the basic physics controlling the neutron skin, we can simplify further by assuming that $B \gg i_3$ (or, equivalently, $\delta \ll 1$. We insert this identity and remove a factor of B/B, to rearrange the radii as

$$R_p^2 \approx r_{rms}^2 - \delta\left(\frac{u^{(2)}}{u} - r_{rms}^2\right) \implies R_p \approx r_{rms}\left[1 - \frac{\delta}{2}\left(\frac{u^{(2)}}{r_{rms}^2 u} - 1\right)\right]. \tag{2.162}$$

Hence the NST is given by

$$\Delta R_{np} \approx \delta\left(\frac{u^{(2)}}{u r_{rms}^2} - 1\right) r_{rms}\,. \tag{2.163}$$

The quantity $u^{(2)}/u$ measures the root-mean-squared radius associated to the isospin density. Hence, the sign and magnitude of the neutron skin depends on the difference between the matter and isospin charge radii, $u^{(2)}/u - r_{rms}^2$.

Experimentally, the NST is measured to depend linearly on the isospin asymmetry, with a slope that seems to be independent on the baryon number in the range $16 < B < 238$ (see fig. 2 in [Nov+23]) and parametrized by

$$\Delta R_{np} = 1.32\,\delta - 0.024 \pm 0.026\,\text{fm}. \tag{2.164}$$

This linear behavior is expected to break up for smaller nuclei, in which few body interactions may be dominating over bulk effects [Nov+23]. It is precisely in this range of the baryon charge where the solutions of the Skyrme model have been extensively studied, including a recent exhaustive description of the landscape of all known local minima in the Skyrmion configuration space up to $B = 16$ [GH22].

Nevertheless, we are able to generate (classical) Skyrmions with $B > 16$, thus can in principle compute the NST of these large B configurations and compare to the experimental results.

	B	Z	δ	ΔR_{np} (fm)	Exp (± 0.026) (fm)
^{34}S	34	16	0.059	0.067	0.0536
^{108}Cd	108	48	0.111	0.261	0.122

Table 2.2: NST of ^{34}S and ^{108}Cd from the Skyrme model and the corresponding data from the experimental relation (2.164)

2.5.3 Mass and scalar radii

In its classical version, the total EMT of QCD [HRT18]

$$T^{\text{QCD}}_{\mu\nu} = -\eta^{\alpha\beta} F^{\text{A}}_{\mu\alpha} F^{\text{A}}_{\nu\beta} + \frac{1}{4}\eta^{\mu\nu} F^2 + i\bar{\psi}\gamma^{(\mu}\overleftrightarrow{D}^{\nu)}\psi \tag{2.165}$$

should be traceless in the chiral limit, i.e. $T^{\text{QCD}}_{\mu\nu}\eta^{\mu\nu} \propto m_q$. However, the (renormalized) quantum operator associated to this observable is given by

$$\hat{T}^{\mu}_{\mu} = \frac{\beta(g)}{2g} F^{\mu\nu}_{\text{A}} F^{\text{A}}_{\mu\nu} + (1 + \gamma_{m_f}(g)) \sum_f m_f \bar{\psi}_f \psi_f, \tag{2.166}$$

where $\beta(g)$ is the beta function of QCD $\beta(g) = \partial g / \partial \log \mu$, which governs the renormalization group running of the QCD coupling constant g with the scale μ, and γ_{m_f} are the anomalous quark mass dimensions. The fact that (2.166) does not vanish for $m_f \to 0$ implies that the approximate conformal symmetry of the classical QCD Lagrangian (8) is broken by the quantum effects, giving rise to the so-called TRACE ANOMALY of QCD. In the chiral limit, the trace of the renormalized EMT operator contains only the glounic self-interaction term, which is also known to be the major contribution to the total nucleon mass. Indeed, taking the matrix element of the EMT trace operator in the rest frame of the nucleon, and the zero momentum transfer (forward) limit, we get[5]

$$\langle \mathbf{p}' = 0 | \, T^{\mu}_{\mu} \, | \mathbf{p} = 0 \rangle = \langle \mathbf{p}' = 0 | \, T^{00} \, | \mathbf{p} = 0 \rangle = 2M^2, \tag{2.167}$$

as can be seen from taking the forward limit in eq. (2.123).

Now, in analogy with the electromagnetic charge, a natural question that arises is how to determine the nucleon mass density of a nucleon. Theoretically, as we have seen, the various density distributions within a nucleon correspond to the Fourier transforms of the associated form factors as a function of momentum transfer (q), which are experimentally

[5] we remind the reader that the nucleon spinors are being normalized to $2P_0$.

measured in elastic scattering processes. Furthermore, the root-mean-squared radius associated to these distributions can be directly read from the first derivative of these form factors.

However, the definition of the proton mass radius [Kha21] is the subject of heated discussions in the nuclear physics community. This mass radius characterizes how the mass is distributed inside the proton, namely the mass density distribution, so it makes sense to define it from the form factor associated to the T^{00} component of the EMT.

$$r_m^2 = \frac{1}{M}\int r^2 T^{00}(\mathbf{x}) d^3x. \tag{2.168}$$

On the other hand, such operator is not a Lorentz scalar, and thus it will be in general a frame-dependent quantity. By virtue of (2.167), one could also define the mass radius of a hadron in terms of the scalar (gravitational) form factor $G(t)$, the form factor associated to the nucleon matrix element of the QCD EMT trace operator [Kha21],

$$\langle p'|\, T^\mu_\mu \,|p\rangle = \sqrt{\frac{M^2}{p_0 p_0'}}\bar{u}(p')G(t)u(p), \tag{2.169}$$

i.e.

$$r_s^2 = \frac{1}{M}\int r^2 T^\mu_\mu(\mathbf{x}) d^3x \tag{2.170}$$

is also known as the SCALAR RADIUS of the nucleus. We may also define ΔR_{sm} as the difference between their root-mean-squared scalar and mass radii:

$$\Delta R_{sm} = r_s - r_m. \tag{2.171}$$

We can compute the scalar and mass radii (eqs. (2.168) and (2.170)) from the classical solutions in the Skyrme model. Their values for the $B = 1-6$ and $B = 32, 108$ cases are shown in table 2.3. The associated ΔR_{sm} is shown in fig. 2.11, together with a simple fitting function.

B	1	2	3	4	5	6	32	108
r_{s} (fm)	1.0036	1.359	1.3936	1.4395	1.5235	1.5897	2.7445	4.0558
r_{m} (fm)	0.7803	1.0606	1.157	1.2444	1.3601	1.4487	2.6842	4.005

Table 2.3: Gravitational scalar and mass radii of the lightest nuclei from the Skyrme model.

The values of the parameters have been chosen to fit the charge radius and mass of the $B = 1$ Skyrmion to the proton values. If we compare the values of the scalar and mass radii of the nucleon with those given in [Dur+23], we see a perfect agreement (see table 2.4).

Furthermore, in the Skyrme model approach, it is easy to obtain the radial profile of the mass and EMT trace densities, as shown in fig. 2.12 for the nucleon.

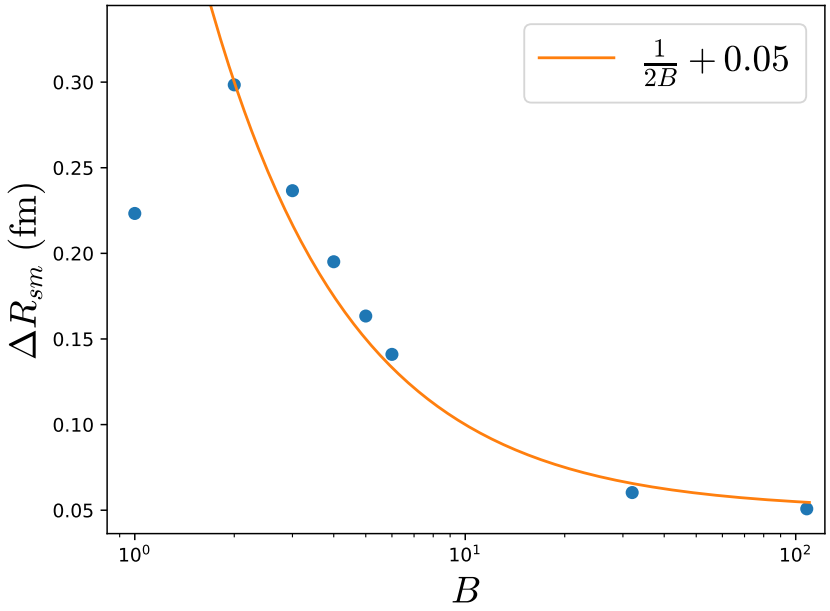

Figure 2.11: Difference between the mean scalar and mass radius of nuclei in the Skyrme model

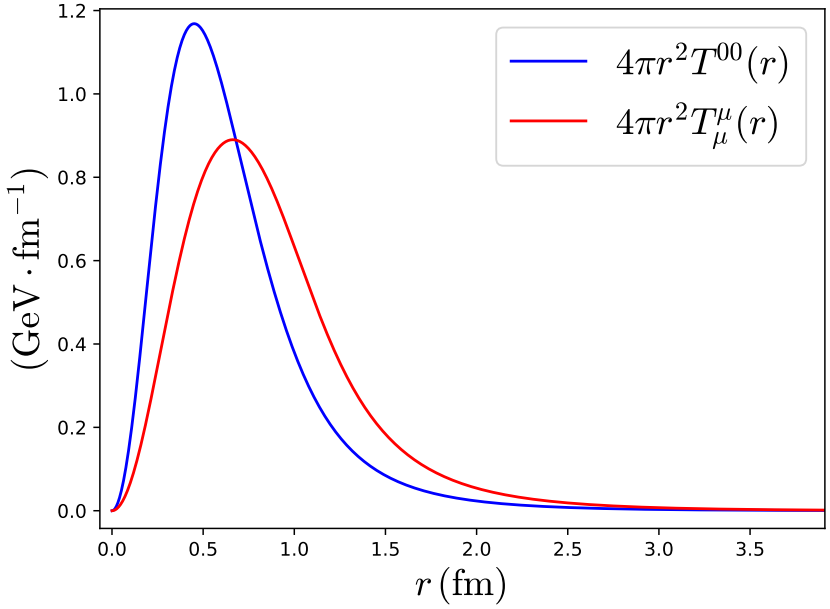

Figure 2.12: Radial profile of the mass and trace of the EMT densities for the nucleons

B	our work	[Dur+23] (Holographic QCD)	[Dur+23] (Lattice)
r_{s} (fm)	1.0036	1.069 ± 0.056	1.073 ± 0.066
r_{m} (fm)	0.7803	0.755 ± 0.035	0.7464 ± 0.025

Table 2.4: Comparison of mass and scalar radii of nucleons.

2.6 Final remarks

The Skyrme model, and most generally, chiral soliton models, constitute a versatile framework to study several properties of nucleons and light nuclei. Traditionally, these analysis mostly focused on global properties, such as total energies; or electromagnetic form factors. In this chapter we have shown that not only one can study these, but lots of other different properties, such as local charge and mass densities, neutron skin thickness and beta-decay multipole form factors. One of the main results of this part has been to adapt the formalism of multipolar expansion of weak hadronic currents, which has been well-known in the nuclear physics literature for a while, to the Skyrme model. We have illustrated this by computing a simple example of such multipoles in the beta decay of lithium-6. On the other hand, we have also presented the results of the computation of the D-term for several light nuclei, as well as other quantities related to the EMT form factors. Most of these properties are the object of intense active research, both from the experimental and theoretical ends. With our results, we demonstrate the feasibility of computing all of these low-energy nuclear properties within the Skyrme model, although only a qualitative agreement with experimental quantities can be achieved in some cases (especially for multi-Skyrmions).

A key feature that we have exploited in the computations mentioned above is the semi-classical nature of nuclei from the solitonic point of view, which makes the task of computing local densities of nuclei remarkably simple, as it does not involve the definition of a spatial, many-body wavefunction (at least in the rigid rotor approximation). Indeed, the spatial structure is determined, in the first semiclassical approximation, by the classical soliton solution alone. In practice, this facilitates the task of obtaining some properties of nuclei, such as charge densities and form factors, which are very difficult to obtain via other approaches like chiral effective theories or quantum montecarlo methods.

On the other hand, the main drawback of this method is the vast landscape of almost-degenerate, local minima in the configuration space of classical Skyrmions for sufficiently large baryon charge. This implies that the semi-classical rigid-rotor approximation must break down at some point, and more complex spatial wavefunctions involving superpositions of different classical configurations are probably a better way to describe such nuclei.

We would like to conclude with a comment about the open problems that we have not addressed in our analysis throughout this chapter. The first, most obvious one involves the quantum corrections to the binding energies of nuclei beyond the rigid rotor quantization, and its possible effects in other properties such as form factors. Indeed, it has been known from almost a decade that the zero mode quantization alone does not correctly reproduce even the ground state quantum numbers of some light nuclei (eg the $B = 5$ and $B = 7$).

When computing the gravitational form factors, we have neglected the quantum corrections from isospin and spin degrees of freedom, invoking their higher order nature in

the large N_c expansion. However, It would be interesting to compute such corrections for the different gravitational form factors, in order to check whether this approximation is consistent.

Finally, we have shown that the computation of beta decay multipolar operators of Skyrmions is a ponderous, but straightforward calculation once the relevant quantum states are known. In spite of our promising results, the analysis carried out in the thesis is a rather superficial one, and of course the subject of beta decay of intermediate-mass nuclei deserves a more profound study.

Part II

Dense Nuclear Matter and Neutron Stars

CHAPTER 3

Skyrmion crystals and the Equation of State of dense Nuclear Matter

Articles partially reproduced in this chapter: [Ada+22b; Ada+23]. See *permissions*.

> *"Brednia. A w dodatku nie do rymu. Wszystkie przyzwoite przepowiednie są do rymu"*
>
> – Geralt z Rivii, in *Ostatnie życzenie (The Last Wish)*, by A. Sapkowski

3.1 The EOS of dense nuclear matter

A unified theoretical understanding of the structure and interactions of nuclei, as well as the phenomenology of neutron stars and supernova explosions, requires a deep knowledge of the EOS of strong-interaction matter at saturation and supra-saturation densities and at large isospin chemical potential. Indeed, realistic models of nuclear matter inside neutron stars do not predict an isospin-symmetric state at all. Due to electromagnetic repulsion, a system with a large number of protons rapidly becomes unstable. On the other hand, for large neutron excess nuclear matter becomes unstable against β-decay. Therefore, only a small fraction of protons over total nucleons is generally allowed for big stable nuclei. For a nuclear system with total number of baryons $A = N + Z$, where N is the number of neutrons and Z the number of protons, and defining the isospin asymmetry parameter as $\delta = (N - Z)/A = (1 - 2\gamma)$, with γ the proton fraction or ratio between Z and A, the binding energy is usually defined as a function of both the baryon density and the asymmetry parameter,

$$\frac{E}{A}(n_B, \delta) = E_N(n_B) + S_N(n_B)\delta^2 + \mathcal{O}\left(\delta^3\right), \tag{3.1}$$

where the term $E_N(n_B)$ would be the binding energy of isospin-symmetric nuclear matter, and $S_N(n_B)$ is the so-called SYMMETRY ENERGY. The energy of symmetric nuclear matter is usually constrained around SATURATION DENSITY, n_0, which is the typical density of nucleons and nuclei. The dependence of the nuclear matter energy with density is thus described in terms of the first coefficients in a Taylor expansion around saturation,

$$E_N(n_B) = E_0 + \frac{1}{18}K_0\epsilon^2 + \cdots \tag{3.2}$$

with $\epsilon = (n - n_0)/n_0$, E_0 the energy of symmetric, infinite nuclear matter at saturation, and

$$K_0 = 9n_0^2 \frac{\partial^2 E_N}{\partial n^2}\bigg|_{n=n_0} \tag{3.3}$$

is the COMPRESSION MODULUS (or incompressibility) of nuclear matter at saturation [Bur+21].

Different measurements of nuclear masses and density distributions have allowed to precisely constrain the value of $n_0 = 0.16 \pm 1\,\mathrm{fm}^{-3}$ and $E_0 = -16 \pm 1\,\mathrm{MeV}$, while the value of K_0 can be extracted from the analysis of isoscalar giant monopole resonances in heavy nuclei. For the latter, results suggest $K_0 \approx 240\,\mathrm{MeV}$ [SSM14] thus pointing to a rather soft EOS, as confirmed by heavy ion collider experiments [Sor+23].

On the other hand, the symmetry energy is a measure of the change in the binding energy of the system as the neutron-to-proton ratio is changed at a fixed value of the total baryon number, and its knowledge is essential to determine the composition of nuclear matter at high densities. However, its dependence on the density has proven difficult to measure experimentally, and usually it is parametrized as an expansion in powers of the baryon density around nuclear saturation n_0,

$$S_N(n_B) = S_0 + \frac{1}{3}L\epsilon + \frac{1}{18}K_{\mathrm{sym}}\epsilon^2 + \cdots \tag{3.4}$$

and

$$L = 3n_0 \frac{\partial S_N}{\partial n}\bigg|_{n=n_0}, \quad K_{\mathrm{sym}} = 9n_0^2 \frac{\partial^2 S_N}{\partial n^2}\bigg|_{n=n_0} \tag{3.5}$$

the slope and curvature of the symmetry energy at saturation, respectively. The symmetry energy at saturation is well constrained ($S_0 \sim 30$ MeV) by nuclear experiments [FF18], but the values of the slope and higher order coefficients are still very uncertain. However, recent efforts on the analysis of up to date combined astrophysical and nuclear observations have allowed to constrain the value of these quantities with reasonable uncertainty above nuclear saturation [Ess+21; Tan+21; TFP21; GPH22; Li+21].

3.2 Skyrmion crystals and their quantization

The classical Skyrme crystal

One of the main features of the Skyrme model is that, being an intrinsically non-perturbative approach, we can in principle use the same effective lagrangian to describe in a unified manner the physics of nuclear matter at zero and non-zero densities. In our approach, infinite skyrmionic matter is described by a field configuration on a finite cell of fixed size and baryon number, which minimizes the static energy functional (1.7) after imposing periodic boundary conditions. Hence, the only difference between isolated Skyrmions and crystalline configurations comes from the fact that the boundary conditions imposed on the Skyrme field are of different nature: instead of imposing the vacuum at large distances, one must impose periodicity conditions on the boundary of a compact space region- the UNIT CELL- and hence these solutions do not yield a finite value when its energy density is integrated over all space. Instead, this requirement is relaxed to yield a finite value

of the energy over the unit cell, or, equivalently, a finite energy per baryon. We would like to remark that, although the boundary conditions imposed on the Skyrme fields are different from those of regular solitonic solutions, the topological properties of the field configurations remain the same. Indeed, a cubic, three-dimensional lattice with periodic boundary conditions is topologically equivalent to a three torus, T^3, so that crystalline configurations are described by maps $U_{\text{crystal}} : T^3 \to S^3$. As T^3 is still a compact and oriented manifold, mappings from T^3 to S^3 are still characterized by their topological degree, as ensured by Hopf's degree theorem[2]. Due to these periodic boundary conditions, such configurations are usually referred to as SKYRME CRYSTALS.

Skyrmion crystals were first proposed as models of infinite nuclear matter by Klebanov in [Kle85], and the exploration of the different crystals was further developed in [KS89; Cas+89]. Let us now shortly review some properties of these crystalline configurations.

As in the non-periodic case, Skyrme units are adopted for numerical purposes, in which energy and length are measured in units of $3\pi^2 f_\pi/e$ and $\hbar/(f_\pi e)$, respectively. Obviously, the total energy of the crystal will diverge, as so does its total volume, but the energy per baryon number remains finite,

$$\frac{E}{B} = \frac{N_{\text{cells}}\, E_{\text{cell}}}{N_{\text{cells}}\, B_{\text{cell}}} = \frac{E_{\text{cell}}}{B_{\text{cell}}}. \tag{3.6}$$

Here, N_{cells} is the number of cells and E_{cell}, B_{cell} are the energy and baryon charge in a single, periodic cell. The energy of the unit cell strongly depends on the assumed geometry and its size, characterized by the length parameter L, as well as on the total baryon charge that the cell contains. Concretely, L is the distance between nearest-neighbor skyrmions in the maximally attractive channel. As a consequence, the resulting field configuration is *not* periodic in L. The period length and the size of the unit cell is $2L$, instead.

As with isolated Skyrmions, the symmetry group of a crystalline configuration is reduced from the total symmetry group of the Lagrangian $\widetilde{G}$ (1.8) due to these periodicity conditions, which in turn result in a particular point group symmetry for the full crystal. However, it is well known that there is no unique crystalline solution, but there are different local minima of the energy functional with periodic boundary conditions at a given density. All these local minima present different crystalline structures, i.e. different point symmetries, although all of them are based on a simple cubic group.

By studying all possible geometries of the unit cell, i.e., types of crystals, at a particular volume of the cell, one could find the ground state crystalline solution (global minimizer) at any given density (Note that a particular geometry of the crystal translates into particular point symmetries of the chiral fields). For the purposes of this thesis, we will restrict ourselves to the study of cubic crystals, which present a unit cell of cubic shape and the chiral fields satisfy cubic symmetries, i.e. they obey the following relations:

$$\begin{aligned} &\mathrm{A}_1 : (x, y, z) \to (-x, y, z), \\ &\qquad (\sigma, \pi_1, \pi_2, \pi_3) \to (\sigma, -\pi_1, \pi_2, \pi_3), \end{aligned} \tag{3.7}$$

$$\begin{aligned} &\mathrm{A}_2 : (x, y, z) \to (y, z, x), \\ &\qquad (\sigma, \pi_1, \pi_2, \pi_3) \to (\sigma, \pi_2, \pi_3, \pi_1). \end{aligned} \tag{3.8}$$

[2] In fact, the theorem asserts that the topological degree is the *only* homotopy invariant in such situations

These are the simple cubic and Face Centered Cubic (FCC) crystals of Skyrmions as well as the Body-Centered Cubic (BCC) and FCC crystals of *half-Skyrmions*.

In this work we will focus on the FCC crystal of half-skyrmions, which has two additional symmetries,

$$\mathrm{C}_3 : (x, y, z) \to (x, z, -y),$$
$$(\sigma, \pi_1, \pi_2, \pi_3) \to (\sigma, -\pi_1, \pi_3, -\pi_2), \tag{3.9}$$
$$\mathrm{D}_4 : (x, y, z) \to (x + L, y, z), \tag{3.10}$$
$$(\sigma, \pi_1, \pi_2, \pi_3) \to (-\sigma, -\pi_1, \pi_2, \pi_3). \tag{3.11}$$

A more detailed description of the construction of the Skyrme crystal and the comparison of different symmetries can be found in [Ada+22a], and we have kept the same notation for this work. As in that previous work, the unit cell has size $2L$ and a baryon content of $B_{\text{cell}} = 4$. Then, for each value of L we obtain the minimum of energy as explained in [Ada+22a]. It turns out that the energy-size curve, $E_{\text{cell}}(L)$, is a convex function which has a minimum at a certain L_*.

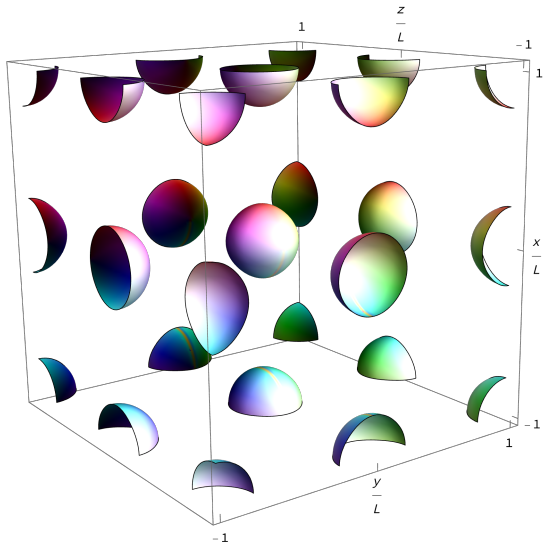

Figure 3.1: Energy density iso-contour for the Half-Skyrmion FCC crystal

3.2.1 The Skyrme crystal EoS for symmetric nuclear matter

For the crystal solutions one can define the relevant thermodynamical quantities in the usual way, that is, energy density ρ, pressure p and baryon charge density n_B

$$\rho = \frac{E}{V} = \frac{E_{\text{cell}}}{V_{\text{cell}}}, \tag{3.12}$$
$$p = -\frac{\partial E}{\partial V} = -\frac{\partial E_{\text{cell}}}{\partial V_{\text{cell}}}, \tag{3.13}$$
$$n_B = \frac{B}{V} = \frac{B_{\text{cell}}}{V_{\text{cell}}}. \tag{3.14}$$

Again they are functions of L or, in other words, the volume of the unit cell V_{cell}.

At the point where $L = L_*$, the given crystal solution describes skyrmionic matter at equilibrium, i.e., at zero pressure. We may thus identify such a minimum with the saturation point, and the associated baryon density value should be identified with the nuclear saturation density, n_0. This will allow us to find a point with respect to which we shall fit all the calculated observables.

In the region where $L < L_*$ the volume of the cell decreases, which corresponds to a squeezed crystal, i.e. $n > n_0$. This translates into growing pressure and density. The remaining region $L > L_*$, where the volume increases in comparison to the equilibrium, is thermodynamically unstable. Indeed, it formally gives negative pressure. Due to that, the low density regime cannot be described by any of the previously mentioned crystals. On the contrary, it is expected that the crystal is replaced by an inhomogeneous phase, where lumps of nontrivial energy density are surrounded by regions of void. In fact, the correct ground state solution for the $L > L_*$ region in the Skyrme model is a very difficult open problem, as it most probably requires obtaining periodic solutions with larger baryon number per unit cell and/or different symmetries. Indeed, different inhomogeneous configurations with lower classical energies than the FCC crystal have been proposed [Ada+22a; HLS23] which point towards this fact.

A related problem is the fact that the ratio between the compressibility K_0 (as defined in (3.3)) and the energy per baryon of Skyrmion crystals at saturation is overestimated by a factor of 4 or larger, independently of the values of the parameters. This implies that the Skyrme model (with and without sextic term), implies that nuclear matter is too stiff around saturation (provided the Skyrmion crystal solution is assumed to be the correct ground state). This is also an open problem that deserves further study. However, we will not address such problem in this thesis, as it may require a further generalization of the Skyrme model, possibly via the inclusion of additional degrees of freedom such as ρ vector mesons. Therefore, in what follows we shall ignore the compressibility and try to compute other nuclear observables at saturation.

On the other hand, in the absence of the sextic term, the landscape of the crystal energy minimizers at high densities is very well understood. Namely, for $L \leq L_*$ the ground state is formed by the FCC half-Skyrmion phase, which at extremely high density is replaced by the BCC half-Skyrmions. This phase transition occurs at densities much beyond the values expected at the cores of neutron stars. It has been recently shown [Ada+22a] that this picture is significantly modified if the sextic term is added. First of all, the FCC to BCC phase transition moves towards much smaller densities, approximately $4 - 5$ times saturation density, which can be easily found in the center of heavy NS. In addition, the appearance of the sextic term introduces a fluidity into the model which mathematically results from the volume diffeomorphism invariance of this part of the action. Such a fluidity translates into an almost homogenous distribution of the energy density as the pressure increases, which is a characteristic trait of the pure-BPS Skyrmions.

However, perhaps the most crucial result is that the equation of state, which relates energy density and pressure, stiffens in the GSM. Indeed, the sextic term alone leads to the maximally stiff EOS, $\rho = p$. In the full, generalized model it occurs asymptotically at high density. In any case, this stiffening is responsible for a significant rising of the maximal masses of NS to values which are in accordance with current observations (as we will extensively discuss in the next chapter).

Up to this point, we have referred to the classical regime of the Skyrme model, which, as we already underlined, corresponds to symmetric nuclear matter. However, it is of vital importance to semiclassically quantize the isospin degrees of freedom of the skyrmionic crystal as a first step to describe (isospin asymmetric) nuclear matter, which is known to be the ground state of the matter in the core of NS.

Quantization of the Skyrme crystal

It is well known that the largest quantum correction to the classical energy of Skyrmion configurations comes from the contribution of the isospin degrees of freedom, which are usually quantized as zero-modes via some collective coordinate parametrization. However, it is not straightforward to define the isospin subgroup $SU(2)_I$ in such configurations, since the vacuum value is no longer imposed at the boundaries. Instead, one should in principle consider internal rotations of the full chiral group $SO(4)_{\text{chiral}}$, since there is not a natural way to select the diagonal subgroup corresponding to isospin.

The problem of defining the isospin group in crystal configurations is treated in [Bas96]. As explained there, the procedure of defining the isospin subgroup in crystalline configurations is subject to some ambiguities, but the energy per baryon spectrum in the infinite crystal limit is unique. Indeed, it turns out that the 4-dimensional representation of the cubic point group of minimal energy crystals is *reducible* into the trivial 1-D irrep and a 3-D irrep, which singles out one direction in isospin space. We may then choose the σ field to transform in the trivial irrep, and then to define the isospin group as the subgroup of isorotations within the 3-D irrep, i.e. rotations between the three pion fields.

In the rest of this work, we will use this definition of isospin in crystals, as it is also the natural choice if a symmetry-breaking potential (such a mass term for the pions) is added to the Skyrme Lagrangian.

To add the contribution of the quantization of the global isospin zero modes to the total energy, we need to know the quantum isospin state of the full crystal. This task, however, becomes impossible in the thermodynamic limit in which the number of particles forming the crystal goes to infinity. Instead, we can make the following assumptions on the quantum wavefuntion of the full crystal:

- The isospin wavefuntion of the total crystal $|\Psi\rangle$ can be written as a superposition of states constructed from the (infinite) product of isospin wavefuntions of individual unit cells, $|\Psi\rangle = \bigotimes_{\text{cells}} |\psi\rangle$. In other words, as a first approximation we will not consider the quantum correlation on the isospin state between cells.

- The symmetry of the classical crystal configuration is inherited by the total wavefunction, and shared with the wavefunction of each of the unit cells, i.e. both $|\Psi\rangle$ and $|\psi\rangle$ share the same point symmetry group.

These two assumptions imply that finding the quantum states of the total crystal is equivalent to finding the state of each unit cell. The latter is in fact a more plausible task as we may use the tools developed for the quantization of multi-skyrmion configurations.

Quantum isospin states and Hilbert space

As discussed in section 3.2.1, On each subspace given by a fixed value of total spin and isospin, the allowed (physical) states will be those which retain the same point symmetries as the corresponding classical solution. This is imposed via the FR constraints, which relate the values of third component of the body-fixed spin and isospin eigenvalues.

In the case of a Skyrmion crystal, the unit cell presents a concrete set of symmetries, some of which relate rotations both in space and isospace, and hence we should consider as physical states only those that are compatible with such symmetries. Let us now proceed to calculate the FR constraints in order to obtain the corresponding quantum states of the Skyrme crystal. The relevant symmetries of the FCC half-skyrmion crystal linking rotations and isorotations are A_2 and C_3, which are represented by the following operators,

$$\exp\left\{i\frac{\pi}{2}\frac{1}{\sqrt{3}}\left(K_1+K_2+K_3\right)\right\}=\mathcal{R}'\left(0,-\pi/2,-\pi/2\right), \tag{3.15}$$

$$\exp\left\{i\frac{\pi}{2}K_1\right\}=\mathcal{R}'\left(\pi/2,-\pi/2,\pi/2\right). \tag{3.16}$$

We only write the operators that correspond to isospin transformations, since the rotations in the real space are the same. Recall that we are using the Euler angles representation for the rotation and isorotation operators in the ZYZ convention,

$$\mathcal{R}\left(\alpha,\beta,\gamma\right)=R_z\left(\alpha\right)R_y\left(\beta\right)R_z\left(\gamma\right). \tag{3.17}$$

From (1.36) we know how these operators act on a state $|j,l_3\rangle\otimes|i,k_3\rangle$ (again we will only consider the isospin part, the quantum numbers resulting from the spin quantization are the same),

$$\mathcal{R}\left(\alpha,\beta,\gamma\right)|i,k_3\rangle=\sum_{k_3'}D^i_{k_3,k_3'}\left(\alpha,\beta,\gamma\right)|i,k_3'\rangle, \tag{3.18}$$

where $D^I_{k_3,k_3'}$ are the Wigner D-matrices. Then we can consider this as a problem of finding the eigenvalues and eigenvectors of the Wigner D-matrices, and the quantum states will be the combination of J,L_3,I,K_3 that satisfy the FR constraints (1.30). In our case, we will consider the possible quantum states of a unit cell, which carries a baryon number $B_{\text{cell}}=4$. We will not prove here that the transformations (1.30) with the corresponding spatial rotations (3.16) correspond to contractible loops on the configuration space. Instead, we will assume that this is indeed the case, i.e. $\chi_{FR}=+1$, as tends to be the case for $B=0$ mod 4 Skyrmions [Kru06]. Also, we will consider all the possible values of i, namely $i=0,1,2$ (eigenvalue of the isospin moment of inertia) and show the (unnormalized) eigenvectors for each symmetry.

A_2 symmetry: $\mathcal{R}(0,-\pi/2,-\pi/2)$

- For $i=0$, $D^0_{00}=1$ and there is only one state $|i=0,i_3=0\rangle$.
- For $i=1$, we have

$$D^1_{k_3,k_3'}=\begin{pmatrix} i/2 & -1/\sqrt{2} & -i/2\\ i/\sqrt{2} & 0 & i/\sqrt{2}\\ i/2 & 1/\sqrt{2} & -i/2\end{pmatrix}. \tag{3.19}$$

This matrix has three different eigenvalues and corresponding eigenstates

$$\begin{aligned}
&\lambda_1 = 1, \\
&\left|\psi_1^1\right\rangle = -i\left|1,-1\right\rangle + (1+i)/\sqrt{2}\left|1,0\right\rangle + \left|1,1\right\rangle \\
&\lambda_2 = -1/2 - \sqrt{3}/2i, \\
&\left|\psi_2^1\right\rangle = (2-\sqrt{3})i\left|1,-1\right\rangle - \sqrt{2-\sqrt{3}}(1+i)\left|1,0\right\rangle + \left|1,1\right\rangle \\
&\lambda_3 = -1/2 + \sqrt{3}/2i, \\
&\left|\psi_3^1\right\rangle = (2+\sqrt{3})i\left|1,-1\right\rangle + \sqrt{2+\sqrt{3}}(1+i)\left|1,0\right\rangle + \left|1,1\right\rangle
\end{aligned} \tag{3.20}$$

- For $i = 2$, we have

$$D^2_{k_3,k_3'} = \begin{pmatrix} -1/4 & -1/2i & \sqrt{6}/4 & 1/2i & -1/4 \\ -1/2 & -1/2i & 0 & -1/2i & 1/2 \\ -\sqrt{6}/4 & 0 & -1/2 & 0 & -\sqrt{6}/4 \\ -1/2 & 1/2i & 0 & 1/2i & 1/2 \\ -1/4 & 1/2i & \sqrt{6}/4 & -1/2i & -1/4 \end{pmatrix} \tag{3.21}$$

which shares the same eigenvalues as the corresponding $i = 1$ case, but this time λ_2 and λ_3 present multiplicity two. The corresponding eigenstates are

$$\begin{aligned}
&\lambda_1 = 1, \\
&\left|\psi_1^2\right\rangle = -\left|2,-2\right\rangle + (1-i)\left|2,-1\right\rangle + (1+i)\left|2,1\right\rangle + \left|2,2\right\rangle,
\end{aligned} \tag{3.22}$$

$$\begin{aligned}
&\lambda_2 = -1/2 - \sqrt{3}/2i, \\
&\left|\psi_{2a}^2\right\rangle = \left|2,-2\right\rangle - \sqrt{2}i\left|2,0\right\rangle + \left|2,2\right\rangle, \\
&\left|\psi_{2b}^2\right\rangle = -\left|2,-2\right\rangle - \frac{(1+\sqrt{3})}{2}(1-i)\left|2,-1\right\rangle + \frac{(\sqrt{3}-1)}{2}(1+i)\left|2,1\right\rangle + \left|2,2\right\rangle,
\end{aligned} \tag{3.23}$$

$$\begin{aligned}
&\lambda_3 = -1/2 + \sqrt{3}/2i, \\
&\left|\psi_{3a}^2\right\rangle = \left|2,-2\right\rangle + \sqrt{2}i\left|2,0\right\rangle + \left|2,2\right\rangle, \\
&\left|\psi_{3b}^2\right\rangle = -\left|2,-2\right\rangle + \frac{(\sqrt{3}-1)}{2}(1-i)\left|2,1\right\rangle - \frac{(1+\sqrt{3})}{2}(1+i)\left|2,1\right\rangle + \left|2,2\right\rangle.
\end{aligned} \tag{3.24}$$

C_3 symmetry: $\mathcal{R}'(\pi/2, -\pi/2, \pi/2)$

- Again, for $i = 0$, the only state is $|0,0\rangle$.
- For $i = 1$, the corresponding Wigner matrix

$$D^1_{k_3,k_3'} = \begin{pmatrix} -1/2 & i/\sqrt{2} & 1/2 \\ -i/\sqrt{2} & 0 & -i/\sqrt{2} \\ 1/2 & i/\sqrt{2} & -1/2 \end{pmatrix} \tag{3.25}$$

has two eigenvalues, with multiplicity 2 and 1, respectively. The associated eigenstates are

$$\begin{aligned}&\lambda_1 = -1,\\ &\left|\phi^1_{1a}\right\rangle = -\left|1,-1\right\rangle + \left|1,1\right\rangle,\\ &\left|\phi^1_{1b}\right\rangle = \left|1,-1\right\rangle + \sqrt{2}i\left|1,0\right\rangle + \left|1,1\right\rangle\end{aligned} \tag{3.26}$$

$$\begin{aligned}&\lambda_2 = 1,\\ &\left|\phi^1_{2}\right\rangle = \left|1,-1\right\rangle - \sqrt{2}i\left|1,0\right\rangle + \left|1,1\right\rangle\end{aligned} \tag{3.27}$$

- $i = 2$,

$$D^2_{k_3,k_3'} = \begin{pmatrix} 1/4 & -i/2 & -\sqrt{6}/4 & i/2 & 1/4\\ 1/2i & 1/2 & 0 & 1/2 & -i/2\\ -\sqrt{6}/4 & 0 & -1/2 & 0 & -\sqrt{6}/4\\ -i/2 & 1/2 & 0 & 1/2 & i/2\\ 1/4 & i/2 & -\sqrt{6}/4 & -i/2 & 1/4 \end{pmatrix} \tag{3.28}$$

$$\begin{aligned}&\lambda_1 = -1,\\ &\left|\phi^2_{1a}\right\rangle = -\left|2,-2\right\rangle + i\left|2,-1\right\rangle - i\left|2,1\right\rangle + \left|2,2\right\rangle,\\ &\left|\phi^2_{1b}\right\rangle = \left|2,-2\right\rangle + \sqrt{6}\left|2,0\right\rangle + \left|2,2\right\rangle\end{aligned} \tag{3.29}$$

$$\begin{aligned}&\lambda_2 = 1,\\ &\left|\phi^2_{2a}\right\rangle = \left|2,-1\right\rangle + \left|2,1\right\rangle,\\ &\left|\phi^2_{2b}\right\rangle = -\left|2,-2\right\rangle - 2i\left|2,-1\right\rangle + \left|2,2\right\rangle,\\ &\left|\phi^2_{2c}\right\rangle = \left|2,-2\right\rangle - \sqrt{2/3}\left|2,0\right\rangle + \left|2,2\right\rangle.\end{aligned} \tag{3.30}$$

Physical states with fixed i will correspond to mutual eigenstates of both spin-i Wigner matrices corresponding to the two symmetries, A_2 and C_3. For each value of total isospin, we have been able to find a unique state that satisfies this property,

$$\begin{aligned}&i = 0 \to \left|0,0\right\rangle,\\ &i = 1 \to \left|\psi^1_1\right\rangle = (1+i)/2\left|\phi^1_{1a}\right\rangle + (1-i)/2\left|\phi^1_{1b}\right\rangle,\\ &i = 2 \to \left|\psi^2_1\right\rangle = \left|\phi^2_{2b}\right\rangle + (1+i)\left|\phi^2_{2a}\right\rangle,\end{aligned} \tag{3.31}$$

and the corresponding normalized states will be denoted by $|\psi^i\rangle$. Note that each $|\psi^i\rangle$ corresponds to an isospin multiplet with degeneracy i, since the i_3 quantum number is not restricted by the FR constraints (and the same happens to the corresponding spin states, in which j_3 is not constrained either).

Then, we just find the quantum ground state of the crystal as the state with lower total energy. Naively, one would think that it corresponds to the $|\psi^0\rangle = |0,0,0\rangle$ state, as the isospin contribution vanishes. However, this would result in a non-vanishing total electric charge of each unit cell, so the crystal will be unstable due to an infinite contribution of the Coulomb energy, as was already noticed in [Kle85]. Thus, electrical neutrality implies that the true ground state of pure skyrmion matter corresponds to the $i_3 = -2$ state in the multiplet $|\psi^2\rangle$.

Following the previous reasoning we have obtained the allowed quantum states for a single unit cell. On the other hand, we have assumed that a basis for the Hilbert space of the total crystal isospin state can be constructed from the direct product of states of individual cells. We are now in a position to be more specific about this statement. Indeed, consider the quantum state of two unit cells with $i = \{i_1, i_2\}$ and $i_3 = \{m_1, m_2\}$. The allowed values of $\{i_1, i_2\}$ are $\{0, 1, 2\}$, and $-i_a \leq m_a \leq i_a$, $a = 1, 2$. The total quantum state will be an eigenstate of the total isospin, so it will be better described in the coupled angular momenta basis. Indeed, from representation theory, the tensor product of two spin j_a representations may be decomposed as a direct sum as

$$D^{j_1} \otimes D^{j_1} = \bigoplus_{k=|j_2-j_1|}^{j_2+j_1} D^k. \tag{3.32}$$

Thus, the basis of states for the two-cell system will be $|I, I_3, i_1, i_2\rangle$, with $|j_1 - j_2| \leq I \leq j_1 + j_2$ the total isospin number and $-I \leq I_3 \leq I$ the third component of total isospin. Therefore, to find a general basis state for an arbitrary number of unit cells, we should just need to generalize the previous construction to the coupling of an arbitrary number of different angular momenta. There are arbitrarily many ways to do it, which should be equivalent up to a unitary transformation (at least, for an arbitrary, but finite, number of unit cells). An important final remark is that, following such construction, the total isospin and third component of isospin of the full crystal will remain good quantum numbers, independently of the quantum state, so they will correspond to well defined observables in the quantum theory, as opposed to the isospin of each of the individual cells.

Isospin correction to the energy per baryon

Let us rewrite the Skyrme Lagrangian (1.1) as

$$\mathcal{L} = \frac{1}{24\pi^2}\big[a\,\mathrm{Tr}\{L_\mu L^\mu\} + b\,\mathrm{Tr}\{[L_\mu, L_\nu]^2\} + c\,B_\mu B^\mu + d\,\mathrm{Tr}(U - I)\big]. \tag{3.33}$$

The values of a, b, c, d are easily obtained from (1.7),

$$a = -\frac{1}{2}, \quad b = \frac{1}{4}, \quad c = -8\lambda^2\pi^4\frac{f_\pi^2 e^4}{\hbar^3}, \quad d = \frac{m_\pi^2}{f_\pi^2 e^2}. \tag{3.34}$$

We now consider a (time-dependent) isospin transformation of a static Skyrme field configuration,

$$U(\mathbf{x}) \to \tilde{U}(\mathbf{x}, t) \equiv g(t)U(\mathbf{x})g^\dagger(t). \tag{3.35}$$

The Maurer-Cartan (M-C) form transforms as ($\dot{g} = dg/dt$)

$$\tilde{U}^\dagger\partial_\mu\tilde{U} = \begin{cases} gU^\dagger\partial_i U g^\dagger, & (\mu = i = 1, 2, 3) \\ g(U^\dagger[g^\dagger\dot{g}, U])g^\dagger, & (\mu = 0). \end{cases} \tag{3.36}$$

We now define the isospin angular velocity ω as $g^\dagger\dot{g} = \frac{i}{2}\omega_a\tau_a$. Then, we may write the time component of the Maurer-Cartan current as $\tilde{U}^\dagger\partial_0\tilde{U} = gT_a g^\dagger\omega_a$, where T_a is the $\mathfrak{su}(2)$-valued current,

$$T_a = \frac{i}{2}U^\dagger[\tau_a, U] = i(\pi_a\pi_b - \pi_c\pi_c\delta_{ab} + \sigma\pi_c\epsilon_{abc})\tau_b \equiv iT_b^a\tau_b, \tag{3.37}$$

where we have made use of the parametrization (1.2). Moreover, the spatial components of the M-C form can be written in terms of the sigma and pion fields as well,

$$\begin{aligned} L_k =&(\sigma - i\pi_a\tau_a)(\partial_k\sigma + i\partial_k\pi_b\tau_b) = \\ =&i(\sigma\partial_k\pi_c - \pi_c\partial_k\sigma + \pi_a\partial_k\pi_b\varepsilon_{abc})\tau_c \equiv L_k^c\tau_c. \end{aligned} \tag{3.38}$$

The time dependence of the new Skyrme field induces a kinetic term in the energy functional, given by [3]

$$T = \frac{1}{24\pi^2}\int \{a\,\mathrm{Tr}\{L_0L_0\} - 2b\,\mathrm{Tr}\{[L_0,L_k][L_0,L_k]\} - c\;B^iB_i\}d^3x, \tag{3.39}$$

with B^i the spatial components of the topological current:

$$B^i = \frac{1}{24\pi^2}\varepsilon^{i\alpha\beta\gamma}\,\mathrm{Tr}\{L_\alpha L_\beta L_\gamma\} = \frac{3}{24\pi^2}\varepsilon^{ijk}\,\mathrm{Tr}\{L_0L_jL_k\}. \tag{3.40}$$

We may rewrite the kinetic isorotational energy in the standard way as a quadratic form acting on the components of the isospin angular velocity,

$$T = \frac{1}{2}\omega_i\Lambda_{ij}\omega_j \tag{3.41}$$

where Λ_{ij} is the isospin inertia tensor, given by

$$\begin{aligned} \Lambda_{ij} = \frac{1}{24\pi^2}\int d^3x\,\{&2a\,\mathrm{Tr}\{T_iT_j\} - 4b\,\mathrm{Tr}\{[T_i,L_k][T_j,L_k]\} \\ &- \frac{c}{32\pi^4}\varepsilon^{abc}\,\mathrm{Tr}\{T_iL_bL_c\}\varepsilon_{ars}\,\mathrm{Tr}\{T_jL_rL_s\}\Big\}\,. \end{aligned} \tag{3.42}$$

The high degree of symmetry of the fields inside the unit cell implies that the complete isospin inertia tensor for the unit cell of a cubic crystal will be proportional to the identity, and its eigenvalue (the isospin moment of inertia) will be given by

$$\Lambda = \frac{1}{24\pi^2}\left[2a\Lambda^{(2)} - 4b\Lambda^{(4)} - \frac{c}{32\pi^4}\Lambda^{(6)}\right]. \tag{3.43}$$

The numerical results for Λ for the $\mathcal{L}_{240}$, and the full $\mathcal{L}_{2460}$ cases are plotted as a function of the lattice parameter in fig. 3.2, for different values of the sextic term coupling constant λ^2. The Λ curve for $\mathscr{L}_{24}$ was obtained by Baskerville in [Bas96] so it has been helpful to check our results. The value of Λ becomes smaller at high densities both without sextic or with a small value of λ^2, hence the isospin correction to the energy will grow with n_B. However the increase of the sextic coupling constant produces a final increase of Λ at high densities (at which the sextic term becomes more relevant), so a non-trivial behavior will be found in the symmetry energy. Therefore, the result for $\mathcal{L}_{2460}$ diverges from that for $\mathcal{L}_{240}$ at high densities, whereas both join in the opposite, low density limit. Note that the pion mass potential term does not directly contribute to the value of Λ, but it does so indirectly because it modifies the classical solution.

[3] Remember that we are using the mostly minus convention for the metric signature.

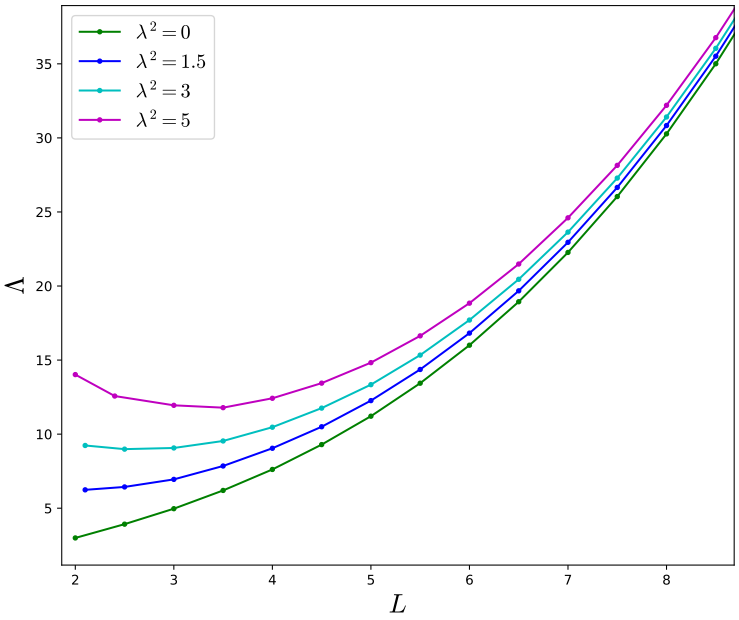

Figure 3.2: The eigenvalue Λ of the isospin inertia tensor is displayed against the lattice length parameter in Skyrme units.

The kinetic term in the Lagrangian of an isospinning cubic crystal with a number $N_{\text{cells}} \equiv N$ of unit cells can thus be written in terms of the isospin moment of inertia Λ (3.43) as

$$T = \frac{1}{2}\omega_i \Lambda_{ij} \omega_j = N \frac{1}{2} \Lambda \omega_a \omega^a, \tag{3.44}$$

and, by defining the corresponding canonical momentum $J_a = \partial L / \partial \omega^a = N \Lambda \omega_a$, we may write it in Hamiltonian form,

$$H = \frac{1}{2N\Lambda} J_a J^a. \tag{3.45}$$

Now, following the standard canonical quantization procedure, we promote the isospin angular momentum variables to operators, so that we may diagonalise the Hamiltonian in a basis of eigenstates with a definite value of the total isospin angular momentum,

$$H = \frac{\hbar^2}{2N\Lambda} J^{\text{tot}} (J^{\text{tot}} + 1) \tag{3.46}$$

The total isospin angular momentum of the full crystal will be given by the product of the total number of unit cells times the total isospin of each unit cell, which can be obtained by composing the isospin of each of the cells. In the charge neutral case, all cells will have the highest possible value of isospin angular momentum, so that in each unit cell with baryon number B_{cell}, the total isospin will be $\frac{1}{2} B_{\text{cell}}$, and hence the total isospin of the full crystal will be $J^{\text{tot}} = \frac{1}{2} N B_{\text{cell}}$.

Therefore, the quantum correction to the energy (per unit cell) due to the isospin degrees of freedom will be given by (assuming $N \to \infty$)

$$E_{\text{iso}} = \frac{\hbar^2}{8\Lambda} B_{\text{cell}}^2. \tag{3.47}$$

For example, for the unit cell of the FCC half-Skyrmion lattice, the isospin contribution to the energy per baryon is

$$\left.\frac{E_{\rm iso}}{B_{\rm cell}}\right|_{\rm FCC} = \frac{\hbar^2}{2\Lambda}. \tag{3.48}$$

The value of $\hbar$ in Skyrme units is important to calculate the contribution of the isospin energy, however for our choice of the parameters $\hbar = e^2/(3\pi^2) \approx 1$.

The classical Skyrmion crystal configurations can be understood as models for isospin-symmetric nuclear matter, i.e. nuclear matter with zero total isospin. Indeed, since the Skyrme Lagrangian is symmetric under isospin rotations of the chiral fields, in principle there is no distinction between nucleons in classical configurations. However, as we have seen, the quantum isospin correction to the crystal energy per baryon does depend on the difference between protons and neutrons through the total isospin number per unit cell. Hence, by considering the effect of iso-rotations over classical solutions we are effectively breaking the isospin symmetry of the static energy functional by adding a correction of quantum origin that explicitly breaks it. Moreover, such correction could also have been obtained through the inclusion of an isospin chemical potential. Indeed, we may introduce a nonzero isospin chemical potential μ_I in any chiral effective theory (and the Skyrme model in particular) in terms of a covariant derivative of the chiral fields of the form [SS01]

$$\partial_\mu U \to D_\mu U = \partial_\mu U - \frac{i\mu_I}{2}\delta_{\mu 0}[\tau^3, U], \tag{3.49}$$

so that, if U is a static configuration, the time component of the Maurer-Cartan form becomes

$$L_0 = -\frac{i}{2}\mu_I U^\dagger[\tau^3, U] = -\mu_I T_3. \tag{3.50}$$

Comparing with eq. (3.36), one sees that this expression is equivalent to that of an iso-rotating field with angular velocity $\omega_a = -\mu_I \delta_{3a}$. Thus, it is straightforward to obtain the isospin chemical potential for the Skyrmion crystal using its thermodynamical definition $\mu_I = -\frac{\partial E}{\partial n_I}$, where n_I is the (third component of) the isospin number density. Given that $(J^{\rm tot})^2 = J_1^2 + J_2^2 + J_3^2$ and $n_I = J_3/N$, we may write the isospin energy per unit cell as

$$E_{\rm iso} = \frac{\hbar^2}{2\Lambda}\left(n_I^2 + \frac{J_2^2}{N^2} + \frac{J_1^2}{N^2}\right) \tag{3.51}$$

and then

$$\mu_I = -\frac{\partial E_{\rm iso}}{\partial n_I} = -\frac{\hbar^2}{\Lambda} n_I. \tag{3.52}$$

As we have seen in the previous subsection, the ground state of the Skyrme crystal is forced by the charge neutrality condition to have

$$(J^{\rm tot})^2 = J_3^2, \tag{3.53}$$

and for a unit cell of $B_{\rm cell}$ baryon number, the chemical potential is simply $\mu_I(L) = -\hbar^2 B_{\rm cell}/(2\Lambda)$. This indeed coincides with the expression of ω_a in terms of the isospin angular momentum and the isospin moment of inertia. As a final comment, we remark that the inclusion of isospin may have non-trivial effects on the geometry of classical solitonic solutions. In

particular, it was shown in [LMR06] that the isospin chemical potential may alter the stability of classical Skyrmion configurations. Hence, a thorough analysis of dense Skyrmion matter at finite isospin chemical potential should focus on its effects on the classical crystal configuration. However, as the contribution to the isospin energy per unit cell $E_{\text{iso}}(L)$ is never dominating for any L, we may neglect the backreaction of the isospin term into the background and consider it simply as a (quantum) correction to the energy.

3.3 Symmetry energy

Let us consider a finite Skyrme crystal of N unit cells, and let $B = N \times B_{\text{cell}}$, where B_{cell} is the baryon number of a unit cell. We do not enforce charge neutrality at this step, and further leave unknown the quantum state $|\Psi\rangle$ of the crystal. We have seen that the total charge of this system is

$$Q = \left\langle e \int d^3x \{B^0/2 + I_3^0\} \right\rangle = eN \left[\frac{B_{\text{cell}}}{2} + \frac{\left\langle \int I_3^0 d^3x \right\rangle}{N} \right]. \tag{3.54}$$

As argued at the end of section 3.2.1, the total third component of isospin is a good quantum number for the total quantum state of the crystal, although this is not true for individual unit cells. In other words, the expectation value

$$\langle I_3 \rangle = \langle \Psi | \int I_3^0 d^3x \, |\Psi\rangle \tag{3.55}$$

is well defined in an arbitrary quantum state, but $\int \langle I_3^0 \rangle \, d^3x$ is not. Since we are seeking for a definition of the isospin density in the quantum theory, we may perform a mean field approximation and consider that the isospin density in an arbitrary skyrmion crystal quantum state is approximately uniform so that

$$\langle I_3^0 \rangle = \frac{\langle I_3 \rangle}{\int d^3x} = \frac{\langle I_3 \rangle}{N V_{\text{cell}}} \doteq \frac{n_I}{V_{\text{cell}}}, \tag{3.56}$$

where n_I is the effective isospin charge per unit cell in this arbitrary quantum state. We also notice that, for a fixed value of total I_3, the quantum state $|\Psi\rangle$ will satisfy condition (3.53) in order to minimize the total isospin energy (3.51). We may further consider the effective proton fraction that would yield such an isospin charge per unit cell with baryon number B_{cell} to write

$$n_I = -\frac{1}{2}(1 - 2\gamma) B_{\text{cell}} = -\frac{B_{\text{cell}}}{2}\delta. \tag{3.57}$$

Hence, we may write the isospin energy per unit cell of the Skyrmion crystal in such a state in terms of the asymmetry parameter

$$E_{\text{iso}} = \frac{\hbar^2 B_{\text{cell}}^2}{8\Lambda}\delta^2, \tag{3.58}$$

and thus the symmetry energy for Skyrme crystals is given by

$$S_N(n_B) = \frac{\hbar^2 L^3}{\Lambda} n_B. \tag{3.59}$$

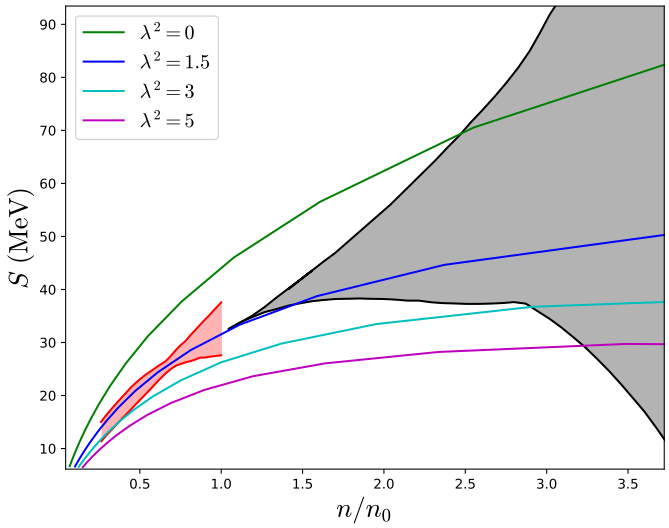

Figure 3.3: Symmetry energy of Skyrme crystals as a function of the density for different values of λ. Constraints of the symmetry energy at sub-saturation densities from isobaric analog states [DL14] are plotted in red. The grey region corresponds to recent constraints from the analysis of neutron star observations [Li+21]

In fig. 3.3 we plot the symmetry energy of Skyrmion crystals for the generalized Skyrme model with different values of the sextic coupling constant.

We can observe that, for this choice of parameters, the symmetry energy of the crystal in the $\mathcal{L}_{240}$ submodel ($\lambda^2 = 0$) comes out too big with respect to the constraints at saturation density n_0, while the inclusion the sextic term reduces the value. We found that a value of $\lambda^2 \sim 1.5\,\text{MeV fm}^3$ fits to the correct value at saturation. Moreover, we may also compute the slope and curvature parameters at saturation for all cases, shown in table 3.1. Interestingly, for values of λ^2 between $1.5 - 3$ MeV fm^{-3} we find that both the saturation density and the symmetry energy parameters agree quite well with the most up-to-date experimental values. Here we have defined the saturation density as the density where the energy per baryon of the skyrmion crystal takes its minimum value. Hence, the constraints on the symmetry energy yield rather stringent bounds on the value

λ^2 (MeV fm^3)	n_0 (fm^{-3})	S_0 (MeV)	L (MeV)	K_{sym} (MeV)
0	0.33	44.4	72.9	-143
1.5	0.22	31.9	46.4	-130
3	0.18	26.4	35.4	-118
5	0.15	22.2	27.5	-105
Exp.	0.16 ± 0.01	31.7 ± 3.2	57.7 ± 19	-107± 88

Table 3.1: Symmetry energy coefficients in the Skyrme model with different sextic couplings. In the last row, we show the most up-to-date fiducial values of n_0, S_0, L and K_{sym} [Li+21]

of λ^2, where the precise numerical values of these bounds will, of course, depend on the choices made for the other model parameters f_π and e. We remark that a lower bound

for this constant can also be obtained from the maximum mass requirement of neutron star EoS [Ada+21].

We end our discussion on the Symmetry energy of Skyrme crystals by pointing out the absence of the *cusp structure* predicted by Lee et al. [LPR11] in our results of S. Their argument (recently reviewed in [Lee+21]) for the appearance of a minimum in the symmetry energy at a given density $n_{1/2} > n_0$ is based on the Skyrmion to half-Skyrmion transition, which is proposed to happen at $n_{1/2} \sim 2 - 3n_0$. In our pure Skyrme model setting, however, such a transition has been shown to occur in a thermodynamically unstable branch of the Skyrmion crystal phase diagram once the pion mass is taken into account (see, eg. [PV10; Ada+22a]). Therefore, we do not find such a transition, as we consider a crystal of (nearly) half-Skyrmions to be the correct ground state for densities $n > n_0$. The ground state of the Skyrme model for densities $n \leq n_0$ is still not well understood, and some inhomogeneous configurations have been proposed [PPV19; Ada+22a] that point towards a complicated phase structure predicted by the Skyrme model near saturation. In particular, the transition from regular nuclear matter to a crystal of half-Skyrmions should take place in such a range of densities.

3.3.1 Particle fractions of $npe\mu$ matter in β-equilibrium

As previously argued, any quantum state that deviates from the ground state in pure skyrme matter would lead to a divergence in the Coulomb energy in the infinite crystal limit. Indeed, an isolated system of positively charged matter is unstable due to Coulomb repulsion. Therefore, it is assumed that there exists a neutralizing background of negatively charged leptons (electrons and possibly muons), such that this Coulomb repulsion is compensated. Such a system of nuclear matter plus leptons is characterized in the equilibrium phase by two equilibrium conditions, namely the *charge neutrality condition*

$$n_p = \frac{Z}{V} = n_e + n_\mu, \tag{3.60}$$

i.e., the densities of positively charged nucleons (protons) and negatively charged leptons (electrons and muons) are equal, and the *β-equilibrium condition*

$$\mu_n = \mu_p + \mu_l \implies \mu_I = \mu_l, \qquad l = e, \mu, \tag{3.61}$$

i.e., the isospin chemical potential must equal that of charged leptons, such that the neutron decay and electron capture processes

$$n \to p + l + \bar{\nu}_l \quad , \quad p + l \to n + \nu_l \tag{3.62}$$

take place at the same rate. Moreover, leptons inside a neutron star are usually described as a non-interacting, highly degenerate fermi gas, so that the chemical potential for each type of leptons can be written

$$\mu_l = \sqrt{(\hbar k_F)^2 + m_l^2}, \tag{3.63}$$

where $k_F = (3\pi^2 n_l)^{1/3}$ is the corresponding Fermi momentum, and m_l is the mass of the corresponding lepton. Indeed, for sufficiently large densities the electron chemical

potential will be larger than the muon mass, $\mu_e \geq m_\mu$, and the appearance of muons in the system will be energetically favorable. We may now estimate the total proton fraction by enforcing both charge neutrality and beta equilibrium. Let us start by neglecting the contribution of muons to the charge density. Then, from the charge neutrality condition (3.60), we relate the electron density to the proton fraction parameter, $n_e = \gamma B_{\rm cell}/(2L)^3$, and the β equilibrium condition yields an equation that implicitly defines γ as a function of the lattice length parameter,

$$\frac{\hbar L}{\Lambda}(1-2\gamma) = \left(\frac{3\pi^2}{B_{\rm cell}^2}\right)^{1/3}\gamma^{1/3}, \tag{3.64}$$

where we have also made the ultrarelativistic electron approximation, i.e. $m_l/k_F \simeq 0$.

Including the muon contribution to the charge density yields a slightly more complicated expression for the β-equilibrium condition, given by

$$\frac{\hbar B_{\rm cell}}{2\Lambda}(1-2\gamma) = \left[3\pi^2\left(\frac{\gamma B_{\rm cell}}{8L^3} - n_\mu\right)\right]^{\frac{1}{3}}, \tag{3.65}$$

where

$$n_\mu = \frac{1}{3\pi^2}\left[\left(\frac{\hbar B_{\rm cell}(1-2\gamma)}{2\Lambda}\right)^2 - \left(\frac{m_\mu}{\hbar}\right)^2\right]^{\frac{3}{2}}. \tag{3.66}$$

On the other hand, the proton fraction inside the beta-equilibrated matter also determines whether a proto-neutron star will go through a cooling epoch via neutrino emission through the Direct Urca (DU) process $n \to p + e + \bar{\nu}_e$, which is expected to occur if the proton fraction reaches a critical value, $\gamma_p > x_{DU}$, the so-called DU-threshold [Lat+91; Kla+06]. As the DU process allows for an enhanced cooling rate of NS, whether it takes place or not in the hot core of proto-neutron stars or during the merge of binary NS systems [Alf+21] would determine the proton fraction (hence, the symmetry energy) of matter at ultra-high densities. However, it is not clear whether such enhanced cooling actually takes place, although there is recent evidence that supports it [Bro+18].

In $npe\mu$ matter, the DU threshold is given by [Kla+06]

$$x_{DU} = \frac{1}{1+(1+(\frac{n_e}{n_e+n_\mu})^{1/3})^3}. \tag{3.67}$$

Once the proton fraction and the asymmetry parameter are obtained, the total energy of the system may be also calculated as

$$E = E_{\rm class} + E_{\rm iso}(\delta) + E_e(\gamma) + E_\mu(\gamma), \tag{3.68}$$

where $E_{\rm clas}$ is the classical energy of the Skyrme field, $E_{\rm iso}$ is given by eq. (3.58) and $E_{\rm lep}$ is the energy density of a relativistic lepton gas with mass m_l at zero temperature

$$E_{\rm lep} = \int_0^{k_f}\frac{k^2dk}{\pi^2}\sqrt{k^2+m_l^2} = \frac{m_l^4}{8\pi^2}\Big[x_r(1+2x_r^2)\sqrt{1+x_r^2} - \ln x_r + \sqrt{1+x_r^2}\Big], \tag{3.69}$$

where $x_r = k_F/m_l$. For densities $n \geq n_0$, the electrons become ultra-relativistic, i.e. $m_e \ll k_{Fe}$ and the corresponding energy becomes

$$E_e \simeq \frac{3}{4}k_{Fe}n_e. \tag{3.70}$$

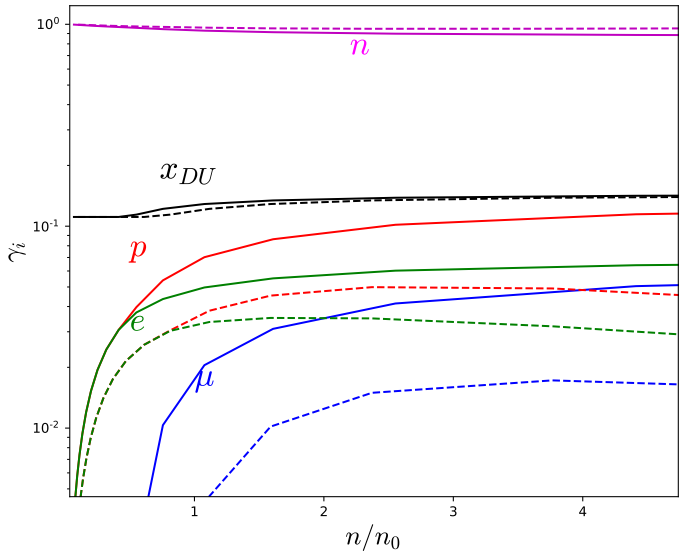

Figure 3.4: Fraction density γ_i for each particle as a function of the baryon density for $\lambda^2 = 0$ (solid) and $\lambda^2 = 1.5$ (dashed). The corresponding DU threshold is also shown in black.

The particle populations γ_i in the beta-equilibrated Skyrmion matter are shown in fig. 3.4 for the cases $\lambda^2 = 0, 1.5$ MeV fm^3.

In both cases, a persistent population of protons and leptons with increasing nucleon density is expected, although in the case with sextic term we see that the fraction of charged particles is smaller. This is the impact of the sextic term, since it is much easier to convert protons into neutrons due to the lower symmetry energy. Finally, the DU-threshold is not reached in any case for the values of the parameters (f_π, e, λ^2) that we have chosen. However, one should not take this fact as a prediction of the Skyrme model, as it strongly depends on the parameter values. Also, it is generally assumed that around $2-3$ times the nuclear saturation density, additional degrees of freedom (strange baryons) become important for the description of nuclear matter, which in particular may affect the proton fraction at such densities.

3.4 Strangeness and Kaon condensation

In QCD with three quark flavors $(up, down, strange)$, there are $3^2 - 1 = 8$ (pseudo) Goldstone bosons after SSB of the chiral symetry [4], which can be compactly collected in terms of the $SU(3)$-valued chiral field

$$U = e^{i\theta_A \lambda_A / f_\pi}, \quad \text{where} \quad \theta_A \lambda_A = \begin{pmatrix} \frac{\pi^0}{\sqrt{2}} + \frac{\eta}{\sqrt{6}} & \pi^+ & K^+ \\ \pi^- & -\frac{\pi^0}{\sqrt{2}} + \frac{\eta}{\sqrt{6}} & K^0 \\ K^- & \bar{K}^0 & -\sqrt{\frac{2}{3}}\eta \end{pmatrix}. \tag{3.71}$$

[4] There is actually nine, as the complete spontaneously broken subgroup includes the axial $U(1)_A$. However, the associated pseudo-Goldstone, η', is much more massive beacuse of the anomalous breaking of such symmetry, which is known as the chiral anomaly of QCD.

where λ_{A} ($\text{A} = 1, \cdots 8$) are the Gell-Mann matrices (see (5)).

Apart from the three pion fields that we have already worked with, there are other pseudoscalar mesons with nonzero STRANGENESS, the quantum number associated with the presence of the s quark, within the same multiplet. These are the η meson and the KAONS (see fig. 3) The latter come in four different types, two electrically charged with opposite charges and two neutral, with opposite strangeness content. The masses of the three types of kaons differ only in less than 1%. As with the pions, this fact reflects the approximate charge symmetry in nuclear physics. The mass of kaons ($m_K \approx 495\,\text{MeV}$) are almost four times bigger than that of pions. Therefore, at the energy scales we will be mostly interested, we may assume that the light quark masses are degenerate, and thus isospin symmetry is preserved, while the s quark mass is different, so that, in a good approximation, we have the following (explicit) symmetry breaking pattern

$$SU(3)_L \times SU(3)_R \xrightarrow{\chi\text{SSB}} SU(3)_V \xrightarrow{m_s \gg m_{u,d}} SU(2)_I \times U(1)_Y. \tag{3.72}$$

Many calculations for the EoS in dense matter predict that strangeness degrees of freedom may become important in the interior of compact stars, in the form of hyperons (strange baryons) or a Bose-Einstein condensate of negatively charged kaons, for densities just a few times nuclear saturation [TF20]. Indeed, hyperons may become stable at sufficiently high isospin chemical potential, where the decay of neutrons relieve the Fermi pressure exerted by the nucleons. On the other hand, the strong attraction between K^- mesons and baryons increases with density and lowers the energy of the zero momentum state. A condensate is formed when this energy equals the kaon chemical potential, since kaons are favored over negatively charged fermions for achieving charge neutrality, as they are bosons and can condense in the lowest energy state.

It is generally assumed that strange degrees of freedom should become relevant at densities above $\sim 2-3$ times the nuclear saturation density n_0, whereas the critical density for kaon condensation is usually predicted to be a bit larger, around $\sim (3-4)n_0$ (although the specific values are of course model and parameter dependent). A density of this order is smaller than the central density of a typical NS, so a kaon condensate could be present in its core. The possibility of kaon condensates in the core of neutron stars has been extensively investigated in the literature, using different approaches. Its appearance tends to soften the EoS, producing smaller values for the allowed maximum masses. Therefore, the presence of hyperons at too low densities is not compatible with the stiffness required by the existence of such massive stars. This is the so-called *Hyperon puzzle*, presently a subject of very active research [Bom17; Vid16].

Having obtained the proton fraction (hence the electron chemical potential) in $npe\mu$-matter as a function of density in the last chapter, we can now turn to the question of whether kaon fields may condense inside a Skyrme crystal for a sufficiently high density, and, if so, whether this critical density value is relevant for the description of matter inside compact stars.

Kaon fluctuations in the Skyrme model

Following the bound-state approach first proposed in [CK85] we may include strange degrees of freedom in the Skyrme model by extending the skyrmion field to a $SU(3)$-valued field U through modelling kaon fluctuations on top of a $SU(2)$ skyrmion-like background

u With the only requirement that unitarity must be preserved, different ansätze have been proposed in the literature for the total $SU(3)$ field describing both pions and kaons [Kle90]. In this work, we choose the ansatz proposed by Blom et al in [BDR89]:

$$U = \sqrt{U_K} U_\pi \sqrt{U_K}. \tag{3.73}$$

In this ansatz U_π represents the $SU(3)$ embedding of the purely pionic part u, and the field U_K are the fluctuations in the strange directions. It can be shown that this ansatz is equivalent to the one first proposed by Callan and Klebanov in [CK85] when computing static properties of hyperons, although both may differ in other predictions of the model [NR90].

In the simplest $SU(3)$ embedding, the $SU(2)$ field u is extended to U_π by filling the rest of entries with ones in the diagonal and zeros outside. On the other hand, the kaon ansatz is modelled by a $\mathfrak{su}(3)$ -valued matrix $\mathcal{D}$ which is non trivial in the off-diagonal elements:

$$\begin{gathered} U_\pi = \begin{pmatrix} u & 0 \\ 0 & 1 \end{pmatrix}, \quad U_K = e^{i\frac{2\sqrt{2}}{f_\pi}\mathcal{D}}, \\ u = \sigma + i\pi_a\tau_a \equiv i n_\alpha \tau_\alpha, \quad \mathcal{D} = \begin{pmatrix} 0 & K \\ K^\dagger & 0 \end{pmatrix}, \end{gathered} \tag{3.74}$$

where $a = 1,2,3$, $\alpha = 0,1,2,3$, $\tau_\alpha = (-i\mathbf{1}, \boldsymbol{\tau})$, and K consists of a scalar doublet of complex fields representing charged and neutral kaons:

$$K = \begin{pmatrix} K^+ \\ K^0 \end{pmatrix}, \quad K^\dagger = (K^-, \bar{K}^0). \tag{3.75}$$

The extension of the GSM Lagrangian (1.1) to include strange degrees of freedom in a way consistent with the symmetry group (3.72) consists in the replacement of the pion mass term $\mathscr{L}_0$ by [NR90]:

$$\mathscr{L}_0^{\text{new}} = \frac{f_\pi^2}{48}\left(m_\pi^2 + 2m_K^2\right)\mathrm{Tr}\{U + U^\dagger - 2\} + \frac{\sqrt{3}}{24} f_\pi^2 \left(m_\pi^2 - m_K^2\right)\mathrm{Tr}\{\lambda_8\left(U + U^\dagger\right)\}, \tag{3.76}$$

with m_K the vacuum kaon mass. The kaon mass differs from that of pions because kaons involve a strange mass. Moreover, as it is well known in the three-flavor case one needs to additionally include the Wess-Zumino-Witten (WZW) term, which accounts for intrinsic parity-violating processes, such as the scattering of two kaons to three pions $K^+K^- \to \pi^+\pi^-\pi^0$ or the decay of π^0 to two photons. It can be expressed in terms of a 5-dimensional action integral [Wit83b]:

$$S_{WZ} = -i\frac{N_c}{240\pi^2}\int d^5x\, \epsilon^{\mu\nu\alpha\beta\gamma}\,\mathrm{Tr}\{L_\mu L_\nu L_\alpha L_\beta L_\gamma\}. \tag{3.77}$$

The onset of kaon condensation in the Skyrme model takes place at a critical density n_{cond} at which μ_e becomes greater than the energy of the kaon zero-momentum mode (s-wave condensate). Thus, for baryon densities $n \geq n_{\text{cond}}$, the macroscopic contribution of the kaon condensate to the energy must be taken into account when obtaining the EoS of dense matter. To do so, we follow the standard procedure to describe Bose-Einstein

condensation of a (complex) scalar field (see eg [Sch10]) in which the field condensates correspond to the non-zero vacuum expectation values (vev), $\langle K^{\pm}\rangle$, which are assumed to be constant in space and whose time dependence is given by:

$$\left\langle K^{\mp}\right\rangle = \phi e^{\mp i\mu_K t} \tag{3.78}$$

The real constant ϕ corresponds to the zero-momentum component of the fields, which acquires a nonvanishing, macroscopic value after the condensation. Its exact value is determined from the minimization of the corresponding effective potential, to whose calculation we will dedicate the rest of this section. On the other hand, the phase μ_K is nothing but the corresponding kaon chemical potential. First, we will need an explicit form of the $SU(3)$ Skyrme field in the kaon condensed phase. Assuming the charged kaons will be the first mesons to condense [5], we can safely drop the neutral kaon contribution, and define the following matrix

$$\tilde{\mathcal{D}} = \begin{pmatrix} 0 & 0 & \phi e^{i\mu_K t} \\ 0 & 0 & 0 \\ \phi e^{-i\mu_k t} & 0 & 0 \end{pmatrix}, \tag{3.79}$$

which results from substituting the kaon fields in $\mathcal{D}$ as defined in (3.74) by their corresponding vev in the kaon condensed phase. Also, taking advantage of the property $\mathcal{D}^3 = \phi^2\mathcal{D}$, we may write the $SU(3)$ element generated by $\tilde{\mathcal{D}}$ explicitly in matrix form:

$$\Sigma = e^{i\frac{\sqrt{2}}{f_\pi}\tilde{\mathcal{D}}} = \begin{pmatrix} \cos\tilde{\phi} & 0 & ie^{i\mu_K t}\sin\tilde{\phi} \\ 0 & 1 & 0 \\ ie^{-i\mu_K t}\sin\tilde{\phi} & 0 & \cos\tilde{\phi} \end{pmatrix}, \tag{3.80}$$

where $\tilde{\phi} = \frac{\sqrt{2}}{f_\pi}\phi$ is the dimensionless condensate amplitude.

Furthermore, assuming the backreaction from the kaon condensate to the skyrmion crystal is negligible, and thus the classically obtained crystal configuration will be the physically correct background even in the kaon condensed phase, we may write the $SU(3)$ field in this phase as $U = \Sigma U_\pi \Sigma$, where U_π is the $SU(3)$ embedding of the $SU(2)$ skyrmion background as in (3.74). Introducing this U in the total action yields the standard Skyrme action for the $SU(2)$ field plus an effective potential term for the kaon condensate:

$$S_{Sk}(U) + S_{\text{WZW}}(U) = S_{Sk}(U_\pi) - \int dt V_K(\tilde{\phi}), \tag{3.81}$$

where

$$V_K = \frac{1}{24\pi^2}\int d^3x\left[V_K^{(2)} + V_K^{(4)} + V_K^{(6)} + V_K^{(0)}\right] + V_K^{(WZW)}. \tag{3.82}$$

Let us now calculate the contribution to the effective potential V_K of each term in the action:

[5] Actually, that the charged (in particular, the negatively charged) kaons will condense first is true in our approach (whenever $\mu_e > 0$), since the chemical potential associated to neutral kaons is zero, so that the onset of neutral kaon condensation is given by $m_K^* = 0$.

- Quadratic term: Given that the crystal background is static and the kaon condensate does not depend on spatial coordinates, the kaon part of the quadratic term may be written as

$$\mathrm{Tr}\{L_0^2\} = -[\mathrm{Tr}\{\partial_t\Sigma^\dagger\partial_t\Sigma\} + \mathrm{Tr}\{\Sigma^\dagger\partial_t\Sigma U_\pi^\dagger\Sigma\partial_t\Sigma^\dagger U_\pi\}]. \tag{3.83}$$

  Introducing the explicit expression for Σ, (3.80), yields

$$V_K^{(2)} = \mu_K^2\sin^2\tilde{\phi}[(1+\sigma^2+\pi_3^2)\sin^2\tilde{\phi} - 2(1+\sigma\cos^2\tilde{\phi})]. \tag{3.84}$$

- Quartic term: In the quartic term, the kaon effective potential comes from the terms with time derivatives of the total field,

$$\mathrm{Tr}\{[L_0, L_i]^2\} = 2[\mathrm{Tr}\{\partial_t U^\dagger\partial_i U\partial_t U^\dagger\partial_i U\} - \mathrm{Tr}\{\partial_i U^\dagger\partial_t U\partial_i U^\dagger\partial_t U\}],$$

  which, after substitution of the expression for Σ, gives

$$\begin{aligned} V_K^{(4)} = -2\mu_K^2\sin^2\tilde{\phi}\big\{&(1+\sigma)(\partial_i n_\alpha)^2\cos^2\tilde{\phi} + \\ &+2[\partial_i\sigma^2(1-\pi_3^2) + \partial_i\pi_3^2(1-\sigma^2) + 2\sigma\pi_3\partial_i\sigma\partial_i\pi_3]\sin^2\tilde{\phi}\big\}. \end{aligned} \tag{3.85}$$

- Mass term: The kaon part associated to the mass term gives the following contribution,

$$V_K^{(0)}(\tilde{\phi}) = 2\frac{m_K^2}{f_\pi^2 e^2}(1+\sigma)\sin^2\tilde{\phi}. \tag{3.86}$$

- Wess-Zumino-Witten term: The WZW term is written as a 5-form integrated over an auxiliar 5-dimensional disk D whose boundary is the spacetime manifold M, but in appendix C we show that the variation after the kaon fluctuations of the pion background yields a local term which may be written as an effective four-dimensional lagrangian. Indeed, we show that

$$\begin{aligned} S_{\mathrm{WZW}}(U) = \quad & S_{\mathrm{WZW}}(U_\pi) - \frac{iN_C}{2}\int_M B^0\,\mathrm{Tr}\left\{\begin{pmatrix}\mathbf{1}_2 & 0\\ 0 & 0\end{pmatrix}\left(\Sigma\partial_t\Sigma^\dagger + U_\pi^\dagger\Sigma^\dagger\partial_t\Sigma U_\pi\right)\right\} = \\ &= -N_C\int\mu B_{\mathrm{cell}}\sin^2(\phi)dt = \int V_K^{(\mathrm{WZW})}(\phi)dt. \end{aligned} \tag{3.87}$$

- Sextic term: The contribution from the sextic term is also obtained in appendix C to be

$$V_K^{(6)} = -\frac{\lambda^2 f_\pi^2 e^4}{16}\,\mathrm{Tr}\{[R_j, R_k]\xi_0\}^2, \tag{3.88}$$

  where $\xi_\mu = U_\pi\Sigma\partial_\mu\Sigma^\dagger U_\pi^\dagger - \Sigma^\dagger\partial_\mu\Sigma$. Once the traces are evaluated, we end up with

$$V_K^{(6)} = -\lambda^2 f_\pi^2 e^4\mu_K^2\sin^4(\tilde{\phi})(\partial_i\pi_3\partial_j\sigma - \partial_i\sigma\partial_j\pi_3)^2. \tag{3.89}$$

In the above calculations, we have taken separately the contributions of a kaon condensate and an isospin angular momentum of the skyrmion crystal, and the kaon condensate

interacts with the skyrmion isospin only indirectly via the charge neutrality and β equilibrium conditions, which relate their corresponding chemical potentials. However, since kaons possess an isospin quantum number, we should consider a (time-dependent) isospin transformation of the full Skyrme field + kaon condensate configuration $U = \Sigma U_\pi \Sigma$:

$$U \to \tilde{U} \equiv A(t) U A^\dagger(t), \tag{3.90}$$

where A is an element of $SU(3)$ modelling an isospin rotation,

$$A = \begin{pmatrix} a & 0 \\ 0 & 1 \end{pmatrix}, \quad a \in SU(2). \tag{3.91}$$

The Maurer-Cartan form transforms as ($\dot{A} = dA/dt$)

$$\tilde{U}^\dagger \partial_\mu \tilde{U} = \begin{cases} A U^\dagger \partial_i U A^\dagger, & (\mu = i = 1,2,3), \\ A U^\dagger \partial_0 U A^\dagger + A(U^\dagger [A^\dagger \dot{A}, U]) A^\dagger, & (\mu = 0). \end{cases} \tag{3.92}$$

We now define the isospin angular velocity ω as $A^\dagger \dot{A} = \frac{i}{2}\omega_a \lambda_a$ ($a = 1,2,3$), with λ_{A} the Gell-Mann matrices generating $SU(3)$ for $\text{A} = 1, \cdots 8$. Notice that ω is a three-vector, since $A^\dagger \dot{A}$ belongs to the isospin $\mathfrak{su}(2)$ subalgebra of $\mathfrak{su}(3)$ Then, we may write the time component of the Maurer-Cartan current as $\tilde{U}^\dagger \partial_0 \tilde{U} = A L_0 A^\dagger + A T_a A^\dagger \omega_a$, where T_a is the $\mathfrak{su}(3)$-valued current:

$$T_a = \frac{i}{2} U^\dagger [\lambda_a, U] \equiv i T_a^{\text{A}} \lambda_{\text{A}}, \tag{3.93}$$

where now we have used the parametrization (3.74).

The time dependence of the new Skyrme field induces the existence of a kinetic term in the energy functional, given by [6]

$$\begin{aligned} T = \int \{ & a(\operatorname{Tr}\{L_0 L_0\} + 2\operatorname{Tr}\{L_0 T_a\}\omega_a + \operatorname{Tr}\{T_a T_b\}\omega_a \omega_b) \\ & -2b\big(\operatorname{Tr}\{[(L_0 + T_a\omega_a), L_k][(L_0 + T_b\omega_b), L_k]\}\big) - c\ B^i B_i \} d^3x, \end{aligned} \tag{3.94}$$

with B^i the spatial components of the topological current (1.3), which now read:

$$B^i = \frac{3}{24\pi^2} \varepsilon^{ijk} \operatorname{Tr}\{(L_0 + T_a\omega_a) L_j L_k\}. \tag{3.95}$$

We may rewrite the kinetic isorotational energy in the standard way as a quadratic form acting on the components of the isospin angular velocity,

$$T = \frac{1}{2}\omega_a \Lambda_{ab} \omega_b + \Delta_a \omega_a - V_K, \tag{3.96}$$

where Λ_{ab} is the isospin inertia tensor and Δ_a is the kaon condensate isospin current, given by

$$\Lambda_{ab} = \int \left\{ 2a \operatorname{Tr}\{T_a T_b\} - 4b \operatorname{Tr}\{[T_a, L_k][T_b, L_k]\} - \frac{c}{32\pi^4} \varepsilon^{lmn} \operatorname{Tr}\{T_a L_m L_n\} \varepsilon_{lrs} \operatorname{Tr}\{T_j L_r L_s\} \right\} d^3x, \tag{3.97}$$

$$\Delta_a = \int \left\{ 2a \operatorname{Tr}\{L_0 T_a\} - 4b \operatorname{Tr}\{[T_a, L_k][L_0, L_k]\} - \frac{c}{32\pi^4} \varepsilon^{lmn} \operatorname{Tr}\{L_0 L_m L_n\} \varepsilon_{lrs} \operatorname{Tr}\{T_a L_r L_s\} \right\} d^3x, \tag{3.98}$$

[6] Remember that we are using the mostly minus convention for the metric signature.

where a, b and c are those in eq. (3.34).

The symmetries of the crystalline configuration that we consider in this work, concretely the S_1 and S_2 transformations, imply that the isospin inertia tensor becomes proportional to the identity, i.e. $\Lambda_{ab}^{\text{crystal}} = \Lambda\delta_{ab}$. However, the presence of a kaon condensate breaks this symmetry to a $U(1)$ subgroup, so that Λ_{ab} presents two different eigenvalues in the condensate phase, $\Lambda_{\text{cond}} = \text{diag}(\Lambda, \Lambda, \Lambda_3)$. Similarly, $\Delta_a = 0$ in the purely barionic phase, and its third component acquires a non-zero value in the condensate phase, $\Delta_{\text{cond}} = (0, 0, \Delta)$. The explicit expressions for Λ_3 and Δ in the condensed phase are written in appendix C. One can easily check that in the non-condensed phase, $\phi = 0$ and the results of the previous section are recovered, namely, $\Lambda_3 = \Lambda$, $\Delta = 0$.

The quantization procedure now goes along the same lines as in the first section. However, the isospin breaking due to the kaon condensate implies that the canonical momentum associated to the third component of the isospin angular velocity will now be different, and given by $I_3 = \Lambda_3\omega_3 + \Delta$.

Thus, after a Legendre transformation to rewrite (3.96) in Hamiltonian form, and making the $N \to \infty$ approximation, one can write the quantum energy correction per unit cell of the crystal in the kaon condensed phase as

$$E_{\text{quant}} = \frac{1}{2\Lambda_3}(I_3^2 - \Delta^2). \tag{3.99}$$

The first term on the right hand side above is just the isospin correction, while now there is an additional second term due to the isospin of the kaons. Indeed, since the kaon field enters also in the expression of the isospin moment of inertia Λ_3, both terms will depend nontrivially on the kaon vacuum expectation value (vev). When the kaon field develops a nonzero vev, apart from the neutron decay and lepton capture processes, additional processes involving kaons may occur:

$$n \leftrightarrow p + K^-, \qquad l \leftrightarrow K^- + \nu_l, \tag{3.100}$$

such that the chemical equilibrium conditions

$$\mu_n = \mu_p + \mu_K, \qquad \mu_l = \mu_K \tag{3.101}$$

are satisfied. The last expressions are the extension of eq. (3.61) to the condensate phase. The total energy within the unit cell may be obtained as the sum of the baryon, lepton and kaon contributions:

$$E = E_{\text{class}} + E_{\text{iso}}(\gamma, \tilde{\phi}) + E_K(\mu_K, \tilde{\phi}) + E_e(n_e) + \Theta(\mu_e^2 - m_\mu^2)E_\mu(n_\mu). \tag{3.102}$$

where the kaon contribution is the effective potential energy given by

$$E_K(\mu_K, \tilde{\phi}) = V_K - \frac{\Delta^2}{2\Lambda_3}, \tag{3.103}$$

which depends on the condensate $\tilde{\phi}$ and on the kaon chemical potential through the explicit dependence on μ_K of both V_K and Δ.

In order to determine whether or not a condensate of kaons will appear at some point in the interior of NS, one needs to obtain the values of the proton fraction γ, kaon vev

ϕ and electron chemical potential μ_e that minimize the total energy for a given baryon density n_B (or equivalently, fixed L) under the constraints of charge neutrality and beta equilibrium. Thermodynamically, this can be achieved by minimizing the grand potential

$$\Omega = E - \mu_e(N_e + \Theta(\mu_e^2 - m_\mu^2)N_\mu - \gamma B) \tag{3.104}$$

with respect to its variables, *i.e.* $\tilde{\phi}$ and μ_e (the equilibrium conditions (3.101) implying $\mu_I = \mu_K = \mu_\mu = \mu_e$ are already imposed)

$$\frac{\partial\Omega}{\partial\mu_e}\bigg|_{n_B}(\tilde{\phi},\mu_e) = \frac{\partial\Omega}{\partial\tilde{\phi}}\bigg|_{n_B}(\tilde{\phi},\mu_e) = 0. \tag{3.105}$$

Indeed, the thermodynamical conditions (3.105) in turn translate into a system of (differential) equations for μ_e and $\tilde{\phi}$, which can be solved for each value of the lattice length L. A detailed description of the minimization process can be found in [Ada+23].

In particular, at a given THRESHOLD DENSITY n_{cond}, the kaon vev will acquire a nonzero value, and a phase transition will take place towards a new phase of the system, which we will call $npe\mu\overline{K}$. We show in the table below the density at which kaons condense for a choice of values of the parameters as well as the values of some nuclear observables this choice yields. All the values are given in units of MeV or fm, respectively.

label	f_π	e	λ^2	E_0	n_0	S_0	$L_{\rm sym}$	$n_{\rm cond}/n_0$
values	133.71	5.72	5	920	0.165	23.5	29.1	2.3

Table 3.2: Parameter values and observables at nuclear saturation

We choose some representative parameter values such that the energy per baryon and baryon density at saturation are reasonably close to their experimental values. However, it is indeed possible to choose other set of values that better adjust the symmetry energy and slope at saturation [Ada+23].

In fig. 3.5 we show the resulting particle fractions for our choice of parameter values. When the kaon condensate phase is taken into account, we observe that *i)* the electric charge neutralization is almost exclusively provided by the negatively charged kaons, with a small contribution of electrons and a negligible contribution of muons, and that *ii)* the proton fraction gets rather close to the neutron fraction for large densities. In fig. 3.6 we plot the symmetry energy as a function of n_B. One can clearly appreciate that the contribution of the kaon condensate enhances the symmetry energy.

Effects on the EoS for (a-)symmetric nuclear matter.

As we have shown, the $SU(3)$ version of the Skyrme model (in the Callan-Klebanov approach) predicts the phase transition from the standard $npe\mu$ matter to a kaon-condensed phase, $npe\mu\overline{K}$, at a threshold density of $n_{cond} \sim 2 - 3n_0$. Further, the kaon vev has a nontrivial effect in symmetry energy (and thus the particle fractions) of the system, which directly translates into the EOS.

On the other hand, the main ingredient to obtain the EOS for the Skyrme crystal is the dependence of the total energy on the unit cell size, and the relevant thermodynamical variables can be obtained from this relation as explained at the beginning of this chapter.

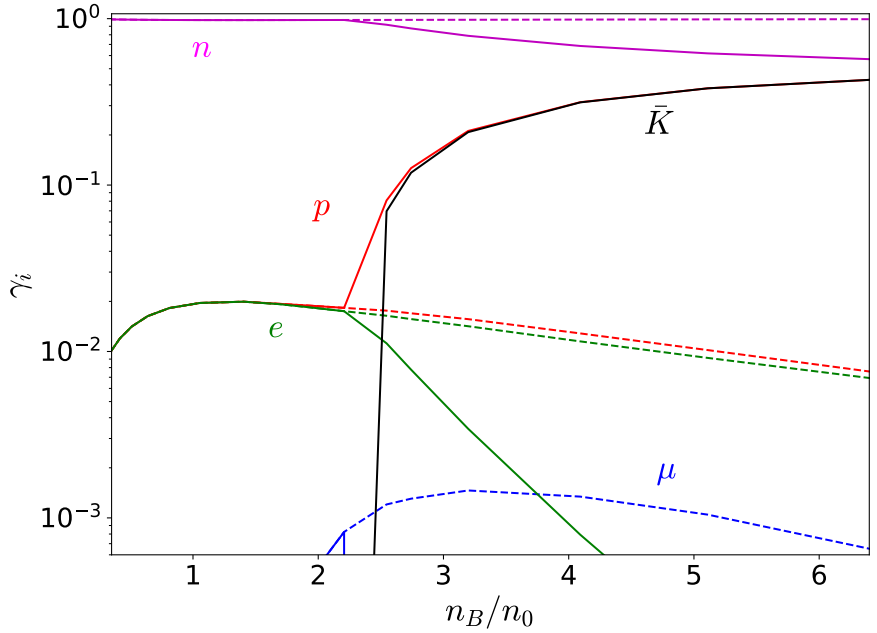

Figure 3.5: Particle fractions as a function of baryon density, both with (solid lines) and without (discontinuous lines) kaon condensate. For the case with kaon condensate, the contribution of muons is negligible.

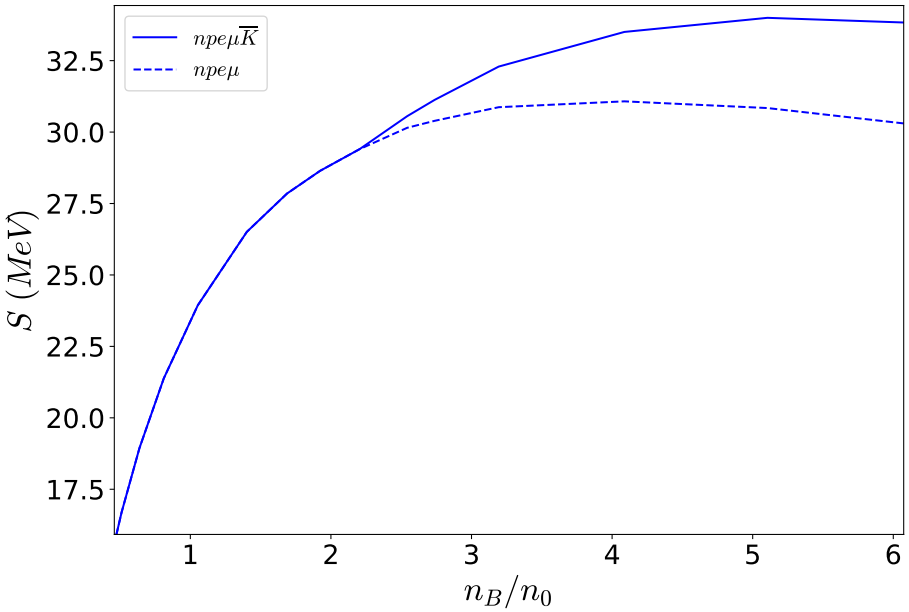

Figure 3.6: Symmetry energy of nuclear matter as a function of baryon density for the values of parameters considered. The thick line represents the symmetry energy when kaons are considered in the system and the dashed line does not include kaons.

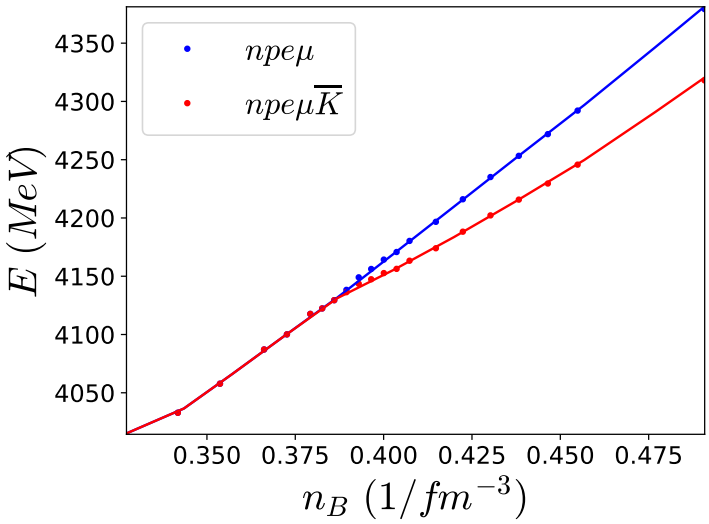

Figure 3.7: Energy per baryon against the baryon density of the crystal and their interpolations in the $npe\mu$ and $npe\mu\bar{K}$ phases.

In the $npe\mu$ phase, this is a straightforward task: one just finds the minimum energy configuration for different values of L, and then the $\beta-$equilibrium and charge neutrality conditions must be solved for $\gamma(L)$. Such a relation contains all the needed information to compute particle fractions as a function of density (see the previous section). However, once we include kaons, the change in the energy curve displayed (in red) in fig. 3.7 leads to a first order phase transition. Indeed, one concludes that the kaon condensation produces a first order phase transition for our choice of parameters after analyzing the dependence of the energy density with the pressure. It was shown in [Ada+23] that there is a non-physical region in the $\rho-p$ relation which must be bridged by a first order phase transition. Similar results, indicating a first-order transition, are found for the other parameter sets used in that work. The phase transition to kaon condensation has been investigated previously, e.g., within a relativistic mean field theory framework [GS99; Pon+00]. The kaon optical potential, which is the relevant parameter for the phase transition, was allowed to vary within a rather large range in these investigations. This lead to a large variety of possible situations, from a second order phase transition for a weak optical potential to a strongly first-order transition for a strong one, where the number of protons outweighs the number of neutrons at sufficiently high density. For intermediate optical potentials, their results are similar to ours.

In the presence of a first order transition, constructing the equation of state of the system requires a nontrivial step which allows to take into account the possibility of a MIXED PHASE, i.e. a region of the phase diagram in which two (or more) different phases coexist. Formally, this can be achieved by means of the so-called GIBBS CONSTRUCTION [Gle92; GS99]. The Gibbs construction is based on a mixed phase of constant pressure which connects the two solutions, in which the chemical potential is also enforced to be common for both phases in the mixed phase [Gle92]. In other words, in the mixed phase the Gibbs conditions for the phase equilibrium,

$$p^{\mathrm{I}} = p^{\mathrm{II}},\ \ \mu_i^{\mathrm{I}} = \mu_i^{\mathrm{II}},\ \ i = B, q \tag{3.106}$$

must be satisfied. In the last expression μ_B and μ_q represent the chemical potentials associated to the conserved baryon and electric charges, respectively. We note that, within this mixed phase, charge neutrality does not necessarily hold on each phase individually, as long as the total mixed phase is charge neutral.

Although we will not be interested in the details on the Gibbs construction between the two phases at hand (they can be found in [Ada+23]), it is remarkable that allowing for a mixed phase implies that the effect of kaons on the nucelar matter EOS become noticeable much earlier (even around nuclear saturation) [Ada+23]. This is a direct consequence of the presence of a first order phase transition at the kaon condensation threshold, which is a genuine prediction of the Skyrme model for a wide range of physically-relevant parameters.

Of course, this fact will be directly reflected on the properties of the NS that can be obtained from such EOS, as we will discuss in the next chapter.

3.5 Final remarks

The description of the nuclear EOS at saturation and supra-saturation densities is a challenging task that nonetheless any serious candidate to a nuclear matter model must confront. In this chapter, we push forward this goal from the Skyrme model approach, focusing on the computation of the relevant physical magnitudes that have been (or could be) measured and constrained from laboratory experiments and astrophysical observations, such as the binding energy or symmetry energy at saturation. In particular, first the procedure to obtain an EOS from the (classical) crystalline solutions of the Skyrme model is reviewed. Then, we show how the effects of isospin can be included by means of canonical quantization, which, together with a mean field approximation, yields a well-defined procedure to compute observables such as the symmetry energy (as a function of density) and the associated particle fractions, i.e. the equation of state of asymmetric nuclear matter in the $npe\mu$ phase.

Finally, we address the possibility of the appearance of a charged kaon condensate in neutron star cores described within a GSM. Our treatment of strange degrees of freedom is based on the bound state approach by Callan and Klebanov, which allows to obtain an in-medium effective potential for the s-wave kaon condensate. One of the main results in this chapter is the prediction of the kaon condensation onset at a certain threshold density—whose value depends on the parameters of the model, and ranges between 1.5 and 2.5 times saturation density—, and how it affects the particle fractions and equation of state for dense matter in the kaon condensed phase, $npe\mu\bar{K}$. Moreover, we observe that the transition between the $npe\mu$ matter and kaon-condensate phases is of first order, which has tremendous impact on the resulting EOS.

Let us end with a final comment about some of the natural ways of extending the results presented in this chapter. The generalization of the Skyrme model to the three flavor chiral symmetry, in which the whole $SU(3)$ group is quantized, is a fascinating endeavor that, however, has been mostly limited to obtaining properties of $SU(3)$ hyperons in the $B = 1$ sector. On the other hand, the Callan-Klebanov approach has also been extended to include additional exotic degrees of freedom coming from even heavier quarks (such as charm or bottom). It would be interesting to explore all these scenarios, focusing on the periodic solutions, in order to provide an understanding of the role that heavy baryons (those with nonzero strange, bottom or charm quantum numbers) play in the EOS of

ultra-dense matter. In particular, this is related to the very relevant *hyperon problem*, in which the appearance of strange baryons has been argued to bring maximum neutron star masses towards rather small, unphysical values.

CHAPTER 4

Neutron stars within the Skyrme model

Articles partially reproduced in this chapter: [Ada+21]. See *permissions*.

"Episodios gravitatorios con los folios,
un laboratorio es mi escritorio "

– Javier Ibarra (Kase.O), *Booty song*

Neutron stars (NS) constitute perfect laboratories for exploring the properties of strongly interacting matter at the most extreme range of densities that are allowed by the laws of Physics. Indeed, NS are the densest known compact objects that lack an event horizon (as opposed to black holes), and repulsive forces originating from strong interaction effects are the only responsible for avoiding their gravitational self-collapse.

Unfortunately, it is precisely the fact that they are so compact what makes it difficult to make accurate observations of their properties, such as their masses and/or radii, due to their small size ($\sim 10\,\mathrm{km}$) relative to their mean distance to the Earth (the closest detected neutron stars are several hundred light years away). Nevertheless, the relation between the masses and radii of neutron stars imposes very strong constraints on the possible Equations of state (EOS) of nuclear matter at high densities, as there exists a one-to-one correspondence between the EOS and the $M - R$ curve of NS.

There are several methods for measuring masses and radii of NS. While masses are relatively easy to measure by studying the orbits of NS in binary systems, their radii are more difficult to measure in general. The radius of a NS can be estimated from its thermal emission under some assumptions, as well as from the gravitational redshift of absorbed lines in gamma-ray burst from the stars's surface, as well as x-ray bursts from binary systems. A more recent alternative method is that used by the NASA instrument Neutron star Interior Composition ExploreR (NICER) [GAO12], which exploits relativistic effects on X-rays emitted from milisecond pulsars, and relies in the high-precision timing of X-rays to detect their variation as the star rotates, which allows to determine the mass and radius of the star [Ril+21]. The NICER experiment has allowed to measure the mass-radius relation of multiple pulsars, such as PSR J0030+0451 [Mil+19] and PSR J0740+6620 [Mil+21].

Finally, the most recent way of measuring NS properties comes from the observation of the gravitational waves emitted during the inspiral (and merging) phases of binary NS-NS or black hole-NS mergers. These are cataclysmic events in spacetime that release an enormous amount of energy in the form of gravitational waves, whose waveform codifies the information abut the parent objects before the merger. Such information, including the stars' masses, radiii and deformabilities, can the be extracted after measuring the

gravitational waves in observatories such as Laser Interferometer Gravitational-wave Observatory (LIGO) [Aas+15], Advanced Virgo [Ace+15] or KAGRA [Som12]. A the time of writing this thesis, only a few of such events have been detected that involve neutron star-like compact objects: The first one was GW170817 [Abb+17], originated from a binary NS merger, was also observed electromagnetically, providing the first multi-messenger observation of this type. A couple of years later, another binary NS merger candidate event (GW190425) was detected in 2020 at LIGO-Virgo [Abb+20a]. Furthermore, two events corresponding to a black-hole-neutron star merger have been detected [Abb+21], although the properties of the parent neutron stars could not be well determined due to the absence of electromagnetic counterpart signals. Furthermore, a third event was detected, GW190814 [Abb+20b], from the coalescence of a 23 $M_\odot$ black hole with a compact object of around 2.6 solar masses. Such an object poses a challenge to the current theories of NS and black hole formation, as it lies precisely in the so-called MASS GAP [Sie+22]: it is either too light to be a black hole (which are expected to be at least of $5M_\odot$) or too heavy to be a neutron star. Furthermore, a recent measurement of the mass of the pulsar PSR J0952-0607 using Saphiro-delay technique gave the value of $M = 2.35 \pm 0.17\, M_\odot$ [Rom+22], making it the most massive neutron star known to date.

Therefore, combined observations from pulsars and GW observatories have made it clear that neutron star masses can pass the limit of $2\, M_\odot$ that was previously expected, and the maximum mass constraint has been lifted to around 2.6 solar masses for non-rotating NS. This fact implied a revision of the known, microscopically obtained EOS that did not allow for such big masses, while the ones that reached them were favored. As we will show in the following sections, the NS obtained from different approaches based on Skyrme models will generally allow for maximum masses of 2.5 or higher solar masses, and hence they are very interesting as models for studying the phenomenology of highly compact and dense stars.

4.1 Early attempts. BPS neutron stars

In order to determine whether the Skyrme model and its generalizations are able to describe the properties of matter inside NS, there are two main approaches that one may take. The first one is based in obtaining self-gravitating, star like solutions of the coupled Einstein-Skyrme system. In the second one, the matter that conforms the star is modelled as a perfect fluid, whose EOS is obtained directly from the Skyrme model. While the latter approach is almost straightforward once the EOS is known (to which we have devoted the previous chapter), the former is much more difficult to take in practice, not only due to the complicated structure of such a differential equation system, but also because the required solution should have $B \sim 10^{57}$ —the estimated number of baryons in a regular NS— for which a stable ansatz is not known. Therefore, additional approximations must be taken into account if one is to take this route.

A first attempt to compute these kind of solutions was made in [NP12], in which they use nested rational maps of increasingly high baryon charge in order to find star-like configurations. However, such method does not yield phenomenologically satisfactory solutions that may be identified with neutron stars, as the maximal mass of these solutions (i.e., the maximum mass these solutions can reach before becoming unstable under gravitational collapse) was too small.

A clever way around this problem comes from the BPS Skyrme model, proposed by Adam et al. in [ASW10b]. The BPS Skyrme model can be thought of as a submodel of the GSM, which can be reached if one makes the (inverse of the) Skyrme parameter e^{-1} and the pion decay constant f_π go to zero in eq. (1.1). Although it represents a limiting case of the generalized model, the BPS model and its solutions present several attractive mathematical features. One of the most important, after which the model receives its name, is that the total energy of field configurations presents a TOPOLOGICAL BOUND that can be saturated. Solutions that saturate this bound are called BPS SKYRMIONS. Another very interesting property of the BPS model is that the associated EMT is of perfect fluid form, which in turn facilitates the solution of the self-gravitating skyrmions [Ada+15d; Ada+15b].

As it turns out, solutions of such model, when coupled to gravity, can reach maximum masses of several times the mass of the Sun [Nay19], which indicates that the associated EOS of such stars is very stiff, i.e. speeds of sound close to that of light. Further studies of neutron stars within this model suggest that it could be a great candidate to describe matter at extreme densities, such as the innner core of neutron stars.

In the following sections, we shall review the properties of the BPS-Skyrme model coupled to gravity, and describe the self-gravitating solutions obtained from such model, that we call BPS stars. It will be also interesting to compare the properties of the self-gravitating BPS star solutions to other star solutions obtained via the first approach, namely, as gravitating perfect fluids with an EOS given by the same BPS model, as well as the generalized model.

4.1.1 Stress-energy tensor and energetics of the BPS model

Let us first consider the BPS submodel coupled to gravity. We start from the following action functional

$$S = \int \sqrt{g}\left(\mathscr{L}_{BPS} - \frac{R}{16\pi G}\right) d^4x, \tag{4.1}$$

where R is the Ricci scalar of the spacetime metric, G is the gravitational constant, g is the determinant of the tensor metric and it is defined as its absolute value ($g \coloneqq |g|$) and now $\mathscr{L}_{BPS}$ corresponds to the minimally coupled BPS Skyrme Lagrangian, which reads

$$\mathscr{L}_{BPS} = -\lambda^2\pi^4 g^{-1} g_{\mu\nu}\mathcal{B}^\mu\mathcal{B}^\nu - \mu^2\mathcal{U}(U). \tag{4.2}$$

Note that in the presence of a non-trivial spacetime metric, the topological current corresponds to the following tensor density of weight +1:

$$\mathcal{B}^\mu = \frac{1}{24\pi^2}\varepsilon^{\mu\nu\rho\sigma}\,\mathrm{Tr}\{L_\nu L_\rho L_\sigma\} \equiv \sqrt{g}B^\mu, \tag{4.3}$$

so that the topological charge enclosed in an arbitrary (spacelike) hypersurface Σ with volume element dS_μ is given by

$$B = \int_\Sigma B^\mu dS_\mu. \tag{4.4}$$

For the special case of a hypersurface of constant time, we have $dS_\mu = k_\mu d^3x$, with $k = \partial_t$ the Killing vector field corresponding to the time coordinate and d^3x the natural volume element of the spatial sections at a given time.

We now consider the stress-energy tensor for the Skyrme field:

$$T^{\mu\nu}_{BPS} = 2\lambda^2\pi^4 B^\mu B^\nu - \big(\lambda^2\pi^4 g_{\rho\sigma}B^\rho B^\sigma - \mu^2\mathcal{U}\big)g^{\mu\nu}, \tag{4.5}$$

which can be brought into the form of a perfect fluid stress-energy tensor, $T^{\mu\nu}_{BPS} = (p+\rho)u^\mu u^\nu - pg^{\mu\nu}$, with the following definitions:

$$\begin{aligned} u^\mu &= \frac{\varepsilon B^\mu}{\sqrt{g_{\rho\sigma}B^\rho B^\sigma}}, \\ p &= \lambda^2\pi^4 g_{\rho\sigma}B^\rho B^\sigma - \mu^2\mathcal{U}, \\ \rho &= p + 2\mu^2\mathcal{U}. \end{aligned} \tag{4.6}$$

where $\varepsilon = 1$ or -1. Since both of these values represent the same model, we will always choose $\varepsilon = 1$ unless otherwise specified. Thus, the BPS Skyrme model behaves as a perfect fluid whose four-velocity, baryon number, pressure, and mass densities are related through (4.6). Note that this perfect fluid would be non-barotropic, since the potential term introduces in both the pressure and mass densities a non-trivial dependence on the Skyrme field, so that no closed relation can be found between ρ and p alone.

Topological energy bound

Consider the proper energy-momentum density of the BPS Skyrme field, which is given by $P_\mu = T_{\mu\nu}u^\nu$.[2] Let the energy functional E_Σ be defined as the integral of P_μ on a spacelike hypersurface with volume form dS_μ:

$$E_\Sigma = \int_\Sigma T^\mu_\nu u^\nu dS_\mu. \tag{4.7}$$

We thus may obtain the energy of the field as measured by an observer comoving with the fluid at any given value of its proper time, writing $dS_\mu = u_\mu d^3S$, so that

$$E = \int T^\mu_\nu u^\nu u_\mu d^3S = \int \big(\lambda^2\pi^4 g_{\rho\sigma}B^\rho B^\sigma + \mu^2\mathcal{U}\big)d^3S, \tag{4.8}$$

where $d^3S = \sqrt{g}d^3x$ is the volume element of the spacelike hypersurfaces defined by $\tau = \text{const}$, and τ is the proper time parameter of the comoving observer. We will now show that the value of this proper energy is bounded from below, in other words, the model presents a BPS bound [Bog76; ASW10a].

Indeed, define the following vectors:

$$W^\mu_\pm = \lambda\pi^2 B^\mu \pm \mu\sqrt{\mathcal{U}}u^\mu = \Big(\varepsilon\lambda\pi^2\sqrt{g_{\rho\sigma}B^\rho B^\sigma} \pm \mu\sqrt{\mathcal{U}}\Big)u^\mu, \tag{4.9}$$

so that we may write the proper energy as

$$E = \int \Big(g_{\mu\nu}W^\mu_\pm W^\nu_\pm \mp \varepsilon 2\lambda\mu\pi^2\sqrt{g_{\rho\sigma}B^\rho B^\sigma}\sqrt{\mathcal{U}}\Big)d^3S. \tag{4.10}$$

[2] Note that P_μ is not a conserved quantity in general, since u^μ will not be in general a Killing field. However, for static and stationary configurations, it will.

Since u^μ is a timelike vector, we have $g_{\mu\nu}W^\mu_\pm W^\nu_\pm \geq 0$, with the equality reached only when $W^\mu_\pm = 0$, i.e.

$$W^\mu_\pm = 0 \implies \varepsilon\lambda\pi^2\sqrt{g_{\rho\sigma}B^\rho B^\sigma} \pm \mu\sqrt{\mathcal{U}} = 0, \tag{4.11}$$

which is the BPS condition. Note that $W^\mu_\pm = 0$ is satisfied only if $\varepsilon = \mp 1$. This is an important property that allows us to write

$$E \geq 2\lambda\mu\pi^2 \int \sqrt{g_{\rho\sigma}B^\rho B^\sigma}\sqrt{\mathcal{U}}d^3S = E_{BPS}, \tag{4.12}$$

where E_{BPS} is the proper energy of the lowest energy configurations, which are called BPS configurations, since they satisfy the BPS equation (4.11), and therefore

$$E \geq E_{BPS} = 2\mu^2 \int \mathcal{U}d^3S. \tag{4.13}$$

4.1.2 Energy conditions

Even though the stress-energy tensor of the BPS Skyrme model presents the structure of a perfect fluid, one can ask whether it satisfies the energy conditions for being a consistent model for a realistic description of gravitating matter even at extreme density regimes such as that present at neutron star cores. It is easy to see that the EMT of this model satisfies the *Dominant Energy Condition (DEC)*, as defined in [HE73]: $T_{\mu\nu}u^\mu u^\nu \geq 0$ and $T^\nu_\mu u^\mu$ is causal for any timelike vector u^μ. This is equivalent to the statement that all observers measure a positive energy density and causal energy fluxes, and, in particular, for a perfect fluid stress-energy tensor, the DEC implies [HE73; MV17]:

$$\rho \geq |p|, \qquad \rho \geq 0, \tag{4.14}$$

which is satisfied by construction for the BPS Skyrme model for any positive potential $\mathcal{U} \geq 0$. Indeed, by definition, ($A = \lambda^2\pi^4 g^{-1} g_{\rho\sigma}B^\rho B^\sigma \geq 0$)

$$|p| = \left|A - \mu^2\mathcal{U}\right| \leq \left|A + \mu^2\mathcal{U}\right| = A + \mu^2\mathcal{U} = \rho \geq 0. \tag{4.15}$$

As a matter of fact, the potential terms usually chosen in the literature are always positive (see e.g. [Ada+15d]), so that the DEC is satisfied at all of those cases.

Another energy condition present in the literature, which is not implied by the DEC, is the *Strong Energy Condition (SEC)*, which states that the gravitational field generated by a stress-energy tensor $T_{\mu\nu}$ will be attractive as measured by an arbitrary observer with 4-velocity u^μ if [VB00]:

$$(T_{\mu\nu} - \frac{1}{2}g_{\mu\nu}T^\alpha{}_\alpha)u^\mu u^\nu \geq 0, \qquad \forall\, \text{timelike vector}\, u^\mu. \tag{4.16}$$

It is easy to see that for any static configurations of a minimally coupled scalar field with an arbitrary positive potential (and canonical kinetic term) without topological energy terms, it is violated (See [VB00]). However, the nontrivial topological structure of the model at hand may allow to overcome this issue, so that static configurations with nontrivial topology which do not violate any energy condition may be found. For the standard Skyrme model (without potential term) it was shown by Gibbons that both DEC and

SEC are satisfied [Gib03]. In the case of the BPS Skyrme model, it is interesting to analyze whether the SEC is satisfied for the usually chosen potentials in the literature. Substituting (4.5) into (4.16), we find the following conditions [MV17]:

$$\rho + p = 2A \geq 0; \qquad \rho + 3p \geq 0 \implies 4A - 2\mu^2\mathcal{U} \geq 0 \implies 2A \geq \mu^2\mathcal{U}. \tag{4.17}$$

The first condition is satisfied trivially, and, since both terms at each side of the last inequality are definite positive, (assuming a positive potential), we may write it as

$$2\int A d^3S \geq \int \mu^2\mathcal{U} d^3S \implies 2E \geq 3\mu^2 \int \mathcal{U} d^3S, \tag{4.18}$$

where E is the energy functional, which, as we have seen, is topologically bounded from below, i.e. $E \geq E_{BPS}$ with E_{BPS} corresponding to the energy of the BPS configurations, so that

$$2E \geq 2E_{BPS} = 4\mu^2 \int \mathcal{U} d^3S \geq 3\mu^2 \int \mathcal{U} d^3S, \tag{4.19}$$

from where we conclude that the SEC is satisfied in the BPS Skyrme model for any positive potential term.

4.1.3 Mean field approximation

As we have stated before, the BPS skyrme model can be seen as a non-barotropic fluid, for which the thermodynamical energy and pressure densities may be found exactly without further approximations. Nevertheless, one may still perform a mean-field approximation in order to obtain an effective, barotropic equation of state for the BPS Skyrme fluid. This will allow for a direct comparison between the results obtained within the exact and the mean-field approaches.

In order to perform the mean-field approximation, consider a static BPS fluid element Ω with finite volume $V = \int_\Omega d^3x$ (as measured by an observer comoving with the fluid element). The volume V must be small enough that we can neglect the effects of the gravitational field (and assume $g_{\mu\nu} = \eta_{\mu\nu}$) on it, but large enough that the topological charge enclosed by its boundary does not vanish. For static BPS configurations in flat space, the conservation of the stress-energy tensor implies that the pressure of these configurations must be constant, and related with the baryon number density via

$$\lambda^2\pi^4 B_0^2 - \mu^2\mathcal{U} = P = \text{const.} \tag{4.20}$$

Thus, the baryon density can be written $B_0 = \pm\frac{\mu}{\lambda\pi^2}\sqrt{\mathcal{U} + \tilde{P}}$, with $\mu^2\tilde{P} = P$, the plus (minus) sign corresponding to baryon (antibaryon) configurations. For simplicity, we shall assume $B_0 > 0$ in the following.

On the other hand, from (1.4), we have

$$V = \int_\Omega \frac{1}{2\pi^2 B_0} U^*(d\Omega_3) = \frac{\lambda}{2\mu}\int_\Omega U^*\left(\frac{d\Omega_3}{\sqrt{\mathcal{U} + \tilde{P}}}\right) = \frac{B\lambda}{2\mu}\int_{S^3}\frac{d\Omega_3}{\sqrt{\mathcal{U} + \tilde{P}}}, \tag{4.21}$$

whereas the total energy of the fluid element will be given by

$$E = \int_\Omega \rho d^3x = \int_\Omega (P + 2\mu^2\mathcal{U}) d^3x = \frac{B\lambda\mu}{2}\int_{S^3}\frac{2\mathcal{U} + \tilde{P}}{\sqrt{\mathcal{U} + \tilde{P}}} d\Omega_3. \tag{4.22}$$

Therefore, we are able to define the mean-field energy and baryon densities as functions of pressure on Ω as the averages of the total energy and baryon number on V:

$$\bar{\rho}(P) = \frac{E(P)}{V(P)}, \qquad \bar{\rho}_B(P) = \frac{B}{V(P)}. \tag{4.23}$$

Since the above quantities do not depend on the particular size of Ω, the mean-field approximation consists on promoting them to local relations between the pressure, energy and baryon number densities (i.e, making the limit $V \to 0$). In particular, within this approximation, one obtains a barotropic equation of state $\bar{\rho}(p)$, whose particular form will depend on the specific potential.

4.1.4 Static NS solutions

Here and in the following sections, we will obtain solutions to the Einstein equations that describe NS within the different Skyrme models presented above. As a first step, we will consider static, spherically symmetric configurations, which is usually done following the Tolman-Oppenheimer-Volkoff (TOV) approach, in which the Einstein equations are solved using the stress-energy tensor of a perfect fluid. Thus, we suppose the spherically symmetric (Schwarzschild) ansatz for the metric,

$$ds^2 = -e^{\alpha(r)}dt^2 + e^{\beta(r)}dr^2 + r^2(d\theta^2 + \sin^2\theta d\phi^2). \tag{4.24}$$

We extract from the Einstein equations

$$R_{\mu\nu} - \frac{1}{2}Rg_{\mu\nu} = 8\pi T_{\mu\nu} \tag{4.25}$$

and the conservation of the stress-energy tensor of the perfect fluid type ($\nabla_\mu T^\mu_\nu = 0$) the following system of Ordinary Differential Equations (ODEs), also known as the TOV system,

$$\frac{d\alpha}{dr} = 2\frac{4\pi r^3 p + M}{r(r-2M)} \tag{4.26a}$$

$$\frac{dM}{dr} = 4\pi r^2 \rho \tag{4.26b}$$

$$\frac{dp}{dr} = -\frac{(p+\rho)}{2}\frac{d\alpha}{dr}, \tag{4.26c}$$

where we have made the usual definition

$$\exp(-\beta) = 1 - 2M/r, \tag{4.27}$$

so that the value $M_* = M(R_*)$ of the function $M = M(r)$ coincides with the (static) Arnowitt-Desser-Misner (ADM) mass of the star [ADM59] when evaluated at its radius $r = R_*$.

To close the system (4.26), we have to know the relations between the pressure and the energy density, *i.e.*, an EOS. It is at this point where the classical Skyrmion solutions with a very large value of the topological charge become relevant.

4.1.5 Skyrme neutron stars

Next, we briefly review the current status of the description of static properties of neutron stars from the Skyrme model perspective.

The BPS Skyrme neutron stars

In the case of the BPS Skyrme submodel $\mathscr{L}_{BPS}$, which is a genuine perfect fluid theory for any potential $\mathcal{U}$, one can find lowest energy Skyrmions for any value of the topological charge B in an exact form. There are, in fact, infinitely many solutions for a given B related via volume-preserving diffeomorphisms, which corresponds very well with the fluid nature of the BPS Skyrmions. Interestingly, the perfect fluid form of the action allows to obtain the mean field EOS in an exact form without solving the field equations [Ada+15c; Ada+15b]. This occurs because the pressure enters as an integration constant into the generalized Bogomolny equation. As a consequence, the pressure dependence of both the energy $E(p)$ and the volume $V(p)$ of BPS Skyrmions can be found as target space integrals (averages). The details of the resulting EOS obviously depend on the particular choice of the potential (but, of course, do not depend on a particular solution). On the other hand, since the sextic term provides the leading behavior in the high pressure limit, the EOS tends to the maximally stiff equation of state as the pressure increases

$$\rho_{BPS}(p) \approx p. \tag{4.28}$$

As a consequence of this stiffness, it is not surprising that the neutron stars provided by the BPS Skyrme model have rather big maximal masses, easily exceeding $3M_{\odot}$—see Fig. 4.1, black, purple and blue curves which correspond to three of the different potentials introduced in [Ada+15c; Ada+15b], namely the θ-potential $\mathcal{U}_{\Theta} = \Theta(\mathrm{Tr}\{1-U\})$, the standard pion mass potential $\mathcal{U}_{\pi} = 1/2\mathrm{Tr}\{1-U\}$, and the pion mass potential squared $\mathcal{U}_{\pi}^2$. The first one corresponds to the constant density compacton limit for BPS Skyrmions in flat space. The motivation for choosing the other two potentials comes from nuclear phenomenology [Ada+15b]

Owing to its perfect fluid nature, the BPS model offers the possibility to close the TOV system without any mean-field approximation. In this case, referred to as the exact case, the pressure and energy densities ρ, p can already be read from the stress-energy tensor (4.5), as we have shown in the previous section. Furthermore, one can see from (4.6) that they are related in a non-algebraic way, by construction, as the potential $\mathcal{U}$ may have an arbitrary spatial dependence. This also means that the obtained matter is an example of a NON-BAROTROPIC FLUID where constant pressure does not correspond to constant energy density in general. Hence, this exact approach may serve as a laboratory where the impact of non-barotropic EOS on properties of NS can be studied. Further, the different BPS models provide a wealth of new and different EOS which will allow us to test the universal, EOS-independent character of certain universal relations, like the *I-Love-Q* relations (see next section), in new environments not considered previously.

More precisely, in the exact case the Skyrme field U enters in the Einstein equations as an additional degree of freedom, so that we have to obtain its own differential equation in order to close the TOV system. To do this, we choose the hedgehog ansatz for the

Skyrme field,

$$U(x) = e^{i\xi(r)\hat{\mathbf{n}}(\theta,\phi)\cdot\boldsymbol{\tau}},$$
$$\hat{\mathbf{n}}(\theta,\phi) = (\sin\theta\cos(B\phi), \sin\theta\sin(B\phi), \cos\theta), \tag{4.29}$$

which is compatible with the chosen ansatz of the metric, since it yields a spherically symmetric energy density, which is relevant for static NS. Here $\boldsymbol{\tau}$ are the Pauli matrices and (r,θ,ϕ) are spherical coordinates. The only degree of freedom in this ansatz corresponds to the radial profile $\xi(r)$, and inserting the hedgehog ansatz into the definition of p it can be shown that this function satisfies the differential equation

$$p = \frac{4B^2\lambda^2\xi'^2\sin^4\xi}{e^{\beta}r^4} - \mu^2\mathcal{U}, \tag{4.30}$$

which is added to (4.26) to close the system. For simplicity, when solving the TOV system we will define the new variable $\chi := \sin^2(\xi/2)$, which satisfies

$$\frac{d\chi}{dr} = \frac{e^{\beta/2}r^2}{2B\lambda}\sqrt{\frac{p+\mu^2\mathcal{U}}{\chi(1-\chi)}}. \tag{4.31}$$

Once the system of ODEs is closed, only a set of initial conditions are needed as an input in order to obtain a particular solution. However, in the exact case, the baryon number B of the star is an additional input parameter, and the value of the pressure at the center of the star (p_0) that yields the input value must be found via a shooting method, with initial conditions

$$\alpha(0) = \alpha_0,\ M(0) = 0,\ \chi(0) = 1,\ p(0) = p_0, \tag{4.32}$$

requiring that the pressure vanishes at some finite value $p(r = R_*) = 0$. This value R_* is precisely the radius of the star. The value of α_0 is not needed to solve the system. However, only one value is correct, and it can be obtained by imposing continuity of the metric at the radius of the star, R_*, for which, and onwards, the metric is given by the Schwarzschild solution:

$$e^{\alpha} = e^{-\beta} = 1 - \frac{2M_*}{r}, \quad r \geq R_*, \quad \text{where } M_* = M(R_*). \tag{4.33}$$

Also, the central value of the energy density ρ_0 is determined from (4.30) using the BPS relations (4.6).

On the other hand, in the Skyrme crystal and the mean-field version of the BPS submodels, we do have a barotropic EOS $\rho(p)$, so that the energy density only depends on the pressure. In these cases, the equation (4.31) is no longer needed and the input parameter is the pressure in the center of the star p_0, along with the rest of initial conditions for α and M. The system of differential equations is then solved up to the star radius (R_*), in that point the static ADM mass of the star $M_* = M(R_*)$ is also obtained.

In Fig. 4.1 mass-radius curves for the exact case are presented - see black, blue and purple stars. For the θ-potential the mean field and exact computations obviously coincide. Therefore, for relatively flat potentials (e.g., the pion mass potential) the difference between the mean field and exact approach is rather small, while it strongly increases for more peaked potentials (e.g., the pion mass potential squared).

Neutron stars in the GSM

The GSM given by (1.1) is a field theory whose energy-momentum tensor does not have a perfect fluid form. Therefore, a suitable mean-field approximation has to be performed. In practice, it means a spatial averaging. For any given set of values for e, f_π, λ, the ground state is a crystal with a given lattice structure and lattice spacing l_0 (we assume the isotropic case). Obviously, the energy per baryon $E(l)$ has a minimum at $l = l_0$. As explained in chapter 3, this minimum may be identified with the nuclear saturation point. We thus choose the values of parameters that best fit some nuclear physics observables at saturation density. The solution at the minimum (saturation) is also a zero-pressure (equilibrium) solution, because

$$p = -\frac{\partial E}{\partial V}, \tag{4.34}$$

where $V = l^3$ is the volume of the cell. Diminishing the lattice spacing l is equivalent to imposing a nonzero pressure. Finally, as the pressure and the energy density are both functions of l, we can find the corresponding EOS, $\rho_{GSM} = \rho_{GSM}(p)$.

An interesting observation is that, if inserted into the TOV system, the crystal EOS with zero sextic term coupling constant amounts to neutron stars with rather small maximal masses, significantly below the observed NS masses. For example, for the cubic, face-centered lattice of $B = 4$ Skyrmions (α particles) $M_{\max} \simeq 1.49 M_\odot$ [NP12; Nay19]. The corresponding mass-radius curve is presented in Fig. 4.1, with a golden dashed line. The corresponding parameter values are those that fit the energy per baryon and baryon density at the minimum with their values at nuclear saturation. Therefore, the standard Skyrme model crystal and the BPS Skyrme fluid result in too small or too large maximal masses of neutron stars, respectively. It can be expected that these two extremal cases can be balanced in the full GSM, i.e. when including a nonzero value of the sextic term. In Fig. 4.1 we show the mass-radius curve for the EOS from the generalized model - see the orange line. As expected, the maximal mass of NS is between the two previously discussed versions of the Skyrme model and reads $M_{\max} \simeq 2.55 M_\odot$. The values of the parameters are chosen to be those of set 1 in table 3.2.

Neutron star crusts and the hybrid EoS

By construction, the generalized Skyrme model contains only pionic degrees of freedom (with some other heavier mesons effectively also taken into account). This means that it is relevant for describing nuclear matter above the saturation density. For lower densities, the electromagnetic interaction starts to have a nontrivial impact on the properties of nuclear matter, leading to the appearance of inhomogeneous phases (usually called NUCLEAR PASTA phases [CH08]). Although the Skyrme model can be coupled with the electromagnetic $U(1)$ gauge field, which in principle may allow to study such phases within the framework of the Skyrme model, the resulting theory is very complicated and currently no large B Skyrmions are known. However, it is possible to take into account this low density regime, relevant for the crust region of NS, by assuming a transition of the generalized Skyrme EOS to a more standard nuclear EOS obtained by other techniques. Concretely, we choose the Barcelona-Catania-Paris-Madrid (BCPM) equation of state, developed in [Bal+10]. The BCPM is based on a semi-phenomenological energy functional, obtained via microscopic many-body calculations in the Bruekner-Hartree-Fock approach,

including two and three-body interaction potentials between nuclei (see [Sha+15] for a detailed review). Within this EOS, the outer crust is modelled as a regular lattice of neutron-rich nuclei in the Wigner-Seitz approxiation, whilst the outer crust presents the so-called nuclear pasta phases of different shapes. At some point close to nuclear saturation, the crust-core transition takes place, and the pasta phases gradually become $nep\mu$ matter. We model the crust-core transition with a *hybrid* EOS that smoothly interpolates between thr crust EOS (BCPM) and the Skyrme model-based EOS for the inner core:

$$\rho_{\mathrm{Hyb}}(p) = (1 - \alpha(p))\rho_{\mathrm{BCPM}} + \alpha(p)(\rho_{\mathrm{GSM}}(p)), \tag{4.35}$$

where the interpolating function

$$\alpha(p, p_{PT}, \beta) = \frac{\left(\frac{p}{p_{PT}}\right)^{\beta}}{1 + \left(\frac{p}{p_{PT}}\right)^{\beta}} \tag{4.36}$$

tends from 0 for $p/p_{PT} \to 0$ to 1 for $p/p_{PT} \to \infty$. The parameter p_{PT} can be identified with the position of the crust-core transition, whereas β measures how rapid the transition occurs. The resulting mass-radius curve is presented in Fig. 4.1, in dark red (for $\beta = 2$, and $p_{PT} = 25\,\mathrm{MeV\,fm^{-3}}$).

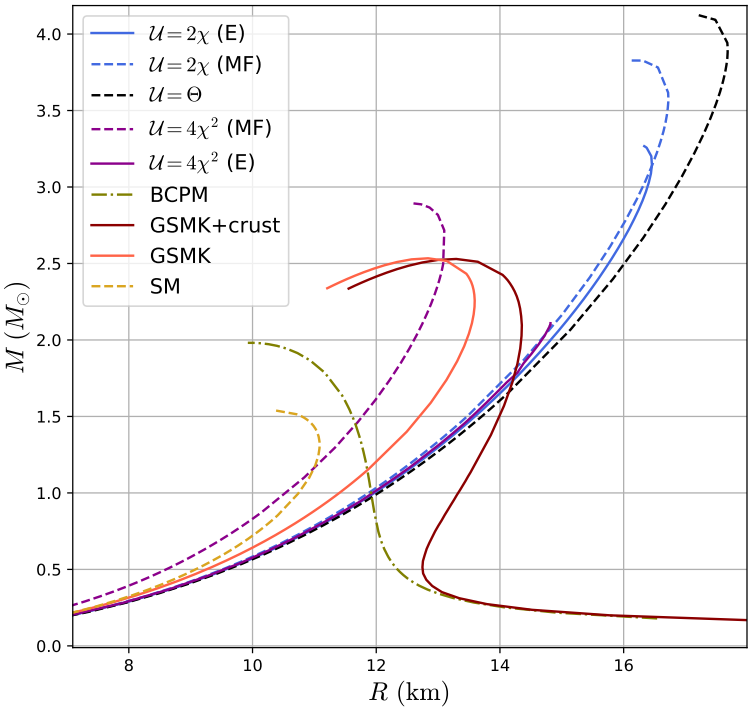

Figure 4.1: Mass-Radius diagram for the different EoS within the Skyrme model.

In the mass-radius diagram of fig. 4.1 one can observe two different qualitative behaviors. Indeed, those curves with a finite energy density at zero pressure present a minimum energy density, and thus they are characterized by the absence of a crust. The radii of these stars will grow monotonically with their masses, up until some value close to the

maximum mass in which the radius (as a function of mass) presents a maxium value, close to the maximum mass point. For larger masses, the radius decreases, and the maximum mass is reached. Other curves present a crust (which is related to the property of vanishing energy density at zero pressure). The radii of such stars grows decreases rapidly with mass for very small values until it stabilizes at around $12 - 14\,\mathrm{km}$ when the masses reach $\sim 0.5 M_\odot$ In general, for $M < M_{\max}$ there are two branches of solutions on the mass-radius curves. The equilibrium states on the decreasing (right) branch are stable, while the equilibrium states on the increasing (left) branch are unstable.

4.2 NS phenomenology with Skyrme-based EOS

In this section we will show that star-like solitonic solutions of different Skyrme-type models not only exist, but also reproduce to a good extent some of the currently best known properties of NS—like the typical values of mass, radius, moment of inertia, Love numbers, etc—coming from astrophysical measurements, GW observations and/or computer simulations.

We also address the issue of whether the compact star solutions obtained within different Skyrme-based models and the corresponding EOS satisfy the *I-Love-Q* relations, and find that they indeed do satisfy them, even though the equations of state for different models present big differences. The Skyrme model, being relatively simpler than other phenomenological or first-principle based relativistic field theories describing nuclear matter, therefore not only stands as an excellent candidate to describe nuclear matter at very high densities such as those inside NS. In addition, it provides a simple toolkit for the construction of a wide range of models of nuclear matter and their corresponding EOS which allow to investigate the resulting NS properties and universal relations in environments not considered previously—like, e.g., for non-barotropic EOS, as we will argue in the next section.

4.2.1 Slowly rotating stars: Hartle-Thorne formalism

To analyze the properties of rotating Skyrmion stars, we will make use of the Hartle-Thorne formalism for slowly rotating stars, introduced in [Har67]. This formalism establishes a perturbative framework which consists in an expansion of the metric in powers of a perturbation parameter—related with the rotational frequency—and solving the Einstein equations order by order in this parameter. This perturbative expansion has proven particularly useful in the literature since it allows to obtain approximate solutions to the Einstein equations both for the interior and exterior of the star, hence, it enables to retrieve information about the equation of state for the matter inside the star from the multipolar expansion of the external solution. We will now review the procedure to obtain the solution in this approximation for the metric in the interior of a compact star, and in the following sections we will do the same for the exterior solution and the matching between both solutions at the star surface.

The starting point of the slow rotation approximation is to consider a static solution for the metric of a non-rotating configuration, and subsequently add perturbation terms up to a given order in a suitable parameter related to the spin of the star. In our case, we will start from the static metric with line element (4.24) and, as in [Ber+05], defining the

spin parameter $\epsilon = \Omega_*/\Omega_K$ in terms of Ω_*—the angular velocity of the star as measured by an external, static observer located at spatial infinity—and the characteristic frequency $\Omega_K = \sqrt{M_0/R_0^3}$, where M_0 and R_0 are the non-spinning mass and radius of the star. The characteristic frequency Ω_k corresponds to the Keplerian orbital period of a test particle at a radius R_0 around a mass M_0 and thus can be thought of as the rotational frequency for which the mass shedding occurs, i.e., an upper limit for the rotational frequency of the star [Bau+13]. For spin frequencies much smaller than this characteristic frequency, the parameter ϵ serves as a suitable small parameter about which we can expand the metric. On the other hand, for spin frequencies near the Keplerian limit, $\epsilon \sim 1$ and the Hartle-Thorne approximation is no longer valid. Despite the dependence of the Keplerian frequency on the EOS, the slow-rotation approximation is valid for even the most rapidly spinning neutron stars observed to date [Ber+05].

Therefore, let us consider the background spacetime whose metric is given by the static line element (4.24). We now extend this metric by defining a one-parameter family of metrics $g(\epsilon)$ whose components may be expanded in powers of ϵ, $g(\epsilon) = g^{(0)} + \epsilon g^{(1)} + \frac{1}{2}\epsilon^2 g^{(2)} + \cdots$, with $g^{(0)}$ given by (4.24). Note that this construction introduces an inherent gauge freedom (for details see, for example, [SBG04; RV15]) Thereby, following [YY13b], up to second order in ϵ, we may write the metric of a slowly rotating star in the Regge-Wheeler gauge as:

$$\begin{aligned} ds^2 = &-(1+2\epsilon^2\bar{h})e^{\bar{\alpha}}dt^2 + \left(1 + 2\epsilon^2\frac{\bar{m}}{r-2\bar{M}}\right)e^{\bar{\beta}}dr^2 + \\ &+(1+2\epsilon^2\bar{k})r^2\left[d\theta^2 + \sin^2(\theta)(d\phi + \epsilon\bar{\omega}dt)^2\right], \end{aligned} \tag{4.37}$$

where $\bar{\omega} = \bar{\omega}(\theta, r)$, $\bar{h} = \bar{h}(\theta, r)$, $\bar{m} = \bar{m}(\theta, r)$, $\bar{k} = \bar{k}(\theta, r)$, and $\bar{M}(r)$ is related to $\bar{\beta}(r)$ in the same form as in (4.27). Comparing with the general expansion of $g(\epsilon)$, we find:

$$g^{(1)} = 2r^2\bar{\omega}\sin^2\theta dt d\phi, \tag{4.38}$$

$$g^{(2)} = -\left(4e^{\bar{\alpha}}\bar{h} + 2r^2\sin^2\theta\bar{\omega}^2\right)dt^2 + 4e^{\bar{\beta}}\frac{\bar{m}}{r-2\bar{M}}dr^2 + 4r^2\bar{k}(d\theta^2 + \sin^2\theta d\phi^2). \tag{4.39}$$

Note that the metric perturbation function $\bar{\omega}$ enters at first order in the spin parameter, whereas $\bar{h}$, $\bar{m}$ and $\bar{k}$ correspond to second order perturbations. This can be easily understood with the following argument [Har67]: a transformation of the metric for a stationary and axially symmetric rotating spacetime of the form $\Omega \to -\Omega$ should be equivalent to $t \to -t$. This, in particular, implies that an expansion of the diagonal components of the metric in powers of ϵ must contain only even powers (since they are unchanged under time reversal), whilst an expansion of the $g_{0,3}$ term will only contain odd powers of ϵ. Furthermore, since $\bar{\omega}$ corresponds essentially with the g_{03} term of the metric, it is responsible for the dragging of inertial frames. In other words, it measures the rate of rotation that a freely falling observer would undergo with respect to a static one (Lense-Thirring effect).

Due to these perturbation terms in the spacetime metric, both the Einstein tensor for the metric and the stress-energy tensor for the matter field will develop perturbation terms, as well. Indeed, just as with the metric tensor, we may define the one-parameter families of perturbed quantities $G_{\mu\nu}(\epsilon)$ and $T_{\mu\nu}(\epsilon)$, expand them in powers of ϵ and impose that Einstein equations are satisfied order by order in the expansion parameter. In

particular, both the pressure and mass densities of the matter field will be perturbed, acquiring an angular dependence, i.e.

$$p(\epsilon; r, \theta) = p_0(r) + \epsilon p_1(r, \theta) + \frac{1}{2}\epsilon^2 p_2(r, \theta) + \mathcal{O}(\epsilon^3), \tag{4.40}$$

$$\rho(\epsilon; r, \theta) = \rho_0(r) + \epsilon \rho_1(r, \theta) + \frac{1}{2}\epsilon^2 \rho_2(r, \theta) + \mathcal{O}(\epsilon^3), \tag{4.41}$$

as well as the fluid four-velocity, $u(\epsilon)$. For this latter quantity, we further impose the normalization condition $g(\epsilon)_{\mu\nu}u^\mu(\epsilon)u^\nu(\epsilon) = 1$. Also, stationarity, axial symmetry and rigidity of the fluid flow requires $u(\epsilon)$ to be proportional to both killing vectors, i.e. $u(\epsilon) = f_1(\epsilon)(\partial_t + f_2(\epsilon)\partial_\phi)$. The f_1 function is obtained by the normalization condition at each order, and, since the background configuration corresponds to a static fluid, $f_2(\epsilon) = \epsilon C + \mathcal{O}(\epsilon^3)$. We therefore have

$$u(\epsilon)^\mu = (u^t(\epsilon), 0, 0, \epsilon C u^t(\epsilon)), \tag{4.42}$$

thus the constant C corresponds to the angular velocity of the fluid as measured within the inner coordinate system. Note also that only odd powers of ϵ enter the expansion of f_2, for the same symmetry arguments as for $\bar{\omega}$.

It is important to notice that all these (one-parameter families of) objects so defined are gauge-dependent, although the Einstein equations themselves do not depend on the gauge (i.e, they must be fulfilled in any gauge). We thus may take advantage of this gauge freedom to choose the most convenient form of the metric functions. In particular, we may choose $C = \Omega_K$ in (4.42), so that the coordinate system in the interior of the star is taken to be that of a static observer which measures the angular velocity of the fluid to be $du^\phi/du^t = \varepsilon\Omega_K = \Omega_*$. It can be shown that any other choice of the constant $C = C_0$ is equivalent to a gauge transformation of the first order metric perturbation defined by the vector $V = (\Omega_K - C_0)t\partial_\phi$[RV15].

On the other hand, the coordinate system we have chosen so far is not quite well suited to perform the integration of the Einstein field equations from the inside of the star, for the following reason: in order to find a numerical solution for the interior metric, we will have to solve Einstein equations with a non-vanishing stress-energy tensor up to the surface of the star, which is usually defined by the surface of vanishing pressure. While in the spherically symmetric case the surfaces of constant density (or pressure) are trivially those of constant radial coordinate, this is no longer the case once the second order perturbations of the metric due to rotation are taken into account. Indeed, the (perturbed) pressure and mass densities (4.41) will depend both on r and θ, so that the surface of the star will be deformed with respect to the static case.

Therefore, we will consider a choice of gauge in which the surfaces of constant pressure (density) of the perturbed configuration are those of constant radial coordinate. This is in fact equivalent to a change of coordinates in the perturbed configuration from the original (background) coordinate system $\{t, r, \theta, \phi\}$ to another, $\{t, \bar{r}, \theta, \phi\}$, in which the new radial coordinate is defined by

$$p(\epsilon; r, \theta) = p_0(\bar{r}), \quad r \equiv r(\epsilon; \bar{r}, \theta) = \bar{r} + \epsilon^2 \zeta(\bar{r}, \theta) + \mathcal{O}(\epsilon^3), \tag{4.43}$$

so that r coincides with $\bar{r}$ in the background configuration ($\epsilon = 0$), whilst the function $\zeta(\bar{r}, \theta)$ measures the deviation from spherical symmetry of the perturbed configurations.

The new radial coordinate $\bar{r}$ is defined so that $p_0(\bar{r}) = \text{const}$ defines the isobaric surfaces of the rotating star.

Strictly speaking, one could think that, in the exact case, also the perturbations of the Skyrme profile function χ must be taken into account. However, these will be by construction directly related to the energy and pressure perturbations, and, since we will get rid of these perturbations by a suitable radial coordinate change, also the perturbation on the radial Skyrme profile will disappear. We have checked that this is in fact the case, and that no extra degrees of freedom appear in the perturbative formalism for the exact BPS Skyrme case up to second order in ϵ.

In the new coordinate system, the metric (4.37) is rewritten, up to second order in ϵ:

$$\begin{aligned} ds^2 = &-(1+2\epsilon^2\bar{h})\big(1+\epsilon^2\bar{\alpha}'\zeta\big)e^{\bar{\alpha}}dt^2 + 2\epsilon^2 e^{\bar{\beta}}\partial_\theta\zeta d\bar{r}d\theta + \\ &+\left[1+2\epsilon^2\left(\frac{\bar{m}}{\bar{r}-2\bar{M}}+\partial_{\bar{r}}\zeta\right)\right](1+\epsilon^2\bar{\beta}'\zeta)e^{\bar{\beta}}d\bar{r}^2 + \\ &+(1+2\epsilon^2\bar{k})(\bar{r}^2+2\epsilon^2\bar{r}\zeta)\big[d\theta^2+\sin^2\theta(d\phi+\epsilon\bar{\omega}dt)^2\big], \end{aligned} \tag{4.44}$$

where all the metric functions are written as functions of $\bar{r}$ (and possibly θ), and the $'$ denotes a derivative with respect to $\bar{r}$.

The metric (4.44) has a rather complicated form. However, we may simplify it by redefining, the metric functions:

$$\begin{aligned} e^{\alpha}(\bar{r}) = &\quad e^{\bar{\alpha}(r)} = e^{\bar{\alpha}(\bar{r})}(1+\epsilon^2\bar{\alpha}'(\bar{r})\zeta(\bar{r},\theta)+\mathcal{O}(\epsilon^3)), \\ e^{\beta}(\bar{r}) = &\quad e^{\bar{\beta}(r)} = e^{\bar{\beta}(\bar{r})}(1+\epsilon^2\bar{\beta}'(\bar{r})\zeta(\bar{r},\theta)+\mathcal{O}(\epsilon^3)), \\ \varpi(\bar{r},\theta) = &\quad \bar{\omega}(\bar{r},\theta), \quad M(\bar{r}) = \bar{M}(\bar{r}), \\ k(\bar{r},\theta) = &\quad \bar{k}(\bar{r},\theta),\ m(\bar{r},\theta) = \bar{m}(\bar{r},\theta),\ h(\bar{r},\theta) = \bar{h}(\bar{r},\theta), \end{aligned} \tag{4.45}$$

so that the new metric

$$\begin{aligned} ds^2 = &-(1+2\epsilon^2 h)e^{\alpha}dt^2 + \\ &+\left[1+2\epsilon^2\left(\frac{m}{\bar{r}-2M}+\partial_{\bar{r}}\zeta\right)\right]e^{\beta}d\bar{r}^2 + 2\epsilon^2 e^{\beta}\partial_\theta\zeta d\bar{r}d\theta + \\ &+(\bar{r}^2+2\epsilon^2\bar{r}^2(k+\zeta/\bar{r}))\big[d\theta^2+\sin^2\theta(d\phi+\epsilon\varpi dt)^2\big] \end{aligned} \tag{4.46}$$

coincides with (4.44) up to second order in ϵ. Although both metrics (4.46) and (4.37) are different, they are related through a gauge transformation, so that both must satisfy Einstein equations, and the gauge-independent results obtained in both approaches must be the same (at least, up to second order in ϵ). Note that these metrics are compatible with the general form for the Hartle-Thorne metric in an arbitrary gauge, obtained in [RV15], which have two commuting killing vector fields $k_{(\phi)} = \partial_\phi$ and $k_{(t)} = \partial_t$.

Although a priori the metric perturbation functions can have an arbitrary dependence on r and θ, an expansion of these functions is always possible in spherical harmonics [Har67]. Moreover, the angular dependence of the perturbation functions may be further reduced by additional arguments. For example, axial and reflection symmetry in the equatorial plane implies that the m (axial) number in the spherical harmonic expansion does not play any role, so that it may be reduced to an expansion in terms of Legendre polynomials. Therefore, we may expand the metric perturbation functions into a series of

Legendre polynomials or their derivatives, depending on the parity of the corresponding perturbation function (see eg [MP05] or appendix B for details). Thus, for the odd parity perturbation function $\varpi(\bar{r},\theta)$, we have

$$\varpi(\bar{r},\theta) = \sum_l \varpi_l(\bar{r}) \frac{\mathrm{d}}{\mathrm{d}\cos\theta} P_l(\cos\theta), \tag{4.47}$$

whereas for the even parity functions h, m and k:

$$\begin{aligned} h(\bar{r},\theta) &= \sum_l h_l(\bar{r}) P_l(\cos\theta), \\ m(\bar{r},\theta) &= \sum_l m_l(\bar{r}) P_l(\cos\theta), \\ k(\bar{r},\theta) &= \sum_l k_l(\bar{r}) P_l(\cos\theta), \end{aligned} \tag{4.48}$$

and the same holds for $\zeta(\bar{r},\theta)$. Furthermore, one can show that the requirements of asymptotic flatness and regularity of the metric at the center of the star impose that only the $l = 0$ term of (4.47) survives, and similar arguments can be made for the second order perturbation functions, in which case only the $l = 0, 2$ terms are non vanishing [Har67]. Thus, the spacetime metric is reduced to (4.46), where $\varpi(\bar{r},\theta) = \varpi_1(\bar{r}) \equiv \varpi(\bar{r})$, $h(\bar{r},\theta) = h_0(\bar{r}) + h_2(\bar{r}) P_2(\cos\theta)$, and so forth. Also, in the following, it will become useful to work with the shifted function $\omega(\bar{r})$ defined by

$$\varpi(\bar{r}) \equiv (\Omega_K - \omega(\bar{r})). \tag{4.49}$$

Furthermore, we can make use of the residual gauge freedom of reparametrizations of the radial coordinate to set $k_0(\bar{r}) = 0$ in the expansion.

On the other hand, with these gauge choices, the stress-energy tensor of the system will be given by

$$T^\mu_\nu = (\rho(\bar{r}) + p(\bar{r})) u^\mu u_\nu + p(\bar{r}) \delta^\mu_\nu, \tag{4.50}$$

where, from the normalization condition for the four-velocity, we have $u^\mu = u^t(1, 0, 0, \Omega_*)$, and

$$u^t = \frac{1}{\sqrt{-g_{tt} - 2\Omega_* g_{t\phi} - \Omega_*^2 g_{\phi\phi}}}, \tag{4.51}$$

which, up to second order in ϵ, reads

$$u^t = e^{-\frac{\alpha}{2}} + \epsilon^2 \left(\frac{\bar{r}^2}{2} \omega^2 \sin^2\theta - [h_0 + h_2 P_2(\cos\theta)] e^{\alpha} \right) e^{-\frac{3\alpha}{2}}. \tag{4.52}$$

To sum up, we have described the metric of spacetime associated to a slowly rotating perfect fluid star up to second order in the spin parameter. To do so, a perturbative expansion must be performed from a spherically symmetric, non-rotating metric in terms of a certain set of perturbation functions. We have chosen a particular coordinate system in which the surfaces of constant pressure coincide with those of constant radial coordinate, and written the stress-energy tensor of the rotating fluid in these coordinates. Therefore, we are now ready to obtain the Einstein equations for the system.

Interior Einstein equations

Let us now consider the Einstein equations (4.25), which can be written as $E = 0$ with $E := G - 8\pi T$, for the interior metric (4.46). The Einstein equations imply different equations for the perturbation functions, at each order in ϵ. Indeed, we may write

$$E(\epsilon) = E^{(0)} + E^{(1)}\epsilon + \frac{1}{2}E^{(2)}\epsilon^2 + \cdots \tag{4.53}$$

where $E^{(1)} = \partial_\epsilon E|_{\epsilon=0}$, and so forth, so that all terms in this expansion must vanish. For example, the zeroth-order equations correspond to the TOV system of equations (4.26).

At first order in ϵ, the only nontrivial equation is obtained from the first-order Einstein equation $E^{(1)} = 0$, and corresponds to the (t, ϕ) component, $E^{(1)\phi}{}_t = 0$, which yields

$$\omega'' = 4\left(\pi\bar{r}e^{\beta}(p+\rho) - \frac{1}{\bar{r}}\right)\omega' + 16\,\pi e^{\beta}(p+\rho)\omega. \tag{4.54}$$

The second order Einstein equations are given by $E^{(2)} = 0$. As we have seen, the second order perturbation functions can be divided into two sectors, corresponding to the $l = 0$ and $l = 2$ terms in the Legendre expansion. Furthermore, these sectors appear uncoupled in the Einstein equations, so that we may separate these into different sets of equations for each sector. At quadratic order in ϵ, it will also be useful to consider, apart from the Einstein equations, the stress-energy tensor conservation equation. In particular, from the $l = 0$ sector of $\nabla_\mu T^{(2)\mu}{}_r = 0$, one finds

$$h_0' = \frac{1}{3}\left(\bar{r}^2\omega^2 e^{-\beta}\right)' - \frac{1}{2}\left[\frac{\zeta_0}{\bar{r}}e^{\alpha}(2M + 8\pi\bar{r}^2 p)\right]'. \tag{4.55}$$

This equation can be integrated to yield an algebraic equation for ζ_0 in terms of h_0 and its initial condition, $h_0^{(0)}$ which is in a priori unknown and will be determined once the system is solved by matching with the exterior solutions. Further, from $\nabla_\mu T^{(2)\mu}{}_\theta = 0$, we have

$$\zeta_2 = -\frac{(\bar{r}^2 - 2\,\bar{r}M)[\bar{r}^2 e^{-\alpha}\omega^2 + 3\,h_2]}{3\,(4\,\pi\bar{r}^3 p + M)}, \tag{4.56}$$

where we have used the zeroth order TOV equations. The last two equations are only valid inside the star since we are supposing $p, \rho \neq 0$. In particular, as they both correspond to algebraic instead of differential equations, the variable ζ_2 will not appear in the second-order system of differential equations since we can substitute directly by (4.56), and the same will happen to h_0'.

Let us now obtain the differential equations for the rest of metric perturbation functions. The $l = 0$ contribution of $E^{(2)}{}_t^t = 0$ gives

$$m_0' = \frac{8}{3}\pi\bar{r}^4 e^{-\alpha}\omega^2(\rho + p) + \frac{1}{12}\,\bar{r}^4 e^{-(\alpha+\beta)}(\omega')^2 - 4\,\pi\bar{r}^2\zeta_0\rho'. \tag{4.57}$$

For the $l = 2$ sector, $E^{(2)\theta}{}_\theta - E^{(2)\phi}{}_\phi = 0$ and $E^{(2)r}{}_\theta = 0$ yield, respectively,

$$m_2 = \left[\frac{8}{3}\,\pi\bar{r}^5 e^{\beta}\omega^2(p+\rho) + \frac{\bar{r}^5}{6}(\omega')^2 - \bar{r}e^{(\alpha+\beta)}h_2\right]e^{-(\alpha+2\beta)}, \tag{4.58}$$

$$k_2' = -h_2' + \frac{\bar{r} - 3M - 4\pi p\bar{r}^3}{\bar{r}^2}e^{\beta}h_2 + \frac{\bar{r} - M + 4\pi p\bar{r}^3}{\bar{r}^3}e^{2\beta}m_2. \tag{4.59}$$

On the other hand, the Einstein equation $E^{(2)r}{}_r = 0$ yields two independent equations which must be satisfied separately, namely, one for the $l = 2$ sector (obtained from the terms proportional to $P_2(\cos\theta)$), and other for the $l = 0$ sector (from the terms independent of the Legendre polynomial). The equation for the $l = 2$ sector can be written

$$\begin{aligned} h_2' = &- \frac{\bar{r} - M + 4\pi p \bar{r}^3}{\bar{r}} e^{\beta} k_2' + \frac{3 - 4\pi(\rho + p)\bar{r}^2}{\bar{r}} e^{\beta} h_2 + \\ &+ \frac{2}{\bar{r}} e^{\beta} k_2 + \frac{1 + 8\pi p \bar{r}^2}{\bar{r}^2} e^{2\beta} m_2 + \frac{\bar{r}^3}{12} e^{-\alpha} (\omega')^2 - \\ &- \frac{4\pi(\rho + p)\bar{r}^4 \omega_1^2}{3\bar{r}} e^{-\alpha+\beta}, \end{aligned} \tag{4.60}$$

whereas for the $l = 0$ sector we have

$$\begin{aligned} h_0' = &- \frac{r^3}{12}(\omega')^2 e^{-\alpha} - \frac{e^{\beta}}{2\bar{r}^2}\left(\frac{2M}{\bar{r}} - \bar{r}\alpha'\right)\zeta_0 - \frac{\alpha''}{2}\zeta_0 \\ &+ \left[\frac{m_0}{\bar{r}^2} + \left(4\pi\rho - \frac{2M}{\bar{r}^3}\right)\zeta_0\right] e^{\beta}(1 + \bar{r}\alpha'). \end{aligned} \tag{4.61}$$

Substitution of eq. (4.55) into (4.61) yields a differential equation for ζ_0, which, together with eq. (4.57), constitutes a system of two ODEs independent of h_0. Thus, once this system is solved, h_0 can be found algebraically using the integrated version of (4.55) up to an arbitrary constant.

Exterior equations and solutions

Following [Har67; YY13b], we may take (4.37) as an ansatz for the metric of spacetime in the star exterior. We can indeed do this, since $\zeta(r, \theta)$ is defined only inside the star, and taken to be constant outside. This means that the exterior metric in terms of r and $\bar{r}$ will be the same, where now the radial coordinate r goes from a finite value in the star surface R_*, –corresponding to the star radius at zeroth-order– to infinity. Following the same steps as in the previous section, the Einstein equations in the exterior of the star can be obtained at each order in ϵ simply by setting $\rho = p = 0$ in Equations (4.54) and (4.58) to (4.60), with the exterior solution of the zeroth-order equations (TOV system) corresponding to the Schwarzschild solution by virtue of Birkhoff's theorem. Hence, to first order in ϵ, we have: $\epsilon\omega^{\text{ext}} = K_1 - K_2/r^3$ where K_1 and K_2 are two integration constants which can be related to the total spin velocity and angular momentum of the star. Indeed, at $r \to \infty$, the metric function $\epsilon\omega^{\text{ext}}$ must approach the angular velocity of the star as measured by an static observer, so that $K_1 = \Omega_*$. On the other hand, we may calculate the conserved total angular momentum J of the star by integrating the angular momentum density current $J^{\mu} = T^{\mu}{}_{\nu} k^{\nu}_{(\phi)}$ over a spacelike hypersurface Σ:

$$J = \int_{\Sigma} T_{\mu\nu} k^{\mu} dS_{\mu} = \int T^{t}_{\varphi} |g|^{1/2} dr d\theta d\phi = K_2/2 + \mathcal{O}(\epsilon^2), \tag{4.62}$$

from where it is straightforward to see that

$$\epsilon\omega^{ext} = \Omega_* - \frac{2J}{r^3}. \tag{4.63}$$

On the other hand, at second order in ϵ, the system given by eqs. (4.58) to (4.60) must be solved with vanishing ρ and p. Using the expressions for the exterior solution of the first and zeroth-order metric functions, and imposing asymptotic flatness of the metric, one finds the analytic expressions [Har67; YY13b]:

$$m_0^{\rm ext} = \delta M - \frac{J^2}{r^3}, \tag{4.64}$$

$$h_0^{\rm ext} = -\frac{\delta M}{(r-2M)} + \frac{J^2}{r^3(r-2M)}, \tag{4.65}$$

$$h_2^{\rm ext} = \frac{1}{M_* r^3}\left(1+\frac{M_*}{r}\right)J^2 + AQ_2^2\left(\frac{r}{M_*}-1\right), \tag{4.66}$$

$$k_2^{\rm ext} = -\frac{1}{M_* r^3}\left(1+\frac{2M_*}{r}\right)J^2 + \frac{2AM_*}{\sqrt{r\,(r-2M_*)}}Q_2^1\left(\frac{r}{M_*}-1\right) - AQ_2^2\left(\frac{r}{M_*}-1\right), \tag{4.67}$$

$$m_2^{\rm ext} = -\frac{1}{M_* r^2}\left(1-7\frac{M_*}{r}+10\frac{M_*^2}{r^2}\right)J^2 + \\ + \frac{3Ar^2}{M_*}\left[1-3\frac{M_*}{r}+\frac{4}{3}\frac{M_*^2}{r^2}+\frac{2}{3}\frac{M_*^3}{r^3}+\frac{r}{2M_*}f(r)^2\ln f(r)\right], \tag{4.68}$$

being $f(r) = (1-2M_*/r)$, and where δM and A are integration constants. As we will see, δM corresponds to the correction of the gravitational mass, whereas A will be associated to the Love numbers.

Numerical solution for the interior and matching

Once we have obtained the system of differential equations for the metric functions, we need now the initial conditions in order to solve it. In this section we will explain how to obtain them and also how to solve the system numerically.

At this point there are no differences between how to solve the exact case and the mean-field case since the shooting method for the exact case is required only for the zeroth-order equations and those have already been solved. Thus we do know which value of the pressure in the center of the star corresponds to a given baryon number.

To obtain the initial conditions, as before, we expand our metric functions in powers of the radial coordinate and insert them in the differential equations to obtain the relations between the coefficients. In the zeroth-order (non-rotating) problem it is enough to expand until the zeroth order coefficient (in powers of $\bar{r}$), however when dealing with the second-order functions we need to expand them to the first nontrivial order (with nonvanishing coefficients). The reason is that the metric functions h_2 and k_2 vanish at the center of the star. Furthermore, for the next term of the expansions we find that they are equal and opposite, thus cancelling each other when substituting into their equations. This implies that: 1. We need a really good accuracy in the step of the numerical integration and 2. We cannot obtain the value of the first nontrivial coefficient of h_2, in its expansion in powers of $\bar{r}$. To solve both problems, we follow [Yag+13] and start the integration in some small radius R_ϵ (instead of $\bar{r}=0$) such that the expansions (4.69) are sufficiently accurate and the integration does not depend on the value of R_ϵ. The expansions of the

metric functions, with the nontrivial coefficients expressed in terms of the functions in $\bar{r} = 0$ are

$$\alpha = \alpha_0 + \frac{4\pi}{3}(\rho_0 + 3p_0)\,\bar{r}^2 + \mathcal{O}\left(\bar{r}^3\right), \tag{4.69a}$$

$$M = \frac{4\pi}{3}\rho_0\bar{r}^3 + \frac{4\pi}{5}\rho_2\bar{r}^5 + \mathcal{O}\left(\bar{r}^6\right), \tag{4.69b}$$

$$p = p_0 - \frac{2\pi}{3}(\rho_0 + p_0)(\rho_0 + 3p_0)\,\bar{r}^2 + \mathcal{O}\left(\bar{r}^3\right), \tag{4.69c}$$

$$\rho = \rho_0 + \rho_2\bar{r}^2 + \mathcal{O}\left(\bar{r}^3\right), \tag{4.69d}$$

$$\chi = 1 - \frac{1}{2}\chi^{(2)}\bar{r}^2 + \mathcal{O}\left(\bar{r}^3\right) \text{(Exact case)}, \tag{4.69e}$$

$$\omega = \omega_0 + \frac{8\pi}{5}(\rho_0 + p_0)\,\omega_0\bar{r}^2 + \mathcal{O}\left(\bar{r}^3\right), \tag{4.69f}$$

$$h_2 = h_2^{(2)}\bar{r}^2 + \mathcal{O}\left(\bar{r}^3\right), \tag{4.69g}$$

$$m_0 = \frac{8e^{-\alpha_0}}{5}\omega_0^2\left[\frac{2\pi}{9}(2\rho_0 + 3p_0) - \frac{3}{8}\frac{\rho_2}{\rho_0 + 3p_0}\right]\bar{r}^5 + \mathcal{O}\left(\bar{r}^6\right), \tag{4.69h}$$

$$\zeta_0 = \frac{3\omega_0^2 e^{-\alpha_0}}{8\pi(\rho_0 + 3p_0)}\bar{r} + \mathcal{O}\left(\bar{r}^2\right), \tag{4.69i}$$

where ω_0, as p_0, is an input parameter when it comes to solve the system. This parameter will determine the angular velocity of the star Ω_*, as can be seen from the matching condition of ω with the exterior solution, ω^{ext}, obtained in the previous section. This matching condition is simply given by imposing that the metric function ω and its first derivative are continuous throughout the star surface [YY13b], i.e.

$$\omega(R_*) = \omega^{\text{ext}}(R_*), \qquad \omega'(R_*) = \omega'^{\text{ext}}(R_*). \tag{4.70}$$

Therefore, in the rotating case, the stars are identified by a two-parameter family (ω_0, p_0). The values of ρ_2 and N_2 are easily obtained from the EOS ($\rho(p)$, $n(p)$), and $h^{(2)}$ is obtained from (4.31). The functions k_2 and m_2 are found to satisfy $k_2^{(2)} = m_2^{(2)} = -h_2^{(2)}$, around the center. As we have said, the odd powers in $\bar{r}$ of almost all the metric functions are null, however the definitions of M (4.27), m and ζ_0 (4.46) lead to the expansions given in (4.69).

Now we start the integration with a non-zero, but still unknown, seed for the second-order functions h_2 and k_2. To solve the unknown initial condition issue we will follow the approach given in [Yag+13; Har67]. First we must obtain a particular solution for h_2 and k_2 (h_p, k_p) by solving the equations (4.60) and (4.59) for an arbitrary initial value (that must satisfy the regularity conditions given in (4.69)). Next, we obtain a homogeneus solution (h_h, k_h) again for an arbitrary initial condition, using the same equations but with vanishing source terms. With these two functions we can construct the solution

$$h_2(\bar{r}) = h_p(\bar{r}) + Bh_h(\bar{r}), \quad k_2(\bar{r}) = k_p(\bar{r}) + Bk_h(\bar{r}). \tag{4.71}$$

In these expressions B is a constant that can be obtained by matching the functions h_2 and k_2 at the surface of the star with their corresponding exterior solutions. This matching condition is simply given by continuity of both functions at R_*, i.e.

$$h_2(R_*) = h_2^{\text{ext}}(R_*), \quad k_2(R_*) = k_2^{\text{ext}}(R_*). \tag{4.72}$$

By doing this we are introducing the integration constant that appears in (4.68), hence we have an algebraic system of two equations that can be solved for A and B.

On the other hand, to solve the $l = 0$ sector of the second order system, we first solve the coupled ODEs for ζ_0 and m_0 as explained in the previous section, and then we obtain the solution for h_0 up to a constant h_0^c whose value is determined from the matching conditions

$$m_0^{\rm int}(R_*) - 4\pi R_*^2 \rho(R_*)\zeta_0(R_*) = m_0^{\rm ext}(R_*), \tag{4.73a}$$
$$h_0^{\rm int}(R_*) = h_0^{\rm ext}(R_*), \tag{4.73b}$$

where the constant term in (4.73a) is due to a nonvanishing energy density at the surface of the star, as pointed out in [RV15; Rei+17]. To obtain this constant term we can integrate (4.93) in the interval $[R_* - \epsilon, R_* + \epsilon]$ and take $\epsilon \to 0$. By doing this we have that all terms in the surface of the star vanish but the term $d\rho/dr$, which is unbounded at R_* and contributes with a constant term. From (4.73a) we can obtain the value of δM, which reads

$$\delta M = m^{\rm int}(R_*) + \frac{J^2}{R_*^3} - 4\pi R_*^2 \rho(R_*)\zeta_0(R_*). \tag{4.74}$$

We would also like to remark a subtle detail concerning the second-order equations. When solving the TOV numerically, the metric function α is not fixed to its correct initial value since it does not affect the observables of the star. However, for solving the second order problem it is necessary to find the correct initial value of this function since the second order perturbation functions depend directly on $\alpha(0)$ and an incorrect value will affect the values of the quadrupole moment and gravitational mass correction of the star. This can be done by first solving the TOV system, finding the correct initial value of α using the matching condition (4.33) and then solving both zeroth and second order systems.

4.2.2 Global properties of compact stars

A key feature of the Hartle-Thorne perturbative formalism is that it allows us to obtain the values of these observable parameters from the solutions of the Einstein equations for the interior of the star at each order in the expansion parameter. Indeed, once these solutions have been obtained, they can be matched to the exterior solutions, from which observational parameters such as the quadrupole moment can be obtained systematically.

Take for example the moment of inertia I, which is defined as the quantity measuring how fast a star can spin given a fixed spin angular momentum J, and is given by

$$I = \frac{J}{\Omega_*}. \tag{4.75}$$

To obtain the value of I for a given (interior) solution of the second-order Hartle-Thorne equations is straightforward: we simply obtain J from (4.63), by matching the exterior solution to the interior one at R_* (4.70) and dividing by Ω_*. It will be convenient also to define the dimensionless moment of inertia as

$$\bar{I} = \frac{I}{M_*^3}. \tag{4.76}$$

On the other hand, the metric generated by an isolated, static gravitating body at a given point sufficiently far from the source may be written using a multipolar expansion in a system of *Asymptotically Cartesian and Mass Centered* coordinates [Tho80; TH85], whose (0,0) component will be of the form

$$g_{00} = -1 + \frac{2M}{r} + 3\frac{Q_{ij}}{r^5}x^i x^j + \mathcal{O}\left(\frac{1}{r^4}\right), \tag{4.77}$$

where M is the gravitational mass of the star [3], and Q_{ij} is the (traceless) quadrupolar tensor.

The induced quadrupolar deformation of the star can be described in terms of the star's $l = 2$ sector perturbation functions in spherical coordinates. Indeed, defining $x^i = rn^i(\theta, \phi)$, where n^i is the unit three-vector in spherical coordinates, we may write:

$$Q_{ij}\frac{x^i x^j}{r^2} = Q_{ij}n^i n^j(\theta, \phi) = \sum_{m=-2}^{2} Q^m Y_{2m}(\theta, \phi), \tag{4.78}$$

(where Y_{2m} are the $l = 2$ spherical harmonics). We find, in the case of an axially symmetric deformation, that the expansion (4.77) reduces to

$$g_{00} = -1 + \frac{2M}{r} + \frac{Q}{r^3}P_2(\cos\theta) + \mathcal{O}\left(\frac{1}{r^4}\right), \tag{4.79}$$

which defines the quadrupole moment of the metric, Q.

Thus, we may perform an asymptotic expansion of the Hartle-Thorne perturbative solution for the exterior spacetime metric and identify the gravitational mass and quadrupole moment as the coefficients proportional to $2/r$ and the $P_2(\cos\theta)/r^3$ term, respectively. Clearly, these quantities get corrections due to the star rotation.

Indeed, for example, the gravitational mass of the star, up to second order in ϵ, receives a correction

$$M(\epsilon) = M_* + \epsilon^2 \delta M \tag{4.80}$$

which can be obtained from the expansion of the h_0^{ext} perturbation function. Furthermore, taking into account the asymptotic expansion for large r of h_2^{ext} and ω^{ext} one finds that the spin-induced quadrupole moment of the star, up to second order in the spin parameter, is given by

$$Q^{\text{rot}} = -\frac{J^2}{M_*} - \epsilon^2 \frac{8}{5} A M_*^3. \tag{4.81}$$

For later convenience we also define the dimensionless rotationally-induced quadrupole moment as

$$\bar{Q}^{\text{rot}} = -\frac{M_*}{J^2}Q^{\text{rot}}. \tag{4.82}$$

Dropping the staticity assumption, nontrivial current multipole moments may appear in the expansion of the $(0, j)$ components of the metric,

$$g_{0j} = -2\epsilon_{jkl}\frac{J_k}{r^2}x^l - 4\epsilon_{jqk}\frac{S_l^k}{r^5}x^q x^l + \mathcal{O}\left(\frac{1}{r^4}\right), \tag{4.83}$$

[3] In stationary spacetimes, the gravitational mass is defined via a Komar surface integral [Gou10], and coincides with the ADM mass in asymptotically flat spacetimes.

the first term corresponding to a non-vanishing angular momentum.

Finally, another interesting property that can be obtained from the solutions is the binding energy, which physically corresponds to the amount of energy that keeps all the particles (baryons) in the star from dispersing to infinity. It is defined as $E_t = M_g - M_b$ where M is the gravitational (or ADM) mass (in the static case, $M = M_*$) and M_b is the baryon mass of the star. The binding energy so defined includes both the gravitational binding energy and the nuclear binding energy. However, we will be mostly interested in the gravitational contribution to the total binding energy, i.e. the *gravitational* binding energy, since it contains EOS-independent information about the mass distribution of the star [JWC19]. The gravitational binding energy is defined as $E_g = M - M_p$, being M_p the proper mass, given by the proper energy-momentum density, $P_\mu = T_{\mu\nu}u^\nu$, integrated on a spacelike hypersurface with volume form dS_μ:

$$M_p = \int_\Sigma T^\mu_\nu u^\nu dS_\mu. \tag{4.84}$$

In a stationary spacetime, this integral does not depend on the chosen hypersurface, so we may take $dS_\mu = n_\mu d^3S$, where $d^3S = \sqrt{\gamma}d^3x$ is the volume element of the spacelike hypersurfaces defined by $t = \text{const}$, γ is the determinant of the three-metric associated with these hypersurfaces and $n_\mu = \nabla_\mu t/\sqrt{(\nabla_\nu t \nabla^\nu t)}$ is the corresponding normal vector, so that, for the static case,

$$M_p^* = \int T^\mu_\nu u^\nu n_\mu d^3S = 4\pi \int_0^{R_*} \frac{\rho(r)}{\sqrt{1-\frac{2M(r)}{r}}} r^2 dr. \tag{4.85}$$

In the slowly rotating case, the perturbed proper mass $M_p(\epsilon)$ will also get corrections. Expanding both γ and the product $u^\mu n_\mu$ in powers of ϵ, we have, up to second order, $M_p(\epsilon) = M_p^* + \epsilon^2 \delta M_p$, where

$$\delta M_p = 8\pi \int_0^{R_*} \rho \bar{r}^4 e^{\beta/2} \left\{ \left(\frac{m_0}{\bar{r} - 2M} \right) + \frac{\bar{r}^2}{6}\omega^2 e^{-\alpha/2} \right\} d\bar{r}. \tag{4.86}$$

Hence, it is straightforward to obtain the second order perturbation to the gravitational binding energy $E_g(\epsilon) = E_g + \epsilon^2 \delta E_g$, with $\delta E_g = \delta M - \delta M_p$.

4.3 Tidally deformed stars and Love numbers.

Until now we have studied the deformation of stars resulting from their own rotation. However, we can also study (non-rotating) stars which are deformed due to some external tidal force. Tidal forces are one of the principal signatures of the presence of a nontrivial gravitational field in spacetime. Such forces are responsible for relative acceleration among freely falling particles. This acceleration induces, on extended gravitating bodies, a field of strains that causes a deformation, which may be measured. By measuring the deformation response of a body to a tidal gravitational field, we may obtain information about the kind of matter that conforms the body, as well as its equation of state. In particular, in the case of binary systems involving neutron stars, it is very useful to analyze the deformation of the stars due to tidal effects, which may be measured from its gravitational wave spectrum previous to the merging.

On the other hand, as we have previously stated, a spherical body immersed in an external tidal field may deform due to tidal forces. Owing to this deformation, the metric in the exterior spacetime will develop a non trivial multipolar structure. To characterize the tidal field generated by a given source, consider an observer immersed in a tidal field generated by an external source. We may expand the metric of spacetime in a region surrounding the observer's worldline in Fermi normal coordinates, with the $(0,0)$ and $(0,j)$ component of the metric given by [TH85; PPV11],

$$g_{00} = -1 + \mathcal{E}_{ij}x^i x^j + \mathcal{O}\big(r^3\big), \tag{4.87a}$$

$$g_{0j} = \frac{2}{3}\epsilon_{jqk}\mathcal{B}^q_l x^k x^l + \mathcal{O}\big(r^3\big), \tag{4.87b}$$

where $\mathcal{E}_{ij}$ and $\mathcal{B}_{ij}$ are the (quadrupolar) tidal multipole moments of electric and magnetic type, respectively. These two are related to the Riemann tensor through $\mathcal{E}_{ij} = R_{i0j0}$ and $\mathcal{B}^i_j = \frac{1}{2}\epsilon^{ijk}R_{0jkl}$ [TH85]. The quadrupolar tidal moments are independent of the distance to the source, but may depend on the time coordinate if the source is not stationary. Now, instead of the worldline of an observer, we may consider the worldtube of an extended, gravitating body immersed in an external tidal field. We thus may be able to write the (0,0) component of the metric outside this body by combining both eqs. (4.77) and (4.87a),

$$g_{00} = -1 + \frac{2M}{r} + 3\frac{Q_{ij}}{r^5}x^i x^j + \mathcal{O}\left(\frac{1}{r^4}\right) + \mathcal{E}_{ij}x^i x^j + \mathcal{O}\big(r^3\big), \tag{4.88}$$

whereas the $(0,j)$ component of the metric will be given by the combination of eqs. (4.83) and (4.87b),

$$g_{0j} = -4\epsilon_{jqk}\frac{S^k_l}{r^5}x^q x^l + \mathcal{O}\left(\frac{1}{r^4}\right) + \frac{2}{3}\epsilon_{jqk}\mathcal{B}^q_l x^k x^l + \mathcal{O}\big(r^3\big). \tag{4.89}$$

Note that, by writing the metric as in eqs. (4.88) and (4.89), we are assuming that there exists a region of the exterior spacetime, called the BUFFER REGION, in which the expansions of eqs. (4.77), (4.83) and (4.87) converge simultaneously. This will be well justified in the limit in which the source of the external tidal field is very far away from the body that gets deformed and does not evolve rapidly with time. It can also be shown that, in this limit, the multipole moments appearing in (4.88) are defined unambiguously [Gür83].

4.3.1 Electric quadrupolar Love number

Since we are considering that the body gets deformed due to the external tidal field, the quadrupole tensor Q_{ij} will be a more or less complicated function of the tidal field $\mathcal{E}_{ij}$. However, working to linear order in the tidal moment, we define the (tidal) ELECTRIC QUADRUPOLAR DEFORMABILITY λ_t as

$$Q_{ij} = -\lambda_t \mathcal{E}_{ij}. \tag{4.90}$$

Assuming that the terms with non-zero axial number m vanish, we may write (4.87a) in spherical coordinates as

$$g_{00} = -1 + r^2\mathcal{E}P_2(\cos\theta) + \mathcal{O}\big(r^3\big), \tag{4.91}$$

so that the tidal electric Love number can be obtained as the ratio $\lambda_t = -Q/\mathcal{E}$, where Q is the quadrupole moment of the star as defined in (4.79).

That the deformation of the star resulting from an external tidal field will be well described by its deformability λ is consistent with the assumption that the source of this external field is far from the body, since the tidal field will be weak and the linear approximation will be well justified.

The quadrupolar deformation of the star due to an external tidal field and to a slow rotation can be described by a similar spacetime metric (up to second order) [Hin08; Hin+10], hence we can take advantage of the differential equations derived above to obtain the results for a tidally deformed star. Indeed, to describe a tidally deformed star, one introduces the metric perturbation $h_{\mu\nu}$ as in appendix B. By direct comparison between the metric (4.37) and (150), it is straightforward to see that the $l = 2$ even perturbation functions H_2, M_2 and K_2 in the tidally deformed case play a similar role as the functions h_2, m_2, k_2 in the slowly rotating case. Indeed, this can be seen by redefining these functions as

$$H_2 = 2e^{\alpha} h_2, \quad M_2 = 2e^{\beta} \frac{m_2}{\bar{r} - 2M}. \tag{4.92}$$

In order to calculate the quadrupolar deformation of the metric due to an external gravitational field, the odd perturbations to the metric are not needed. Therefore, the metric functions of non-rotating tidally deformed stars can be directly obtained from eqs. (4.58) to (4.60) by imposing $\omega = 0$. Then, these equations can be arranged into only one equation for h_2,

$$\begin{aligned} h_2'' = &- \left\{ \frac{2}{\bar{r}} + \left[\frac{2M}{\bar{r}^2} + 4\pi \bar{r}(p - \rho) \right] e^{\beta} \right\} h_2' \\ &+ \left\{ \frac{6e^{\beta}}{\bar{r}^2} - 4\pi \left[5\rho + 9p + (\rho + p) \frac{d\rho}{dp} \right] e^{\beta} + (\alpha')^2 \right\} h_2. \end{aligned} \tag{4.93}$$

This is a second-order differential equation which can be solved as a first-order system as in [Hin08] by defining $H \equiv h_2'$, while H' is given by (4.93). To do this we need, again, to expand the function h_2 in powers of $\bar{r}$ and introduce it in (4.93) to obtain the initial condition

$$\begin{aligned} h_2 &= h_2^{(2)} \bar{r}^2 + \mathcal{O}\left(\bar{r}^3\right) \\ H &= h_2' = 2h_2^{(2)} \bar{r} + \mathcal{O}\left(\bar{r}^2\right). \end{aligned} \tag{4.94}$$

Once more, the value of $h^{(2)}$ can not be found from the limit $\bar{r} \to 0$ of the field equations. However, we will see that this is unimportant to find the correct value of the tidal deformability (see below), so that we can start the integration with an arbitrary value for $h_2^{(2)}$, as long as (4.94) are satisfied.

Once the internal solution has been found numerically, we can calculate the (tidal) Love number from the external solution of the metric after matching with the internal solution using the matching conditions

$$h_2^{\text{int}}(R_*) = h_2^{\text{ext}}(R_*), \tag{4.95a}$$

$$H^{\text{int}}(R_*) - 4\pi \frac{R_*^2}{M_*} \rho(R_*) h_2^{\text{int}}(R_*) = H^{\text{ext}}(R_*). \tag{4.95b}$$

where, as in the case of (4.73a), there is a constant contribution in (4.95b) due to a nonvanishing energy density at the surface of the star [Hin+10; Yag+13; DN09].

Hence, as before, the vacuum ($\rho = p = 0$) version of (4.93) can be analytically solved,

$$h_2^{\rm ext} = c_1 \left(\frac{r}{M_*}\right)^2 \left(1 - \frac{2M_*}{r}\right) \left[-\frac{2M_*\left(r - M_*\right)\left(3r^2 - 6M_* r - 2M_*^2\right)}{r^2\left(r - 2M_*\right)^2} + 3\ln\left(\frac{r}{r - 2M_*}\right)\right] + \\ + c_2 \left(\frac{r}{M_*}\right)^2 \left(1 - \frac{2M_*}{r}\right). \tag{4.96}$$

where $c_{1,2}$ are constants that can be determined through the matching conditions in terms of $H^{\rm int}(R_*), h_2^{\rm int}(R_*)$. Studying the behavior of this function in the buffer zone we can extract the expression for Q and $\mathcal{E}$ in terms of these constants c_1 and c_2 in order to obtain the tidal electric deformability. Indeed, in the buffer zone

$$h_2^{\rm ext} = \frac{16}{5} c_1 \frac{M_*^3}{r^3} + c_2 \frac{r^2}{M_*^2} + \mathcal{O}\left(\frac{M_*^4}{r^4}, \frac{r}{M_*}\right), \tag{4.97}$$

and comparing with eqs. (4.79) and (4.91) we have

$$\lambda_t = \frac{16}{15} M^5 \frac{c_1}{c_2}, \tag{4.98}$$

and, defining the tidally induced, quadrupolar electric Love number $k_2^E = \frac{3}{2}\frac{\lambda_t}{R_*^5}$, we can write

$$k_2^E = \frac{8}{5} C^5 (1-2C)^2 [2 + 2C(y-1) - y] \times \\ \{2C[6 - 3y + 3C(5y-8)] + 4C^3\left[13 - 11y + C(3y-2)\right. \\ \left. + 2C^2(1+y)\right] + 3(1-2C)^2[2 - y + 2C(y-1)]\ln(1-2C)\}^{-1}, \tag{4.99}$$

where $y = R_* H^{\rm ext}(R_*)/h_2^{\rm ext}(R_*)$ and $C = M_*/R_*$ is the compactness of the zeroth-order solution. From the definition of y it is clear that $k_2^{(\rm tid)}$, and hence λ_t, does not depend on the value of $h^{(2)}$ chosen in the numerical integration of the interior equation. Again, for later convenience we will define the adimensional tidal deformability as

$$\bar{\lambda}_t = \frac{2}{3} k_2^{(\rm tid)} C^{-5}. \tag{4.100}$$

4.3.2 Magnetic quadrupolar Love number

While electric-type Love numbers measure the induction of different multipole moments on a star due to an external gravitational field and can also be calculated in the Newtonian limit of general relativity, the current multi-pole moments induced by an external magnetic-type tidal field have no analogue in Newtonian gravity, and thus the magnetic tidal Love numbers are a genuine prediction of general relativity. In the simplest (quadrupolar) case, the tidal magnetic deformability, in analogy with the electric case, measures the magnitude of the quadrupolar current S_{ij} induced in the star by an external tidal field of magnetic type, $\mathcal{B}_{ij}$. At the linear level, the relation between both is

$$S_{ij} = -\sigma_t \mathcal{B}_{ij}. \tag{4.101}$$

Therefore, it is interesting to study the response of a NS under a magnetic-type external gravitational field, whose effects may be relevant for such compact objects. To do so, we consider an axially-symmetric perturbation of the spherical metric. For the calculation of magnetic-type Love numbers, only the odd metric perturbations are relevant. The magnetic Love number can be obtained by assuming a perturbation of the static metric of the form $g(\epsilon) = g^{(0)} + \epsilon h^{\rm odd}$ where $g^{(0)}$ is the static spherically symmetric metric (4.24), ϵ here does not have to do anything with rotation, but will play the role of a bookkeeping parameter, and $h^{\rm odd}$ is the odd-parity perturbation:

$$h^{\rm odd}_{\mu\nu} dx^\mu dx^\nu = 2V(r,\theta) dr d\phi + 2\omega(r,\theta) dt d\phi. \tag{4.102}$$

In particular, for the simplest (quadrupolar) perturbations, we take into account only $l = 2$ in (150) and we have

$$\begin{aligned} V(r,\theta) &= V_2(r) \sin\theta\, \partial_\theta P_2(\cos\theta), \\ \omega(r,\theta) &= \omega_2(r) \sin\theta\, \partial_\theta P_2(\cos\theta). \end{aligned} \tag{4.103}$$

Notice that we have dropped the barred radial coordinate, since the star shape will not be altered by the odd metric perturbations.

On the other hand, using the notation of appendix B, we define $n^i_A = \partial_A n^i$. Then, we can transform the $(0, j)$ components of the metric to spherical coordinates by $g_{0j} \to g_{0A} = r n^j_A g_{0j}$, and expand into odd-parity vector harmonics (see appendix B), for instance,

$$\epsilon_{jqk} \frac{S^k_l}{r^3} x^q x^l \to n^j_A \epsilon_{jqk} S^k_l n^q n^l = \sum_{m=-2}^{m=2} S_m X^{2m}_A(\theta,\phi), \tag{4.104}$$

so that eq. (4.89) is transformed into

$$h^{\rm odd}_{0A} = \sum_{m=-2}^{m=2} \left\{ \frac{-4}{r^2} S_m + \frac{2}{3} r^3 B_m \right\} X^{2m}_A(\theta,\phi) + \cdots \tag{4.105}$$

In particular, for the simplest case of axially symmetric perturbations, we have, for instance,

$$h^{\rm odd}_{0\phi} = \left[\frac{-4S}{r^2} + \frac{2}{3} r^3 B \right] \sin\theta \partial_\theta P_2(\cos\theta) + \cdots, \tag{4.106}$$

where $\cdots$ in eqs. (4.105) and (4.106) denotes the non-leading terms in the expansion at the buffer zone. Hence, the magnetic tidal deformability can be obtained as the ratio

$$\sigma_t = -\frac{S}{B}, \tag{4.107}$$

where the constants S and B will be determined from the buffer zone expansion of the odd-parity metric perturbation functions (4.103).

To find these functions, the Einstein equations must be solved for the star interior, and matched to a suitable exterior solution, as we have previously done for the even parity case. However, in the case of odd-parity tidal perturbations, the energy-momentum tensor of the fluid will also get perturbed through a perturbation of the 4-velocity, $u^\mu(\epsilon) = u^\mu + \epsilon \delta u^\mu$,

$$\delta T^\mu{}_\nu = (\rho + p)(u_\nu \delta u^\mu + u^\mu \delta u_\nu) - p g^{(0)\mu\sigma} h^{\rm odd}_{\sigma\nu}, \tag{4.108}$$

working to first order in ϵ, and $\delta u_\mu = g^{(0)}_{\mu\nu}\delta u^\nu + h^{\rm odd}_{\mu\nu}u^\nu$.

Now, in principle, the four-velocity perturbations are independent of the metric perturbations, and the latter are only related with the former through the perturbative Einstein equations. However, there are two simple cases for which these perturbations are closely related to each other: the *static* case, in which the fluid remains static — with vanishing spatial four-velocity components i.e. $\delta u^\mu = 0$ — even when the metric perturbations are taken into account, and the *irrotational* fluid, which is based on the assumption that the fluid perturbations preserve the relativistic circulation theorem [RZ13], and can be shown to be equivalent to the condition of a vorticity-free fluid, i.e. with vanishing vorticity four-vector $\omega^\alpha = \frac{1}{2}\epsilon^{\alpha\beta\mu\nu}u_\beta\nabla_\mu u_\nu = 0$ which in turn implies $\delta u_\mu = 0$ [LP15], since the static initial configuration is trivially vorticity-free. The latter assumption is usually considered as more physically relevant, as the static fluid is only adequate for the non-physical case of time-independent tidal perturbations [Pan+18]. Hence in the following we will only consider the case of an irrotational fluid and write the four-velocity perturbation as

$$\delta u^\mu = g^{(0)\mu\nu}h^{\rm odd}_{\nu\alpha}u^\alpha = -\frac{2\omega_2(r)}{r^2}\frac{\partial_\theta P_2(\cos\theta)}{\sin\theta}\delta^\mu_\phi. \tag{4.109}$$

Substituting this expression into the stress-energy tensor perturbation, we may expand the Einstein equations as in (4.53) and solve the linearized equations $E^{(1)} = 0$, which yield $V_2 = 0$ and the following equation:

$$\omega_2'' - 4\pi(\rho+p)re^\beta\omega_2' - \frac{e^\beta}{r^3}\left(6r - 4M - 8\pi(\rho+p)r^3\right)\omega_2 = 0, \tag{4.110}$$

for the metric perturbation function ω_2. The above equation is numerically integrated in the star interior starting with an initial condition

$$\omega_2 = \omega_2^{(3)}r^3 + \mathcal{O}(\bar{r}^5), \tag{4.111}$$

where, as in the electric case, the exact value of $\omega_2^{(3)}$ is undetermined from the equations but will not be needed for obtaining the corresponding Love number.

On the other hand, the exterior solution of eq. (4.110) can be written in terms of the hypergeometric function ${}_2F_1(\alpha,\beta,\gamma;x)$ as [Yag14]

$$\omega_2^{\rm ext}(r) = d_1\left(\frac{r}{2M}\right)^3 {}_2F_1\left(-1,-4,-4;\frac{2M}{r}\right) + d_2\left(\frac{2M}{r}\right)^2 {}_2F_1\left(1,4,6;\frac{2M}{r}\right), \tag{4.112}$$

where $d_{1,2}$ are integration constants that can be related to the interior solution through the matching conditions

$$\omega_2^{\rm ext}(R_*) = \omega_2(R_*), \quad \omega'^{\rm ext}_2(R_*) = \omega_2'(R_*). \tag{4.113}$$

The expansion of (4.112) in powers of r and r^{-1} in the buffer region reads

$$\omega_2^{\rm ext}(r) = \frac{1}{8}d_1\frac{r^3}{M_*^3} + 4d_2\frac{M_*^2}{r^2} + \mathcal{O}\left(\frac{M_*^3}{r^3}, \frac{r^2}{M_*^2}\right), \tag{4.114}$$

and, comparing with (4.106), we have

$$\sigma_t = \frac{16}{3}\frac{d_1}{d_2}M^5, \tag{4.115}$$

so that the magnetic quadrupolar Love number $k_2^M = 48\frac{\sigma_t}{R_*^5}$ can be written as

$$\begin{aligned} k_2^M = \frac{96C^5}{5}[3+2C(y-2)-y]\big\{2C\{9-3y+C[3(y-1)+ \\ +2C(C+y+Cy)]\}+3[3+2C(y-2)-y]\log(1-2C)\big\}^{-1}, \end{aligned} \tag{4.116}$$

where now $y = R_*\omega_2'(R_*)/\omega_2(R_*)$, and once more it is clear from this expression that the initial condition for ω_2 does not enter in the expression for the magnetic Love number.

4.4 Quasi-universal relations

4.4.1 I-Love-Q

In their original paper [YY13b], Yagi and Yunes present a set of EOS-independent relations between the dimensionless moment of inertia, quadrupole moment and Love numbers of slowly rotating and tidally deformed compact stars, the so-called *I-Love-Q* relations. Soon after these relations where proposed, in [Yag+14] two possible reasons for these relations to exist were given. The first one relies on the fact that these relations depend mostly on the outer core ($10^{13} \leq \rho \leq 5\,10^{14}$ g/cm^3) of the NS, where all the EOS nuclear experimental data follow the same behavior. The second is related to the no-hair conjecture of black holes, since the three parameters ($\bar{I}, \bar{\lambda}$ and $\bar{Q}$) must approach the limiting values of a black hole for stars with large compactness.

In fig. 4.2 we show that these relations for the BPS (both exact and mean-field limits) also satisfied. We also show the data for the standard Skyrme crystal, generalized and hybrid EOS of [Ada+20] (which satisfy these relations as well) and the numerical fit for each of these relations obtained in [YY13b] is plotted with a black line. Although somewhat expected, this result is remarkable at least for the case of exact BPS models, for which the *I-Love-Q* relations are satisfied even when they present a non-barotropic EOS which varies depending on the chosen potential. Furthermore, the relations are satisfied for these models in the exact and mean-field cases. As we will see, this will not be true anymore for other quasi-universal relations. This points out the universality and EOS independence of the *I-Love-Q* relations.

Additionally, more quasi-universal relations have been found between electric, magnetic and higher multipole Love numbers [Yag14]. For example, in 4.3 we show how there is as well an EOS independent relation between the (dimensionless) electric and magnetic quadrupolar tidal deformabilities in all models considered.

4.4.2 I-Love-C

Apart from the *I-Love-Q* relations, there exists other set of relations between the moment of inertia, the Love numbers and the compactness of neutron stars that share some chatracteristics with the *I-Love-Q* but are accurate only up to $\sim 10\%$. These *I-Love-C*

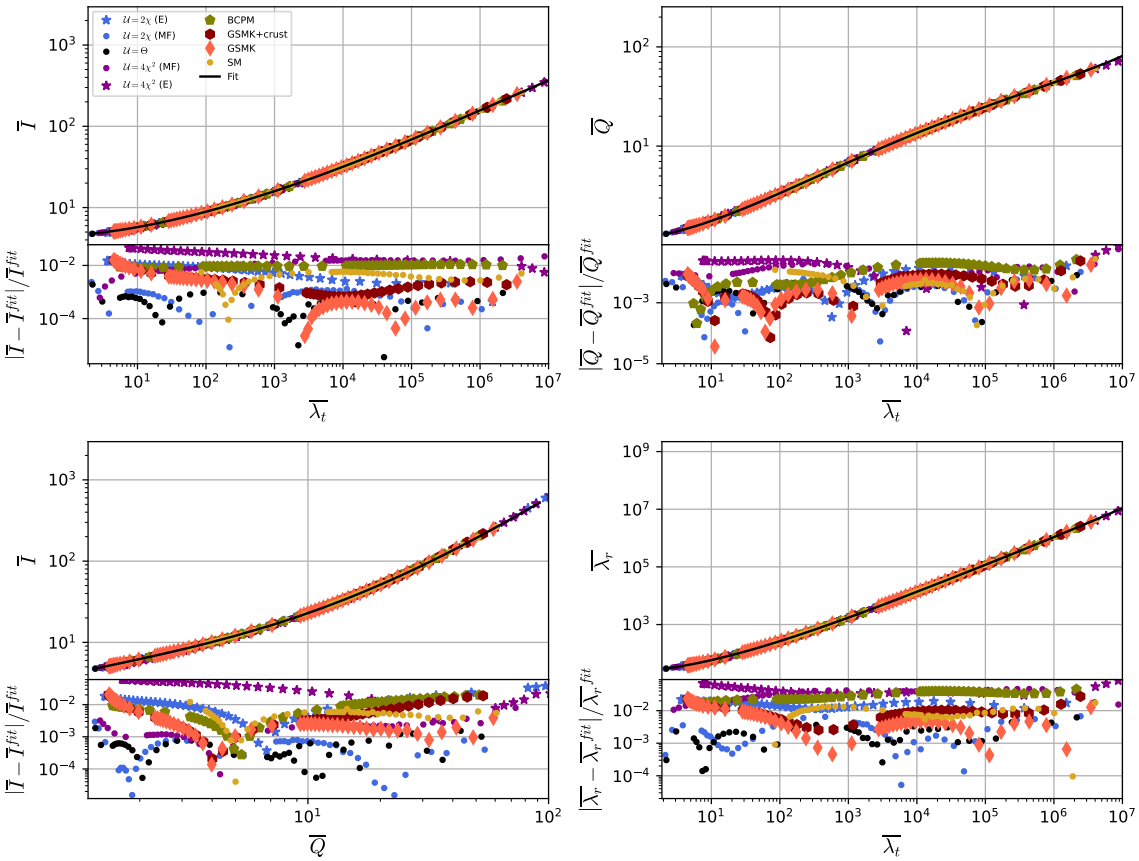

Figure 4.2: I-Love-Q relations and relation between the rotationally induced and tidally induced deformabilities for different Skyrme models, both the exact and mean field solutions. The black line corresponds to the numerical fit obtained in [YY13b].

relations were approximately derived analytically in [JY20], as well as a possible explanation for these relations, in terms of the behavior of the energy density in the star interior. It turns out that these relations, as opposed to the *I-Love-Q* relations, are not universally satisfied for all the models we have considered. Indeed, from fig. 4.4 it can be seen that the relation between I, Q and C generally splits into two branches, corresponding to usual neutron stars and incompressible stars. This is consistent with the findings of [JY20]. However, we also find that, although the mean field version of the BPS models does lie in the incompressible star branch, the exactly solved cases behave quite differently. Whereas the behavior of the 2χ- BPS model is better adjusted by the NS branch, the $4\chi^2-$ BPS model does not fit in neither branch. This behavior can be traced back to the radial dependence of the energy density in each model. Indeed, from fig. 4.6 we can see that the mean field approximation is not good in order to describe the low-density regime of neutron stars within the BPS Skyrme models in general, which translates into very different behaviors of the *I-Love-C* relations for these models. Indeed, it is clear from this figure that the mean field approach overestimates the energy density of the stars in the outer regions.

Furthermore, the energy density profile for the different BPS models highly depends on the chosen potential. For example, while the θ-potential yields almost incompressible

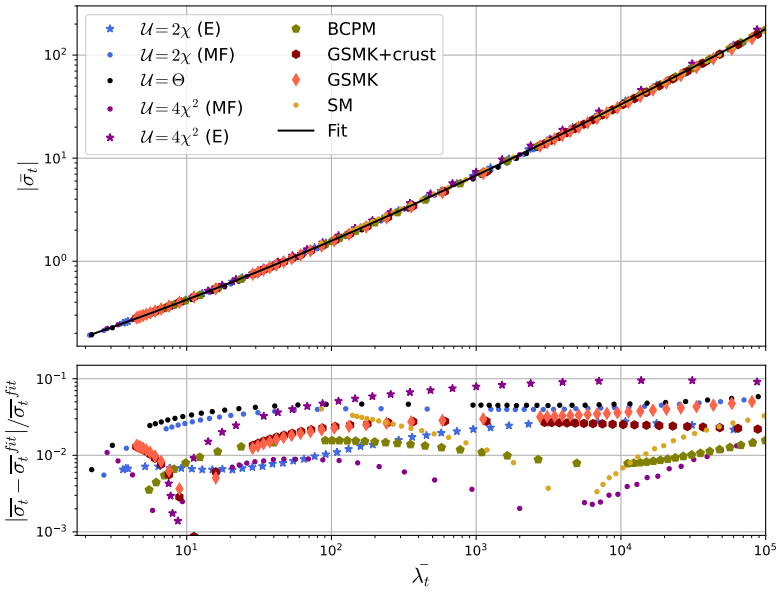

Figure 4.3: Quasi-universal relation between electric and magnetic quadrupolar deformabilities.

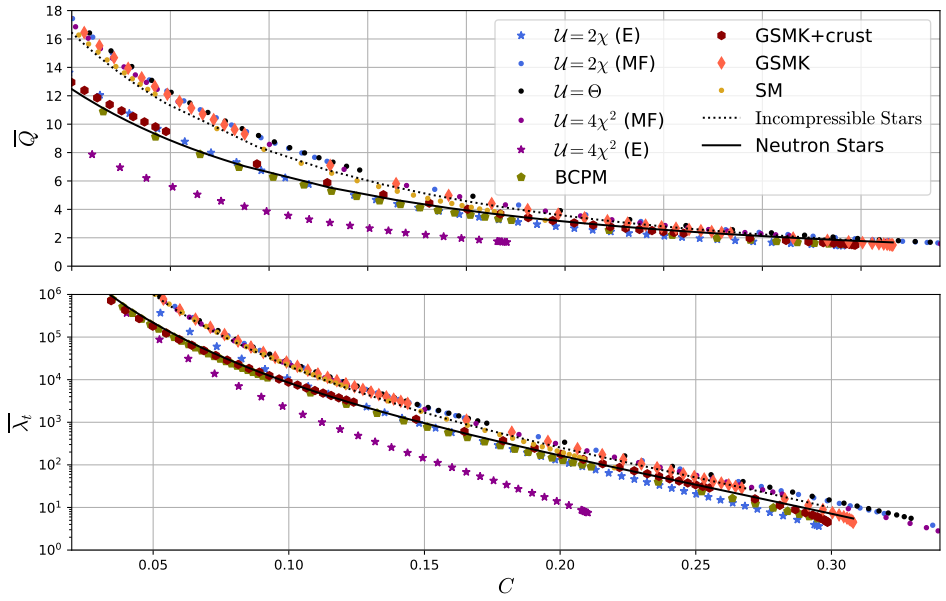

Figure 4.4: Relations of the dimensionless quadrupolar moment and electric quadrupolar Love number with compactness.

stars, the 2χ-potential curve can be well approximated by a quadratic function. This quadratic behavior is in fact expected for realistic neutron stars, whilst the behavior of the density profile for the $4\chi^2$-model is actually more similar to that of white dwarfs [JY20]. Indeed, as we have seen in figs. 4.4 and 4.5, the (exact) 2χ- BPS model *I-Love-C* relations are very close to the NS fit from [JY20].

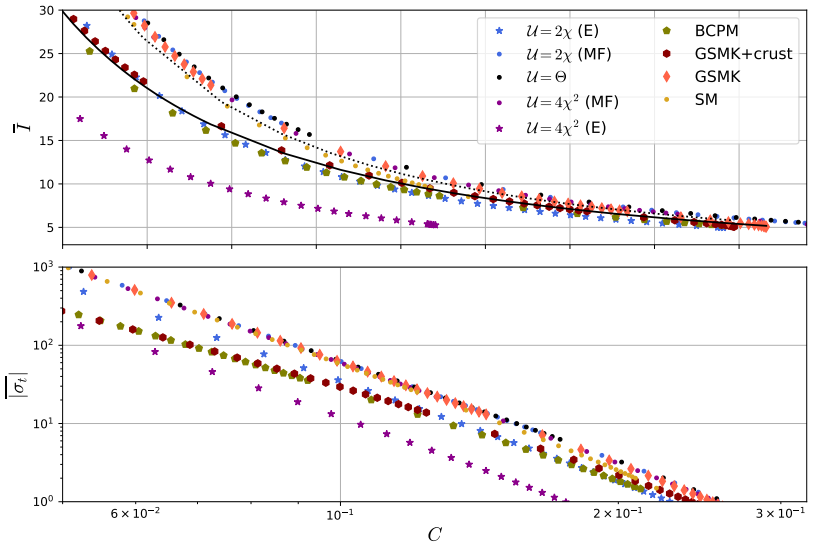

Figure 4.5: Relations of the dimensionless moment of inertia and magnetic quadrupolar Love number with compactness.

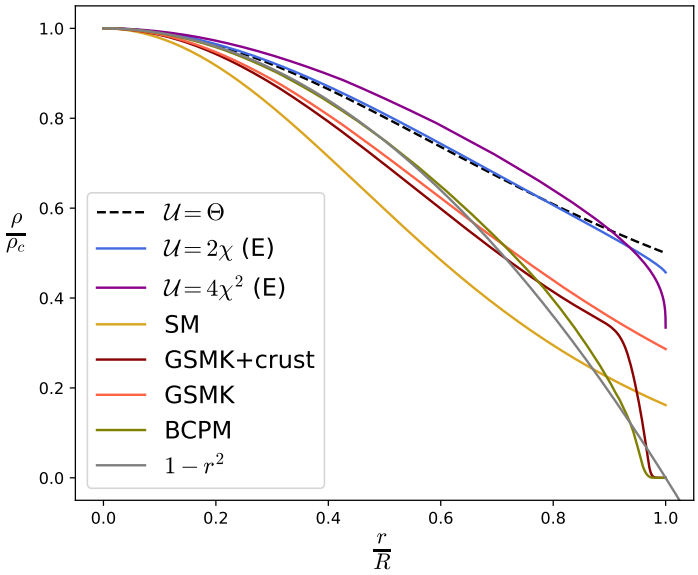

Figure 4.6: Normalized energy density profiles of Skyrme stars with nearly maximum mass for different models. We include the nuclear based EOS BCPM, as well as the quadratic curve $1 - r^2$.

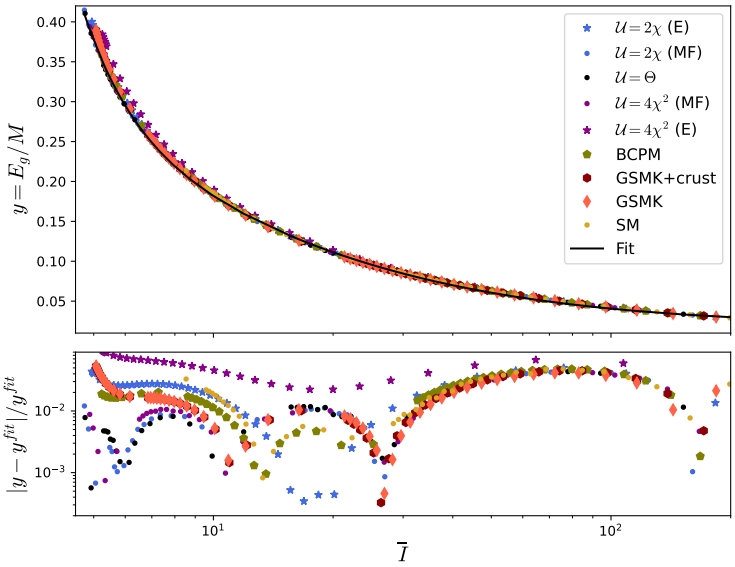

Figure 4.7: Relation between the adimensional moment of inertia and normalized gravitational binding energy.

4.4.3 Gravitational binding energy relations

A different set of quasi-universal relations involving the static gravitational binding energy and other global properties of neutron star solutions have been recently proposed in [JWC19]. For instance, we show in fig. 4.7 the universal behavior of the static gravitational binding energy normalized to the TOV mass and plotted against the adimensional moment of inertia. From the error plot one can see that all models follow the same universal behavior with a deviation of $\lesssim 5\%$ (but the exact $4\chi^2$ BPS model, in which case the error is as high as ten percent) with respect to the numerical fit obtained in [JWC19]. Further, the rotation of the star has measurable effects both in the gravitational and proper mass of the star. Indeed, as we have seen, the gravitational mass of the star receives a correction δM, the dimensionless version of which, $\overline{\delta M} = \delta M \times M^3/J^2$, was also shown in [Rei+17] to satisfy a universal relation when plotted against the (dimensionless) tidal deformability. We show this relation in fig. 4.8, together with the numerical fit of [Rei+17] obtained for the region $\overline{\lambda_t} < 10^3$, at which the deviation for all models is less than ten percent.

On the other hand, the gravitational binding energy will also get a second order correction, namely, δE_g. Remarkably, as opposing to its zeroth-order counterpart, the correction to the gravitational binding energy does not seem to follow a simple, quasi-universal relation. Since the correction to the gravitational mass indeed does follow a relation as shown in fig. 4.8, the non-universal nature of δE_g can be traced back to the correction to the proper mass δM_p, which involves an integral over the star, see (4.86). In fig. 4.9 we show the behavior of $\overline{\delta M_p} = \delta M_p \times M^4/J^2$ with the proper mass of the static solution, M_p^*. From this figure a curve describing a quasi-universal behavior may be inferred, which corresponds to the numerical fit we have obtained. However, this behavior has not the same universality as others previousy analyzed, as the deviation can grow up to 30% for realistic masses.

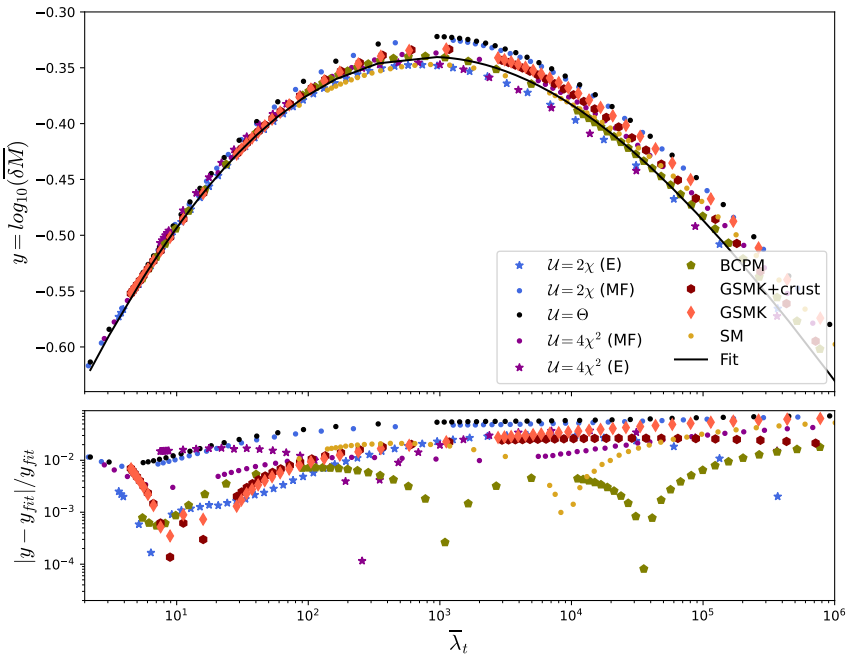

Figure 4.8: Quasi-universal relation for the (dimensionless) gravitational mass correction δM, and normalized deviation from the fitted relation of [Rei+17].

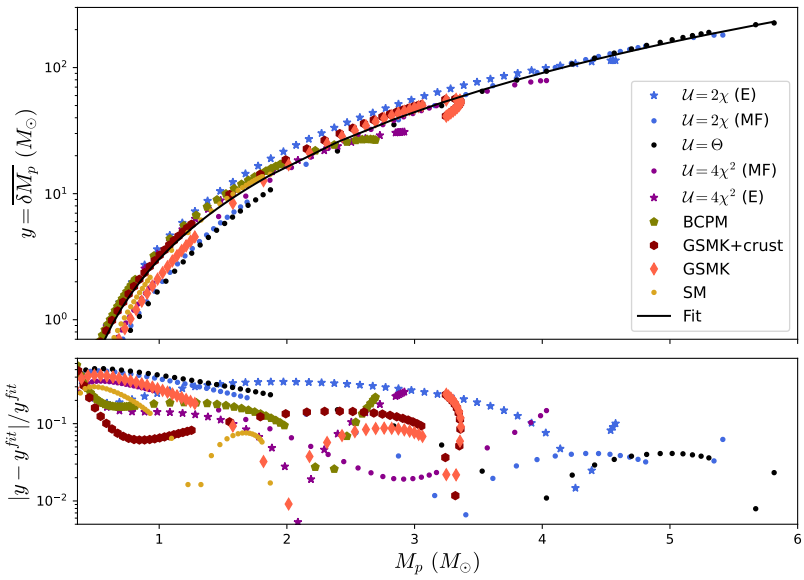

Figure 4.9: Normalized second order proper mass correction versus static proper mass

4.5 Deformability constraints from observations

In addition of constituting an outstanding experimental confirmation of the validity of General Relativity, the direct observation of gravitational waves can be used to place direct constraints on the neutron star EOS (see [LEC20; Gre+20; Cha20] for a recent review of nuclear EOS constraints from GW observations). Indeed, the waveform produced by the coalescence of two realistic extended bodies deviates significantly from a point-particle waveform and thus this difference can be observed with Advanced LIGO. The degree of the deviation, in the case of binary neutron star mergers, depends on the underlying EoS. Although the magnitude of the deviation is strongest at later times in the inspiral and during the merger, Flanagan and Hinderer found that the early phase of the inspiral depends mostly on the tidal Love number of the neutron stars, introducing a phase shift with respect to the point-particle waveform [Hin+10].

However, the individual Love numbers for each component of the merger cannot be separately distinguished in the observed gravitational waveform. Instead, what can be sharply measured is the so-called effective tidal deformability, $\tilde{\Lambda}$ a mass-weighted average of the dimensionless deformabilities $\tilde{\lambda}_1$ and $\tilde{\lambda}_2$ of both components (with masses m_1 and m_2), given by

$$\tilde{\Lambda} \equiv \frac{16}{13} \frac{(m_1 + 12m_2)\, m_1^4 \lambda_1 + (m_2 + 12m_1)\, m_2^4 \lambda_2}{(m_1 + m_2)^5}. \tag{4.117}$$

Similarly, the two component masses are not measured directly. Instead, it is the chirp mass,

$$M_c = \frac{(m_1 m_2)^{3/5}}{(m_1 + m_2)^{1/5}} = m_1 \frac{q^{3/5}}{(1+q)^{1/5}}, \tag{4.118}$$

where $q = m_1/m_2$ is the mass ratio, what can actually be constrained. In the case of the GW170817 event, the chirp mass was measured to be $1.188^{+0.004}_{-0.002}$ at the 90% confidence level. Moreover, within the same confidence level, the mass ratio was found to be in the range $0.7 - 1$, and the effective tidal deformability to be smaller than 800 [Abb+17].

Such such measurements of the NS properties can be used to further reduce the set of Skyrme models able to reproduce physically realistic NS solutions and impose some constraints on the possible values of the free parameters of these models. Indeed, once the equations for the tidally deformed stars of section 4.3 are solved for a specific model, we may obtain the dimensionless tidal deformability of stars described by this model as a function of their TOV mass, so that $\tilde{\Lambda}$ may be seen as a function of both m_1 and m_2, or, equivalently, of M_c and q. On the other hand, since the chirp mass of the binary progenitor of GW170817 is well measured, for any given EOS the effective deformability reduces to a simple EOS-dependent function of the mass ratio.

In fig. 4.10 we show the effective tidal deformability as a function of the mass ratio for a chirp mass of 1.19 $M_\odot$ for different Skyrme models, together with the constraints from the GW170817 event. It is clear from this figure that, as we have already argued, the mean field approximation is not suitable for describing the low energy region of BPS stars, which makes the most relevant contribution to the deformability of the stars. Indeed, this approximation overestimates the values of effective deformability by at least a factor of ~ 2. In addition, we see again that the exact BPS Skyrme models present very different

behaviors —in this case, different values of $\tilde{\Lambda}$— depending on the chosen potential. For example, the contribution from the Θ potential is clearly too big as compared with the GW observation, which sets an upper value of $\tilde{\Lambda} \leq 800$, whereas the 2χ potential yields very large $\tilde{\lambda}$, near the upper value, although still allowed by the bound). On the other hand, we find that both the GSM (without crust) and the hybrid EOS provide very similar values of the tidal deformability, which comes out a bit too big than what has been measured. This may signal that the GSM produces an EOS that is too stiff at intermediate densities (which could be expected from the fact that the compression modulus at saturation comes out too big, see the discussion in chapter 3). Nevertheless, further constrains on these properties coming from GW observations are necessary to definitively rule out these EOS.

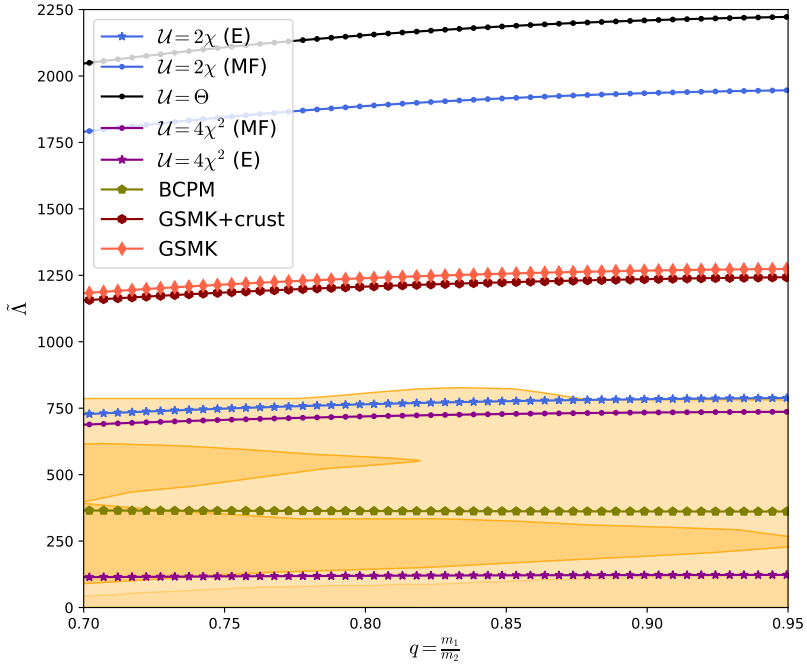

Figure 4.10: Effective tidal deformability versus mass ratio of the two merging stars.

Indeed, it is likely that additional observations of gravitational waves from binary NS mergers will further constrain the tidal deformability of these compact stars. In particular, some recently observed GW events [Abb+20a; Abb+20b] strongly suggest that highly massive NS and compact objects within the NS-Black Hole mass gap (around $2.5\,M_\odot$) could exist.

However, it is difficult to distinguish between an extremely massive neutron star and a small black hole from the GW waveform alone with first generation GW detectors, since the tidal deformability and quadrupole moment of such massive stars is usually very low due to their high compactness, and almost no realistic EOS is able to produce stars with such big mass.

In fig. 4.11, we show the dimensionless moment of inertia, quadrupolar moment and tidal deformability of all the Skyrme models as well as for the BCPM EOS. These plots show that not only high mass NS solutions can be found for any BPS Skyrme model (as well as for the generalized and the hybrid EOS). We also find that, depending on the potential, these parameters can acquire sufficiently high values to be able to be

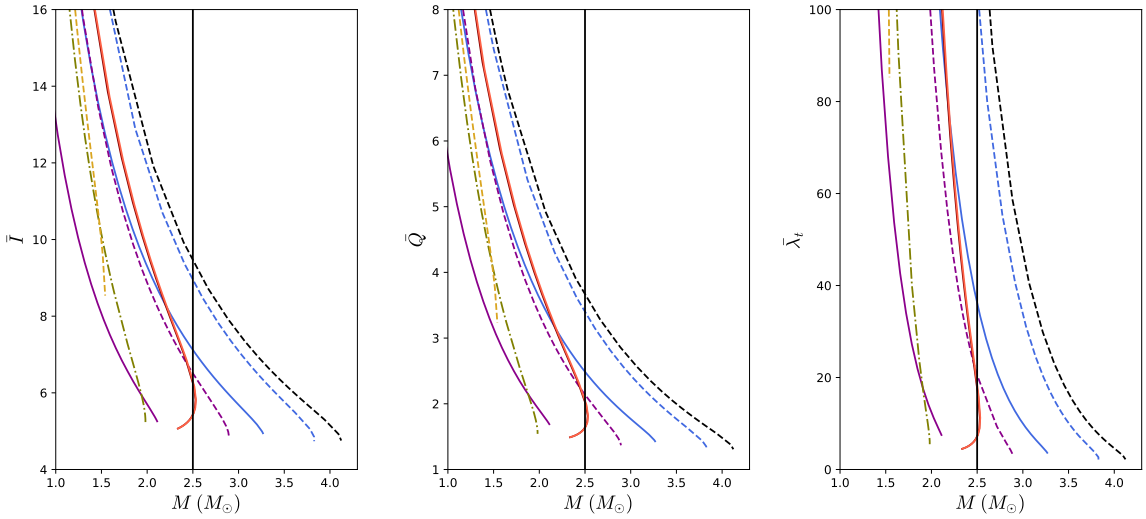

Figure 4.11: Dimensionless moment of inertia, quadrupolar moment and tidal deformability versus mass of stars for different models and EoS

measured by current generation GW observatories. Therefore, we conclude that if the tidal deformability of a mass-gap compact object were measured to be non-zero, it is very likely that its EOS will be well approximated by a BPS Skyrme model and/or by the hybrid model we have presented, which approaches the BPS behavior at high densities.

4.6 Final remarks

In this final chapter, we have solved the Einstein equations using the Hartle-Thorne perturbative formalism to find slowly rotating NS solutions with nuclear and Skyrme model-based EOS. Moreover, we have presented perturbative solutions to the Einstein-BPS Skyrme system describing slowly rotating and tidally deformed, self-gravitating solitons which can also be considered as idealized models for Neutron Stars. For all these models, we have computed different global properties of the corresponding star configurations, such as the moments of inertia, quadrupole moments, gravitational masses or binding energies, and checked whether or not all the models satisfy some (quasi-)universal relations previously proposed in the literature. As we have found, the *I-Love-Q* relations presented in [YY13b] are satisfied up to a $\sim 2\%$ error, even for the exact, non-barotropic BPS Skyrme models, which reaffirms the universality of these relations. Other relations involving the second-order correction to the gravitational mass (including the correction proposed in [Rei+17]) and those involving the (gravitational) binding energy are also quite well satisfied for all models at hand.

On the other hand, we have found that while the *I-Love-C* quasi-universal relations still hold for the mean-field BPS and Skyrme-based EOS, these relations break up for the exact BPS Skyrme models. This fact, as argued, can be traced back to the behavior of the energy density profiles of the solutions for such models, which strongly depends on the particular potential chosen due to the non-barotropic nature of these models. This finding is consistent with the explanation given in [Yag+14] about the difference in nature

between these relations and the *I-Love-Q*. Furthermore, a remarkable property of the solutions based on generalized Skyrme models is that very high masses (of approximately $2.5M_{\odot}$) can be reached even for not too large energy densities at the center of the stars. In other words, such massive stars can be produced from mesonic degrees of freedom alone without the need of additional degrees of freedom such as unconfined quarks. This is consistent with the assumption that the Skyrme model is a valid approximation for the description of matter at the core of a NS, which, if true, implies that the pressure and density reached at NS cores are still far from the energy density regimes in which perturbative QCD becomes relevant.

Although some recent GW events can be seen as possible evidence that such massive stars may exist, additional observations are required to further clarify the detailed properties of massive NS cores.

We conclude by summarizing the main results of this chapter:

- We find that a hybrid EOS, in which the generalized Skyrme model is complemented by a standard nuclear physics EOS for low densities, is compatible with current observational constraints of static NS observables and allows to reach maximum masses that enter the mass gap (around $2.5\,M_{\odot}$). However, other observables such as the tidal deformation come out a bit too big than expected, due to the big stiffness of these EOS at intermediate densities. As argued, this is related to another one of the main open probles in the Skyrme model approach to nuclear matter: the compressibility problem. Nevertheless, additional GW observations are necessary to impose further constraints on the deformability of neutron stars, which are expected to happen in the next observing run (O4) of LIGO.

- We verify (quasi-)universal relations, like *I-Love-Q*, for a broad range of models, based on the minimal Skyrme model, the BPS Skyrme model with a variety of potentials, the generalized Skyrme model, and the hybrid model, respectively. In particular, the BPS Skyrme model also allows for an exact field-theoretic treatment (beyond mean-field theory), because it represents a non-barotropic perfect fluid.

These results contribute to a deeper understanding of the range of validity of these relations, because we investigate them for qualitatively different models not considered previously in the literature.

Summary, conclusions and outlook

In this final chapter, we briefly summarize the main results of this thesis, and state the conclusions that we have drawn from them, as well as an overall picture of possible further work scenarios.

Summary

This thesis is devoted to the study of the physics of strongly interacting matter, namely, that whose dynamics is mainly governed by the strong nuclear force, albeit the effects of other fundamental interactions such as the electromagnetic and/or weak nuclear forces play a decisive role in some processes, such as nuclear flavor-changing decays or β-equilibrium of nuclear matter at high densities.

Therefore, a unified description of nucleons, nuclei and nuclear matter and the strong interactions between them, as well as the effects of other fundamental interactions over them is crucial to the understanding of a plethora of physical processes in a very wide range of densities. This includes not only the phenomenology of light nuclei: their ground and excited states, as well as transitions between them, but also the shape of the equation of state of ultra-dense matter inside neutron stars, which ultimately will determine their properties, for instance, the relation between their mass and radius.

However, this ambitious goal gets truncated due to the properties of quantum chromodynamics (QCD), the quantum field theory that describes the underlying degrees of freedom of strong interactions, i.e. quarks and gluons. Indeed, the fact that the relevant degrees of freedom for nuclear matter (namely, baryons and mesons) appear only as a byproduct of chiral symmetry breaking at low energies, and their dynamics is completely governed by nonperturbative aspects of QCD, renders a first-principles description of the dynamics of strongly interacting matter extremely hard in practice, and thus other methods such as effective field theories or phenomenological models must be used.

Concretely, in this thesis we choose to approach the problem from the Skyrme model perspective. The Skyrme model is a phenomenological, relativistic field theory first proposed by Tony Skyrme in the 60s [Sky61], whose principal feature is that both baryonic and mesonic degrees of freedom are described by a single $SU(2)$-valued field (also known as chiral field), and its dynamics is given by a Lorentz and chirally symmetric Lagrangian that includes a nonlinear interaction term (quartic in derivatives of the chiral field). In this model, mesons are parametrized as the perturbative degrees of freedom, describing the small fluctuations around the vacuum state in terms of three pseudo Nambu-Goldstone scalar fields, the pions, originated after the spontaneous symmetry breaking of chiral symmetry to the residual isospin symmetry. On the other hand, baryons and their bound states (nuclei) are described as non-perturbative, solitonic states: field configurations with

a localized energy density and a nontrivial inner structure, that minimize the energy subject to some boundary conditions. The solitons in the Skyrme model are topological: they can be characterized in terms of the topological degree of mappings between three-spheres. Therefore, they carry a topological charge that is conserved under evolution, which can be identified with the baryon number. These topological solitons are called Skyrmions, and, together with their interactions, conform the main objects of study of the present work.

The main results of this thesis are divided into two principal categories, namely, the physics of light nuclei, and the physics of dense nuclear matter and neutron stars, both studied from the same starting point: the generalized Skyrme model (GSM) Lagrangian. It generalizes the one initially introduced by Skyrme in the sense that two additional interaction terms are included. The first one accounts for the fact that pions (the mesons in the $SU(2)$ effective theory) are massive. The other term is a self-interaction term wich is of sextic order in derivatives (the only one that still allows for a well defined Hamiltonian evolution), and can be interpreted as coming from integrating out the ω mesons of an underlying chiral effective theory, resulting in a repulsive interaction term that has been shown to be very relevant for describing nuclear matter at high densities.

Therefore, in the first chapter of the thesis we carefully review the procedure of obtaining nuclear states from the Skyrme model. To do so, in the first place one needs to obtain classical Skyrmion configurations via the minimization of the corresponding static energy functional. Further, one needs to identify the corresponding zero modes (each associated to a symmetry transformation of the Skyrmion solution), and canonically-quantize them via promoting the associated collective coordinates to quantum mechanical operators. This is a well defined procedure, called rigid-rotor quantization, that allows to define a physical Hilbert space of common eigenstates of spatial momentum, spin and isospin angular momentum operators by means of the Finkelstein-Rubinstein constraints that select, among all the kinematically possible states, those which implement the symmetries of the classical solution.

Once the physically-allowed nuclear states have been identified on each topological sector, many different nuclear observables may be computed within the Skyrme model approach. Apart from the quantum correction to classical energies coming from spin and isospin quantum numbers, especially relevant are those observables that make a direct contribution to any kind of nuclear transition matrix element. In the case of nucleons, these are the so-called form factors, which parametrize the strength of the coupling between the nucleon to some other external current. Indeed, we devote chapter 2 of the thesis to review and, in some cases, extend, the existent theoretical formalism for the computation of electromagnetic, weak and gravitational form factors for nucleons but also for nuclei.

Concretely, an interesting application is the computation of the multipolar operators associated to the $V-A$ nuclear current, because they play a fundamental role in the β-decay transition rates of nuclei. Indeed, some nuclei are stable under strong nuclear forces, but decay via weak-mediated processes that involve the β -decay or electron capture of a neutron (or proton) inside the nucleus. In section 2.2.2 we describe in detail the procedure for obtaining explicit expressions for each of these multipole operators in terms of integrals of local densities depending on the Skyrme field, assuming only the rigid rotor quantization and that the decay is mediated by the emission (and decay) of a single gauge boson, at

tree level in perturbation theory.

In addition, other properties of light nuclei are also computed in chapter 2 for the first time in the Skyrme model. An example of these is the D term, an intrinsic property of all nuclei that is related to the stress-energy tensor form factors, concretely, to its traceless part, in the zero momentum transfer limit. The form factors associated to the energy-momentum tensor are collectively known as gravitational form factors (GFFs). Amongst all of the different interactions between nuclei and other fundamental particles, the gravitational force is the hardest to measure as it is the weakest in nuclear processes. For this reason, the GFFs of nuclei are poorly known experimentally as compared to the electromagnetic or weak form factors. Nevertheless, their knowledge (even if qualitative) is essential to uncover the distribution of pressure and energy densities inside nuclei, and, in particular, to shed some light into the so called *trace anomaly*, a non-perturbative, purely quantum effect in which the stress-energy tensor of QCD develops a non-zero trace (even in the chiral limit of massless quarks), and which is thought to be the responsible of generating the largest contribution to the masses of baryons (and nuclei). In the Skyrme model, the effects of the trace anomaly are naturally implemented by construction (as nucleons are massive also in the chiral limit), but in terms of pionic self-interactions (instead of gluonic), and thus it can be a useful tool to study the effects induced by the trace anomaly on the structure of nucleons and nuclei.

Finally, charge densities and radii of small nuclei are also interesting observables that store information about the inner structure of nuclei and the distribution of strong forces within them. These are intrinsically related to electromagnetic form factors, and, as oposed to GFFs, they are more experimentally acessible, so they can be used to benchmark the predictive power of the model, or as fitting observables to fix the values of the free parameters. In any of the cases, their computation is important, so we present the general procedure to compute even in the nonzero isospin case, in which the details of the particular quantum state become relevant. For larger nuclei, however, the relevant observable is the neutron skin thickness (which measures the excess density of neutrons than that of protons, and is related to the isospin-breaking effects of nuclear strong forces). We present an approximation to compute such observable in the Skyrme model that does not rely on the specific quantum state but only in terms of the moments of classical currents.

On the other hand, a natural question that arises is whether the same methods that we have made use for studying light nuclei can be applied to investigate the phenomenology of nuclear matter at finite densities, which is much less known due to the extreme conditions needed for its experimental study. Thus, in the third chapter of the thesis we focus on this interesting idea, with the final goal of obtaining an Equation of State (EOS) that effectively describes the relation between energy and density of nuclear matter.

In the Skyrme model, infinite nuclear matter can be modelled as a periodic field configuration, an example of which was first found by Klebanov [Kle85]. Such configurations are known as Skyrmion crystals, which minimize the Skyrme energy functional on a three-torus (i.e. subject to periodic boundary conditions on the three spatial directions over a compact, cubic spatial region –the unit cell–) of size L, for sufficiently small values of L, and with finite baryon charge $B = 4$ per unit cell. In fact, the classical energy of the crystal depends on the size of its unit cell, and the curve $E(L)$ presents a minimum at a given $L = L_0$. Hence, this minimum corresponds to the equilibrium configuration of the crystal at zero pressure, and thus it can be identified with the saturation point of

infinite, symmetric nuclear matter. This identification, together with the standard thermodynamical definitions of pressure, baryon and energy densities that can be obtained from the $E(L)$ curve, allow to compute several properties of the Skyrmion crystal as a function of density (or, equivalently, the lattice length), in order to make predictions for nuclear matter at saturation and supra-saturation densities. In order to do so, we first fit the free parameters of the model to some observables at saturation, (for example, the binding energy and baryon density), and then their values are completely determined at any other (higher) density.

On the other hand, the effects of isospin asymmetry (namely, the asymmetry between the number of protons and neutrons) must be taken into account if one is interested in describing physically realistic nuclear matter. In the Skyrme model, this is achieved by quantizing the isospin degrees of freedom. For the case of Skyrmion crystals, we show in chapter 3 that canonically quantizing the isospin of each unit cell, together with a mean field approximation of the isospin density per unit cell, yields a well defined procedure to determine observables such as the symmetry energy or, when the effects of Coulomb and weak interactions are taken into account, the proton fraction of β-equilibrated asymmetric nuclear matter. Furthermore, it is expected that, at sufficiently high densities, the degeneracy and isospin pressures are so high that the usually stable phases of matter become unstable, and exotic states may appear to relieve these pressures, reducing the global energy. For example, the appearance of hyperons (baryonic states with nonzero strangeness) is expected in standard approaches to nuclear matter at around two or three times nuclear saturation density. In order to account for this effect in the Skyrme model, one needs to extend the $SU(2)$ flavor group manifold into the $SU(3)$ case. We explicitly show how to to this in the second part of chapter 3, using the Callan-Klebanov parametrization of strange degrees of freedom. After extending the formalism of isospin quantization to the $SU(3)$ case, we analyze the possibility of a phase transition to a nonzero vacuum expectation value of kaon fields (the lightest meson states with nonzero strangeness), which is usually called a kaon condensate. Moreover, we find that this transition does indeed take place at around 2.3 times nuclear saturation, for a given choice of the parameters that is physically well-motivated. Taking all the above considerations into account, our analysis of Skyrmion crystals allows to obtain a realistic EOS for isospin-asymmetric nuclear matter at saturation and supra-saturation, and the question remains wether it reproduces any of the known properties of neutron stars that are currently well measured.

Therefore, in chapter 4, we focus on obtaining neutron star solutions to the Einstein field equations sourced by a perfect fluid with Skyrme model-based EOS. We consider different cases, mainly the GSM but also the BPS submodel, due to its nice properties. Indeed, the BPS model, which includes only the effects of the potential and sextic terms in the GSM Lagrangian, can be understood as a non-barotropic perfect fluid, that can be exactly solved in the spherically symmetric, static case. The use of this model is justified as the limiting case of ultra-high density, as the sextic term becomes the most relevant term in the GSM Lagrangian, and thus it can be understood as a model of ultracompact neutron stars, in whose interiors matter can reach densities of several times the nuclear saturation density.

We thus solve the Tolman-Oppenheimer-Volkov system of equations in order to obtain the mass-radius curves associated to each one of the models we have considered, resulting in maximal masses of $2.5\,M_\odot$ or even higher. We go further and study the case of slowly

rotating stars, in order to be able to obtain additional, dynamical observables such as quadrupole moment. This is a well known perturbative procedure, via the Hartle-Thorne (slow rotation) approximation, in which the metric is expanded in powers of the spin parameter, which is interpreted as the angular frequency of rotation of a distant observer. The Einstein equations are then solved perturbatively, at each order up to second order in the angular frequency, both in the interior and exterior of the star, and the interior and exterior metric functions must be matched, which in turn allows to obtain information about the interior (such as the mass, angular momentum or quadrupolar moment) of the star from the asymptotic expansion of the exterior metric. A very similar perturbative analysis can be made for tidally deformed stars, in which the metric perturbations now come from an external tidal field (for example due to a companion star or black hole in a binary system). Again, one first perturbatively solves Einstein's equations both inside and outside the star, which have the same form as in the slow rotation case at second order. The quadrupolar deformation due to tidal forces can then be extracted from the exterior solution. This determines the tidal deformability, or (quadrupolar) Love number, as (minus) the ratio between the quadrupolar moment of the star and the quadrupolar moment of the tidal gravitational field, $\lambda = -Q/\mathcal{E}$. Therefore, it contains information about the stiffness of the EOS of the star in terms of its strain response to a quadrupolar gravitational force. Furthermore, the definition of Love numbers can be extended to other multipoles of the gravitational field, both of electric and magnetic type.

The extension of previous works on Skyrmion stars [Nay19] to include the effects of small rotations and tidal deformations allows to enlarge the set of observable quantities that can be compared to actual measurements. Owing to the increasing number of observed GW events in recent years (and the ones estimated to be detected in the current observing run, with improved sensibility), those observables that can be inferred from the waveform of a GW produced at a binary NS (or NS-Black Hole) coalescence are of particular interest. An example is the (effective) tidal deformability of the binary, which, together with the quasi-universal relations, allows to constrain the EOS of strongly interacting matter in the extremely high density regime.

Therefore, to conclude this analysis, we study the presence of universal (and quasi-universal) relations between different sets of observables obtained in this perturbative approach. An example of these universal relations are the well known $I - Love - Q$ relations [YY13b] between the moment of inertia, quadrupole moment and tidal deformability (or Love number). Such relations are universal, in the sense that they are satisfied independently of the particular EOS used to describe the matter content in the Einstein equations, up to an error of $\sim 1\%$. We also study other relations that are also universal, such as the relation between the electric and magnetic quadrupolar Love numbers, or that of the moment of inertia and the gravitational binding energy. These relations are important from a phenomenological point of view, since they allow to partially break the degeneracy between some NS properties in the waveforms of binary inspirals, but also very interesting at a fundamental level, as the ultimate reason for their appearance is still not well understood. Furthermore, being insensitive to the details of the matter content of the stars, these relations may be thought of as genuine predictions for the structure of compact stars in General Relativity, and studying deviations from them could allow to explore other fundamental theories of gravity. With our analysis, we aim to contribute to the understanding of such universal relations, as we show that they are also satisfied even

in the case of non-barotropic perfect fluids, and thus the current experimental bounds on NS deformabilities can be well accounted for within the Skyrme model.

Conclusions and outlook

The results obtained in the present thesis have allowed us to sketch a general picture of the state of the art of theoretical nuclear physics in the solitonic approach, from which several different conclusions may be drawn.

In the first place, the Skyrme model, understood as a very simple phenomenological model for the description of nuclear dynamics, allows for a qualitative, and in some cases even quantitative, understanding of a wide range of different low-energy nuclear properties in terms of the (quantized) zero-mode degrees of freedom of topological solitons and their interactions with external sources.

An interesting feature of this model, that is shared with other similar chiral soliton approaches, is the fact that, when considering nuclei as semi-classical states, the spatial (local) currents and densities are straightforwardly determined by the classical solutions of some differential equations. These are, in general, much easier to solve numerically than the equivalent matrix elements involving a complicated many-body wavefunction in the fully quantum-mechanical problem. In practice, this means that some observables, such as form factors, of large B nuclei are very easily obtained in the Skyrme model as compared with other theoretical nuclear models. Even though these computations rely on the semi-classical rigid rotor approximation (which is not well-justified for large baryon number solutions), the dependence of some properties that are not even well measured (for example, the D term computed in this thesis) with the baryon charge may be determined as an estimation of the order of magnitude. Our principal goal in the first part of the thesis has been to provide a broad picture of the available methods for the computation of all the different nuclear observables mentioned above. However, once the methodology and formalism are established, a careful analysis of these properties, trying to find a global fitting of the parameters that provides reasonably good values for them, is in order. Due to its striking simplicity (as compared to other nuclear phenomenological models), the generalized Skyrme model presented in this thesis may not be able to predict the values of the experimentally measured quantities, such as masses and charge radii of light nuclei, as accurately as other, more involved models. Indeed, the computations performed in this thesis, as well as previous attempts to determine some of these quantities have confirmed that the Skyrme model, or some simple generalizations of it, cannot reliably predict the measured properties of medium mass nuclei with high precission.

However, it is fascinating that nuclear properties, including not only nuclear states and masses, but also charge densities and form factors of all kinds, can be computed to a certain degree of precission from such a simple idea: a semi-classical soliton of a nonlinear scalar field theory. Therefore, it is our hope that the results of this thesis may further encourage the search of a soliton-based model that is able to describe nuclear phenomenology with greater accuracy. Some natural extensions of the GSM presented in this thesis that may help towards this goal include the explicit addition of ω and/or ρ vector mesons, both of which have been shown to reduce binding energies as compared to the standard Skyrme model [GS20; NS18b]. It would be interesting to study the effects of these additional fields on other nuclear observables, such as charge radii. Furthermore,

the formalism developed in the first part of this thesis is of general character, and could be in principle applied even outside of the Skyrme model, for example in the context of Holographic QCD, in order to compute, for instance, gravitational form factors or beta decay matrix elements in this kind of models.

On the other hand, even though we present some promising results in the Skyrmion crystal approach to modelling neutron star matter, there are several open questions that deserve further study. Firstly, the ground state of Skyrmionic matter at the intermediate and low density regimes of Skyrmion matter ($n \leq n_0$) is still very poorly known. As argued in chapter 3, it is precisely in such regime where the (residual) nuclear forces become of the same order as the Coulomb repulsive forces, and thus neglecting the latter is not a well justified approximation anymore. Moreover, it is well known from other models of nuclear matter that the competition of these two interactions may result in exotic arrangements of nucleons into what is usually known as "nuclear pasta" phases. Although small, these pasta phases have a non-negligible effect on the NS EOS, and strongly influence the crust-core transition. Thus, a better understanding of this phenomenon is one of the most urgent open problems in the Skyrmionic approach to nuclear matter.

An additional problem regarding the low density regime of Skyrmion crystals is the fact that, in the Skyrme model, the nuclear incompressibility (or equivalently, the compression modulus) is over-estimated by a factor of ~ 4, which translates into an EOS that is too stiff around saturation as compared to experimental data. It seems that this is a feature of the standard Skyrme model, and not of the classical solutions we are considering. Thus, this points also to the necessity of extending the model to consider additional degrees of freedom (for example, vector mesons) that soften the EOS around nuclear saturation. We would like to point out here a recent approach to the description of the low-density regime purely within the Skyrme model, based on a new 'double sheet' solution at low densities [LHW23]. This would eliminate the dependence on an ad-hoc nuclear EOS for lower densities, but the problems concerning the stiffness of the EOS around saturation remain.

Finally, we hope that our results serve as a motivation to explore other regions of the QCD phase diagram in terms of Skyrmion crystals. Indeed, the effects of a nonzero magnetic field on the nuclear matter EOS could in principle follow from the coupling of an external, nondynamical gauge field to the Skyrme field, and considering solutions of the coupled system in the three torus, with the magnetic field strength as an external parameter. Although there is a nontrivial complication when considering gauge fields with periodic boundary conditions (the field configurations will be in general periodic up to a gauge transformation), in principle the basic computational methods should follow straightforwardly from what we have presented in this thesis.

A further generalization of our results would be to include the effect of finite temperatures of the Skyrme crystal, which is more complicated in practice as it becomes necessary to consider the dynamics of perturbations around classical static configurations. Although complicated, the theory of small fluctuations on top of solitonic backgrounds is well known in the literature, and the dynamics of Skyrmion normal and quasi-normal modes was recently studied in [BH18]. A thorough study of normal modes in Skyrmion crystals (which, being a periodic system, should be identified with phonons) would pave the way to the classical solid-state treatment of Skyrmion lattices, and allow the study of phonon dispersion relations, thermal and transport properties, etc.

Resumo en Galego

Esta tese está adicada ao estudo da física da materia fortemente interaccionante, é dicir, aquela na que a dinámica está gobernada pola forza nuclear forte, polo que os efectos das outras interaccións, como a electromagnética e/ou a forza nuclear feble, xogan un papel decisivo nalgúns procesos, tales como o decaemento nuclear por cambio de sabor ou o equilibrio β da materia nuclear a altas densidades.

Polo tanto, unha descrición unificada dos nucleóns, núcleos, materia nuclear e as interaccións fortes entre os anteriores elementos, así como os efectos de outras interaccións fundamentais sobre os mesmos, é esencial co gallo de entender un bo feixe de procesos físicos, para un amplo abano de posibles densidades. Todo isto non inclúe só a fenomenoloxía dos núcleos lixeiros: os estados fundamentais e excitados, así como as transicóns entre os mesmos, senón que tamén dá conta da forma da ecuación de estado (EOS) da materia altamente densa no interior das estrelas de neutróns (NS), o que, en última instancia, determina as propiedades das mesmas, como por exemplo, as relacións entre masas e radios.

Con todo, esta meta tan ambiciosa vese coutada por mor das propiedades da cromodinámica cuántica (QCD), a teoría cuántica de campos que describe os restantes graos de liberdade das interaccións fortes, é dicir, quarks e gluóns. En efecto, o feito de que os graos de liberdade relevantes para a materia (os ben coñecidos barións e mesóns) xurdan tan só como subproduto da ruptura da simetría quiral a baixas enerxías, estando a dinámica completmante gobernada por aspectos non-perturbativos da QCD, leva de seu unha descrición de primeiros principios da dinámica da materia fortemente interactuante, moi complicada na práctica, e polo tanto, é preciso empregar outros métodos tales como teoreías de campo efectivas ou modelos fenomenolóxicos.

Particularmente, nesta tese, emprégase un achegamento ao problema co modelo de Skyrme como marco de referencia. O modelo de Skyrme é unha teoría relativista e fenomenolóxica de campos, proposta por Tony Skyrme nos anos 60 [Sky61], sendo a súa característica principal, que tanto os graos de liberdade barióncos como os mesónicos están descritos por un mesmo campo de $SU(2)$ (tamén coñecido como campo quiral), e a súa dinámica vén dada por un Lagranxiano con simetría quiral e de Lorentz, o cal inclúe un termo de interación nonlineal (cuártico nas derivadas do campo quiral). Neste modelo, os mesóns están parametrizados como os graos de liberdade perturbativos, describindo pequenas flutuacións arredor do estado do baleiro en termos de tres campos pseudo-escalares de Nambu-Goldstone, os pións, orixinados logo da ruptura espontánea da simetría quiral, permanecendo residualmente a simtría de isoespín. Por outra banda, os barións e os correspondentes estados ligados (os núcleos) están descritos como estados solitónicos non perturbativos: configuracións de campo con densidade de enerxía localizada e estrutura interna non trivial, o cal minimiza a enerxía suxeita a unhas certas

condicións de contorno. Os solitóns no modelo de Skyrme son topolóxicos: poden ser caracterizados en termos do grao topolóxico de mapeos entre 3−esferas. Polo tanto, estes levan de si unha carga topolóxica que se conserva baixo evolución, a cal pode ser identificada co número bariónico. Estes solitóns topolóxicos coñécense co nome de Skyrmións, e xunto coas interaccións que levan de man, conforman o obxectivo principal de estudo deste traballo.

Os resultados principais desta tese están divididos en dúas categorías principais, sendo estas, a física dos núcleos lixeiros, e a física da materia nuclear densa e das estrelas de neutróns, ambas partes estudadas dende o mesmo punto de partida: eprengando o Lagranxiano do modelo de Skyrme xeralizado (GSM). Este, xeraliza o modelo inicialmente introducido polo propio Skyrme no sentido de que se engaden dous termos de interacción adicionais. O primeiro dá conta do feito de que os pións (os mesóns na teoría efetiva de $SU(2)$) son masivos. O restante é un termo de auto-interacción, séxtico nas derivadas (o único que permite evolución ben definida do Hamiltoniano), podéndose interpretar que provén da integración efectiva dos mesóns ω, resultando ser un termo de interacción repulsiva. Isto viuse que é importante á hora de describir a materia nuclear a altas densidades.

Así pois, no primeiro capítulo desta tese, farase unha revisión coidadosa do procedemento mediante o cal se obteñen os estados nucleares empregando o modelo de Skyrme. Para facer tal cousa, en primeiro lugar, precísase obter as configuracións clásicas dos Skyrmións, empregando unha minimización do funcional de enerxía correspondente. Ademais, precísase identificar os modos cero correspondentes (cada un, vencellado a unha transformación simétrica da solución de Skyrmión), e logo cuantizalos canonicamente por medio da promoción das coordenadas colectivas asociadas a operadores mecano-cuánticos. Este é un proceso ben definido, coñecido como cuantización do rotor ríxido, o que permite definir un espazo de Hilbert físico de autoestados comúns para os operadores momento espacial, esípn e momento angular de isoespín, isto quere dicir que as ligaduras de Finkelstein-Rubinstein, escollen entre todos os posibles estados cinemáticos, aqueles que implementan as simetrías da solución clásica.

Unha vez que se identifican os estados nucleares físicamente permitidos en cada sector topolóxico, moitos observables nucleares diferentes poden ser calculadaos no marco do modelo de Skyrme. Ademais das correccións cuánticas ás enerxías clásicas, procedentes dos números cuánticos de espín e isoespín, son especialmente relevantes aqueles observables que fan unha contribución directa a calequera clase de elemento de matriz da transicón nuclear. Para o caso dos nucleóns, estes son os ben coñecidos facotres de forma, que parametrizan a forza do acoplamento entre os nucleóns e calquera corrente externa. De feito, adicamos o capítulo 2 da tese a revisar, e nalgúns casos, ampliar, o formalismo teórico existente para a computación de factores de forma electromagnéticos, felbles e gravitatorios, tanto para nucleóns como tamén para núcleos.

En concreto, unha aplicación interesante é a computación dos operadores multipolares asociados á corrente nuclear $V - A$ posto que xogan un papel esencial nos ratios de transicón en decaementos β nucleares. En efecto, algúns núcleos son estables baixo a forzas nucleare fortes, pero decaen mediante procesos mediados pola interacción feble, vía decaemento beta ou captura dun electrón por un neutrón (ou protón) dentro do propio núcleo. Na sección 2.2.2, describimos con detalle o procedemento polo cal obtemos explicitamente as expresións para cada un dos operadores multipolares en termos de

integrais de densidades locais, dependendo do campo de Skyrme, e asumindo únicamente a cuantización do rotor ríxido e que o decamento está mediado pola emisión (e decaemento) dun só bosón de gauge, a nivel árbore na teoría de perturbacións.

Ademais, no capítulo 4, calcúlanse algunhas propiedades por vez primeira, empregando o modelo de Skyrme e para os núcleos lixeiros. Exemplo disto é o D term, unha propiedade intrínseca de todos os núcleos, relacionada cos factores de forma do tensor enerxía-momento, concretamente, coa parte sin traza no límite de nula transferencia de momento. Os factores de forma asociados ao tensor enerxía-momento coñécense en conxunto como factores de forma gravitacionais (GFFs). Entre todas as interaccións distintas que se dan entre núcleos e outras partículas elemnetais, a forza gravitacional é a máis complicada de medir, por mor de ser a máis feble no eido dos procesos nucleares. É este o motivo polo que os GFFs para os núcleos son pouco coñecidos dende un punto de vista experimental, en comparación por exemplo cos seus análogos no eido das interacións electromagnética ou feble. Porén, o coñecemento dos mesmos (ata a nivel cualitativo) é primordial á hora de descubrir a distribución da presión e da densidade de enerxía dentro dos núcleos.

Específicamente, esto permitiría clarexar un pouco o que se coñece como *anomalía da traza*, un efecto puramente cuántico e non perturbativo, no cal o tensor enerxía-momento de QCD, adquire un unha traza non nula (mesmo no límite quiral de quarks sen masa), do que se pensa que é o causante de xerar as maiores contribucións ás masas dos barións (e dos núcleos). No modelo de Skyrme, os efectos da anomalía da traza son implementados de xeito natural por construción (xa que os nucleóns son masivos tamén no límite quiral), pero en termos das auto-interacións piónicas (no canto das gluónicas), o que pode facer disto unha ferramenta útil á hora de estudar os efectos inducidos pola anomalía da traza nas estruturas de nucleóns e núcleos.

Finalmente, as densidades de carga e radios de núcleos pequenos, son observables moi interesantes que agochan información sobre a estrutura interna dos núcleos e da distribucións das forzas fortes entre eles. Estes están relacionados de xeito directo cos factores de forma electromagnéticos, que contrariamente aos GFFs, estes están moito mellor estudados experimentalmente, polo que poden ser empregados como punto de referencia en canto ao poder preditivo do modelo, ou como observables axustables para fixar os valores dos parámetros libres. En calquera dos casos, o cálculo dos mesmos é importante, polo que presentamos o procedemento xeral para obtelos, mesmo para o caso no que o isoespín é distinto de cero, para o cal os detalles do estado cuántico particular vólvense relevantes. Así e todo, para núcleos maiores, o observable relevante é *neutron skin thickness* (esta mide o exceso de densidade neutrónica con relación á protónica, e está relacionada cos efectos da ruptura do isoespín da interación nuclear forte). Presentamos unha aproximación para a computación de tal observable, empregando o modelo de Skyrme, que no canto de basearse nalgún estado cuántico en específico, fundaméntase nos momentos das correntes clásicas.

Por outra banda, está naturalmente xustificado pór en dúbida se os mesmos métodos empregados no estudo dos núcleos lixeiros, poden ser empregados para investigar sobre a fenomenoloxía da materia nuclear a densidades finitas, a cal é moito menos coñecida por mor de seren extremas as condicións necesarias experimentais para tratala. Polo tanto, no terceiro capítulo desta tese, centrámonos nestas interesantes ideas, co gallo de obter unha (EOS) que de xeito efectivo, describa a relación entre a enerxía e a densidade de

materia nuclear.

A materia nucelar infinita, no modelo de Skyrme, pode ser modelada como unha configuración periódica de campo, sendo os traballos de Klebanov os pioneiros neste eido [Kle85]. Tales configuracións coñécense como cristais de Skyrme, e minimizan o funcional da enerxía de Skyrme nun tres-toro (o que se traduce por estar suxeitos a condicións de contorno periódicas nas tres direccións espaciais, sobre unha rexión espacial cúbica e compacta -a cela unidade-) de tamaño L, sendo os valores de L pequenos, e con carga bariónica finita $B = 4$ por cela unidade. De feito, a enerxía clásica do cristal, depende do tamaño da cela unidade, e a curva $E(L)$ presenta un mínimo para un certo $L = L_0$. Este mínimo correspóndese entón coa configuración de equilibrio do cristal, a presión cero, e polo tanto pode ser identificado co punto de saturación da materia nuclear simétirca infinita. Esta identificación, xunto coas definicións termodinámicas habituais das densidades de presión, barións e enerxía, que poden ser obtidas da curva $E(L)$, permite calcular moitas propiedades dos cristais de Skyrme como función da densidade (ou equivalentemente, a lonxitude da malla) co gallo de facer predicións para a materia nuclear nos réximes de densidade de saturación e supra saturación. Co fin de facer isto, primeiramente axustamos os parámetros libres do modelo a algúns observables no punto de saturación (como por exemplo as enerxías de enlace ou a densidade bariónica), quedando logo os seus valores totalmente determinados para calquera outra densidade.

Doutra banda, os efectos da asimetría do isoespín (é dicir, a asimetría entre o número de protóns e neutróns) deben ser tomados en consideración sempre e cando se desexe describir a realidade física da materia nuclear. No modelo de Skyrme, isto lógrase logo de cuantizar os graos de liberdade do isoespín. No capítulo 3, amósase para o caso dos cristais de Skyrme, como a cuantización canónica do isoespín para cada cela, xunto coa aproximación de campo medio da densidade de isoespín por cela unidade, isto leva de man un proceso ben definido para determinar tales observables como a enerxía de simetría, ou tamén, tendo en conta efectos de Coulomb e interacións febles, permite obter a fracción de protóns do equilibrio beta asimétrico da materia nuclear. É máis, agárdase que, para densidades suficientemente altas, a dexeneración e a presión de isoespín son tan elevadas que as fases de materia habitualmente estables, vólvense inestables, e novos e exóticos estados poden aparecer para aliviar a presión, reducindo a enerxía global. Por exemplo, baixo certos tratamentos estándar da materia nuclear, agárdase a aparición de hiperóns (estados bariónicos con extrañeza non nula), arredor dun valor de dúas ou tres veces a densidade de saturación. Para dar conta deste efecto co modelo de Skyrme, precísase expandir a variedade do grupo de sabor de $SU(2)$ ao caso de $SU(3)$. Amosamos explicitamente como facer tal cousa na segunda parte do capítulo 3, empregando a parametrización de Callan-Klebanov dos graos de liberdade con extrañeza. Logo de expandir o formalismo da cuantización do isoespín ao caso de $SU(3)$, analizamos a posibilidade de que haxa unha transición de fase a un baleiro cun valor agardado non nulo para os campos kaónicos (os estados mesónicos máis lixeiros, con extrañeza), coñecéndose isto habitualmente co nome de condensado de kaóns. Ademais, atopamos que esta transición toma lugar para valores arredor de 2.3 veces a saturación nuclear, para unha certa escolla de parámetros, ben motivados físicamente. Tendo o anterior en conta, a análise realizada dos cristais de Skyrmións, permite obter unha EOS realista para a materia nuclear con asimtería de isoespín, nos puntos de saturación e supra-saturación, quedando a cuestión de se con isto se poden reproducir algunhas das propiedades das estrelas de neutróns, hoxe en día

ben medidas e coñecidas. Polo tanto, no capítulo 4, centrámonos en obter solucións de estrelas de neutróns para as ecuacións de campo de Einstein, empregando como fonte, un fluído perfecto con EOS baseada no modelo de Skyrme. Temos en conta diferentes casos, principalmente o GSM pero tamén o submodelo BPS, por mor de posuír este unhas propiedades moi boas. Dende logo, o modelo BPS, o cal inclúe soamente os efectos do potencial e do termo séxtico en termos do Lagranxiano de GSM, pode ser entendido coma un fluído perfecto non-barotrópico, que se pode resolver de xeito exacto no caso esfericamente simétrico e estático. O emprego deste modelo está xustificado como o caso límite para densidades moi altas, xa que o termo séxtico vólvese o máis relevante no Lagranxiano GSM, e polo tanto este pódese entender como un modelo de estrelas de neutróns moi compactas, para as cales a materia no seu interior, chega a acadar densidades varias veces a densidade nuclear de saturación.

Así pois, resolvemos o sistema de ecuacións de Tolman-Oppenheimer-Volkov, co fin de obter as curvas masa-radio asociadas a cada un dos modelos considerados, tendo as masas máis maiores, valores de $2.5\,M_\odot$ ou mesmo máis. Fomos un pouco máis aló no noso estudo, e tratamos o formalismo de rotación lenta para as estrelas, para así obter observables dinámicos adicionais tales como o momento cuadrupolar. Este proceso perturbativo é ben coñecido, empregando a aproximación de pouca rotación de Hartle-Thorne, na cal a métrica é expandida en potencias do parámetro de espín, o cal se pode interpretar como a frecuencia angular de rotación vista por un observador a distancia. As ecuacións de Einstein son entón resoltas perturbativamente, orde a orde, ata a segunda orde na frecuencia angular, tanto no interior coma no exterior da estrela. As funcións da métrica tanto fóra coma dentro da estrela deben empalmar na superficie da mesma, o que permite obter infomración sobre o interior (masa, momento angular, momento cuadrupolar) dende a expansión asintótica da métrica exterior. Unha análise perturbativa semellante, pode facerse para estrelas deformadas por forzas de marea, no cal as perturbacións da métrica teñen agora orixe nunha forza de marea externa (por exemplo por mor dunha estrela acompañante ou dun buraco negro nun sistema binario). De novo, resolvemos primeiramente as ecuacións de Einstein, tanto dentro coma fóra da estrela, de igual xeito ca no caso da rotación lenta, e ata segunda orde. A deformación cuadrupolar debida ás forzas de marea, pódese obter da solución exterior. Isto determina a deformación por marea, ou o número de Love (cuadrupolar) , como (menos) o cociente entre o momento cuadrupolar da estrela e o momento cuadrupolar do campo gravitacional de marea $\lambda = -Q/\mathcal{E}$. Como resultado, esto contén información sobre a rixidez da EOS da estrela, en termos da tensión da resposta á forza cuadrupolar gravitacional. A un tempo, a definición dos números de Love, pode extenderse a outros multipolos do campo gravitacional, tanto de tipo eléctrico como magnético.

A expansión de traballos anteriores a estrelas de Skyrmións [Nay19], incuíndo os efectos por rotacións pequenas e deformacións de marea, permite ampliar o número de cantidades observables que poden ser medidas a día de hoxe. Debido ao aumento de eventos observados nos últimos anos grazas á tecnoloxía das ondas gravitacionais (e os que se agarda medir nos vindeiros tempos, debido á mellora na sensibilidade dos detectores), estes observables que poden ser inferidos empregando a forma da onda dunha GW producida nun sistema binario de NS (ou tamén NS-BH) en coalescencia, son de elevado interese. Un exemplo disto é a deformación de marea (efectiva) dun sistema binario, a cal, en conxunto coas relacións cuasi-universais, permite restrinxir a EOS da materia altamente interaccionante

ao réxime de densidade extremadamente alta.

Xa para ir rematando coa análise, estudamos a existencia de relacións universais (e cuasi-universais) entre distintos conxuntos de observables, obtidos nesta aproximación perturbativa. Exemplo das mesmas son as coñecidas relacións $I - Love - Q$ [YY13b], entre o momento de inercia, momento cuadrupolar e a deformación de marea (ou números de Love). Tales realcións son universais dende que se satisfan independentemente da EOS particular que se empregue para describir o contido de materia nas ecuacións de Einstein, cun marxe de erro baixo o $\sim 1\%$. Tamén estudamos outras relacións que son universais, como as que xorden entre os números de Love eléctricos e magnéticos, ou as existentes entre os momentos de inercia e as enerxías gravitacionais de enlace. Estas relacións son importantes dende un punto de vista fenomenolóxico, xa que permiten romper parcialmente a dexeneración existente entre algunhas propiedades das NS, nas formas de onda para sistemas binarios en coalescencia. E son tamén moi importantes a nivel fundamental, xa que a última razón da súa existencia, aínda non está moi ben comprendida. É máis, sendo insensibles con respecto a certos detalles do contido da materia das estrelas, estas relacións poden ser entendidas como predicións xenuínas sobre a estrutura das estrelas compactas na Teoría Xeral da Relatividade, e o estudo de desviacións das memsas, permite explorar outras teorías fundamentais de gravitación. Coa nosa análise, gustaríanos contribuír no eido da comprensión de tales relacións universais, xa que amosamos que as mesmas son satisfeitas para o caso dun fluído perfecto non-barotrópico, e polo tanto, os límites acutais experimentais para as deformabilidades das NS, poden ser ben descritos no marco do modelo de Skyrme.

Appendices

A Gradient-based Optimization methods for functionals

The gradient flow relaxation method

Consider a general nonlinear (scalar) field theory with topologically non-trivial configurations. Static solutions are given by field configurations $\boldsymbol{\phi}_s$ that make the (static) energy functional (26) stationary under first variations, i.e.

$$\left.\frac{\delta E[\boldsymbol{\phi}]}{\delta \phi^a}\right|_{\boldsymbol{\phi}_s} = 0. \tag{119}$$

Starting from an arbitrary initial configuration $\boldsymbol{\phi}^{(i)}$ which, in general, will NOT be a static solution of the system, we want to find a static solution within the same homotopy class as $\boldsymbol{\phi}^{(i)}$. The gradient flow method allows to do so by "relaxing" the input field configuration to the true static solution. This is achieved by locally evolving the field in the direction of maximum (local) variation of the energy functional, i.e. the direction of the gradient of the energy density with respect to the field variables. Indeed, let $\boldsymbol{\phi}^{(i)}$ be the input configuration. Since it will not be in general a static solution, the first variation of the static energy density in the direction of $\delta\boldsymbol{\phi}$ will have the form

$$\delta E[\boldsymbol{\phi}^{(i)}; \delta\boldsymbol{\phi}] = \left.\frac{\mathrm{d}}{\mathrm{d}\epsilon} E[\boldsymbol{\phi} + \epsilon\delta\boldsymbol{\phi}]\right|_{\epsilon=0} = \int d^d x F_a[\boldsymbol{\phi}^{(i)}]\delta\phi^a + \text{B. T.} \neq 0 \tag{120}$$

where B.T. stands for boundary terms, and

$$F_a[\boldsymbol{\phi}] = \frac{\delta E[\boldsymbol{\phi}]}{\delta \phi^a} = \frac{\partial \varepsilon}{\partial \phi^a} - \partial_i \frac{\partial \varepsilon}{\partial \partial_i \phi^a} \tag{121}$$

is the FUNCTIONAL DERIVATIVE of E. Expression (120) is the generalization of the concept of directional derivative to functionals, and hence the functional derivative is the generalization of the gradient to infinite dimensions.

Considering that the variations are taken over field configurations with fixed boundary conditions, the boundary terms vanish identically after integration. The Gradient flow relaxation method may then be implemented iteratively by changing at each iteration the field configuration as:

$$\phi_a^{(i+1)} = \phi_a^{(i)} - \gamma F_a[\boldsymbol{\phi}^{(i)}], \tag{122}$$

where $\gamma \in \mathbb{R}_+$ is the UPDATE PARAMETER. The previous equation is the discrete analogue of the following flow equation in the limit $\gamma \to 0$:

$$\frac{\mathrm{d}\phi_a(x,\gamma)}{\mathrm{d}\gamma} = -F_a[\boldsymbol{\phi}(x,\gamma)], \tag{123}$$

where now γ plays the role of an ancillary time parameter. The evolution along γ describes the relaxation of the initial configuration to a static solution, in the sense that

$$E[\boldsymbol{\phi}^{(i+1)}] \leq E[\boldsymbol{\phi}^{(i)}]. \tag{124}$$

Since the flow (123) describes a smooth transformation of the field, the final and initial field configurations will (in principle) lay in the same homotopy class of maps. Therefore, we may obtain solitonic solutions with different topological charge by using field configurations with different degree as input ansatz. Of course, for the numerical implementation it is necessary to discretize such transformation, into a discontinuous change on each iteration. One then must be careful with the values of the parameters that enter in the discretized version of (123) so that these discrete steps do not involve a transition between homotopy classes.

Constrained Gradient Flow

A complication that arises in multi-dimensional problems as opposed to the one dimensional case is that often the fields whose minimum energy configuration we want to find are subject to some CONSTRAINTS $C_\alpha(\boldsymbol{\phi}) = 0$, $\alpha = 1, ..., m$. Therefore, the problem becomes a constrained minimization of the energy functional. The standard approach to procede in such cases is the method of LAGRANGE MULTIPLIERS, which basically consists on extending the energy functional (26) to include the constraints:

$$\tilde{E}[\boldsymbol{\phi}] = \frac{1}{2}\int \left[h_{ab}(\boldsymbol{\phi})\partial_i\phi^a(x)\partial^i\phi^b(x) + V(\boldsymbol{\phi}) + \lambda^\alpha C_\alpha(\boldsymbol{\phi})\right] d^dx, \tag{125}$$

in which case, the variation of the modified energy density under field variations from an input configuration $\boldsymbol{\phi}^{(i)}$ will be given by

$$\delta\tilde{\varepsilon}[\boldsymbol{\phi}^{(i)}] = F_a[\boldsymbol{\phi}^{(i)}]\delta\phi^a + \lambda^\alpha \frac{\partial C_\alpha}{\partial\phi^a}[\boldsymbol{\phi}^{(i)}]\delta\phi^a + \text{B. T.}. \tag{126}$$

In particular, the (static) on-shell field configurations subject to the constraints $C_\alpha[\boldsymbol{\phi}] = 0$ will satisfy the modified Euler-Lagrange equations:

$$F_a[\boldsymbol{\phi}] = -\lambda^\alpha \frac{\partial C_\alpha}{\partial\phi^a}[\boldsymbol{\phi}]. \tag{127}$$

Usually, one can use the equations of motion, the constraints, and the derivatives of the constraints to solve for the multipliers λ^α in terms of the original phase space variables (in this case, the values of the fields and their time derivatives). Once the relations $\lambda^\alpha(\boldsymbol{\phi}, \partial_i\boldsymbol{\phi})$ are found, we will be interested in the first order (constrained) flow equation:

$$\frac{\mathrm{d}\phi_a(x,\gamma)}{\mathrm{d}\gamma} = -F_a[\boldsymbol{\phi}(x,\gamma)] - \lambda^\alpha \frac{\partial C_\alpha}{\partial\phi^a}[\boldsymbol{\phi}(x,\gamma)]. \tag{128}$$

Numerical implementation

As previously stated, the gradient flow relaxation method can be implemented iteratively by changing at each iteration the field configuration. In the case of three dimensions,

one needs to discretize the space by defining a grid of $N_x \times N_y \times N_z$ sites, with $h_{x,y,z}$ the distance between grid points in the x, y, z direction. Thus, in the $n-th$ iteration of the gradient flow, on each grid point, labeled by $[i, j, k]$, $(i, j, k \in [0, N_{x,y,z}])$ the $a-$th component of the field evolves as

$$\phi_a^{(n+1)}[i,j,k] = \phi_a^{(n)}[i,j,k] - \gamma F_a[\boldsymbol{\phi}^{(n)}[i,j,k]] - \gamma\lambda^\alpha \frac{\partial C_\alpha}{\partial \phi^a}[\boldsymbol{\phi}^{(n)}[i,j,k]]. \tag{129}$$

As in the one dimensional case, for the flow to converge to a (possibly local) minimum, the update parameter γ must be small enough. However, too small values will slow down the convergence.

An important difference with respect to the one dimensional problem is that the value of the topological charge cannot be obtained simply from the value of the field at the boundaries. Instead, the topological degree is obtained via an integral of a certain density over the full space. As a consequence of the space discretisation, this integral will fail to yield an integer number in general. Indeed, if the grid spacing constants h_i are chosen too big, it is likely that the topological charge of the field configuration $\boldsymbol{\phi}$ obtained after numerical integration over all the grid points will be less than the corresponding to such configuration in the continuous limit $h_{x,y,z} \to 0$. Both the number of grid points in each directions and the grid spacing constant will play a role in determining the deviation of the numerically obtained value for the topological charge from the integer value in the continuous limit. Such deviation can allow us to determine whether the parameters chosen for the numerical algorithm are well suited to the problem we are trying to solve.

Accelerated Gradient Descent

An important issue when considering the gradient flow algorithm is that of convergence. Indeed, the gradient flow method is not guaranteed to converge to a local minimum if the configuration space is not convex (which, in general, will not be the case for a sufficiently complex field theory), but it can converge to a metastable state (a paradigmatic example of such states in a field theory are the SPHALERONS of an $SU(2)$ yang mills theory). Furthermore, the fact that the field update is proportional to the functional derivative (129) may produce slow convergence times when the energy valley in field configuration space is very shallow. Indeed, when the field configuration reaches a point of energy close to the minimum, the gradient can be almost zero, making the next update step too small.

These convergence problems can be alleviated by a modification of the gradient flow algorithm which introduces a "memory term" that favours the direction of travelling from previous configurations. The regions with small gradient are then transited faster, like a heavy ball would due to its own inertia. The inclusion of a momentum term in the gradient descent algorithm is a standard strategy in functional optimization problems, which is usually denoted as "heavy ball" method. The drawback of adding such a term appears when the actual minimum is met, and passed by. If the momentum term dominates the evolution, the system may not be able to come back to the desired local minimum, and the system may even not be able to find a local minimum ever.

Using the "heavy ball" idea, Nesterov [Nes83] was able to find the optimal algorithm that is based on single gradients of the energy functional. In such algorithm, the gradient is no longer calculated in the current position. Instead, it is done in the position that the configuration would arrive to with the momentum term alone. This gradient now

favors (disfavors) the momentum direction if it was approaching to (moving away from) the minimum This balance leads the algorithm to convergence. The iterative pattern is then

$$\phi_a^{(i+1)} = \phi_a^{(i)} - \Delta\phi_a^{(i+1)}, \tag{130}$$

where now the actualization of the field depends on the field but also on its previous value:

$$\Delta\phi_a^{(i+1)} = p^{(i)}\Delta\phi_a^{(i)} - \gamma\tilde{F}_a[\boldsymbol{\phi}^{(i)} + p^{(i)}\Delta\boldsymbol{\phi}^{(i)}], \quad \Delta\phi_a^{(0)} = 0. \tag{131}$$

In eq. (131) we have defined

$$\tilde{F}_a[\boldsymbol{\phi}] = F_a[\boldsymbol{\phi}] + \lambda^\alpha \frac{\partial C_\alpha}{\partial \phi^a}[\boldsymbol{\phi}], \tag{132}$$

and the momentum parameter $p^{(i)}$, given by

$$p^{(i)} = \frac{v^{(i)}}{v^{(i)} + 3}, \tag{133}$$

with

$$v^{(i+1)} = \begin{cases} v^{(i)} + 1, & \text{if} \quad E[\boldsymbol{\phi}^{(i+1)}] < E[\boldsymbol{\phi}^{(i)}], \\ 0, & \text{if} \quad E[\boldsymbol{\phi}^{(i+1)}] > E[\boldsymbol{\phi}^{(i)}], \end{cases} \tag{134}$$

and $v^{(0)} = 0$.

The minimization algorithm so defined is often called ACCELERATED GRADIENT FLOW. It is accelerated in the sense that the momentum parameter grows with each iteration, but it is brought back to its initial value ($p = 0$) when the energy minimum is passed by.

B General relativistic perturbation theory

Perturbations of arbitrary backgrounds and gauge freedom

Consider a *background spacetime* $(\mathcal{M}, g_{\mu\nu})$, where $\mathcal{M}$ is a four dimensional differentiable manifold and $g_{\mu\nu}$ is a background metric satisfying the Einstein field equations:

$$E_{\mu\nu}[g] = G_{\mu\nu}[g] - 8\pi T_{\mu\nu}[g] = 0. \tag{135}$$

In order to carry on a perturbation scheme over $(\mathcal{M}, g_{\mu\nu})$, we define a 5-dimensional manifold $\mathcal{N} := \mathcal{M} \times \boldsymbol{R} \equiv \mathcal{M}(\epsilon)$ such that, for each $\epsilon_0 \in \boldsymbol{R}$, $\mathcal{M}(\epsilon_0)$ is a 4-dimensional embedded submanifold —which represents a "perturbed" spacetime— and $\mathcal{M}(0)$ corresponds to the background spacetime manifold. this, we need an identification map between points of $\mathcal{M}(0)$ and $\mathcal{M}(\epsilon)$, so that we may compare the values of $Q(x)$ and those of its extension to the 5-D manifold, $\tilde{Q}(\epsilon, x)$, at any point. Let

$$\begin{array}{rccc} \phi_\epsilon : & \mathcal{N} & \to & \mathcal{N} \\ & \mathcal{M}(0) & \mapsto & \mathcal{M}(\epsilon) \end{array} \tag{136}$$

be a one-parameter family of diffeomorphisms between the background spacetime manifold and the perturbed spacetimes, and let $V := \partial_\epsilon$ the vector field on the 5-dimensional manifold $\mathcal{N}$ whose integral curves are precisely the ones defined by ϕ_ϵ. Therefore, the points at each submanifold of the family are identified through ϕ_ϵ, which allows us to pull back $\tilde{Q}(\epsilon, x)$ onto the background spacetime, and obtain the family of tensors[2]

$$Q(\epsilon, x) = \phi_\epsilon^*(\tilde{Q}(\epsilon, x)) = \exp(\epsilon \mathcal{L}_V)\tilde{Q}(\epsilon, x) = \sum_{k=0}^{\infty} \frac{(\epsilon \mathcal{L}_V)^k}{k!} \tilde{Q}(\epsilon, x) \tag{137}$$

defined on $\mathcal{M}(0)$. For small values of the perturbation parameter ϵ, we may Taylor-expand the pulled-back perturbed tensor $Q(\epsilon, x)$, and we obtain

$$Q(\epsilon, x) = Q(x) + Q^{(1)}\epsilon + \frac{1}{2} Q^{(2)}\epsilon^2 + \cdots, \tag{138}$$

where $Q^{(n)} = \mathcal{L}_V \tilde{Q}(\epsilon, x) = \partial_\epsilon^n \tilde{Q}(\epsilon, x)\big|_{\epsilon=0}$.

Applying the previous construction to the background spacetime metric, we obtain the following one-parameter family of metrics,

$$g_{\mu\nu}(\epsilon, x) = g_{\mu\nu}(x) + g^{(1)}_{\mu\nu}(x)\epsilon + \frac{1}{2} g^{(2)}_{\mu\nu}(x)\epsilon^2 + \cdots \tag{139}$$

such that $(\mathcal{M}(\epsilon), g(\epsilon))$ defines a one-parameter family of spacetimes. Taking into account these perturbations, the Einstein equations read (we omit the dependence on x and the indices for clearness):

$$E[g(\epsilon)] = E[g] + \epsilon E^{(1)}[g, g^{(1)}] + \frac{1}{2} E^{(2)}[g, g^{(1)}, g^{(2)}] + \cdots = 0, \tag{140}$$

[2]Here we use the fact that the action of the flow ϕ_ϵ is generated by V, and

$$\mathcal{L}_V Q = \frac{\mathrm{d}}{\mathrm{d}\epsilon} \phi_\epsilon^*(T)\Big|_{\epsilon=0}$$

is the Lie derivative of an arbitrary tensor Q with respect to the flow generated by V.

which gives a set of equations for each order in the expansion, i.e.

$$E^{(n)}[g, \cdots, g^{(n)}] = 0, \tag{141}$$

so that the metric perturbation quantities are related to each other in such a way that (141) hold. This allows us to find explicit solutions of the Einstein equations from a perturbed background solution to any order in the perturbation parameter.

Note that there is an inherent gauge freedom in this construction, and the perturbation quantities $Q^{(n)}$ are gauge-dependent, in the sense that the family ϕ_ϵ is arbitrarily chosen. Had we chosen a different family of diffeomorphisms, namely ψ_ϵ, with generating vector field W, we would get different perturbation quantities at each order. However, the perturbation quantities at either gauge can be related to each other, order by order.

Indeed, let us consider the two gauge choices ϕ_ϵ and ψ_ϵ. A gauge transformation between these two choices is given by $G_\epsilon = \phi_\epsilon^{-1} \circ \psi_\epsilon$. Therefore, we have

$$G_\epsilon^* = \exp(\epsilon \mathcal{L}_W) \exp(-\epsilon \mathcal{L}_V) = \exp\left(\sum_{n=1}^{\infty} \frac{\epsilon^n}{n!} \mathcal{L}_{X_n} \right), \tag{142}$$

where the properties of the Lie derivative and the Baker–Campbell–Hausdorff formula have been used in the last equation. The vector fields X_n can be written in terms of the gauge generators V and W, and their commutators, the first of them having the form [SBG04]:

$$X_1 = W - V, \quad X_2 = [V, W], \quad X_3 = \frac{1}{2}[V + W[W, V]], \quad \cdots \tag{143}$$

Therefore, G_ϵ^* is a mapping between the perturbed tensorial quantities in both gauges, and expanding into powers of the perturbation parameter ϵ gives the relation between the perturbation quantities order by order.

As an example, consider the case of linearized gravity, in which the background metric corresponds to that of flat spacetime, and only the first order perturbative term is taken into account:

$$g_{\mu\nu}(\epsilon, x) = \eta_{\mu\nu} + \epsilon h_{\mu\nu}(x) + \mathcal{O}(\epsilon^2). \tag{144}$$

Had we chose a different gauge, this expansion may be written $\tilde{g}_{\mu\nu}(\epsilon, x) = \eta_{\mu\nu} + \epsilon \tilde{h}_{\mu\nu}(x) + \mathcal{O}(\epsilon^2)$, where both $h_{\mu\nu}(x)$ and $\tilde{h}_{\mu\nu}(x)$ are related through a gauge transformation. Indeed, we have:

$$\tilde{g}_{\mu\nu}(\epsilon, x) = G_\epsilon^* g_{\mu\nu}(\epsilon, x) \implies \eta_{\mu\nu} + \epsilon \tilde{h}_{\mu\nu}(x) = \eta_{\mu\nu} + \epsilon h_{\mu\nu}(x) + \epsilon \mathcal{L}_X \eta_{\mu\nu} + \mathcal{O}(\epsilon^2), \tag{145}$$

or $\tilde{h}_{\mu\nu}(x) = h_{\mu\nu}(x) + 2\partial_{(\mu}\xi_{\nu)}$, where $X = \xi^\mu \partial_\mu$ is the vector field generating this gauge transformation.

Perturbation of spherically symmetric configurations

Consider a spherically symmetric spacetime $\mathcal{M}$, whose metric is given in general by the Schwarzschild solution. Given its spherical symmetry, the Schwarzschild spacetime manifold has the topology $\mathcal{M} = \mathcal{N} \times \mathcal{S}^2$, where S^2 is the two-sphere and $\mathcal{N}$ is a two-dimensional manifold. Thus we, may write the Schwarzschild line element in a covariant form as

$$ds^2 = g_{ab} dx^a dx^b + r^2(x^a) \Omega_{AB} dx^A dx^B, \tag{146}$$

with lower-case latin indices running over $\{0,1\}$ and upper-case latin indices running over $\{2,3\}$. In particular, r is a scalar function of the lower-case coordinates, the coordinates $x^A = \{\theta, \phi\}$ span the two-spheres $x^a = \text{const}$, and Ω_{AB} is the metric on the unit two-sphere, $\Omega_{AB} = \text{diag}(1, \sin^2\theta)$. Let D_A be the covariant derivative operator compatible with Ω_{AB}, and ε_{AB} the Levi-Civita tensor on the unit two-sphere, with $\varepsilon_{\theta\phi} = \sin\theta$.

We may now introduce the metric perturbation $\delta g_{\mu\nu} := h_{\mu\nu}$, which may be written

$$h_{\mu\nu} = h_{ab}dx^a dx^b + h_{aB}dx^a dx^B + h_{AB}dx^A dx^B. \tag{147}$$

Spherical symmetry of the background spacetime motivates a decomposition of $h_{\mu\nu}$ in spherical harmonics. Note that the h_{ab} transform as scalars on $\mathcal{S}^2$, whereas h_{aB} and h_{AB} transform as covariant vectors and tensors, respectively, on $\mathcal{S}^2$. Therefore, we should decompose them into scalar, vector and tensor spherical harmonics, respectively.

The scalar harmonics are the usual spherical-harmonic functions $Y^{lm}(x^A)$, which satisfy the following eigenvalue equation:

$$[\Omega^{AB} D_A D_B + l(l+1)]Y^{lm} = 0. \tag{148}$$

Vectorial spherical harmonics come into two types, depending on their parity:

a Even parity: $Y^{lm}_A := D_A Y^{lm}$

b Odd parity: $X^{lm}_A := -\varepsilon^B_A D_B Y^{lm}$

Tensorial harmonics are also classified according to their parity:

a) Even parity: there are two kinds: $\begin{cases} Y^{lm}_{AB} & := & \Omega_{AB}Y^{lm} \text{ (traceful, scalar degree of freedom)} \\ \tilde{Y}^{lm}_{AB} & := & [D_A D_B - \frac{1}{2}l(l+1)\Omega_{AB}]Y^{lm} \text{ (traceless)} \end{cases}$

b) Odd parity: $X^{lm}_{AB} := \frac{1}{2}(\varepsilon^C_A D_B + \varepsilon^C_B D_A)D_C Y^{lm}$

Therefore, the components of the metric perturbation (147) can be written:

The even-parity sector of the perturbation (polar perturbations) consists of the associated functions $h^{lm}_{ab}, j^{lm}_a, k^{lm}$ and G^{lm}, whilst the variables h^{lm}_a and h^{lm}_2 make up the odd parity sector (axial perturbations). Up to now, the discussion of the perturbation functions have been made in an arbitrary gauge. It is useful to fix the gauge for the metric perturbations, in order to simplify the problem of determining their explicit expression by solving the perturbed Einstein equations. A useful gauge choice is the so-called Regge-Wheeler gauge [MP05], in which

$$j^{lm}_a = G^{lm} = h^{lm}_2 = 0. \tag{149}$$

Furthermore, for axially symmetric spacetimes, we may discard the $\phi-$dependence of the harmonics, so that the general expression for an axially symmetric metric perturbation with these gauge choices is given by:

$$h_{\mu\nu} = \begin{pmatrix} -H_l & I_l & 0 & 0 \\ I_l & M_l & 0 & 0 \\ 0 & 0 & r^2 K_l & 0 \\ 0 & 0 & 0 & r^2\sin^2(\theta)K_l \end{pmatrix} P_l(\cos\theta) + \begin{pmatrix} 0 & 0 & 0 & V_l \\ 0 & 0 & 0 & \omega_l \\ 0 & 0 & 0 & 0 \\ V_l & \omega_l & 0 & 0 \end{pmatrix} \sin\theta\partial_\theta P_l(\cos\theta), \tag{150}$$

where the first term has even parity and the second term has odd parity.

C The WZW term

Derivation of the WZW and sextic terms contribution to V_K To work with the WZW and sextic terms, it is useful to employ the formalism of Lie algebra-valued differential forms, which we will extensively do in this appendix. Let us first review the basic properties of such objects and establish the notation that we will follow. A $\mathfrak{g}$-valued differential form α can be written in terms of the Lie algebra generators T_a, as $\alpha = \alpha^a \otimes T_a$. The exterior derivative is then simply obtained as $d\alpha = d\alpha^a \otimes T_a$. Furthermore, the wedge product on $\mathfrak{g}$-valued forms is defined as

$$\alpha \wedge \beta = \alpha^a \wedge \beta^b \otimes T_a T_b. \tag{151}$$

So that the following useful properties hold:

$$d\alpha \wedge \beta = (d\alpha) \wedge \beta + (-1)^{|\alpha|} \alpha \wedge (d\beta), \tag{152}$$

$$\mathrm{Tr}\{\alpha \wedge \beta\} = (-1)^{|\alpha||\beta|} \mathrm{Tr}\{\beta \wedge \alpha\}, \tag{153}$$

where $|\alpha|$ denotes the degree of α. Also, by linearity of the trace, both the trace and the exterior derivative commute, i.e.

$$d\,\mathrm{Tr}\{\alpha\} = \mathrm{Tr}\{d\alpha\}. \tag{154}$$

To alleviate the notation, in the following we will drop the wedge product symbol and denote the product (151) simply by $\alpha\beta$. Then, for instance, if α and β denote two 1-forms, we have $\mathrm{Tr}\{\alpha\beta\} = -\mathrm{Tr}\{\beta\alpha\}$, $d(\alpha\beta) = d\alpha\beta - \alpha d\beta$.

Let us now perform the most general chiral transformation to the Skyrme field U_π, given by $U = g_l U_\pi g_r^\dagger$, with $(g_l, g_r) \in SU(3)_L \times SU(3)_R$ and define the following $\mathfrak{su}(3)$-valued differential forms,

$$V = U^\dagger dU,\ L = U_\pi^\dagger dU_\pi,\ \alpha = g_l^\dagger dg_l,\ \beta = g_r dg_r^\dagger. \tag{155}$$

By definition, we have the following relation between the forms above:

$$V = (U_\pi g_r)^\dagger [\alpha + U_\pi (L - \beta) U_\pi^\dagger] U_\pi g_r. \tag{156}$$

On the other hand, the WZW action is then given by the pullback of a volume 5-form Ω_5 by an extended Skyrme field $U : D^5 \to SU(3)$ [3] integrated over an auxiliar 5-dimensional disk D whose boundary is the spacetime manifold M,

$$S_{\mathrm{WZW}} = -i \frac{N_C}{240\pi^2} \int_D U^*(\Omega_5). \tag{157}$$

The form $U^*(\Omega_5)$ can be expressed in terms of L as

$$\begin{aligned} S_{\mathrm{WZW}}(L) &= -i \frac{N_C}{240\pi^2} \int_D \mathrm{Tr}\{V^5\} = \\ &= -\frac{iN_C}{240\pi^2} \int_D \mathrm{Tr}\{[\alpha + U_\pi (L - \beta) U_\pi^\dagger]^5\}. \end{aligned} \tag{158}$$

[3] The result is of course independent of such extension, because $\pi_4(SU(3))$ vanishes.

Let us denote the 1-form $U_\pi(L-\beta)U_\pi^\dagger$ by ω. The exterior derivative of this form is:

$$\begin{aligned} d\omega &= dU_\pi(L-\beta)U_\pi^\dagger + U_\pi(dL-d\beta)U_\pi^\dagger - U_\pi(L-\beta)dU_\pi^\dagger = \\ &= -U_\pi^\dagger(dL+d\beta+L\beta+\beta L)U_\pi, \end{aligned} \tag{159}$$

where we have used the fact that both β and L satisfy the Maurer-Cartan equation $d\beta = -\beta^2$. Moreover, one can straightforwardly see that

$$\omega^2 = U_\pi^\dagger(L-\beta)^2U_\pi = U_\pi^\dagger(-d\beta - dv - \beta v - v\beta)U_\pi = d\omega. \tag{160}$$

Knowing this, we have

$$\begin{aligned} S_{\text{WZW}}(L) =& -i\frac{N_C}{240\pi^2}\int_{\mathcal{M}} \text{Tr}\{[\alpha+\omega]^5\} \\ =& S_{\text{WZW}}(\alpha) + S_{\text{WZW}}(\omega) - \frac{iN_C}{48\pi^2}\int_{\mathcal{M}} \text{Tr}\{\alpha^4\omega + \omega^4\alpha + \alpha^2\omega^3 + \omega^2\alpha^3 + \alpha\omega\alpha\omega^2 + \omega\alpha\omega\alpha^2\} \\ =& S_{\text{WZW}}(\alpha) + S_{\text{WZW}}(\omega) - \frac{iN_C}{48\pi^2}\int_{\partial\mathcal{M}} \text{Tr}\{\omega^3\alpha - \alpha^3\omega - \frac{1}{2}(\alpha\omega)^2\}, \end{aligned} \tag{161}$$

where we have used eqs. (152) to (154), the relation (160) for ω, the M-C equation for α and Stokes' theorem in the last step. Repeating the same calculation for $S_{\text{WZW}}(\omega)$ yields:

$$\begin{aligned} S_{\text{WZW}}(\omega) =& -i\frac{N_C}{240\pi^2}\int_{\mathcal{M}} \text{Tr}\{[L-\beta]^5\} = \\ =& -S_{\text{WZW}}(\beta) + S_{\text{WZW}}(L) - \frac{iN_C}{48\pi^2}\int_{\partial\mathcal{M}} \text{Tr}\{L^3\beta - \beta^3 L - \frac{1}{2}(L\beta)^2\}, \end{aligned} \tag{162}$$

so that

$$\begin{aligned} S_{\text{WZW}}(V) = S_{\text{WZW}}(L) + S_{\text{WZW}}(\alpha) - S_{\text{WZW}}(\beta) - \\ -\frac{iN_C}{48\pi^2}\int_{\partial\mathcal{M}} \text{Tr}\{L^3\beta - \beta^3 L - \frac{1}{2}(L\beta)^2 + \omega^3\alpha - \alpha^3\omega - \frac{1}{2}(\alpha\omega)^2\}. \end{aligned} \tag{163}$$

Eq.(163) shows that a chiral transformation of the $SU(3)$ Skyrme field induces an additional local term in the action due to the nontrivial transformation of the (nonlocal) WZW term. Furthermore, if we fix the chiral transformation fields to only depend on one spacetime coordinate, $g_{l/r}(x) \equiv g_{l/r}(t)$, any power of α and β will vanish in the local, 4-dimensional effective term. Taking this into account, we arrive to the final result:

$$S_{\text{WZW}}(V) = S_{\text{WZW}}(L) - \frac{iN_C}{48\pi^2}\int_{\partial\mathcal{M}} \text{Tr}\{L^3(\beta + U_\pi^\dagger\alpha U_\pi)\}, \tag{164}$$

from where eq. (3.87) is readily obtained.

Let us now turn to the sextic term. The coordinate free version of $\mathcal{L}_6$ is given by

$$\mathcal{L}_6 = \lambda^2\pi^4\mathcal{B}\wedge\star\mathcal{B}, \tag{165}$$

where $\star$ denotes the Hodge star operator, and $\mathcal{B}$ the 1-form in spacetime whose coordinates in a local chart coincide with the Baryon current, $\mathcal{B} = B_\mu dx^\mu$. We can construct such form as the Hodge dual of the baryon number density three-form,

$$\begin{aligned} b &= (24\pi^2)^{-1} U^*(\Omega_3) = \frac{1}{24\pi^2} \operatorname{Tr}\{L_\mu L_\nu L_\rho\} dx^\mu \wedge dx^\nu \wedge dx^\rho \\ &= \frac{1}{3!} b_{\mu\nu\rho} dx^\mu \wedge dx^\nu \wedge dx^\rho, \end{aligned} \tag{166}$$

i.e.

$$\mathcal{B} = \star b = \frac{1}{3!} b^{\nu\rho\sigma} \varepsilon_{\nu\rho\sigma\mu} dx^\mu = \frac{1}{24\pi^2} \varepsilon_\mu{}^{\nu\rho\sigma} \operatorname{Tr}\{L_\nu L_\rho L_\sigma\} = B_\mu dx^\mu. \tag{167}$$

Thus $\mathcal{L}_6 = \lambda^2 \pi^4 \star b \wedge b$. Expressing the sextic term in such form is most useful for calculating its contribution to the kaon potential employing the formalism of differential forms in the same way as for the WZW term. Indeed, we see that

$$b = \frac{1}{24\pi^2} \operatorname{Tr}\{L^3\} = \frac{1}{24\pi^2} \operatorname{Tr}\{\omega^3 + 3w\omega^2\}, \tag{168}$$

where we used the fact that $w^n = 0$ for $n \geq 2$ because the kaon field Σ only depends on time. Hence, also $v^n = 0$ for $n \geq 2$ and $vw = 0$ hold, and, given that $\omega = U_\pi^\dagger(\beta - v)U_\pi$, we may write

$$\begin{aligned} b =& \frac{1}{24\pi^2} \operatorname{Tr}\{\beta^3 + 3(wU_\pi^\dagger(\beta - v)^2 U_\pi - \beta^2 v)\} = \\ =& \frac{1}{24\pi^2} \operatorname{Tr}\{\beta^3 + 3\beta^2(U_\pi w U_\pi^\dagger - v)\}. \end{aligned} \tag{169}$$

Thus, the baryon current density in the kaon condensed phase will be modified by $B^\mu = B_\pi^\mu + C^\mu$, where B_π^μ is the baryon current due to the pionic background and

$$C^\mu = \frac{1}{8\pi^2} \varepsilon^{\mu\nu\rho\sigma} \operatorname{Tr}\{R_\nu R_\rho (U_\pi \Sigma \partial_\sigma \Sigma^\dagger U_\pi^\dagger - \Sigma^\dagger \partial_\sigma \Sigma)\}. \tag{170}$$

For a time independent pion background and a homogeneous kaon condensate, we have $B_\pi^\mu C_\mu = 0$, and hence the only constribution from the sextic term ($\propto B_\mu B^\mu$) to V_K comes from the additional term:

$$\begin{aligned} C_\mu C^\mu &= \frac{1}{64\pi^4} \varepsilon^{\mu\nu\rho\sigma} \epsilon_{\mu\alpha\beta} \operatorname{Tr}\{R_\nu R E_\rho \xi_\sigma\} \operatorname{Tr}\{R_\alpha R_\beta \xi_\gamma\} = \\ &= \frac{-1}{64\pi^4} \varepsilon_{ijk} \varepsilon_{ilm} \operatorname{Tr}\{R_j R_k \xi_0\} Tr\{R_l R_m \xi_0\}, \end{aligned} \tag{171}$$

where $\xi_\mu = U_\pi \Sigma \partial_\mu \Sigma^\dagger U_\pi^\dagger - \Sigma^\dagger \partial_\mu \Sigma$.

Publications and permissions

The research work done during the development of this thesis has given raise to a total of 11 publications in peer-reviewed journals, apart from other non-published preprints. The contents of some of these publications have been (partially) reproduced within the thesis. Here we list these publications (not including the ones that have not been included in the thesis) and the respective authorisations from the corresponding journals, as required by the internal university policy.

Publications reproduced in this thesis

Title: Gravitational form factors of nuclei in the Skyrme model ([GHH23])
Authors: Alberto Garcia Martin-Caro,[a] Miguel Huidobro[a] and Yoshitaka Hatta [b], [a] Departamento de Física de Partículas, Universidad de Santiago de Compostela and Instituto Galego de Física de Altas Enerxias (IGFAE) E-15782 Santiago de Compostela, Spain [b] Physics Department, Brookhaven National Laboratory, Upton, NY 11973, USA and RIKEN BNL Research Center, Brookhaven National Laboratory, Upton, NY 11973, USA
Journal and article information: **Name:** Physical Review D **Publisher:** American Physical Society **Date of publication:**14 August 2023 **ISSN:** 2470-0029 **DOI:** 10.1103/PhysRevD.108.034014 **Impact Factor:** 5.407 (2021 Journal Citation Report)
Contribution from the PhD Student: Performed analytical and numerical computations, contributed to the writing of the manuscript and creation of figures.
The content of this article is partially reproduced in **chapter 1, fig. 1.1** and **chapter 2, section 2.3** of this thesis with standard author permissions from the American Physical Society. (Distributed under the terms of the CC BY 4.0 license).

Title: Quantum skyrmion crystals and the symmetry energy of dense matter ([Ada+22b])

Authors: Christoph Adam[a], Alberto García Martín-Caro[a], Miguel Huidobro[a], Ricardo Vázquez[a], and Andrzej Wereszczynski[b]

[a] Departamento de Física de Partículas, Universidad de Santiago de Compostela and Instituto Galego de Física de Altas Enerxias (IGFAE) E-15782 Santiago de Compostela, Spain

[b] Institute of Physics, Jagiellonian University, Lojasiewicza 11, Kraków, Poland

Journal and article information:

Name: Physical Review D

Publisher: American Physical Society

Date of publication: 28 December 2022

ISSN: 2470-0029

DOI:10.1103/PhysRevD.106.114031

Impact Factor: 5.407 (2021 Journal Citation Report)

Contribution from the PhD Student: Performed analytical and numerical computations, contributed to the writing of the manuscript and creation of figures.

Title: Kaon condensation in skyrmion matter and compact stars ([Ada+23])

Authors: Christoph Adam[a], Alberto García Martín-Caro[a], Miguel Huidobro[a], Ricardo Vázquez[a], and Andrzej Wereszczynski[b]

[a] Departamento de Física de Partículas, Universidad de Santiago de Compostela and Instituto Galego de Física de Altas Enerxias (IGFAE) E-15782 Santiago de Compostela, Spain

[b] Institute of Physics, Jagiellonian University, Lojasiewicza 11, Kraków, Poland

Journal and article information:

Name: Physical Review D

Publisher: American Physical Society

Date of publication: 10 April 2023

ISSN: 2470-0029

DOI:10.1103/PhysRevD.107.074007

Impact Factor: 5.407 (2021 Journal Citation Report)

Contribution from the PhD Student: Performed analytical computations, contributed to the writing of the manuscript and creation of figures.

Title: Quasiuniversal relations for generalized Skyrme stars ([Ada+21])
Authors: Christoph Adam[a], Alberto García Martín-Caro[a], Miguel Huidobro[a], Ricardo Vázquez[a] and Andrzej Wereszczynski[b] [a] Departamento de Física de Partículas, Universidad de Santiago de Compostela and Instituto Galego de Física de Altas Enerxias (IGFAE) E-15782 Santiago de Compostela, Spain [b] Institute of Physics, Jagiellonian University, Lojasiewicza 11, Kraków, Poland
Journal and article information: **Name:** Physical Review D **Publisher:** American Physical Society **Date of publication:** 2021 **ISSN:** 2470-0029 **DOI:** 10.1103/PhysRevD.103.023022 **Impact Factor:** 5.407 (2021 Journal Citation Report)
Contribution from the PhD Student: Performed analytical and numerical computations, contributed to the writing of the manuscript and creation of figures.
The content of this article is partially reproduced in **chapter 4** and **appendix B** of this thesis with standard author permissions from the American Physical Society. (distributed in open access under the terms of the CC BY 4.0 license ).

Title: Constrained instanton approximation of Skyrmions with massive pions. ([Gar22])
Authors: Alberto García Martín-Caro [a] [a] Departamento de Física de Partículas, Universidad de Santiago de Compostela and Instituto Galego de Física de Altas Enerxias (IGFAE) E-15782 Santiago de Compostela, Spain
Journal and article information: **Name:** Physics Letters B **Publisher:** Elsevier **Date of publication:** 24 October 2022 **ISSN:** 1873-2445 **DOI:** 10.1016/j.physletb.2022.137532 **Impact Factor:** 4.95 (2021 Journal Citation Report)
Contribution from the PhD Student: The student is the only author of this article
The content of this article is partially reproduced in **chapter 1, section 1.3** of this thesis with standard author permissions from Elsevier. (Distributed in open access under the terms of the CC BY 4.0 license ).

Figure authorship statement

Fig.2 has been taken from [Ben09]. No especial permissions are required as it was released to the public domain by its author.
The rest of figures have been elaborated by the author of this thesis, Alberto García Martín-Caro, and are subject to the CC BY 4.0 license  .

List of Figures

List of Tables

References

[t H74] Gerard 't Hooft. "Magnetic monopoles in unified gauge theories". In: *Nuclear Physics B* 79.2 (1974), pp. 276–284. ISSN: 0550-3213. DOI: https://doi.org/10.1016/0550-3213(74)90486-6 (cit. on p. xxix).

[t H76] Gerard 't Hooft. "Computation of the quantum effects due to a four-dimensional pseudoparticle". In: *Phys. Rev. D* 14 (12 Dec. 1976), pp. 3432–3450. DOI: 10.1103/PhysRevD.14.3432 (cit. on pp. xxix, 16, 17, 20).

[t H86] Gerard 't Hooft. "How Instantons Solve the U(1) Problem". In: *Phys. Rept.* 142 (1986), pp. 357–387. DOI: 10.1016/0370-1573(86)90117-1 (cit. on p. 15).

[Aas+15] J. Aasi et al. "Advanced LIGO". In: *Class. Quant. Grav.* 32 (2015), p. 074001. DOI: 10.1088/0264-9381/32/7/074001. arXiv: 1411.4547 [gr-qc] (cit. on pp. xxxiv, 96).

[Abb+17] B. P. Abbott et al. "GW170817: Observation of Gravitational Waves from a Binary Neutron Star Inspiral". In: *Phys. Rev. Lett.* 119 (16 Oct. 2017), p. 161101. DOI: 10.1103/PhysRevLett.119.161101 (cit. on pp. 96, 129).

[Abb+18] B. P. Abbott et al. "GW170817: Measurements of Neutron Star Radii and Equation of State". In: *Phys. Rev. Lett.* 121 (16 Oct. 2018), p. 161101. DOI: 10.1103/PhysRevLett.121.161101 (cit. on p. xxxiv).

[Abb+20a] B. P. Abbott et al. "GW190425: Observation of a Compact Binary Coalescence with Total Mass $\sim 3.4 M_{\odot}$". In: *Astrophys. J. Lett.* 892.1 (2020), p. L3. DOI: 10.3847/2041-8213/ab75f5. arXiv: 2001.01761 [astro-ph.HE] (cit. on pp. 96, 130).

[Abb+20b] R. Abbott et al. "GW190814: Gravitational Waves from the Coalescence of a 23 Solar Mass Black Hole with a 2.6 Solar Mass Compact Object". In: *Astrophys. J. Lett.* 896.2 (2020), p. L44. DOI: 10.3847/2041-8213/ab960f (cit. on pp. 96, 130).

[Abb+21] R. Abbott et al. "Observation of Gravitational Waves from Two Neutron Star–Black Hole Coalescences". In: *Astrophys. J. Lett.* 915.1 (2021), p. L5. DOI: 10.3847/2041-8213/ac082e. arXiv: 2106.15163 [astro-ph.HE] (cit. on p. 96).

[Abd+22] R. Abdul Khalek et al. "Science Requirements and Detector Concepts for the Electron-Ion Collider: EIC Yellow Report". In: *Nucl. Phys. A* 1026 (2022), p. 122447. DOI: 10.1016/j.nuclphysa.2022.122447. arXiv: 2103.05419 [physics.ins-det] (cit. on p. 41).

[Abr57] A. Abrikosov. "The magnetic properties of superconducting alloys". In: *Journal of Physics and Chemistry of Solids* 2.3 (Apr. 1957), pp. 199–208. DOI: 10.1016/0022-3697(57)90083-5 (cit. on p. xxix).

[Ace+15] F. Acernese et al. "Advanced Virgo: a second-generation interferometric gravitational wave detector". In: *Class. Quant. Grav.* 32.2 (2015), p. 024001. DOI: 10.1088/0264-9381/32/2/024001. arXiv: 1408.3978 [gr-qc] (cit. on p. 96).

[ASW10a] C. Adam, J. Sánchez-Guillén, and A. Wereszczyński. "A Skyrme-type proposal for baryonic matter". In: *Physics Letters B* 691.2 (July 2010), pp. 105–110. ISSN: 0370-2693. DOI: 10.1016/j.physletb.2010.06.025 (cit. on pp. 3, 98).

[ASW10b] Christoph Adam, J. Sanchez-Guillen, and A. Wereszczynski. "A BPS Skyrme model and baryons at large N_c". In: *Phys. Rev. D* 82 (2010), p. 085015. DOI: 10.1103/PhysRevD.82.085015. arXiv: 1007.1567 [hep-th] (cit. on pp. 43, 97).

[Ada+15a] Christoph Adam et al. "Baryon chemical potential and in-medium properties of BPS skyrmions". In: *Phys. Rev. D* 91.12 (2015), p. 125037. DOI: 10.1103/PhysRevD.91.125037. arXiv: 1504.05185 [hep-th] (cit. on p. 43).

[Ada+15b] Christoph Adam et al. "Neutron stars in the Bogomol'nyi-Prasad-Sommerfield Skyrme model: Mean-field limit versus full field theory". In: *Phys. Rev. C* 92 (2 Aug. 2015), p. 025802. DOI: 10.1103/PhysRevC.92.025802 (cit. on pp. 97, 102).

[Ada+15c] Christoph Adam et al. "The Skyrme model in the BPS limit". In: *The Multifaceted Skyrmion*. Nov. 2015. Chap. 9, pp. 193–232. DOI: 10.1142/9789814704410_0009. arXiv: 1511.05160 [hep-th] (cit. on pp. 42, 102).

[Ada+20] Christoph Adam et al. "A new consistent neutron star equation of state from a generalized Skyrme model". In: *Phys. Lett. B* 811 (2020), p. 135928. DOI: 10.1016/j.physletb.2020.135928. arXiv: 2006.07983 [hep-th] (cit. on pp. 4, 123).

[Ada+21] Christoph Adam et al. "Quasiuniversal relations for generalized Skyrme stars". In: *Phys. Rev. D* 103.2 (2021), p. 023022. DOI: 10.1103/PhysRevD.103.023022 (cit. on pp. 80, 95, 159).

[Ada+22a] Christoph Adam et al. "Dense matter equation of state and phase transitions from a generalized Skyrme model". In: *Phys. Rev. D* 105.7 (2022), p. 074019. DOI: 10.1103/PhysRevD.105.074019. arXiv: 2109.13946 [hep-th] (cit. on pp. 68, 69, 80).

[Ada+22b] Christoph Adam et al. "Quantum skyrmion crystals and the symmetry energy of dense matter". In: *Phys. Rev. D* 106.11 (2022), p. 114031. DOI: 10.1103/PhysRevD.106.114031. arXiv: 2202.00953 [nucl-th] (cit. on pp. 49, 65, 158).

[Ada+23] Christoph Adam et al. “Kaon condensation in skyrmion matter and compact stars”. In: *Phys. Rev. D* 107.7 (2023), p. 074007. DOI: 10.1103/PhysRevD.107.074007. arXiv: 2212.00385 [nucl-th] (cit. on pp. 4, 49, 65, 89, 91, 92, 158).

[Ada+15d] Christoph. Adam et al. “BPS Skyrmions as neutron stars”. In: *Physics Letters B* 742 (Mar. 2015), pp. 136–142. ISSN: 0370-2693. DOI: 10.1016/j.physletb.2015.01.027 (cit. on pp. 97, 99).

[ANW83a] Gregory S Adkins, Chiara R Nappi, and Edward Witten. “Static properties of nucleons in the Skyrme model”. In: *Nuclear Physics B* 228.3 (1983), pp. 552–566 (cit. on pp. 4, 32).

[AN84] Gregory S. Adkins and Chiara R. Nappi. “Stabilization of Chiral Solitons via Vector Mesons”. In: *Phys. Lett. B* 137 (1984), pp. 251–256. DOI: 10.1016/0370-2693(84)90239-9 (cit. on p. 4).

[ANW83b] Gregory S. Adkins, Chiara R. Nappi, and Edward Witten. “Static Properties of Nucleons in the Skyrme Model”. In: *Nucl. Phys. B* 228 (1983), p. 552. DOI: 10.1016/0550-3213(83)90559-X (cit. on pp. x, 3, 7, 12).

[Aff81] Ian Affleck. “On constrained instantons”. In: *Nuclear Physics B* 191.2 (1981), pp. 429–444. ISSN: 0550-3213. DOI: https://doi.org/10.1016/0550-3213(81)90307-2 (cit. on pp. 17, 19).

[Aku+19] T. Akutsu et al. “KAGRA: 2.5 Generation Interferometric Gravitational Wave Detector”. In: *Nature Astron.* 3.1 (2019), pp. 35–40. DOI: 10.1038/s41550-018-0658-y (cit. on p. xxxiv).

[Alf+08] Mark G. Alford et al. “Color superconductivity in dense quark matter”. In: *Rev. Mod. Phys.* 80 (4 Nov. 2008), pp. 1455–1515. DOI: 10.1103/RevModPhys.80.1455 (cit. on p. xxx).

[Alf+21] Mark G. Alford et al. “Beta Equilibrium under Neutron Star Merger Conditions”. In: *Universe* 7.11 (2021). ISSN: 2218-1997. URL: https://www.mdpi.com/2218-1997/7/11/399 (cit. on p. 81).

[AG85] Luis Alvarez-Gaume and Paul H. Ginsparg. “The Structure of Gauge and Gravitational Anomalies”. In: *Annals Phys.* 161 (1985). Ed. by A. Salam and E. Sezgin. [Erratum: Annals Phys. 171, 233 (1986)], p. 423. DOI: 10.1016/0003-4916(85)90087-9 (cit. on p. xxix).

[Ama+17] Pau Amaro-Seoane et al. *Laser Interferometer Space Antenna*. Feb. 2017. DOI: 10.48550/arXiv.1702.00786. arXiv: 1702.00786 [astro-ph.IM] (cit. on p. xxxiv).

[AT07] I. V. Anikin and O. V. Teryaev. “Dispersion relations and subtractions in hard exclusive processes”. In: *Phys. Rev. D* 76 (2007), p. 056007. DOI: 10.1103/PhysRevD.76.056007. arXiv: 0704.2185 [hep-ph] (cit. on p. 41).

[Ann+20] Eemeli Annala et al. “Evidence for quark-matter cores in massive neutron stars”. In: *Nature Phys.* 16.9 (2020), pp. 907–910. DOI: 10.1038/s41567-020-0914-9. arXiv: 1903.09121 [astro-ph.HE] (cit. on p. xxxiii).

[ADM59] Richard L. Arnowitt, Stanley Deser, and Charles W. Misner. "Dynamical Structure and Definition of Energy in General Relativity". In: *Phys. Rev.* 116 (1959), pp. 1322–1330. DOI: 10.1103/PhysRev.116.1322 (cit. on p. 101).

[Arr+23] John Arrington et al. *The Jefferson Lab tritium program of nucleon and nuclear structure measurements*. Apr. 2023. arXiv: 2304.09998 [nucl-ex] (cit. on p. 28).

[AHS77] M. F. Atiyah, Nigel J. Hitchin, and I. M. Singer. "Deformations of Instantons". In: *Proc. Nat. Acad. Sci.* 74 (1977), pp. 2662–2663. DOI: 10.1073/pnas.74.7.2662 (cit. on p. 15).

[AM93] M. F. Atiyah and N. S. Manton. "Geometry and kinematics of two skyrmions". In: *Commun. Math. Phys.* 153 (1993), pp. 391–422. DOI: 10.1007/BF02096649 (cit. on p. 15).

[Ati+78] M. F. Atiyah et al. "Construction of Instantons". In: *Phys. Lett. A* 65 (1978). Ed. by Mikhail A. Shifman, pp. 185–187. DOI: 10.1016/0375-9601(78)90141-X (cit. on p. 23).

[AM89] M.F. Atiyah and N.S. Manton. "Skyrmions from instantons". In: *Physics Letters B* 222.3 (1989), pp. 438–442. ISSN: 0370-2693. DOI: https://doi.org/10.1016/0370-2693(89)90340-7 (cit. on p. 14).

[AS05] Michael Atiyah and Paul M. Sutcliffe. "Skyrmions, instantons, mass and curvature". In: *Physics Letters B* 605.1 (2005), pp. 106–114. DOI: https://doi.org/10.1016/j.physletb.2004.11.015. arXiv: hep-th/0411052 (cit. on p. 24).

[Auc+23] Pierre Auclair et al. *Cosmic string bursts in LISA*. May 2023. arXiv: 2305.11653 [gr-qc] (cit. on p. xxix).

[Bal+10] M Baldo et al. "Energy density functional on a microscopic basis". In: *J. Phys. G* 37 (2010), p. 064015. DOI: 10.1088/0954-3899/37/6/064015. arXiv: 1005.1810 [nucl-th] (cit. on p. 104).

[BI66] Myron Bander and Claude Itzykson. "Group theory and the Hydrogen atom". In: *Rev. Mod. Phys.* 38 (1966), pp. 330–345. DOI: 10.1103/RevModPhys.38.330 (cit. on p. 12).

[Bas96] W. K. Baskerville. "Quantization of global isospin in the Skyrme crystal". In: *Phys. Lett. B* 380 (1996), pp. 106–112. DOI: 10.1016/0370-2693(96)00409-1 (cit. on pp. 70, 75).

[Bat+09] Richard A. Battye et al. "Light Nuclei of Even Mass Number in the Skyrme Model". In: *Phys. Rev. C* 80 (2009), p. 034323. DOI: 10.1103/PhysRevC.80.034323. arXiv: 0905.0099 [nucl-th] (cit. on pp. 3, 4).

[Bau+13] Michi Bauböck et al. "Relations between neutron star parameters in the Hartle-Thorne approximation". In: *Astrophys. J.* 777.1 (Oct. 2013), p. 68. ISSN: 1538-4357. DOI: 10.1088/0004-637x/777/1/68. arXiv: 1306.0569 [astro-ph.HE] (cit. on p. 107).

[Bel+75] A. A. Belavin et al. "Pseudoparticle Solutions of the Yang-Mills Equations". In: *Phys. Lett. B* 59 (1975). Ed. by J. C. Taylor, pp. 85–87. DOI: 10.1016/0370-2693(75)90163-X (cit. on pp. xxix, 18).

[Ben09] BenRG. - *Own work, Public Domain*. 2009. URL: https://commons.wikimedia.org/w/index.php?curid=7900237 (visited on 04/23/2023) (cit. on pp. xxi, 160).

[BL99] O. G. Benvenuto and G. Lugones. "The phase transition from nuclear matter to quark matter during proto-neutron star evolution". In: *Mon. Not. Roy. Astron. Soc.* 304 (1999), p. L25. DOI: 10.1046/j.1365-8711.1999.02458.x (cit. on p. xxxiii).

[Ber+05] E. Berti et al. "Rotating neutron stars: an invariant comparison of approximate and numerical space-time models". English. In: *MNRAS* 358.3 (2005), pp. 923–938. ISSN: 0035-8711. DOI: 10.1111/j.1365-2966.2005.08812.x (cit. on pp. 106, 107).

[Bet90] H. A. Bethe. "Supernova mechanisms". In: *Rev. Mod. Phys.* 62 (4 Oct. 1990), pp. 801–866. DOI: 10.1103/RevModPhys.62.801 (cit. on p. xxxii).

[BH18] Sven Bjarke Gudnason and Chris J. Halcrow. "Vibrational modes of Skyrmions". In: *Phys. Rev. D* 98.12 (2018), p. 125010. DOI: 10.1103/PhysRevD.98.125010. arXiv: 1811.00562 [hep-th] (cit. on pp. 3, 47, 57, 139).

[BOS18] Jose J. Blanco-Pillado, Ken D. Olum, and Xavier Siemens. "New limits on cosmic strings from gravitational wave observation". In: *Phys. Lett. B* 778 (2018), pp. 392–396. DOI: 10.1016/j.physletb.2018.01.050. arXiv: 1709.02434 [astro-ph.CO] (cit. on p. xxix).

[BDR89] U. Blom, K. Dannbom, and D. Riska. "Hyperons as bound states in the skyrme model". In: *Nuclear Physics* 493 (1989), pp. 384–396 (cit. on p. 84).

[Bog76] E B Bogomol'nyi. "The stability of classical solutions". In: *Sov. J. Nucl. Phys. (Engl. Transl.); (United States)* (Oct. 1976). URL: https://www.osti.gov/biblio/7309001 (cit. on p. 98).

[Bom17] Ignazio Bombaci. "The Hyperon Puzzle in Neutron Stars". In: *JPS Conf. Proc.* 17 (2017). Ed. by H. Tamura, p. 101002. DOI: 10.7566/JPSCP.17.101002. arXiv: 1601.05339 [nucl-th] (cit. on p. 83).

[BH20] Renaud Boussarie and Yoshitaka Hatta. "QCD analysis of near-threshold quarkonium leptoproduction at large photon virtualities". In: *Phys. Rev. D* 101.11 (2020), p. 114004. DOI: 10.1103/PhysRevD.101.114004. arXiv: 2004.12715 [hep-ph] (cit. on p. 41).

[BC86] Eric Braaten and Larry Carson. "The Deuteron as a Soliton in the Skyrme Model". In: *Phys. Rev. Lett.* 56 (1986), p. 1897. DOI: 10.1103/PhysRevLett.56.1897 (cit. on p. 3).

[BC88] Eric Braaten and Larry Carson. "The Deuteron as a Toroidal Skyrmion". In: *Phys. Rev. D* 38 (1988), p. 3525. DOI: 10.1103/PhysRevD.38.3525 (cit. on p. 45).

[BC89] Eric Braaten and Larry Carson. "The Deuteron as a Toroidal Skyrmion: Electromagnetic Form-factors". In: *Phys. Rev. D* 39 (1989), p. 838. DOI: 10.1103/PhysRevD.39.838 (cit. on pp. 28, 39).

[BTC90] Eric Braaten, Steve Townsend, and Larry Carson. "Novel Structure of Static Multi - Soliton Solutions in the Skyrme Model". In: *Phys. Lett. B* 235 (1990), pp. 147–152. DOI: 10.1016/0370-2693(90)90111-I (cit. on p. 47).

[BTW86] Eric Braaten, Sze-Man Tse, and Charles Willcox. "Electroweak form factors of the Skyrmion". In: *Phys. Rev. D* 34 (5 Sept. 1986), pp. 1482–1492. DOI: 10.1103/PhysRevD.34.1482 (cit. on pp. 28, 31, 54).

[Bro+18] Edward F. Brown et al. "Rapid neutrino cooling in the neutron star MXB 1659-29". In: *Phys. Rev. Lett.* 120.18 (2018), p. 182701. DOI: 10.1103/PhysRevLett.120.182701 (cit. on p. 81).

[Bur16] Carsten Burgard. *A TikZ diagram of the current standard model of physics*. 2016. URL: https://texample.net/tikz/examples/model-physics/ (visited on 04/18/2023) (cit. on p. xx).

[Bur+21] G. Fiorella Burgio et al. "A Modern View of the Equation of State in Nuclear and Neutron Star Matter". In: *Symmetry* 13.3 (Feb. 2021), p. 400. ISSN: 2073-8994. DOI: 10.3390/sym13030400. URL: http://dx.doi.org/10.3390/sym13030400 (cit. on p. 66).

[Cai+15] Bao-Jun Cai et al. "Critical density and impact of $\Delta(1232)$ resonance formation in neutron stars". In: *Phys. Rev. C* 92 (1 July 2015), p. 015802. DOI: 10.1103/PhysRevC.92.015802 (cit. on p. xxxiii).

[CK85] Curtis G. Callan and Igor R. Klebanov. "Bound-state approach to strangeness in the Skyrme model". In: *Nuclear Physics B* 262.2 (1985), pp. 365–382. DOI: https://doi.org/10.1016/0550-3213(85)90292-5 (cit. on pp. 83, 84).

[Cam+14] A. Camsonne et al. "JLab Measurement of the ^{4}He Charge Form Factor at Large Momentum Transfers". In: *Phys. Rev. Lett.* 112 (13 Apr. 2014), p. 132503. DOI: 10.1103/PhysRevLett.112.132503 (cit. on p. 28).

[Car+15] J. Carlson et al. "Quantum Monte Carlo methods for nuclear physics". In: *Rev. Mod. Phys.* 87 (2015), p. 1067. DOI: 10.1103/RevModPhys.87.1067. arXiv: 1412.3081 [nucl-th] (cit. on p. xxxi).

[Car91a] Larry Carson. "B = 3 nuclei as quantized multiskyrmions". In: *Phys. Rev. Lett.* 66 (1991), pp. 1406–1409. DOI: 10.1103/PhysRevLett.66.1406 (cit. on pp. 14, 45, 49).

[Car91b] Larry Carson. "Static properties of He-3 and H-3 in the Skyrme model". In: *Nucl. Phys. A* 535 (1991), pp. 479–496. DOI: 10.1016/0375-9474(91)90472-I (cit. on pp. 28, 30, 35, 36, 46, 48).

[Cas+89] L. Castillejo et al. "Dense skyrmion systems". In: *Nuc. Phys. A* 501.4 (1989), pp. 801–812. ISSN: 0375-9474. DOI: https://doi.org/10.1016/0375-9474(89)90161-9 (cit. on p. 67).

[Ceb+07] C. Cebulla et al. "The Nucleon form-factors of the energy momentum tensor in the Skyrme model". In: *Nucl. Phys. A* 794 (2007), pp. 87–114. DOI: 10.1016/j.nuclphysa.2007.08.004. arXiv: hep-ph/0703025 (cit. on pp. 42, 47, 49, 52).

[CNS77] Louis S. Celenza, W.T. Nutt, and C.M. Shakin. "Measurement of pion-nucleus total cross sections as a test for the existence of a pion condensate". In: *Physics Letters B* 72.1 (1977), pp. 23–26. ISSN: 0370-2693. DOI: https://doi.org/10.1016/0370-2693(77)90053-3 (cit. on p. xxxiii).

[CH08] Nicolas Chamel and Pawel Haensel. "Physics of Neutron Star Crusts". In: *Living Rev. Relativ.* 11.1 (Dec. 2008), p. 10. DOI: 10.12942/lrr-2008-10. arXiv: 0812.3955 [astro-ph] (cit. on pp. xxxiii, 104).

[Cha20] Katerina Chatziioannou. "Neutron star tidal deformability and equation of state constraints". In: *Gen. Rel. Grav.* 52.11 (2020), p. 109. DOI: 10.1007/s10714-020-02754-3 (cit. on p. 129).

[Chi+16] Ching-Kai Chiu et al. "Classification of topological quantum matter with symmetries". In: *Rev. Mod. Phys.* 88.3 (2016), p. 035005. DOI: 10.1103/RevModPhys.88.035005. arXiv: 1505.03535 [cond-mat.mes-hall] (cit. on p. xxix).

[Cir+19] Vincenzo Cirigliano et al. *Precision Beta Decay as a Probe of New Physics*. July 2019. arXiv: 1907.02164 [nucl-ex] (cit. on p. 37).

[Cor18] Josh Cork. "Skyrmions from calorons". In: *JHEP* 11 (2018), p. 137. DOI: 10.1007/JHEP11(2018)137. arXiv: 1810.04143 [hep-th] (cit. on p. 15).

[CH22] Josh Cork and Chris J. Halcrow. "ADHM skyrmions". In: *Nonlinearity* 35.8 (2022), pp. 3944–3990. DOI: 10.1088/1361-6544/ac72e6. arXiv: 2110.15190 [hep-th] (cit. on pp. 15, 23).

[DN09] Thibault Damour and Alessandro Nagar. "Relativistic tidal properties of neutron stars". In: *Phys. Rev. D* 80 (2009), p. 084035. DOI: 10.1103/PhysRevD.80.084035. arXiv: 0906.0096 [gr-qc] (cit. on p. 120).

[DL14] Pawel Danielewicz and Jenny Lee. "Symmetry Energy II: Isobaric Analog States". In: *Nucl. Phys. A* 922 (2014), pp. 1–70. DOI: 10.1016/j.nuclphysa.2013.11.005. arXiv: 1307.4130 [nucl-th] (cit. on p. 79).

[Dia96] Dmitri Diakonov. "Chiral symmetry breaking by instantons". In: *Proc. Int. Sch. Phys. Fermi* 130 (1996). Ed. by A. Di Giacomo and Dmitri Diakonov, pp. 397–432. DOI: 10.3254/978-1-61499-215-8-397. arXiv: hep-ph/9602375 (cit. on p. 15).

[DGH23] John F. Donoghue, Eugene Golowich, and Barry R. Holstein. "Symmetries and anomalies". In: *Dynamics of the Standard Model*. 2nd ed. Cambridge Monographs on Particle Physics, Nuclear Physics and Cosmology. Cambridge University Press, 2023, pp. 76–105. DOI: 10.1017/9781009291033.004 (cit. on pp. xxii, 26).

[DLP14] Alessandro Drago, Andrea Lavagno, and Giuseppe Pagliara. "Can very compact and very massive neutron stars both exist?" In: *Phys. Rev. D* 89.4 (2014), p. 043014. DOI: 10.1103/PhysRevD.89.043014. arXiv: 1309.7263 [nucl-th] (cit. on p. xxxiii).

[Dra+14] Alessandro Drago et al. "Early appearance of Δ isobars in neutron stars". In: *Phys. Rev. C* 90 (6 Dec. 2014), p. 065809. DOI: 10.1103/PhysRevC.90.065809. arXiv: 1407.2843 [astro-ph.SR] (cit. on p. xxxiii).

[DHW21] C. Drischler, J. W. Holt, and C. Wellenhofer. "Chiral Effective Field Theory and the High-Density Nuclear Equation of State". In: *Ann. Rev. Nucl. Part. Sci.* 71 (2021), pp. 403–432. DOI: 10.1146/annurev-nucl-102419-041903. arXiv: 2101.01709 [nucl-th] (cit. on p. xxxi).

[Dun13] Maciej Dunajski. "Skyrmions from gravitational instantons". In: *Proc. Roy. Soc. Lond. A* 469 (2013), p. 20120576. DOI: 10.1098/rspa.2012.0576. arXiv: 1206.0016 [hep-th] (cit. on p. 15).

[Dur+23] B. Duran et al. "Determining the gluonic gravitational form factors of the proton". In: *Nature* 615.7954 (Mar. 2023), pp. 813–816. DOI: 10.1038/s41586-023-05730-4. arXiv: 2207.05212 [nucl-ex] (cit. on pp. 59, 61).

[Eic+16] Gernot Eichmann et al. "Baryons as relativistic three-quark bound states". In: *Prog. Part. Nucl. Phys.* 91 (2016), pp. 1–100. DOI: 10.1016/j.ppnp.2016.07.001. arXiv: 1606.09602 [hep-ph] (cit. on p. 28).

[Ell17] Joshua Ellis. "TikZ-Feynman: Feynman diagrams with TikZ". In: *Comput. Phys. Commun.* 210 (2017), pp. 103–123. DOI: 10.1016/j.cpc.2016.08.019. arXiv: 1601.05437 [hep-ph] (cit. on p. xii).

[Epe+22] E. Epelbaum et al. "Definition of Local Spatial Densities in Hadrons". In: *Phys. Rev. Lett.* 129.1 (2022), p. 012001. DOI: 10.1103/PhysRevLett.129.012001. arXiv: 2201.02565 [hep-ph] (cit. on pp. 53, 54).

[Esp90] Olivier Espinosa. "High-Energy Behavior of Baryon and Lepton Number Violating Scattering Amplitudes and Breakdown of Unitarity in the Standard Model". In: *Nucl. Phys. B* 343 (1990), pp. 310–340. DOI: 10.1016/0550-3213(90)90473-Q (cit. on pp. 16, 17, 20, 22, 42).

[Ess+21] Reed Essick et al. "Detailed examination of astrophysical constraints on the symmetry energy and the neutron skin of Pb208 with minimal modeling assumptions". In: *Phys. Rev. C* 104.6 (2021), p. 065804. DOI: 10.1103/PhysRevC.104.065804 (cit. on p. 66).

[FR68] D. Finkelstein and J. Rubinstein. "Connection between spin, statistics, and kinks". In: *J. Math. Phys.* 9 (1968), pp. 1762–1779. DOI: 10.1063/1.1664510 (cit. on p. 11).

[FF18] G. Fiorella Burgio and Anthea F. Fantina. "Nuclear Equation of state for Compact Stars and Supernovae". In: *Astrophys. Space Sci. Libr.* 457 (2018), pp. 255–335. DOI: 10.1007/978-3-319-97616-7_6 (cit. on p. 66).

[FC19] Adam Freese and Ian C. Cloët. "Gravitational form factors of light mesons". In: *Phys. Rev. C* 100.1 (2019). [Erratum: Phys.Rev.C 105, 059901 (2022)], p. 015201. DOI: 10.1103/PhysRevC.100.015201. arXiv: 1903.09222 [nucl-th] (cit. on p. 45).

[Fuj+22] Mitsutoshi Fujita et al. "Nucleon D-term in holographic quantum chromodynamics". In: *PTEP* 2022.9 (2022), 093B06. DOI: 10.1093/ptep/ptac110. arXiv: 2206.06578 [hep-th] (cit. on p. 49).

[GV22] Haiyan Gao and Marc Vanderhaeghen. "The proton charge radius". In: *Rev. Mod. Phys.* 94.1 (2022), p. 015002. DOI: 10.1103/RevModPhys.94.015002. arXiv: 2105.00571 [hep-ph] (cit. on p. 53).

[GHH23] Alberto Garcia Martin-Caro, Miguel Huidobro, and Yoshitaka Hatta. "Gravitational form factors of nuclei in the Skyrme model". In: *Phys. Rev. D* 108.3 (2023), p. 034014. DOI: 10.1103/PhysRevD.108.034014. arXiv: 2304.05994 [nucl-th] (cit. on pp. 3, 25, 157).

[Gar22] Alberto García Martín-Caro. "Constrained instanton approximation of Skyrmions with massive pions". In: *Phys. Lett. B* 835 (2022), p. 137532. DOI: 10.1016/j.physletb.2022.137532. arXiv: 2209.06607 [hep-th] (cit. on pp. 3, 19, 159).

[GAO12] Keith C. Gendreau, Zaven Arzoumanian, and Takashi Okajima. "The Neutron star Interior Composition ExploreR (NICER): an Explorer mission of opportunity for soft x-ray timing spectroscopy". In: *Space Telescopes and Instrumentation 2012: Ultraviolet to Gamma Ray*. Ed. by Tadayuki Takahashi, Stephen S. Murray, and Jan-Willem A. den Herder. Vol. 8443. Society of Photo-Optical Instrumentation Engineers (SPIE) Conference Series. Sept. 2012, 844313, p. 844313. DOI: 10.1117/12.926396 (cit. on p. 95).

[Gib03] G. W. Gibbons. "Causality and the Skyrme model". In: *Phys. Lett. B* 566 (2003), pp. 171–174. DOI: 10.1016/S0370-2693(03)00384-8. arXiv: hep-th/0302149 (cit. on p. 100).

[GPH22] Hana Gil, Panagiota Papakonstantinou, and Chang Ho Hyun. "Constraints on the curvature of nuclear symmetry energy from recent astronomical data within the KIDS framework". In: *Int. J. Mod. Phys. E* 31.01 (2022), p. 2250013. DOI: 10.1142/S0218301322500136. arXiv: 2110.09802 [nucl-th] (cit. on p. 66).

[GHS15] Mike Gillard, Derek Harland, and Martin Speight. "Skyrmions with low binding energies". In: *Nucl. Phys. B* 895 (2015), pp. 272–287. DOI: 10.1016/j.nuclphysb.2015.04.005 (cit. on p. 3).

[Giu93] Domenico Giulini. "On the possibility of spinorial quantization in the Skyrme model". In: *Mod. Phys. Lett. A* 8 (1993), pp. 1917–1924. DOI: 10.1142/S0217732393001641. arXiv: hep-th/9301101 (cit. on pp. 10, 11).

[Gle85] Norman K. Glendenning. "Neutron Stars Are Giant Hypernuclei?" In: *Astrophys. J.* 293 (1985), pp. 470–493. DOI: 10.1086/163253 (cit. on p. xxxiii).

[Gle92] Norman K. Glendenning. "First order phase transitions with more than one conserved charge: Consequences for neutron stars". In: *Phys. Rev. D* 46 (1992), pp. 1274–1287. DOI: 10.1103/PhysRevD.46.1274 (cit. on p. 91).

[GS99] Norman K. Glendenning and Jurgen Schaffner-Bielich. "First order kaon condensate". In: *Phys. Rev. C* 60 (1999), p. 025803. DOI: 10.1103/PhysRevC.60.025803. arXiv: astro-ph/9810290 (cit. on pp. xxxiii, 91).

[Gou10] Eric Gourgoulhon. "An Introduction to the theory of rotating relativistic stars". In: *CompStar 2010: School and Workshop on Computational Tools for Compact Star Astrophysics*. Mar. 2010. arXiv: 1003.5015 [gr-qc] (cit. on p. 116).

[Goy+17] V. A. Goy et al. "Sign problem in finite density lattice QCD". In: *PTEP* 2017.3 (2017), p. 031D01. DOI: 10.1093/ptep/ptx018. arXiv: 1611.08093 [hep-lat] (cit. on p. xxx).

[Gre+20] S. K. Greif et al. "Equation of state constraints from nuclear physics, neutron star masses, and future moment of inertia measurements". In: *Astrophys. J.* 901.2 (2020), p. 155. DOI: 10.3847/1538-4357/abaf55. arXiv: 2005.14164 [astro-ph.HE] (cit. on p. 129).

[GM09] W. Greiner and B. Müller. *Gauge Theory of Weak Interactions*. 4th ed. Springer Berlin, Heidelberg, 2009. ISBN: 9783540878438. DOI: 10.1007/978-3-540-87843-8 (cit. on p. 27).

[Gud16] Sven Bjarke Gudnason. "Loosening up the Skyrme model". In: *Phys. Rev. D* 93.6 (2016), p. 065048. DOI: 10.1103/PhysRevD.93.065048 (cit. on p. 3).

[GH22] Sven Bjarke Gudnason and Chris J. Halcrow. "A Smörgåsbord of Skyrmions". In: *JHEP* 08 (2022), p. 117. DOI: 10.1007/JHEP08(2022)117. arXiv: 2202.01792 [hep-th] (cit. on pp. 7, 58).

[GS20] Sven Bjarke Gudnason and James Martin Speight. "Realistic classical binding energies in the ω-Skyrme model". In: *JHEP* 07 (2020), p. 184. DOI: 10.1007/JHEP07(2020)184. arXiv: 2004.12862 [hep-th] (cit. on p. 138).

[GJL21] Yuxun Guo, Xiangdong Ji, and Yizhuang Liu. "QCD Analysis of Near-Threshold Photon-Proton Production of Heavy Quarkonium". In: *Phys. Rev. D* 103.9 (2021), p. 096010. DOI: 10.1103/PhysRevD.103.096010. arXiv: 2103.11506 [hep-ph] (cit. on p. 41).

[Gür83] Yekta Gürsel. "Multipole moments for stationary systems: The equivalence of the Geroch-Hansen formulation and the Thorne formulation". In: *Gen. Relativ. Gravit.* 15.8 (1983), pp. 737–754. DOI: 10.1007/BF01031881. URL: https://doi.org/10.1007/BF01031881 (cit. on p. 118).

[GS06] V. Guzey and M. Siddikov. "On the A-dependence of nuclear generalized parton distributions". In: *J. Phys. G* 32 (2006), pp. 251–268. DOI: 10.1088/0954-3899/32/3/002. arXiv: hep-ph/0509158 (cit. on pp. 42, 52).

[Gyu04] Miklos Gyulassy. "The QGP discovered at RHIC". In: *NATO Advanced Study Institute: Structure and Dynamics of Elementary Matter*. Mar. 2004, pp. 159–182. arXiv: nucl-th/0403032 (cit. on p. xxx).

[HH20] Chris J. Halcrow and Derek Harland. "An attractive spin-orbit potential from the Skyrme model". In: *Phys. Rev. Lett.* 125.4 (2020), p. 042501. DOI: 10.1103/PhysRevLett.125.042501 (cit. on p. 4).

[HH22] Chris J. Halcrow and Derek Harland. "Nucleon-nucleon potential from instanton holonomies". In: *Phys. Rev. D* 106.9 (2022), p. 094011. DOI: 10.1103/PhysRevD.106.094011. arXiv: 2208.04863 [hep-th] (cit. on p. 15).

[HKM17] Chris J. Halcrow, C. King, and Nicholas S. Manton. "A dynamical α-cluster model of ^{16}O". In: *Phys. Rev. C* 95.3 (2017), p. 031303. DOI: 10.1103/PhysRevC.95.031303 (cit. on pp. 3, 4).

[HW21] Chris J. Halcrow and Thomas Winyard. "A consistent two-skyrmion configuration space from instantons". In: *JHEP* 12 (2021), p. 039. DOI: 10.1007/JHEP12(2021)039. arXiv: 2103.15669 [hep-th] (cit. on p. 15).

[HLS23] Derek Harland, Paul Leask, and Martin Speight. *Skyrme crystals with massive pions*. May 2023. arXiv: 2305.14005 [hep-th] (cit. on p. 69).

[HH18] Ian Harry and Tanja Hinderer. "Observing and measuring the neutron-star equation-of-state in spinning binary neutron star systems". In: *Class. Quant. Grav.* 35.14 (2018), p. 145010 (cit. on p. xxxiv).

[Har67] James B. Hartle. "Slowly Rotating Relativistic Stars. I. Equations of Structure". In: *Astrophys. J.* 150 (Dec. 1967), p. 1005. DOI: 10.1086/149400 (cit. on pp. 106, 107, 109, 110, 112–114).

[HSS75] James B. Hartle, R. F. Sawyer, and D. J. Scalapino. "Pion Condensed Matter at High Densities: Equation of State and Stellar Models". In: *Astrophys. J.* 199 (July 1975), pp. 471–481. DOI: 10.1086/153713 (cit. on p. xxxiii).

[HRT18] Yoshitaka Hatta, Abha Rajan, and Kazuhiro Tanaka. "Quark and gluon contributions to the QCD trace anomaly". In: *JHEP* 12 (2018), p. 008. DOI: 10.1007/JHEP12(2018)008. arXiv: 1810.05116 [hep-ph] (cit. on p. 58).

[HS21] Yoshitaka Hatta and Mark Strikman. "ϕ-meson lepto-production near threshold and the strangeness D-term". In: *Phys. Lett. B* 817 (2021), p. 136295. DOI: 10.1016/j.physletb.2021.136295. arXiv: 2102.12631 [hep-ph] (cit. on p. 41).

[HY18] Yoshitaka Hatta and Di-Lun Yang. "Holographic J/ψ production near threshold and the proton mass problem". In: *Phys. Rev. D* 98.7 (2018), p. 074003. DOI: 10.1103/PhysRevD.98.074003. arXiv: 1808.02163 [hep-ph] (cit. on p. 41).

[HE73] Stephen W. Hawking and George F. R. Ellis. *The Large Scale Structure of Space–Time*. Cambridge University Press, 1973. DOI: 10.1017/cbo9780511524646 (cit. on p. 99).

[HPS93] H. Heiselberg, C. J. Pethick, and E. F. Staubo. "Quark matter droplets in neutron stars". In: *Phys. Rev. Lett.* 70 (10 Mar. 1993), pp. 1355–1359. DOI: 10.1103/PhysRevLett.70.1355 (cit. on p. xxxiii).

[Hew+68] A. Hewish et al. "Observation of a Rapidly Pulsating Radio Source". In: *Nature* 217.5130 (Feb. 1968), pp. 709–713. DOI: 10.1038/217709a0 (cit. on p. xxxii).

[Hin08] Tanja Hinderer. "Tidal Love numbers of neutron stars". In: *Astrophys. J.* 677 (2008), pp. 1216–1220. DOI: 10.1086/533487. arXiv: 0711.2420 [astro-ph] (cit. on pp. xxxiv, 119).

[Hin+10] Tanja Hinderer et al. "Tidal deformability of neutron stars with realistic equations of state and their gravitational wave signatures in binary inspiral". In: *Phys. Rev. D* 81 (2010), p. 123016. DOI: 10.1103/PhysRevD.81.123016. arXiv: 0911.3535 [astro-ph.HE] (cit. on pp. 119, 120, 129).

[Hol06] Barry R. Holstein. "Metric modifications for a massive spin 1 particle". In: *Phys. Rev. D* 74 (2006), p. 084030. DOI: 10.1103/PhysRevD.74.084030. arXiv: gr-qc/0607051 (cit. on p. 44).

[HOA91] A. Hosaka, M. Oka, and R. D. Amado. "Skyrmions and their interactions using the Atiyah-Manton construction". In: *Nucl. Phys. A* 530 (1991), pp. 507–531. DOI: 10.1016/0375-9474(91)90766-Y (cit. on p. 15).

[HMS98] Conor J. Houghton, Nicholas S. Manton, and Paul M. Sutcliffe. "Rational maps, monopoles and Skyrmions". In: *Nucl. Phys. B* 510 (1998), pp. 507–537. DOI: 10.1016/S0550-3213(97)00619-6. arXiv: hep-th/9705151 (cit. on p. 6).

[Hoy+16] Carlos Hoyos et al. "Holographic quark matter and neutron stars". In: *Phys. Rev. Lett.* 117.3 (2016), p. 032501. DOI: 10.1103/PhysRevLett.117.032501. arXiv: 1603.02943 [hep-ph] (cit. on p. xxxi).

[Hub75] A. Hubert. "Domain wall structures in thin magnetic films". In: *IEEE Transactions on Magnetics* 11.5 (1975), pp. 1285–1290. DOI: 10.1109/TMAG.1975.1058830 (cit. on p. xxix).

[Hun07] J. D. Hunter. "Matplotlib: A 2D graphics environment". In: *Computing in Science & Engineering* 9.3 (2007), pp. 90–95. DOI: 10.1109/MCSE.2007.55 (cit. on p. xii).

[Irw00] Patrick Irwin. "Zero mode quantization of multi - Skyrmions". In: *Phys. Rev. D* 61 (2000), p. 114024. DOI: 10.1103/PhysRevD.61.114024. arXiv: hep-th/9804142 (cit. on p. 11).

[JR77] R. Jackiw and C. Rebbi. "Degrees of freedom in pseudoparticle systems". In: *Physics Letters B* 67.2 (1977), pp. 189–192. ISSN: 0370-2693. DOI: https://doi.org/10.1016/0370-2693(77)90100-9 (cit. on p. 15).

[Jac+85] A. Jackson et al. "A modified skyrmion". In: *Phys. Lett. B* 154.2 (1985), pp. 101–106. ISSN: 0370-2693. DOI: https://doi.org/10.1016/0370-2693(85)90566-0 (cit. on pp. 3, 4, 49).

[Jaf21] Robert L. Jaffe. "Ambiguities in the definition of local spatial densities in light hadrons". In: *Phys. Rev. D* 103.1 (2021), p. 016017. DOI: 10.1103/PhysRevD.103.016017. arXiv: 2010.15887 [hep-ph] (cit. on p. 53).

[Jär22] Matti Järvinen. "Holographic modeling of nuclear matter and neutron stars". In: *Eur. Phys. J. C* 82.4 (2022), p. 282. DOI: 10.1140/epjc/s10052-022-10227-x. arXiv: 2110.08281 [hep-ph] (cit. on p. xxxi).

[JY20] Nan Jiang and Kent Yagi. "Analytic I-Love-C relations for realistic neutron stars". In: *Phys. Rev. D* 101 (12 June 2020), p. 124006. DOI: 10.1103/PhysRevD.101.124006. arXiv: 2003.10498 [gr-qc] (cit. on pp. 124, 125).

[JWC19] Rongrong Jiang, Dehua Wen, and Houyuan Chen. "Universal behavior of a compact star based upon the gravitational binding energy". In: *Phys. Rev. D* 100 (12 Dec. 2019), p. 123010. DOI: 10.1103/PhysRevD.100.123010. URL: https://link.aps.org/doi/10.1103/PhysRevD.100.123010 (cit. on pp. 117, 127).

[JBR23] Hao Jiao, Robert Brandenberger, and Alexandre Refregier. *Early Structure Formation from Cosmic String Loops in Light of Early JWST Observations*. Apr. 2023. arXiv: 2304.06429 [astro-ph.CO] (cit. on p. xxix).

[KCP05] Alexander C. Kalloniatis, Jonathan D. Carroll, and Byung-Yoon Park. "Neutral pion decay into nu anti-nu in dense skyrmion matter". In: *Phys. Rev. D* 71 (2005), p. 114001. DOI: 10.1103/PhysRevD.71.114001. arXiv: hep-ph/0501117 (cit. on p. 34).

[KN88] D. B. Kaplan and A. E. Nelson. "Kaon Condensation in Dense Matter". In: *Nucl. Phys. A* 479 (1988). Ed. by J. Speth, p. 273c. DOI: 10.1016/0375-9474(88)90442-3 (cit. on p. xxxiii).

[KKM16] M. Karliner, C. King, and N. S. Manton. "Electron Scattering Intensities and Patterson Functions of Skyrmions". In: *J. Phys. G* 43.5 (2016), p. 055104. DOI: 10.1088/0954-3899/43/5/055104. arXiv: 1510.00280 [nucl-th] (cit. on p. 28).

[Kha21] Dmitri E. Kharzeev. "Mass radius of the proton". In: *Phys. Rev. D* 104 (5 Sept. 2021), p. 054015. DOI: 10.1103/PhysRevD.104.054015 (cit. on p. 59).

[Kib76] T. W. B. Kibble. "Topology of Cosmic Domains and Strings". In: *J. Phys. A* 9 (1976), pp. 1387–1398. DOI: 10.1088/0305-4470/9/8/029 (cit. on p. xxix).

[KS21] June-Young Kim and Bao-Dong Sun. "Gravitational form factors of a baryon with spin-3/2". In: *Eur. Phys. J. C* 81.1 (2021), p. 85. DOI: 10.1140/epjc/s10052-021-08852-z. arXiv: 2011.00292 [hep-ph] (cit. on pp. 42, 47).

[Kin+23] Garrett B. King et al. "Ab initio calculation of the β-decay spectrum of He6". In: *Phys. Rev. C* 107.1 (2023), p. 015503. DOI: 10.1103/PhysRevC.107.015503. arXiv: 2207.11179 [nucl-th] (cit. on pp. 37, 40).

[Kla+06] T. Klahn et al. "Constraints on the high-density nuclear equation of state from the phenomenology of compact stars and heavy-ion collisions". In: *Phys. Rev. C* 74 (2006), p. 035802. DOI: 10.1103/PhysRevC.74.035802 (cit. on p. 81).

[Kle85] Igor R. Klebanov. "Nuclear Matter in the Skyrme Model". In: *Nucl. Phys. B* 262 (1985), pp. 133–143. DOI: 10.1016/0550-3213(85)90068-9 (cit. on pp. 67, 73, 135, 144).

[Kle90] Igor R. Klebanov. "Strangeness in the Skyrme Model". In: *Hadrons and Hadronic Matter*. Ed. by D. Vautherin, F. Lenz, and J. W. Negele. Boston, MA: Springer US, 1990, pp. 223–262. ISBN: 978-1-4684-1336-6. DOI: 10.1007/978-1-4684-1336-6_8 (cit. on p. 84).

[Kli93] Frans R. Klinkhamer. "Existence of a new instanton in constrained Yang-Mills Higgs theory". In: *Nucl. Phys. B* 407 (1993), pp. 88–114. DOI: 10.1016/0550-3213(93)90275-T. arXiv: hep-ph/9306208 (cit. on p. 18).

[KO62] I. Yu. Kobzarev and L. B. Okun. "Gravitational interaction of fermions". In: *Zh. Eksp. Teor. Fiz.* 43 (1962), pp. 1904–1909 (cit. on p. 41).

[KMR17] Peter Koch, Berndt Müller, and Johann Rafelski. "From Strangeness Enhancement to Quark–Gluon Plasma Discovery". In: *Int. J. Mod. Phys. A* 32.31 (2017), p. 1730024. DOI: 10.1142/S0217751X17300241. arXiv: 1708.08115 [nucl-th] (cit. on p. xxx).

[KT01] J. B. Kogut and D. Toublan. "QCD at small nonzero quark chemical potentials". In: *Phys. Rev. D* 64 (2001), p. 034007. DOI: 10.1103/PhysRevD.64.034007. arXiv: hep-ph/0103271 (cit. on p. xxxii).

[KHS88] K.S. Krane, D. Halliday, and John Wiley & Sons. *Introductory Nuclear Physics*. Wiley, Nov. 1988. ISBN: 9780471805533. URL: https://www.wiley.com/en-dk/Introductory+Nuclear+Physics,+3rd+Edition-p-9780471805533 (cit. on p. 35).

[Kru03] Steffen Krusch. "Homotopy of rational maps and the quantization of skyrmions". In: *Annals Phys.* 304 (2003), pp. 103–127. DOI: 10.1016/S0003-4916(03)00014-9. arXiv: hep-th/0210310 (cit. on p. 9).

[Kru06] Steffen Krusch. "Finkelstein-Rubinstein constraints for the Skyrme model with pion masses". In: *Proc. Roy. Soc. Lond. A* 462 (2006), pp. 2001–2016. DOI: 10.1098/rspa.2006.1664. arXiv: hep-th/0509094 (cit. on p. 71).

[KS89] M. Kugler and S. Shtrikman. "Skyrmion crystals and their symmetries". In: *Phys. Rev. D* 40 (10 Nov. 1989), pp. 3421–3429. DOI: 10.1103/PhysRevD.40.3421 (cit. on p. 67).

[LEC20] Philippe Landry, Reed Essick, and Katerina Chatziioannou. "Nonparametric constraints on neutron star matter with existing and upcoming gravitational wave and pulsar observations". In: *Phys. Rev. D* 101 (12 June 2020), p. 123007. DOI: 10.1103/PhysRevD.101.123007. arXiv: 2003.04880 [astro-ph.HE] (cit. on p. 129).

[LP15] Philippe Landry and Eric Poisson. "Gravitomagnetic response of an irrotational body to an applied tidal field". In: *Phys. Rev. D* 91 (10 May 2015), p. 104026. DOI: 10.1103/PhysRevD.91.104026. URL: https://link.aps.org/doi/10.1103/PhysRevD.91.104026 (cit. on p. 122).

[Lat+91] James M. Lattimer et al. "Direct URCA process in neutron stars". In: *Phys. Rev. Lett.* 66 (21 May 1991), pp. 2701–2704. DOI: 10.1103/PhysRevLett.66.2701 (cit. on p. 81).

[LM14] P.H.C. Lau and N.S. Manton. "States of Carbon-12 in the Skyrme Model". In: *Phys. Rev. Lett.* 113.23 (2014), p. 232503. DOI: 10.1103/PhysRevLett.113.232503 (cit. on pp. 3, 4).

[LHW23] Paul Leask, Miguel Huidobro, and Andrzej Wereszczynski. *Quantized and gravitating multi-wall skyrmion crystals with applications to neutron stars*. June 2023. arXiv: 2306.04533 [hep-th] (cit. on p. 139).

[LPR11] Hyun Kyu Lee, Byung-Yoon Park, and Mannque Rho. "Half-Skyrmions, Tensor Forces and Symmetry Energy in Cold Dense Matter". In: *Phys. Rev. C* 83 (2011). [Erratum: Phys.Rev.C 84, 059902 (2011)], p. 025206. DOI: 10.1103/PhysRevC.84.059902. arXiv: 1005.0255 [nucl-th] (cit. on p. 80).

[Lee+21] Hyun Kyu Lee et al. “Cusp in the Symmetry Energy, Speed of Sound in Neutron Stars and Emergent Pseudo-Conformal Symmetry”. In: (July 2021). arXiv: 2107.01879 [nucl-th] (cit. on p. 80).

[LM94] R. A. Leese and N. S. Manton. “Stable instanton generated Skyrme fields with baryon numbers three and four”. In: *Nucl. Phys. A* 572 (1994), pp. 575–599. DOI: 10.1016/0375-9474(94)90401-4 (cit. on p. 15).

[Li+21] Bao-An Li et al. “Progress in Constraining Nuclear Symmetry Energy Using Neutron Star Observables Since GW170817”. In: *Universe* 7.6 (2021), p. 182. DOI: 10.3390/universe7060182 (cit. on pp. 66, 79).

[LSW18] Jia Jie Li, Armen Sedrakian, and Fridolin Weber. “Competition between delta isobars and hyperons and properties of compact stars”. In: *Phys. Lett. B* 783 (2018), pp. 234–240. DOI: 10.1016/j.physletb.2018.06.051. arXiv: 1803.03661 [nucl-th] (cit. on p. xxxiii).

[LT05] S. Liuti and S. K. Taneja. “Nuclear medium modifications of hadrons from generalized parton distributions”. In: *Phys. Rev. C* 72 (2005), p. 034902. DOI: 10.1103/PhysRevC.72.034902. arXiv: hep-ph/0504027 (cit. on pp. 42, 52).

[LMR06] M. Loewe, S. Mendizabal, and J. C. Rojas. “Skyrme model and isospin chemical potential”. In: *Phys. Lett. B* 632 (2006), pp. 512–516. DOI: 10.1016/j.physletb.2005.10.082. arXiv: hep-ph/0508038 (cit. on p. 78).

[Lor20] Cédric Lorcé. “Charge Distributions of Moving Nucleons”. In: *Phys. Rev. Lett.* 125 (23 Dec. 2020), p. 232002. DOI: 10.1103/PhysRevLett.125.232002. arXiv: 2007.05318 [hep-ph] (cit. on p. 53).

[Mag+20] Michele Maggiore et al. “Science Case for the Einstein Telescope”. In: *JCAP* 03 (2020), p. 050. DOI: 10.1088/1475-7516/2020/03/050. arXiv: 1912.02622 [astro-ph.CO] (cit. on p. xxxiv).

[MZ22] Kiminad A. Mamo and Ismail Zahed. “J/ψ near threshold in holographic QCD: A and D gravitational form factors”. In: *Phys. Rev. D* 106.8 (2022), p. 086004. DOI: 10.1103/PhysRevD.106.086004. arXiv: 2204.08857 [hep-ph] (cit. on p. 41).

[MMW07] Olga V. Manko, Nicholas S. Manton, and Stephen W. Wood. “Light nuclei as quantized skyrmions”. In: *Phys. Rev. C* 76 (2007), p. 055203. DOI: 10.1103/PhysRevC.76.055203. arXiv: 0707.0868 [hep-th] (cit. on pp. 6, 13, 14, 35).

[Man19] Massimo Mannarelli. “Meson condensation”. In: *Particles* 2.3 (2019), pp. 411–443. DOI: 10.3390/particles2030025. arXiv: 1908.02042 [hep-ph] (cit. on p. xxxii).

[Man22] Nicholas S. Manton. *Skyrmions – A Theory of Nuclei*. 1st ed. World Scientific Publishing Company (Europe), 2022. DOI: 10.1142/q0368 (cit. on p. 4).

[MS04] Nicholas S. Manton and Paul M. Sutcliffe. *Topological Solitons*. Cambridge Monographs on Mathematical Physics. Cambridge University Press, 2004. DOI: 10.1017/CBO9780511617034 (cit. on pp. xxv, xxviii, 4).

[MW08] Nicholas S. Manton and Stephen W. Wood. "Light Nuclei as Quantized Skyrmions: Energy Spectra and Form Factors". In: *15th International Seminar on High Energy Physics*. Sept. 2008. arXiv: 0809.3501 [hep-th] (cit. on p. 28).

[Mar91] Luc Marleau. "Modifying the Skyrme model: Pion mass and higher derivatives". In: *Phys. Rev. D* 43 (1991), pp. 885–890. DOI: 10.1103/PhysRevD.43.885 (cit. on p. 3).

[MP05] Karl Martel and Eric Poisson. "Gravitational perturbations of the Schwarzschild spacetime: A Practical covariant and gauge-invariant formalism". In: *Phys. Rev. D* 71 (2005), p. 104003. DOI: 10.1103/PhysRevD.71.104003 (cit. on pp. 110, 153).

[MV17] Prado Martín–Moruno and Matt Visser. "Classical and Semi-classical Energy Conditions". In: *Wormholes, Warp Drives and Energy Conditions*. Ed. by Francisco S. N. Lobo. Springer International Publishing, 2017, pp. 193–213. ISBN: 978-3-319-55182-1. DOI: {10.1007/978-3-319-55182-1_9} (cit. on pp. 99, 100).

[MP07] Larry McLerran and Robert D. Pisarski. "Phases of cold, dense quarks at large N(c)". In: *Nucl. Phys. A* 796 (2007), pp. 83–100. DOI: 10.1016/j.nuclphysa.2007.08.013. arXiv: 0706.2191 [hep-ph] (cit. on p. xxxiii).

[MR19] Larry McLerran and Sanjay Reddy. "Quarkyonic Matter and Neutron Stars". In: *Phys. Rev. Lett.* 122.12 (2019), p. 122701. DOI: 10.1103/PhysRevLett.122.122701. arXiv: 1811.12503 [nucl-th] (cit. on p. xxxiii).

[MZ86] U. -G. Meissner and I. Zahed. "Skyrmions in the Presence of Vector Mesons". In: *Phys. Rev. Lett.* 56 (10 Mar. 1986), pp. 1035–1038. DOI: 10.1103/PhysRevLett.56.1035 (cit. on p. 3).

[Mei+86] Ulf -G. Meissner et al. "Skyrmions with ρ and ω Mesons as Dynamical Gauge Bosons". In: *Phys. Rev. Lett.* 57 (14 Oct. 1986), pp. 1676–1679. DOI: 10.1103/PhysRevLett.57.1676 (cit. on p. 3).

[Meu+17] Aaron Meurer et al. "SymPy: symbolic computing in Python". In: *PeerJ Computer Science* 3 (Jan. 2017), e103. ISSN: 2376-5992. DOI: 10.7717/peerj-cs.103. URL: https://doi.org/10.7717/peerj-cs.103 (cit. on p. xii).

[Mil07] Gerald A. Miller. "Charge Density of the Neutron". In: *Phys. Rev. Lett.* 99 (2007), p. 112001. DOI: 10.1103/PhysRevLett.99.112001. arXiv: 0705.2409 [nucl-th] (cit. on p. 53).

[Mil+19] M. C. Miller et al. "PSR J0030+0451 Mass and Radius from *NICER* Data and Implications for the Properties of Neutron Star Matter". In: *Astrophys. J. Lett.* 887.1 (2019), p. L24. DOI: 10.3847/2041-8213/ab50c5. arXiv: 1912.05705 [astro-ph.HE] (cit. on p. 95).

[Mil+21] M. C. Miller et al. "The Radius of PSR J0740+6620 from NICER and XMM-Newton Data". In: *Astrophys. J. Lett.* 918.2 (2021), p. L28. DOI: 10.3847/2041-8213/ac089b (cit. on p. 95).

[Müh+09] Sebastian Mühlbauer et al. “Skyrmion lattice in a chiral magnet”. In: *Science* 323.5916 (2009), pp. 915–919. arXiv: 0902.1968 [cond-mat.str-el] (cit. on p. xxix).

[Nah+15] Y. Nahas et al. “Discovery of stable skyrmionic state in ferroelectric nanocomposites”. In: *Nature Communications* 6.1 (2015), p. 8542. DOI: 10.1038/ncomms9542 (cit. on p. xxix).

[Nay19] Carlos Naya. “Neutron stars within the Skyrme model”. In: *International Journal of Modern Physics E* 28.08 (2019), p. 1930006. DOI: 10.1142/S0218301319300066. arXiv: 1910.01145 [astro-ph.HE] (cit. on pp. 97, 104, 137, 145).

[NS18a] Carlos Naya and Paul M. Sutcliffe. “Skyrmions and Clustering in Light Nuclei”. In: *Physical Review Letters* 121 (23 Dec. 2018), p. 232002. DOI: 10.1103/PhysRevLett.121.232002. arXiv: 1811.02064 [hep-th] (cit. on p. 3).

[NS18b] Carlos Naya and Paul M. Sutcliffe. “Skyrmions in models with pions and rho mesons”. In: *JHEP* 05 (2018), p. 174. DOI: 10.1007/JHEP05(2018)174. arXiv: 1803.06098 [hep-th] (cit. on p. 138).

[NP12] Susan Nelmes and Bernard M. A. G. Piette. “Phase transition and anisotropic deformations of neutron star matter”. In: *Phys. Rev. D* 85 (12 June 2012), p. 123004. DOI: 10.1103/PhysRevD.85.123004 (cit. on pp. 96, 104).

[Nes83] Yurii E. Nesterov. “A method of solving a convex programming problem with convergence rate $O\left(\frac{1}{k^2}\right)$”. In: *Proceedings of the USSR Academy of Sciences* 269 (1983), pp. 543–547. URL: https://www.mathnet.ru/eng/dan46009 (cit. on p. 149).

[NO73] Holger Bech Nielsen and P. Olesen. “Vortex Line Models for Dual Strings”. In: *Nucl. Phys. B* 61 (1973). Ed. by J. C. Taylor, pp. 45–61. DOI: 10.1016/0550-3213(73)90350-7 (cit. on p. xxix).

[NN00] Morten Nielsen and N. K. Nielsen. “Explicit construction of constrained instantons”. In: *Phys. Rev. D* 61 (2000), p. 105020. DOI: 10.1103/PhysRevD.61.105020. arXiv: hep-th/9912006 (cit. on pp. 17, 19).

[Nie05] N. K. Nielsen. *Instanton constraints in supersymmetric gauge theories. II. N = 2 Yang-Mills theory*. Mar. 2005. arXiv: hep-th/0503120 (cit. on p. 17).

[Nov+23] S. J. Novario et al. “Trends of Neutron Skins and Radii of Mirror Nuclei from First Principles”. In: *Phys. Rev. Lett.* 130.3 (2023), p. 032501. DOI: 10.1103/PhysRevLett.130.032501. arXiv: 2111.12775 [nucl-th] (cit. on pp. 57, 58).

[NR90] E. M. Nyman and D. O. Riska. “Low-energy Properties of Baryons in the Skyrme Model”. In: *Rept. Prog. Phys.* 53 (1990), pp. 1137–1182. DOI: 10.1088/0034-4885/53/9/001 (cit. on p. 84).

[Pag66] Heinz Pagels. “Energy-Momentum Structure Form Factors of Particles”. In: *Phys. Rev.* 144 (1966), pp. 1250–1260. DOI: 10.1103/PhysRev.144.1250 (cit. on p. 41).

[PBG00] Subrata Pal, Debades Bandyopadhyay, and Walter Greiner. "Anti-K**0 condensation in neutron stars". In: *Nucl. Phys. A* 674 (2000), pp. 553–577. DOI: 10.1016/S0375-9474(00)00175-5. arXiv: astro-ph/0001039 (cit. on p. xxxiii).

[Pan+18] Paolo Pani et al. "Magnetic tidal Love numbers clarified". In: *Phys. Rev. D* 98 (12 Dec. 2018), p. 124023. DOI: 10.1103/PhysRevD.98.124023. URL: https://link.aps.org/doi/10.1103/PhysRevD.98.124023 (cit. on p. 122).

[PPV19] Byung-Yoon Park, Won-Gi Paeng, and Vicente Vento. "The inhomogeneous phase of dense skyrmion matter". In: *Nuclear Physics A* 989 (2019), pp. 231–245. ISSN: 0375-9474. DOI: https://doi.org/10.1016/j.nuclphysa.2019.06.010 (cit. on p. 80).

[PV10] Byung-Yoon Park and Vicente Vento. "Skyrmion approach to finite density and temperature". In: *The multifaceted skyrmion*. Ed. by Gerald E. Brown and Mannque Rho. 2010, pp. 115–146. DOI: 10.1142/9789814280709_0005. arXiv: 0906.3263 [hep-ph] (cit. on p. 80).

[Par+02] Byung-Yoon Park et al. "Atiyah-Manton approach to skyrmion matter". In: *Nucl. Phys. A* 707 (2002), pp. 381–398. DOI: 10.1016/S0375-9474(02)00963-6. arXiv: nucl-th/0201014 (cit. on p. 23).

[PHS22] Dimitra A. Pefkou, Daniel C. Hackett, and Phiala E. Shanahan. "Gluon gravitational structure of hadrons of different spin". In: *Phys. Rev. D* 105.5 (2022), p. 054509. DOI: 10.1103/PhysRevD.105.054509. arXiv: 2107.10368 [hep-lat] (cit. on p. 45).

[PPS16] I. A. Perevalova, M. V. Polyakov, and P. Schweitzer. "On LHCb pentaquarks as a baryon-ψ(2S) bound state: prediction of isospin-$\frac{3}{2}$ pentaquarks with hidden charm". In: *Phys. Rev. D* 94.5 (2016), p. 054024. DOI: 10.1103/PhysRevD.94.054024. arXiv: 1607.07008 [hep-ph] (cit. on p. 42).

[Pia+13] M. Piarulli et al. "Electromagnetic structure of $A = 2$ and 3 nuclei in chiral effective field theory". In: *Phys. Rev. C* 87 (1 Jan. 2013), p. 014006. DOI: 10.1103/PhysRevC.87.014006 (cit. on p. 28).

[Pic95] A. Pich. "Chiral perturbation theory". In: *Rept. Prog. Phys.* 58 (1995), pp. 563–610. DOI: 10.1088/0034-4885/58/6/001. arXiv: hep-ph/9502366 (cit. on p. 34).

[Pic20] Antonio Pich. "Effective Field Theory with Nambu–Goldstone Modes". In: *Effective Field Theory in Particle Physics and Cosmology: Lecture Notes of the Les Houches Summer School: Volume 108, July 2017*. Oxford University Press, Apr. 2020. ISBN: 9780198855743. DOI: 10.1093/oso/9780198855743.003.0003 (cit. on p. xxiii).

[PPV11] Eric Poisson, Adam Pound, and Ian Vega. "The Motion of Point Particles in Curved Spacetime". In: *Living Rev. Relativ.* 14.1 (2011), p. 7. DOI: 10.12942/lrr-2011-7 (cit. on p. 118).

[Pol74] Alexander M. Polyakov. "Particle Spectrum in Quantum Field Theory". In: *JETP Lett.* 20 (1974). Ed. by J. C. Taylor, pp. 194–195 (cit. on p. xxix).

[Pol03] M. V. Polyakov. "Generalized parton distributions and strong forces inside nucleons and nuclei". In: *Phys. Lett. B* 555 (2003), pp. 57–62. DOI: 10.1016/S0370-2693(03)00036-4. arXiv: hep-ph/0210165 (cit. on pp. 42, 52).

[PS18] Maxim V. Polyakov and Peter Schweitzer. "Forces inside hadrons: pressure, surface tension, mechanical radius, and all that". In: *Int. J. Mod. Phys. A* 33.26 (2018), p. 1830025. DOI: 10.1142/S0217751X18300259. arXiv: 1805.06596 [hep-ph] (cit. on p. 41).

[PS19] Maxim V. Polyakov and Bao-Dong Sun. "Gravitational form factors of a spin one particle". In: *Phys. Rev. D* 100.3 (2019), p. 036003. DOI: 10.1103/PhysRevD.100.036003. arXiv: 1903.02738 [hep-ph] (cit. on pp. 44, 45).

[PMG09] J. A. Pons, J. A. Miralles, and U. Geppert. "Magneto–thermal evolution of neutron stars". In: *Astron. Astrophys.* 496 (2009), pp. 207–216. DOI: 10.1051/0004-6361:200811229. arXiv: 0812.3018 [astro-ph] (cit. on p. xxxii).

[Pon+99] J. A. Pons et al. "Evolution of protoneutron stars". In: *Astrophys. J.* 513 (1999), p. 780. DOI: 10.1086/306889. arXiv: astro-ph/9807040 (cit. on p. xxxii).

[Pon+00] Jose A. Pons et al. "Kaon condensation in proto neutron star matter". In: *Phys. Rev. C* 62 (2000), p. 035803. DOI: 10.1103/PhysRevC.62.035803. arXiv: nucl-th/0003008 (cit. on p. 91).

[PPL10] Sergey Postnikov, Madappa Prakash, and James M. Lattimer. "Tidal Love Numbers of Neutron and Self-Bound Quark Stars". In: *Phys. Rev. D* 82 (2010), p. 024016. DOI: 10.1103/PhysRevD.82.024016. arXiv: 1004.5098 [astro-ph.SR] (cit. on p. xxxiv).

[Pun+15] V. Punjabi et al. "The Structure of the Nucleon: Elastic Electromagnetic Form Factors". In: *Eur. Phys. J. A* 51 (2015), p. 79. DOI: 10.1140/epja/i2015-15079-x. arXiv: 1503.01452 [nucl-ex] (cit. on pp. 28, 32).

[RW00] Krishna Rajagopal and Frank Wilczek. "The Condensed matter physics of QCD". In: *At the frontier of particle physics. Handbook of QCD. Vol. 1-3.* Ed. by M. Shifman and Boris Ioffe. Nov. 2000, pp. 2061–2151. DOI: 10.1142/9789812810458_0043. arXiv: hep-ph/0011333 (cit. on p. xxx).

[RDH21] Brendan T. Reed, Alex Deibel, and C. J. Horowitz. "Modeling the Galactic Neutron Star Population for Use in Continuous Gravitational-wave Searches". In: *Astrophys. J.* 921.1 (2021), p. 89. DOI: 10.3847/1538-4357/ac1c04. arXiv: 2104.00771 [astro-ph.HE] (cit. on p. xxxii).

[RV15] Borja Reina and Raül Vera. "Revisiting Hartle's model using perturbed matching theory to second order: amending the change in mass". In: *Class. Quantum Gravity* 32.15 (July 2015), p. 155008. ISSN: 1361-6382. DOI: 10.1088/0264-9381/32/15/155008. arXiv: 1412.7083 [gr-qc] (cit. on pp. 107–109, 115).

[Rei+17] Borja Reina et al. "Completion of the universal I–Love–Q relations in compact stars including the mass". In: *Mon. Not. R. Astron. Soc. Lett.* 470.1 (May 2017), pp. L54–L58. ISSN: 1745-3925. DOI: 10.1093/mnrasl/slx078. arXiv: 1702.04568 [gr-qc] (cit. on pp. 115, 127, 128, 131).

[Rei+19] David Reitze et al. "Cosmic Explorer: The U.S. Contribution to Gravitational-Wave Astronomy beyond LIGO". In: *Bull. Am. Astron. Soc.* 51.7 (2019), p. 035. arXiv: 1907.04833 [astro-ph.IM] (cit. on p. xxxiv).

[RZ13] Luciano Rezzolla and Olindo Zanotti. *Relativistic Hydrodynamics*. Oxford University Press, Sept. 2013. ISBN: 9780198528906. DOI: 10.1093/acprof:oso/9780198528906.001.0001 (cit. on p. 122).

[Ril+21] Thomas E. Riley et al. "A NICER View of the Massive Pulsar PSR J0740+6620 Informed by Radio Timing and XMM-Newton Spectroscopy". In: *Astrophys. J. Lett.* 918.2 (2021), p. L27. DOI: 10.3847/2041-8213/ac0a81. arXiv: 2105.06980 [astro-ph.HE] (cit. on p. 95).

[Rom+22] Roger W. Romani et al. "PSR J0952−0607: The Fastest and Heaviest Known Galactic Neutron Star". In: *Astrophys. J. Lett.* 934.2 (2022), p. L17. DOI: 10.3847/2041-8213/ac8007. arXiv: 2207.05124 [astro-ph.HE] (cit. on p. 96).

[Rot12] Heinz J. Rothe. *Lattice Gauge Theories : An Introduction (Fourth Edition)*. Vol. 43. World Scientific Publishing Company, 2012. ISBN: 978-981-4365-87-1, 978-981-4365-85-7. DOI: 10.1142/8229 (cit. on p. xxiv).

[RS96] V. A. Rubakov and M. E. Shaposhnikov. "Electroweak baryon number non-conservation in the early universe and in high-energy collisions". In: *Usp. Fiz. Nauk* 166 (1996), pp. 493–537. DOI: 10.1070/PU1996v039n05ABEH000145. arXiv: hep-ph/9603208 (cit. on pp. 16, 17).

[Sac62] R. G. Sachs. "High-Energy Behavior of Nucleon Electromagnetic Form Factors". In: *Phys. Rev.* 126 (6 June 1962), pp. 2256–2260. DOI: 10.1103/PhysRev.126.2256 (cit. on pp. 28, 53).

[SS05a] Tadakatsu Sakai and Shigeki Sugimoto. "Low energy hadron physics in holographic QCD". In: *Prog. Theor. Phys.* 113 (2005), pp. 843–882. DOI: 10.1143/PTP.113.843. arXiv: hep-th/0412141 (cit. on pp. 15, 49).

[SS05b] Stefan Scherer and Matthias R. Schindler. *A Chiral perturbation theory primer*. May 2005. arXiv: hep-ph/0505265 (cit. on p. 34).

[Sch10] Andreas Schmitt. *Dense matter in compact stars: A pedagogical introduction*. Vol. 811. 2010. DOI: 10.1007/978-3-642-12866-0. arXiv: 1001.3294 [astro-ph.SR] (cit. on p. 85).

[Sch+08] Andreas Schnyder et al. "Classification of topological insulators and superconductors in three spatial dimensions". In: *Phys. Rev. B* 78.19 (2008), p. 195125. DOI: 10.1103/PhysRevB.78.195125. arXiv: 0803.2786 [cond-mat.mes-hall] (cit. on p. xxix).

[SW97] Brian D. Serot and John Dirk Walecka. "Recent progress in quantum hadrodynamics". In: *Int. J. Mod. Phys. E* 6 (1997), pp. 515–631. DOI: 10.1142/S0218301397000299. arXiv: nucl-th/9701058 (cit. on p. xxxi).

[Sha+15] B. K. Sharma et al. "Unified equation of state for neutron stars on a microscopic basis". In: *Astron. Astrophys.* 584 (Nov. 2015), A103. ISSN: 1432-0746. DOI: 10.1051/0004-6361/201526642 (cit. on p. 105).

[Shi22] Mikhail Shifman. *Advanced Topics in Quantum Field Theory: A Lecture Course*. 2nd ed. Cambridge University Press, 2022. DOI: 10.1017/9781108885911 (cit. on p. 17).

[Shu09] Edward Shuryak. "Physics of Strongly coupled Quark-Gluon Plasma". In: *Prog. Part. Nucl. Phys.* 62 (2009), pp. 48–101. DOI: 10.1016/j.ppnp.2008.09.001. arXiv: 0807.3033 [hep-ph] (cit. on p. xxx).

[Sic01] I. Sick. "Elastic electron scattering from light nuclei". In: *Progress in Particle and Nuclear Physics* 47.1 (2001), pp. 245–318. ISSN: 0146-6410. DOI: https://doi.org/10.1016/S0146-6410(01)00156-9 (cit. on p. 57).

[Sie+22] Jared C. Siegel et al. *Investigating the Lower Mass Gap with Low Mass X-ray Binary Population Synthesis*. Sept. 2022. arXiv: 2209.06844 [astro-ph.HE] (cit. on p. 96).

[Sky61] Tony H. R. Skyrme. "A non-linear field theory". In: *Proceedings of the Royal Society of London. Series A. Mathematical and Physical Sciences* 260.1300 (1961), pp. 127–138. DOI: 10.1098/rspa.1961.0018 (cit. on pp. xxiv, xxviii, 3, 4, 133, 141).

[Som12] Kentaro Somiya. "Detector configuration of KAGRA: The Japanese cryogenic gravitational-wave detector". In: *Class. Quant. Grav.* 29 (2012). Ed. by Mark Hannam et al., p. 124007. DOI: 10.1088/0264-9381/29/12/124007. arXiv: 1111.7185 [gr-qc] (cit. on p. 96).

[SS01] D. T. Son and M. A. Stephanov. "QCD at finite isospin density". In: *Phys. Rev. Lett.* 86 (2001), pp. 592–595. DOI: 10.1103/PhysRevLett.86.592 (cit. on p. 77).

[SS08] D. T. Son and M. A. Stephanov. "Axial anomaly and magnetism of nuclear and quark matter". In: *Phys. Rev. D* 77 (2008), p. 014021. DOI: 10.1103/PhysRevD.77.014021. arXiv: 0710.1084 [hep-ph] (cit. on p. xxxi).

[SBG04] Carlos F. Sopuerta, Marco Bruni, and Leonardo Gualtieri. "Nonlinear N parameter space-time perturbations: Gauge transformations". In: *Phys. Rev. D* 70 (2004), p. 064002. DOI: 10.1103/PhysRevD.70.064002 (cit. on pp. 107, 152).

[Sor+23] Agnieszka Sorensen et al. *Dense Nuclear Matter Equation of State from Heavy-Ion Collisions*. Jan. 2023. arXiv: 2301.13253 [nucl-th] (cit. on p. 66).

[SSM14] J. R. Stone, N. J. Stone, and S. A. Moszkowski. "Incompressibility in finite nuclei and nuclear matter". In: *Phys. Rev. C* 89 (4 Apr. 2014), p. 044316. DOI: 10.1103/PhysRevC.89.044316 (cit. on p. 66).

[Sut94] Paul M. Sutcliffe. "Instanton moduli and topological soliton dynamics". In: *Nucl. Phys. B* 431 (1994), pp. 97–118. DOI: 10.1016/0550-3213(94)90099-X. arXiv: hep-th/9408168 (cit. on pp. 15, 17).

[Sut10] Paul M. Sutcliffe. "Skyrmions, instantons and holography". In: *JHEP* 08 (2010), p. 019. DOI: 10.1007/JHEP08(2010)019. arXiv: 1003.0023 [hep-th] (cit. on pp. 3, 15).

[TCA01] Alexander K. Tagantsev, Eric Courtens, and Ludovic Arzel. "Prediction of a low-temperature ferroelectric instability in antiphase domain boundaries of strontium titanate". In: *Phys. Rev. B* 64 (22 Nov. 2001), p. 224107. DOI: 10.1103/PhysRevB.64.224107 (cit. on p. xxix).

[Tan+21] Shao-Peng Tang et al. "Constraints on the phase transition and nuclear symmetry parameters from PSR J0740+6620 and multimessenger data of other neutron stars". In: *Phys. Rev. D* 104.6 (2021), p. 063032. DOI: 10.1103/PhysRevD.104.063032 (cit. on p. 66).

[Tew+16] I. Tews et al. "Quantum Monte Carlo calculations of neutron matter with chiral three-body forces". In: *Phys. Rev. C* 93.2 (2016), p. 024305. DOI: 10.1103/PhysRevC.93.024305. arXiv: 1507.05561 [nucl-th] (cit. on p. xxxi).

[Tho80] Kip S. Thorne. "Multipole expansions of gravitational radiation". In: *Rev. Mod. Phys.* 52 (2 Apr. 1980), pp. 299–339. DOI: 10.1103/RevModPhys.52.299. URL: https://link.aps.org/doi/10.1103/RevModPhys.52.299 (cit. on p. 116).

[TH85] Kip S. Thorne and James B. Hartle. "Laws of motion and precession for black holes and other bodies". In: *Phys. Rev. D* 31 (8 Apr. 1985), pp. 1815–1837. DOI: 10.1103/PhysRevD.31.1815 (cit. on pp. 116, 118).

[Tin64] M. Tinkham. *Group Theory and Quantum Mechanics*. International series in pure and applied physics. McGraw-Hill, 1964. ISBN: 9780070648951 (cit. on p. 46).

[TF20] Laura Tolos and Laura Fabbietti. "Strangeness in Nuclei and Neutron Stars". In: *Prog. Part. Nucl. Phys.* 112 (2020), p. 103770. DOI: 10.1016/j.ppnp.2020.103770. arXiv: 2002.09223 [nucl-ex] (cit. on p. 83).

[TFP21] Pedro Barata de Tovar, Márcio Ferreira, and Constança Providência. "Determination of the symmetry energy from the neutron star equation of state". In: *Phys. Rev. D* 104.12 (2021), p. 123036. DOI: 10.1103/PhysRevD.104.123036. arXiv: 2112.05551 [nucl-th] (cit. on p. 66).

[VBG09] Sergey Vaintraub, Nir Barnea, and Doron Gazit. "He-6 beta-decay rate and the suppression of the axial constant in nuclear matter". In: *Phys. Rev. C* 79 (2009), p. 065501. DOI: 10.1103/PhysRevC.79.065501. arXiv: 0903.1048 [nucl-th] (cit. on p. 37).

[Vid16] Isaac Vidaña. "Hyperons in Neutron Stars". In: *J. Phys. Conf. Ser.* 668.1 (2016). Ed. by David Alvarez-Castillo et al., p. 012031. DOI: 10.1088/1742-6596/668/1/012031. arXiv: 1509.03587 [nucl-th] (cit. on p. 83).

[VB00] Matt Visser and Carlos Barceló. "Energy conditions and their cosmological implications". In: *3rd International Conference on Particle Physics and the Early Universe*. World Scientific Pub Co Pte Lt, Sept. 2000, pp. 98–112. DOI: 10.1142/9789812792129_0014. arXiv: 0001099 [gr-qc] (cit. on p. 99).

[Wal04] John Dirk Walecka. *Theoretical Nuclear And Subnuclear Physics*. 2nd. World Scientific Publishing Company (co-published with Imperial College Press), 2004. ISBN: 9789813102170. DOI: 10.1142/5500. URL: https://www.worldscientific.com/doi/abs/10.1142/5500 (cit. on pp. 36, 37).

[Wan94] Meng-yuan Wang. *On constrained instanton valleys*. Dec. 1994. arXiv: hep-ph/9502333 (cit. on p. 20).

[WSH86] H. Weigel, B. Schwesinger, and G. Holzwarth. "Exotic Baryon Number $B = 2$ States in the SU(2) Skyrme Model". In: *Phys. Lett. B* 168 (1986), pp. 321–325. DOI: 10.1016/0370-2693(86)91637-0 (cit. on p. 3).

[Wei08] Herbert Weigel. *Chiral Soliton Models for Baryons*. Vol. 743. Lect. Notes Phys. Springer, Berlin Heidelberg, 2008. DOI: 10.1007/978-3-540-75436-7 (cit. on p. 28).

[Wen90] X. G. Wen. "Topological Order in Rigid States". In: *Int. J. Mod. Phys. B* 4 (1990), p. 239. DOI: 10.1142/S0217979290000139 (cit. on p. xxix).

[Wen93] Xiao-Gang Wen. "Topological order and edge structure of ν=1/2 quantum Hall state". In: *Phys. Rev. Lett.* 70 (3 Jan. 1993), pp. 355–358. DOI: 10.1103/PhysRevLett.70.355 (cit. on p. xxix).

[WZ83] Frank Wilczek and A. Zee. "Linking Numbers, Spin, and Statistics of Solitons". In: *Phys. Rev. Lett.* 51 (1983), pp. 2250–2252. DOI: 10.1103/PhysRevLett.51.2250 (cit. on p. 24).

[Wit83a] Edward Witten. "Current Algebra, Baryons, and Quark Confinement". In: *Nucl. Phys. B* 223 (1983), pp. 433–444. DOI: 10.1016/0550-3213(83)90064-0 (cit. on p. xxiv).

[Wit83b] Edward Witten. "Global Aspects of Current Algebra". In: *Nucl. Phys. B* 223 (1983), pp. 422–432. DOI: 10.1016/0550-3213(83)90063-9 (cit. on p. 84).

[Wit88] Edward Witten. "Topological Quantum Field Theory". In: *Commun. Math. Phys.* 117 (1988), p. 353. DOI: 10.1007/BF01223371 (cit. on p. xxix).

[Wol23] Wolfram Research, Inc. *Mathematica*. Version 13.3. Champaign, IL. 2023. URL: https://www.wolfram.com/mathematica (cit. on p. xii).

[Wor+22] R. L. Workman et al. "Review of Particle Physics". In: *PTEP* 2022 (2022), p. 083C01. DOI: 10.1093/ptep/ptac097 (cit. on p. xxiv).

[Yag14] Kent Yagi. "Multipole Love Relations". In: *Phys. Rev. D* 89.4 (2014). [Erratum: Phys.Rev.D 96, 129904 (2017), Erratum: Phys.Rev.D 97, 129901 (2018)], p. 043011. DOI: 10.1103/PhysRevD.89.043011 (cit. on pp. 122, 123).

[YY13a] Kent Yagi and Nicolás Yunes. "I-Love-Q: Unexpected Universal Relations for Neutron Stars and Quark Stars". In: *Science* 341.6144 (2013), pp. 365–368. ISSN: 0036-8075. DOI: 10.1126/science.1236462. arXiv: 1303.1528 [gr-qc] (cit. on p. xxxiv).

[YY13b] Kent Yagi and Nicolas Yunes. "I-Love-Q Relations in Neutron Stars and their Applications to Astrophysics, Gravitational Waves and Fundamental Physics". In: *Phys. Rev. D* 88.2 (2013), p. 023009. DOI: 10.1103/PhysRevD.88.023009. arXiv: 1303.1528 [gr-qc] (cit. on pp. xi, xxxiv, 107, 112–114, 123, 124, 131, 137, 146).

[Yag+13] Kent Yagi et al. "Isolated and Binary Neutron Stars in Dynamical Chern-Simons Gravity". In: *Phys. Rev. D* 87 (2013). [Erratum: Phys.Rev.D 93, 089909 (2016)], p. 084058. DOI: 10.1103/PhysRevD.87.084058. arXiv: 1302.1918 [gr-qc] (cit. on pp. 113, 114, 120).

[Yag+14] Kent Yagi et al. "Why I-Love-Q: Explaining why universality emerges in compact objects". In: *Phys. Rev. D* 90.6 (2014), p. 063010. DOI: 10.1103/PhysRevD.90.063010. arXiv: 1406.7587 [gr-qc] (cit. on pp. 123, 131).

[ZKO74] Ya. B. Zeldovich, I. Yu. Kobzarev, and L. B. Okun. "Cosmological Consequences of the Spontaneous Breakdown of Discrete Symmetry". In: *Zh. Eksp. Teor. Fiz.* 67 (1974), pp. 3–11 (cit. on p. xxix).